Oxidation of

Organic Compounds

Volume III. Ozone Chemistry, Photo and Singlet Oxygen and Biochemical Oxidations

Proceedings of the International

Oxidation Symposium, arranged

by Stanford Research Institute,

in San Francisco, Calif.

Aug. 28-Sept. 1, 1967

Frank R. Mayo

General Chairman

ADVANCES IN CHEMISTRY SERIES **77**

AMERICAN CHEMICAL SOCIETY

WASHINGTON, D.C.   1968

Advances in Chemistry Series

Robert F. Gould, *Editor*

AMERICAN CHEMICAL SOCIETY PUBLICATIONS

FOREWORD

ADVANCES IN CHEMISTRY SERIES was founded in 1949 by the American Chemical Society as an outlet for symposia and collections of data in special areas of topical interest that could not be accommodated in the Society's journals. It provides a medium for symposia that would otherwise be fragmented, their papers distributed among several journals or not published at all. Papers are refereed critically according to ACS editorial standards and receive the careful attention and processing characteristic of ACS publications. Papers published in ADVANCES IN CHEMISTRY SERIES are original contributions not published elsewhere in whole or major part and include reports of research as well as reviews since symposia may embrace both types of presentation.

Ozone Chemistry of Organic Compounds

ROBERT W. MURRAY

Bell Telephone Laboratories, Inc., Murray Hill, N. J.

To the best of my knowledge this is only the third time in just over 10 years that a complete session at a symposium has been devoted to the ozone chemistry of organic compounds. The last occasions were at the Southwest Regional ACS meeting in December 1963, the September 1959 ACS meeting in Atlantic City, N. J., and the International Ozone Conference in Chicago in November 1956. We are concerned here with the ozone chemistry of organic materials only. The larger subject of ozone chemistry and technology is far beyond the capacity of a single session, even straining the bounds of a whole symposium, as was seen at the Chicago meeting. In fact, we shall not even be able to cover all areas of current interest in the limited area of organic ozone chemistry, although we have a fairly representative sample of those interests.

Interest in ozone chemistry has been stimulated by two sources where the practical consequences of this field are of some importance— namely, the space program and the air pollution problem. It seems safe to predict that both areas will continue to be interested in the results of research on the reactions of ozone with both organic and inorganic materials. More recently it has become apparent that ozone will play an increasingly important role in industrial chemistry, owing to the lower cost and greater efficiency of industrial ozone generators. In 1956, at the time of the International Ozone Chemistry Conference, less than a million pounds of ozone were used in industrial chemistry. In 1967 it is expected that 24 million pounds will be used by U.S. chemical and drug manufacturers.

The areas of current interest in organic ozone chemistry fall roughly into five broad categories. The first might be called the classical use of ozone—*i.e.*, either as a synthetic tool to convert unsaturation into carbonyl functions or as a valuable reagent for locating double bonds in structure determinations. Both techniques are still used widely by chemists, and reports of such work probably account for more than one-half of all the papers in this field. This use of ozone has by-products for the chemist who is more interested in mechanism—*i.e.*, products are obtained occa-

sionally which are attributed to anomalous ozonolysis and with which the mechanism chemist will have to deal.

The second general area of research is that concerned with the mechanism of ozonolysis—*i.e.*, that particular ozone reaction which leads to cleavage of a double bond. These efforts have had the benefit of a unifying mechanism proposed in the early 1950's by Prof. Criegee in Germany. Recent work in this area has been directed at determining the influence of several reaction variables on the ozonolysis process, including olefin geometry steric factors, and solvent effects. Some of the results suggest that modifications of the basic mechanism scheme may be required. This area will undoubtedly continue to receive considerable attention. This category also includes efforts directed at defining the stabilities and structures of intermediates, rate studies, and substituent effects on the rate and mechanism. Two papers in this section fall into the category of the mechanism of ozonolysis.

The reaction of ozone with saturated hydrocarbons has been a subject of renewed interest in recent years. Two papers in this section are concerned with this subject, while a third deals with the analogous reaction of organosilicon compounds. These studies are of both synthetic and mechanistic importance and are perhaps most closely associated with the general theme of this symposium since they inevitably involve the question of their relationship to autoxidation processes. The question of the mechanism of these saturated hydrocarbon-ozone reactions is presently an active subject with ionic, free radical, and insertion processes all being considered.

The reactions of ozone with non-hydrocarbons constitutes a fourth category for discussion. Included are the reactions of ozone with heterocycles, amines, aldehydes, alcohols, and others. Two papers in this section deal with this subject. Specifically, the reactions of amines and alcohols are reported. Suggestions for the mechanisms of these reactions are also made, and again, these proposals should be of special interest to those involved with similar reactions of oxygen.

The last general category—namely, the reaction of ozone with aromatic hydrocarbons, has received an enormous amount of attention by ozone chemists. Most of this attention has concerned rate and reactivity studies in an attempt to correlate these experimental quantities with some known parameters of the hydrocarbons. Several reactivity correlations have been proposed, including those with bond localization energy, atom localization energies, and oxidation-reduction potentials. This category is also represented by a paper in this section, in which a possible correlation between ozone reactivity and carcinogenicity of some polycyclic aromatic compounds is explored.

In summary, organic ozone chemistry is an active research area and will continue to see new developments both from theoretical and industrial viewpoints. In particular, we shall likely see the relationship between ozone chemistry, autoxidation, photo-oxidation, and singlet oxygen chemistry more clearly defined, with a noteworthy contribution being made at this symposium.

RECEIVED October 18, 1967.

59

The Reaction Between Ozone and Saturated Compounds

M. C. WHITING, A. J. N. BOLT, and J. H. PARISH

University of Bristol, Bristol 8, England

Ozone oxidizes saturated hydrocarbons (Decalin and ada-mantane) and alcohols even at −78°C. Initial products from hydrocarbons are radical pairs, in which tertiary radicals are formed preferentially from hydrocarbons, and which collapse to alcohols and oxygen with high retention of configuration. Methanol and ethanol are attacked, initially giving radical pairs or ion pairs which yield first α-hydroxy-hydrotrioxides, then formic or acetic acid and hydrogen peroxide. Propan-2-ol similarly gives α-hydroxyisopropyl hydrotrioxide, whose breakdown at higher temperatures is affected by trace substituents, and can give either acetone, oxygen, and water, or acetic acid and hydrogen peroxide. Side reactions lead via *acetone enol and its ozonide to peracetic acid, formaldehyde, acetone, and hydrogen per-oxide, and by a less well understood route to acetic acid and methanol.*

Durland and Adkins (5) described the oxidations of *cis-* and *trans-*Decalin with ozone as giving *cis-* and *trans-*9-decalols, respectively. The specific and stereospecific insertion of an atom into a C-H group appeared to be an interesting and unexpected reaction, and we have reinvestigated it using gas chromatography. It proceeds at temperatures as low as −78°C., leading mainly to tertiary alcohols, although significant quantities of ketones are also formed, and it shows a stereospecificity of *ca.* 90–98%, varying with solvent and temperature. Adamantane is also attacked at −78°C., giving the 1-alcohol and the ketone in ratios of *ca.* 3 to 1. Ozonation of a mixture of *trans-cis-β*-decalol and *trans-*Decalin resulted in preferential attack on the former, with the formation of *trans-β*-decalone. Thus, secondary alcohols are probably intermediates in the formation of ketones from hydrocarbons. We considered the possibility

4

that singlet oxygen rather than ozone might be the effective oxidant; however, pre-prepared solutions of ozone in trichlorofluoromethane at −78°C., in which it is unlikely that significant concentrations of singlet oxygen could be obtained, oxidized adamantane in the same way as did a stream of ozonized oxygen.

Experimental

Materials. Propan-2-ol (Type A) was May & Baker 2-propanol, either untreated or fractionated through a 30-inch Vigreux column. Propan-2-ol (Type B) was refluxed for 1 hour with sodium borohydride before fractionation. Both types had b.p., 82°C. Ethanol (b.p., 78°C.), methanol (b.p., 65°C.), *tert*-butyl alcohol (m.p., 25°C.), cyclohexanol (b.p., 161°C.), cyclohexane (b.p., 81°C.), and adamantane (m.p., 268°–270°C.) were purified by standard methods. *cis*- and *trans*-Decalin were prepared by preparative gas-liquid chromatography (GLC), following removal of Tetralin by passing through silica gel.

Ozone Apparatus and Reaction Procedure. The ozone apparatus was a Gallenkamp GE-150 yielding *ca.* 6% ozone in oxygen at a rate of *ca.* 10 liters/hour. The ozonized oxygen stream was passed by means of a tube terminated in a high porosity sintered glass disc through the substrate in a cylindrical reactor cooled to −78°C. with solid CO_2. Preliminary cooling of the gas stream by passage through a cooled glass coil had no appreciable effect on the result.

Product Analysis. Peroxidic products were estimated by the method of Ledall and Bernatek (7); 2-ml. aliquots were taken with a pipette previously cooled by wrapping in polyethylene sheet and covering with solid CO_2 (this procedure is particularly important when Type A propan-2-ol is involved since temperature increases result in changed product concentrations).

Acids other than peracids were estimated by titration against centinormal sodium hydroxide using bromothymol blue as indicator. (Speed is essential since decomposition of peracid otherwise results in an indefinite end point).

Carbonyl compounds were estimated by thin-layer chromatography (TLC) using diethyl ketone as an internal standard. They were converted to the corresponding 2,4-dinitrophenylhydrazones (DNP) by reaction for 15 hours with an excess of aqueous 2,4-dinitrophenylhydrazine perchlorate. The DNP's were extracted with benzene, the benzene extract was concentrated, and a portion of the concentrate was chromatographed on silica. The DNP's were completely separated by development with a mixture of diethyl ether (20%) and petroleum (b.p., 60°–80°C.; 80%). The resulting bands were removed separately and eluted with ethanol, the volume of each eluate being adjusted to 5 ml. The ultraviolet spectrum of each solution (diluted when necessary) was recorded, and the absolute concentrations of the carbonyl compounds in the original reaction solution were calculated.

GLC analysis of volatile products (*e.g.*, acetone, methanol), involved GPO-50 (Unilever Ltd.; 15%; 3 meters), temperatures between 0° and 20°C. and a heated flame-ionization detector. *n*-Hexane served as an

internal standard for quantitative estimation. Carboxylic acids were analyzed with a Pye 104 flame ionization gas-liquid chromatography apparatus and a mixed stationary phase (5%; 50°C.) of glutaric acid (23%) and GPO-50 (77%). The support (Embacel) and the 11.5-meter glass columns were silanized, and cyclohexanone was used as an internal standard. Peak areas were obtained planimetrically. Sample collection involved the above mixed phase (25%; 40°C.) and a Pye 104 catharometer apparatus.

Gas Evolution. The cold reaction solution was transferred to a calibrated flask at −78°C., connected to a gas buret, and immersed in an ice bath at 0°C. The solution was stirred magnetically at as near a constant rate as possible, and the apparent gas evolution was recorded at convenient time intervals. The gas was identified as oxygen by its absorption in alkaline pyrogallol (no absorption was noted in strong aqueous sodium hydroxide). The real gas evolution was obtained by subtracting from the apparent volume the value obtained in a blank control experiment involving unozonized oxygen.

Low Temperature Infrared Studies. These studies involved a low temperature cell (Research and Industrial Ltd., slightly modified) and a Perkin-Elmer 225 infrared spectrophotometer augmented with a slave recorder to record optical density. The cell temperature was maintained as close to −78°C. as possible with solid CO_2.

Oxidation by Solutions of Ozone. Solutions of ozone in trichlorofluoromethane (b.p., 24°C.) were prepared at −78°C., using the above apparatus and conditions. Passage of ozonized oxygen through the solvent (50 ml.) for 45 min. yielded a solution containing approximately 65 μmole/cc. ozone. Calculated quantities of substrate (generally in small excess) were added, and the mixture was set aside at −78°C. until, for alcohols, loss of color indicated the reaction to be complete. Titrimetric estimations were made as before, and the solvent was removed through a 30-inch Vigreux column before GLC investigation.

Solids precipitated in the reaction of propan-2-ol in CCl_3F with ozone were separated from the supernatant with a filter stick, washed with cold CCl_3F, and dissolved in propan-2-ol before analysis.

Partition of the reaction products of the above reaction between CCl_3F and 80% methanol involved shaking a portion of the supernatant at −78°C. with an equal volume of 80% methanol precooled to −78°C. The aqueous layer, on separation, was rapidly transferred to and mixed with an equal volume of CCl_3F at −78°C. On separation of the two layers, 2-ml. aliquots were removed from each and analyzed for peracid, acetic acid, hydrogen peroxide, acetone, and formaldehyde in the usual way. The temperature was maintained as close to −78°C. as possible until the analysis stage was reached. The procedure was repeated with CCl_3F solutions of the authentic compounds under identical conditions, and partition coefficients were compared.

The reactions of hydrocarbons with CCl_3F solutions of ozone at −78°C., being considerably slower than for alcohols, were allowed to proceed for up to 8 days. Any residual ozone was removed by flushing with nitrogen. Experiments were conducted on either a GLC or a preparative scale.

In a typical GLC scale experiment, adamantane (100 mg.) was added in excess to a CCl_3F solution of ozone, and the mixture was set aside at $-78°C.$ for 6 days. After removing residual ozone, the solvent was evaporated using a 30-inch Vigreux column. GLC of an ethereal solution of the residue on diglycerol (15%; 2 meters; 100°C.) demonstrated two main products, adamantanone (relative retention time $\tau = 22$) and 1-adamantanol ($\tau = 48$). In a similar experiment in which the solvent was a mixture of bromotrichloromethane (13 ml.) and CCl_3F (21 ml.) (this mixture precipitated some solid CCl_3Br at $-78°C.$), GLC analysis demonstrated the presence in the product of 1-chloroadamantane ($\tau = 2.5$), 1-bromoadamantane ($\tau = 4$), adamantanone (low yield), and 1-adamantanol. Five other components ($\tau = 6, 12, 17, 23, 62$) were not investigated.

In a typical preparative scale experiment adamantane (1 gram) was oxidized with a CCl_3F solution of ozone at $-78°C.$ for 8 days. After working up by the usual method, the residue was dissolved in ether and washed with aqueous sodium hydroxide. The ether layer on evaporation yielded a white crystalline solid (870 mg.). Elution with light petroleum (b.p., 30–40°C.) from neutral alumina (175 grams) gave unchanged adamantane (505 mg.), and 30% diethyl ether in petroleum eluted a ketonic fraction (63 mg.). Finally, pure ether eluted 1-adamantanol (227 mg.). TLC of the ketonic fraction separated the major component—adamantanone—from a minor unidentified component.

Hydrocarbons were also oxidized by passing ozonized oxygen through CCl_3F, CCl_3Br, and CCl_4 solutions at temperatures between $-20°$ and $0°C.$

cis- AND *trans*-9-HYDROXYDECALINS. Ozonized oxygen was bubbled through a stirred solution of Decalin (Harrington, 30 grams; 43.5% *trans*) in carbon tetrachloride (250 ml.) at 0°C. for 40 hours. Aromatic ozonides (which would be formed from Tetralin contaminating the Decalin) were removed as follows. Carbon tetrachloride (*ca.* 120 ml.) was evaporated at 21°–25°C./100 mm. The residue was stirred with aqueous hydrogen peroxide (2% w/v, 300 ml.) for 15 min. at 25°C. and for 30 min. at 60°C. Non-acidic products were obtained *via* ether, and distillation afforded unchanged Decalin and an oil (9.28 grams), b.p., 72°–76°C./0.07 mm., from which crystals separated after 20 hours at 18°C. The oil was drained off; recrystallization from light petroleum (boiling range 30°–40°C.) yielded *cis*-9-hydroxydecalin (501 mg.), m.p., 65°–66°C. Elution with light petroleum (b.p., 30°–40°C.) of the residue from aluminum oxide (Peter Spence Grade H, deactivated with 5% w/v of an aqueous solution, 10% w/v of acetic acid; 100 grams) gave ketones. Further elution gave solids (420 mg.) which, after recrystallization from light petroleum (benzene free, b.p., 20°–27°C.) at $-70°C.$ yielded *trans*-9-hydroxydecalin (370 mg.), m.p., 52.5°–53°C., then more of the *cis* isomer (1.93 grams), m.p., 63°C.

The assignment of these isomers was confirmed by nuclear magnetic resonance spectroscopy on a Perkin-Elmer 60 Mc./sec. NMR spectrometer, after removal of -OH by exchange with deuterium oxide. The spectrum of the *cis*-alcohol showed a single broad peak, while that of the *trans*-alcohol showed two peaks; they thus resembled the spectra of the corresponding hydrocarbons (8).

OXIDATION OF *cis*- AND *trans*-DECALIN. *trans*-Decalin (1.02 grams), *cis*-Decalin (1.14 grams) and *trans*-Decalin (1.38 grams) + *trans-cis-β*-decalol (1.54 grams) were dissolved in 25, 25, and 50 ml. of carbon tetra-chloride, respectively. Ozone was passed through each of the solutions for 20 hours, and the resultant solutions were treated with aqueous hydrogen peroxide (6%, 25 ml.) and with concentrated potassium hydrogen carbonate (25 ml.), dried (MgSO$_4$) and evaporated (Dufton column).

Table I. Oxidation of Decalin

Relative Product Concentrations

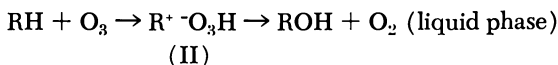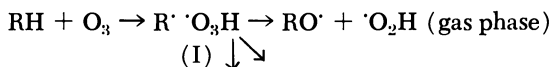|	T, °C.	Solvent	trans-9-ol	cis-9-ol	trans-1-one	cis-1-one	trans-2-one	cis-2-one
trans-Decalin	0	CCl$_4$	100	2	27	—	35	—
	−78	CH$_2$Cl$_2$	100	10	45	—	50	—
cis-Decalin	0	CCl$_4$	4	100	—	5	—	35

Gas-chromatographic analysis involved diglycerol (15%, 2 meters, 50°C.) as stationary phase. From *trans*-Decalin, peaks were *trans*-9-hydroxy-decalin ($\tau = 41$), *trans*-α-decalone ($\tau = 53$), and *trans*-β-decalone ($\tau = 74$); from *cis*-Decalin they were *cis*-α-decalone ($\tau = 30$), *cis*-β-decalone ($\tau = 55$) and *cis*-9-hydroxydecalin ($\tau = 100$). Retention times are relative; products were identified by comparison with authentic specimens, except for *cis*-α-decalone, where structure was assumed from retention time and analogy with the trans-series. Peak areas were obtained planimetrically. Relative product concentrations are given in Table I.

Discussion

Schubert and Pease (*11*) proposed a mechanism for isobutane oxidation in the gaseous state, in which the first stage
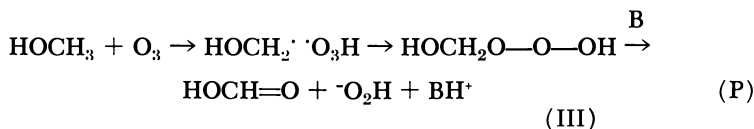
$$RH + O_3 \rightarrow RO^{\cdot} + {}^{\cdot}O_2H$$
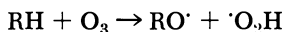
can hardly be elementary. It can be reformulated with a radical pair (I) or an ion pair (II) as an additional intermediate.

$$RH + O_3 \rightarrow R^{\cdot}\ {}^{\cdot}O_3H \rightarrow RO^{\cdot} + {}^{\cdot}O_2H \text{ (gas phase)}$$
$$\text{(I)} \downarrow \searrow$$
$$RH + O_3 \rightarrow R^{+}\ {}^{-}O_3H \rightarrow ROH + O_2 \text{ (liquid phase)}$$
$$\text{(II)}$$

In solution, rapid collapse with consequent high preservation of configuration replaces the complex sequence of changes observed by Schubert and Pease, and this led to an initial preference for intermediate (II). Use of bromotrichloromethane as a component of the solvent in the ozonation of adamantane, however, gave a product mixture which contained several new components—two having retention times correspond-

ing to 1-chloro- and 1-bromo-adamantane; thus, it seems probable that in oxidizing hydrocarbons in nonpolar media, short-lived radical pairs, capable of being intercepted by sufficiently reactive radical traps, are involved. Collapse of the radical pairs evidently gives mainly the alcohol plus oxygen, rather than a hydrotrioxide (Reaction P).

In seeking information about the second stage of the oxidation at secondary positions attention was turned to the ozonation of simple alcohols (Table II). Methanol gave a blue solution with ozonized oxygen; this faded rapidly, and on warming it was found to contain an equimolecular mixture of formic acid and hydrogen peroxide:

$$\text{HOCH}_3 + \text{O}_3 \rightarrow \text{HOCH}_2 \cdot \ \cdot\text{O}_3\text{H} \rightarrow \text{HOCH}_2\text{O}\!\!-\!\!\text{O}\!\!-\!\!\text{OH} \overset{\text{B}}{\rightarrow}$$

$$\text{HOCH}\!\!=\!\!\text{O} + \ ^-\text{O}_2\text{H} + \text{BH}^+ \qquad\qquad (\text{P})$$
$$(\text{III})$$

Performic acid was stable under the reaction conditions and hence was not an intermediate; formaldehyde and oxygen were formed in low yields (Table II). A hydrotrioxide intermediate (III) is almost a necessary postulate; the β-elimination which gives formic acid (Reaction P) and HO_2^- can of course be intramolecular. [Formation of such an intermediate (*see* additional evidence below) might indicate a different precursor from the radical pair (I)—*i.e.*, the ion pair (II), which is of course much more plausible in a polar solvent.] Infrared spectra determined at $-78°\text{C}$. gave no evidence that such a species as (III) could accumulate, however.

The oxidation of ethanol was decidedly faster than that of methanol, and the main products were acetic acid and hydrogen peroxide [molar ratio *ca.* 1:1.0 (Reaction P)]. Small yields of acetaldehyde, formaldehyde, and peracid and the evolution of small quantities of oxygen on warming the ozonized solution to $0°\text{C}$., suggested the incursion of side reactions Q and R (*see below*) (20% and 1–2% of the whole process), analogous to the oxidation reactions of propan-2-ol (Type B), which were much more fully investigated.

Ozonation of propan-2-ol gave results which varied with the history of the alcohol specimen used. All propan-2-ol specimens absorbed ozone readily at $-78°\text{C}$., the solution never becoming blue, and gave solutions which showed a weak infrared band at 1705 cm.$^{-1}$ (Figure 1), attributable (shown by comparison with authentic solutions) to either acetic acid or acetone or both. Addition of excess triethylamine reduced the intensity of this band by 60%, so most of it was evidently attributable to acetic acid; authentic specimens behaved similarly, the acetate ion absorbing at 1550–1600 cm.$^{-1}$. Titration at this stage showed the presence of substantial amounts of peracid, acid, and hydrogen peroxide, while gas chromatography (after warming to $20°\text{C}$.) indicated the presence of acetic acid

Table II.   Oxidation

Propan-2-ol (B)	Number of Runs	Relative	
		$CH_3COCH_3{}^c$	CH_3CHO
before warming after warming	3	100[b]	—
Propan-2-ol (A) before warming after warming	2	100[b]	—
Ethanol	1	—	27
Methanol	1	—	—

[a] Average values, taken from several similar experiments.
[c] Quoted concentrations were obtained by TLC.; in one experiment the corresponding GLC. estimate was 94 μmole/cc.

and methanol, the former in about the same amount as indicated by infrared spectroscopy.

The behavior of the solution thus obtained at −78°C. on warming to 0°C. depended on its history—*i.e.*, on its Type A/B character. If the character were Type B, oxygen was evolved in large quantity, and additional acetone was formed, as estimated by cooling to −78°C. and repeating the infrared examination, by gas chromatography, or by preparing and separating the 2,4-dinitrophenylhydrazones. No increase in the acid titer or hydrogen peroxide titer was observed, and the peracid titer fell slightly. Type A propan-2-ol evolved less oxygen on warming to 0°C. (varying from one specimen to another), but correspondingly the organic products were oxidized to acetic acid, and approximately 1 molecule of hydrogen peroxide was formed for each 2 molecules of oxygen not evolved. Type A propan-2-ol was simply the commercial product before or after fractional distillation; Type B was obtained by distillation from sodium borohydride; their relationship, and the possible nature of contaminants present, were not ascertained until after the symposium. Contrary to our preferred hypothesis then, type A proved to be pure, and Type B contained a contaminant; the simpler Type B behavior could be simulated by adding to Type A 2-propanol 2 p.p.m. or more (even 0.5 p.p.m. had a marked effect) of sodium borohydride as a solution in 2-propanol, which was not inactivated by heating with excess acetone, hence, it was probably present as sodium tetraisopropoxyboron. A similar quantity of sodium acetate was equally effective, but sodium perchlorate had no effect. We are currently investigating these phenomena. In the initial phase of the oxidation, the main process evidently involved is the formation of a compound, itself transparent at 1705 cm.$^{-1}$ but capable of yielding acetone, oxygen, and water on warming
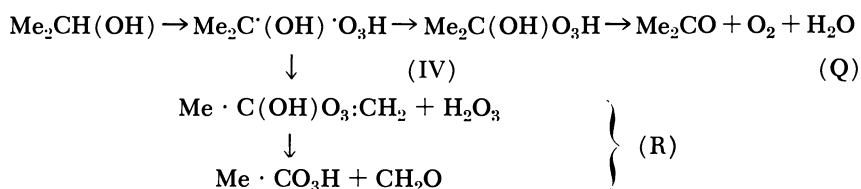
of Alcohols

Product Concentrations[a]

CH_2O	RCO_3H	RCO_2H	H_2O_2	O_2
17	11	11	18	71
	9	16	18	
16	14	8	18	27
	13	42	44	
2	2	100[b]	100	18
15	—	100[b]	93	10

[b] Values based on a concentration of 100 μmole/cc. of major product. Major products are formed at a rate of *ca.* 50 μmole/cc./hr.

(Reaction Q). Formation of water was apparent when filtered homogeneous trichlorofluoromethane solutions were warmed. Solids initially precipitated from these solutions appeared to be either hydrogen peroxide or a mixture of all other products aggregated with hydrogen peroxide. The acetone precursor was in fact shown to be more polar than acetone, as measured by distribution coefficient between trichlorofluoromethane and 80% methanol. Its decomposition rate, 2.3×10^{-3} sec.$^{-1}$ at 0°C., is comparable with that of di-*tert*-butyltrioxide (*1*); slow decomposition even at −78°C. is catalyzed by triethylamine. There is every reason for accepting the obvious formula (IV):

$$Me_2CH(OH) \rightarrow Me_2C^{\cdot}(OH) \cdot O_3H \rightarrow Me_2C(OH)O_3H \rightarrow Me_2CO + O_2 + H_2O$$
$$\downarrow \qquad (IV) \qquad\qquad\qquad (Q)$$
$$Me \cdot C(OH)O_3{:}CH_2 + H_2O_3$$
$$\downarrow \qquad\qquad\qquad\qquad \Big\} \ (R)$$
$$Me \cdot CO_3H + CH_2O$$

for this major intermediate, constituting some 80% of the initial reaction product. Its alternative mode of decomposition in Type A propan-2-ol is considered below.

Peracetic acid and formaldehyde are the expected ozonolysis products for acetone enol (*6*), and they are obtained in roughly equimolecular ratio. Infrared spectra cannot be used to identify them since peracetic acid in propan-2-ol absorbs at 1755 cm.$^{-1}$, coinciding with a minor solvent peak, while formaldehyde monomer would presumably exist as hemiacetal. Peracetic acid does not survive gas chromatography at 40°C. on a polypropylene oxide/glycerol condensate (GPO-50)–glutaric acid phase. However, the peracid titer partitioned between trichlorofluoro-

methane and 80% methanol in the same ratio (1:30) at −78°C. as authentic peracetic acid. Thus, it seems that acetone enol molozonide (V), if an intermediate, must break down even at −78°C. Acetone itself is not attacked at a significant rate by ozone at −78°C., but adding hydrogen chloride results in rapid reaction, presumably *via* the enol, and peracid is in fact found by titration. It seems plausible that an ion pair [II; R = Me₂C(OH)] might give acetone enol and hydrogen trioxide, and the corresponding radical pair (I) might also, or might undergo a redox reaction to give the ion pair. Once formed, acetone enol would be more likely to react with ozone than to ketonize. We therefore charac-
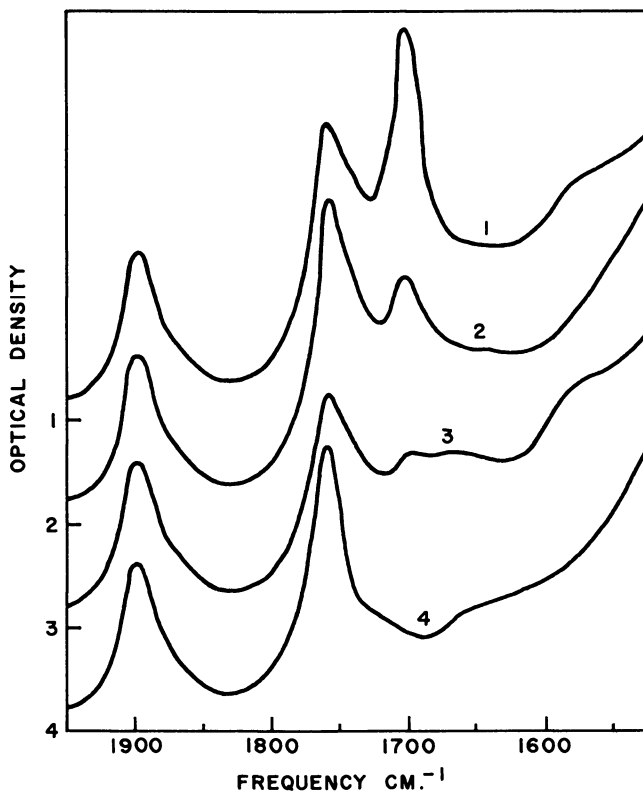
Figure 1.   Infrared spectra of propan-2-ol solutions

*Curve 1: Ozonized at −78°C., warmed to °C. and recooled to
            −78°C.; triethylamine added*
Curve 2: Ozonized at −78°C.
Curve 3: Ozonized at −78°C., triethylamine added
Curve 4: At −78°C. before ozonation
*Peak at 1900 cm.⁻¹ caused by propan-2-ol; that at 1760 cm.⁻¹
caused by propan-2-ol and peracetic acid; that at 1710 cm.⁻¹
caused by acetone and acetic acid. Triethylamine removes the
1710 cm.⁻¹ peak of acetic acid. Successive curves are displaced
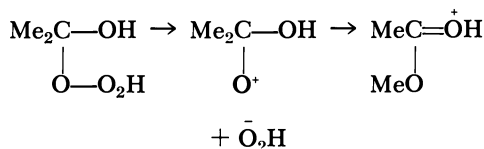   by one unit of optical density*

terize Reaction R as one main side reaction in the case of propan-2-ol, (and in the cases of cyclohexanol and cyclohexane which both yield peracid to an extent of *ca.* 10% of the over-all reaction) and attribute to it the small yields of peracid (performic) and formaldehyde observed in the case of ethanol.

In the oxidation of propan-2-ol substantial yields of hydrogen peroxide are obtained. In view of the reported instability of an intermediate believed to be hydrogen trioxide (*2, 3*), it seems unlikely that the titration for H_2O_2 at 20°C. actually represents H_2O_3; furthermore Reaction R produces H_2O_3, whose fate must now be considered. Fission to $HO\cdot$ and $\cdot O_2H$ seems probable even at low temperatures, and in 2-propanol some such sequence as

$$HO - O_2H \rightarrow HO\cdot + \cdot O_2H$$

$$HO\cdot + H \cdot CMe_2OH \rightarrow H_2O + \cdot CMe_2OH$$

$$\cdot CMe_2OH + \cdot O_2H \rightarrow HO_2 \cdot CMe_2 \cdot OH \rightarrow Me_2CO + H_2O_2$$
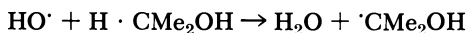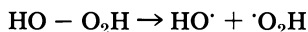
seems plausible in view of the differential reactivity of $HO\cdot$ and $HO_2\cdot$ (*4, 9, 10*). At any rate, Reaction S does rationalize the appreciable yield of hydrogen peroxide found by titration. No pinacol ($< 2\ \mu mole/cc.$) was found in the reaction products; hence, dimerization of α-hydroxylisopropyl is improbable.

The products least easily accounted for in the ozonation of Type B propan-2-ol are acetic acid and methanol. Methyl acetate could be formed easily:

$$\begin{array}{ccc} Me_2C\!-\!OH & \rightarrow\ Me_2C\!-\!OH\ \rightarrow & MeC\!\!=\!\!\overset{+}{O}H \\ | & | & | \\ O\!-\!O_2H & O^+ & MeO \\ & + \overset{-}{O}_2H & \end{array}$$

but, as expected, methyl acetate proved to be stable to the reaction conditions.

There remains the enigma of Type A behavior, as measured by the increase in H_2O_2 titer and acidity titer on warming and the diminution in oxygen evolution. Every specimen of propan-2-ol gave some oxygen on ozonation and warming, whereas Type B material consistently failed to form any additional acid and H_2O_2. We must therefore leave Reaction T in an incomplete state.

$$2\ HOMe_2C \cdot O_3H \rightarrow 2\ Me \cdot CO_2H + H_2O_2 + 2Y \qquad (T)$$
$$X$$
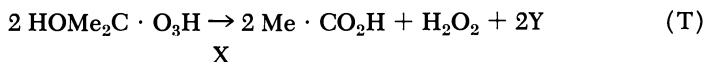
In trichlorofluoromethane, oxidation of *tert*-butyl alcohol proved to be much slower (factor $\not< 20$) than of 2-propanol. This eliminates from consideration mechanisms of oxidation in which an alkoxy radical is a necessary intermediate formed in the rate-determining stage (*4*).

Literature Cited

(1) Bartlett, P. D., Gunther, P., *J. Am. Chem. Soc.* **88**, 3288 (1966).
(2) Benson, S. W., *J. Am. Chem. Soc.* **86**, 3922 (1964).
(3) Czapski, G., Bielski, B. H. J., *J. Phys. Chem.* **67**, 2180 (1963).
(4) Dixon, W. T., Norman, R. O. C., *J. Chem. Soc.* **1963**, 3119.
(5) Durland, J. R., Adkins, H., *J. Am. Chem. Soc.* **61**, 429 (1939).
(6) Kwart, H., Hoffman, D. M., *J. Org. Chem.* **31**, 419 (1966).
(7) Ledaal, T., Bernatek, E., *Anal. Chim. Acta* **28**, 322 (1963).
(8) Musher, J., Richards, R. E., *Proc. Chem. Soc.* **1958**, 230.
(9) Norman, R. O. C., personal communication.
(10) Norman, R. O. C., Lindsay Smith, J. R., "Oxidases and Related Redox Systems," Vol. 1, p. 131, Wiley, New York, 1965.
(11) Schubert, C. C., Pease, R. N., *J. Am. Chem. Soc.* **78**, 2044, 5553 (1956).

RECEIVED April 1, 1968.

Discussion

M. C. Whiting: Two comments during the discussion require an answer. Our mechanism requires that the ozone molecule abstract a hydrogen atom from (*e.g.*) 2-propanol, breaking a bond with a strength of some 90 kcal. S. W. Benson quoted a bond strength of 10 kcal. for O_3-H and therefore categorically rejected our mechanism. He now agrees that the 10 kcal. estimate in fact applied to the energy of the process $O_3 + \frac{1}{2}H_2 \rightarrow \cdot O_3H$—*i.e.*, is low by some 55 kcal., and he gives a current, preferred estimate of 61 $\pm$ 2 kcal. (gas phase). Even allowing for solvation, this situation still presents a problem on which we are trying to shed more light. It is possible that a considerable upward revision of the rather indirectly calculated bond energy estimate may be justified.

Cheves Walling commented on the high chloride/bromide ratio obtained from adamantane $+ O_3 + CBrCl_3$, unusual in a radical-abstraction process. An even higher ratio has, however, been reported (J. I. G. Cadogan, D. H. Hey, and P. G. Hibbert, *J. Chem. Soc.* **1965**, 3939) for attack by a well-authenticated free radical in the presence of oxygen; hence, our interpretation of this reaction as proceeding *via* 1-adamantyl radicals stands.

The Mechanism of Alkane Oxidation by Ozone

GORDON A. HAMILTON, BRUCE S. RIBNER, and
THOMAS M. HELLMAN

Pennsylvania State University, University Park, Pa., 16802 and Princeton
University, Princeton, N. J. 08540

*The characteristics of the initial step in the reaction of
ozone with saturated hydrocarbons have been investigated.
Ozonation of cyclohexane gives initially cyclohexanol and
cyclohexanone in a 3:1 ratio. Cyclohexane is oxidized 4.5
times more rapidly than cyclohexane-d$_{12}$. The relative re-
activity of primary, secondary, and tertiary hydrogens is
approximately 1:13:110. The ozonation of tertiary hydrogens
to tertiary alcohols occurs with 60 to 70% retention of con-
figuration. The presence of good hydrogen atom donors,
antioxidants, and a number of other reagents has only a
small effect on the percent retention of configuration. These
results and others are compared with those obtained for
other hydrocarbon reactions, and a mechanism for the ozona-
tion is suggested.*

As a result of our interest in the mechanism of biological oxidations of saturated hydrocarbons (11), we have investigated the mechanisms of several alkane oxidations (12, 13). This paper reports our studies on the oxidation of saturated hydrocarbons by ozone. Although there are frequent references in the literature to the oxidation of alkanes by ozone (2), the mechanism of the reaction has received relatively little study. Durland and Adkins (7) reported that *cis-* and *trans-*Decalin are oxidized in reasonable yield to tertiary alcohols with retention of configuration. Schubert and Pease (24) studied the gas-phase ozonation of alkanes at room temperature and suggested that the products arose from the formation and further reactions of RO· and HOO·. A complicating feature in these investigations was the necessity to carry out the oxidation to relatively high conversions so that the products could be analyzed. Since

15

the initial alkane oxidation products are more reactive toward ozone than the alkane, the observed products frequently arise as the result of several steps. With the availability of sensitive gas chromatographic methods it is now possible to analyze for products after very low conversions, and thus the initial step in alkane ozonation can be studied separately. In our investigation, some of the characteristics of this initial step were determined.

Experimental

Materials. Unless described otherwise, commercial materials, which were usually redistilled and which were shown by gas chromatography to be either free of impurities or free of interfering impurities, were used throughout. Cyclohexane and 2-methylbutane were refluxed with lithium aluminum hydride before being distilled. *cis*-Decalin was obtained from Aldrich Chemical Company and *trans*-Decalin was obtained by isomerizing commercial Decalin with aluminum trichloride followed by fractional distillation (*14*). Gas chromatographic analysis indicated that there was less than 1% trans in the cis solvent and less than 2% cis in the trans solvent. Cyclohexane-d_{12} was obtained from Nuclear Equipment Chemical Corp. and had 99.3% deuterium.

Cis- and *trans*-1,2-dimethylcyclohexanol-1 were prepared by J. R. Giacin by the method of Chiurdoglu (*6*) and isolated by the procedure of Nevitt and Hammond (*20*). The *cis*-alcohol was not obtained pure but as a mixture of cis and trans. The composition of the mixture was determined by a combination of gas chromatography and nuclear magnetic resonance. The *cis*- and *trans*-9-decalols were prepared by J. R. Giacin by oxidizing the corresponding hydrocarbons with chromic anhydride in acetic acid–acetic anhydride by the method of Lehr (*16*). The crude products were purified by alumina chromatography followed by sublimation. Samples of the isomeric norboranols and norbornanones were obtained from Paul von R. Schleyer.

Reaction Conditions. The ozone–oxygen mixture used in these reactions was obtained from either a Welsbach T-23 or T-408 Laboratory Ozonator. When pure oxygen was fed into the ozonator at the rate of 0.6 liter/min., the effluent was *ca.* 5% ozone as determined by iodometric titration. A small fraction of this stream giving 0.5–1 mg. of ozone per minute was bubbled through 2–10 ml. of hydrocarbon solvent contained in a small flask fitted with a cold finger condenser (to minimize solvent evaporation). Most of our results were obtained from competition experiments either with known mixtures of solvents or with compounds which can react to give several products. In a few experiments the total yield of cyclohexanol and cyclohexanone obtained from the oxidation of cyclohexane at room temperature was estimated to be 0.2 to 0.3 mg./min.

In cases where the reaction solutions were reduced following oxidation, the solution was diluted with *ca.* 50 ml. ether, an excess (0.15 gram) of lithium aluminum hydride was added, the mixture refluxed for 2 hours and then cooled, 0.4 ml. saturated solution of sodium sulfate was added, the resulting suspension was filtered, the ether was distilled off until 5–10 ml. remained, and this solution was injected into the gas chromatograph

for analysis. In controls where known amounts of products were present, essentially all the carbonyl compounds were reduced to alcohols, and over 95% of the alcohols were recovered by this procedure.

Analyses. The oxidation products were determined using a Perkin-Elmer model 800 gas chromatograph equipped with flame ionization detectors. In the competition experiments the relative amounts of material were calculated by multiplying either the peak heights or peak areas by conversion factors determined using known amounts of the products. Preliminary experiments indicated that peak heights or peak areas gave the same amounts of materials when multiplied by the appropriate conversion factors. Perkin-Elmer 12-foot columns packed with Chromosorb W and containing the liquid phases polypropylene glycol (Perkin-Elmer designation R) and fluorinated silicone oil (Perkin-Elmer designation FS-1265) gave convenient separations. The last liquid phase was used for the decalol determinations, and the first was used for all others. Usually a small sample (1–2 μliters) of the reaction solution was injected directly into the gas chromatograph for analysis. However, to ensure that other products were not affecting the stereospecificity experiments, representative samples of the various systems studied were reduced with lithium aluminum hydride before analysis. The ratios of tertiary alcohols obtained following reduction were altered only slightly in a few cases, apparently because some ketonic products were eluted from the column at the same time as the tertiary alcohols. In such cases the results quoted are those obtained after reduction.

Results

Following ozonation of cyclohexane for short periods at room temperature, only two oxidation products—cyclohexanol and cyclohexanone—were observed in significant amounts on gas chromatographic analysis. Possibly some much less volatile products (*e.g.*, ring fragmentation products, *vide infra*) were also formed but not detected by the gas chromatographic procedure. After 5 minutes of ozonation the ratio of cyclohexanone to cyclohexanol was 0.3 to 0.35, but the ratio rapidly increased to 1.5 to 2 after 1 hour. The result indicates that even after very low conversion the initially formed cyclohexanol is oxidized further by ozone (2). Confirmation of this was obtained when a small amount (20 mg.) of cyclohexanol was added to 10 ml. of cyclopentane and the solution was ozonized under the usual conditions. Some cyclopentanol and cyclopentanone were formed, but in addition, over 80% of the cyclohexanol was oxidized to cyclohexanone after 1 hour. However, not all the cyclohexanone obtained in the cyclohexane ozonation arises from further oxidation of cyclohexanol. If the observed ratio of cyclohexanone to cyclohexanol is plotted *vs.* time, and the curve is extrapolated to zero time, one obtains a ratio at time zero of 0.25 to 0.3. This indicates that some of the cyclohexanone is formed directly from an intermediate in the ozonation.

Cyclohexanone is oxidized further only slowly under our ozonation conditions. Ozonation of 30 mg. of cyclohexanone in 7 ml. of cyclopentane for 1 hour led to the oxidation of only 10% of the cyclohexanone. The oxidation of cyclohexane requires the presence of ozone; control experiments, where unozonized oxygen was passed through the cyclohexane with all other conditions the same, gave no detectable amounts of oxidation products.

The kinetic deuterium isotope effect for the reaction of cyclohexane with ozone was obtained from the competition experiments summarized in Table I. Since the solvent is in large excess, the ratio k_H/k_D was calcu-

Table I.   Deuterium Isotope Effect for the Ozonation of Cyclohexane at 22°C.

Ozonation Time, min.	Solvent Composition, mole %	Molar Ratio of Cyclohexane to Cyclopentane Products	$\dfrac{k_H}{k_D}$
20	Cyclohexane (50%) Cyclopentane (50%)	0.94	
20	Cyclohexane-d_{12} (50%) Cyclopentane (50%)	0.21	4.5
50	Cyclohexane (50%) Cyclopentane (50%)	1.10	
50	Cyclohexane-d_{12} (50%) Cyclopentane (50%)	0.27	4.1

lated by simply dividing the molar ratio of cyclohexane to cyclopentane oxidation products obtained with cyclohexane present by that obtained with cyclohexane-d_{12} after the same ozonation time. It is not known why the ratio of products increases slightly or why the apparent isotope effect decreases slightly with time. Perhaps it is caused by different rates for the further oxidation of the initial oxidation products. Nevertheless, it is clear that there is a sizeable isotope effect for the ozonation reaction, and k_H/k_D is probably between 4.5 and 5 for very low conversions when further oxidation of the products would have a minimal effect.

The reactivity of ozone toward primary, secondary, and tertiary hydrogens was determined from experiments where 2-methylbutane was ozonized. These experiments were performed at 0°C. to decrease solvent loss by evaporation during ozonation. To simplify the analysis of the products, the reaction mixture following ozonation was reduced with lithium aluminum hydride. The relative reactivity per hydrogen, calculated from the observed quantities of the four isomeric C_5 alcohols, is: primary, 1; secondary, 13; tertiary, 110. These values are time independent for up to 1 hour ozonation. However, they may not be a com-

pletely accurate measure of the reactivity of the various hydrogens because some fragmentation products, including ethanol, 2-propanol, and other minor products, were also observed. These fragmentation products were formed in smaller quantities than the C_5 alcohols, and they could not alter the relative reactivities quoted by more than 25%. Thus, the relative yields of the C_5 alcohols (following reduction with lithium aluminum hydride) should be a fairly good measure of the relative reactivities of the various hydrogens.

The stereospecificity of the hydrocarbon ozonation was investigated by measuring the isomer distribution of tertiary alcohols formed on ozonating *cis*- and *trans*-1,2-dimethylcyclohexane and *cis*- and *trans*-Decalin. Other oxidation products are formed in these ozonations, but the tertiary alcohols are easily separated from these by gas chromatography. Some results are shown in Table II. The observed isomer distributions of tertiary alcohols are independent of time for up to 3 hours ozonation

Table II. Isomer Distribution of Tertiary Alcohols from the Ozonation of *cis*- and *trans*-Hydrocarbons

Hydrocarbon Solvent	Isomer Distribution of Hydrocarbon Solvent, %		T, °C.	Isomer Distribution of Tertiary Alcohols, %	
	cis	*trans*		*cis*	*trans*
DMC[a]	100	0	22	85	15
	100	0	−48	91	9
	0	100	22	21	79
	0	100	−48	20	80
	68	32	22	78	22
	26	74	22	59	41
Decalin	100	0	22	85	15
	100	0	0	85	15
	0	100	22	20	80
	0	100	0	29	71
	62	38	22	79	21
	36	64	22	68	32

[a] 1,2-Dimethylcyclohexane.

and are reproducible to ±2%. Clearly the formation of tertiary alcohols occurs with considerable but not complete retention of configuration (earlier results by others (7, 17) with less sensitive analytical procedures indicated almost complete retention of configuration). The observation that temperature has such little effect on the isomer distribution suggests that it is unlikely that the lack of complete stereospecificity is caused by two distinctly different mechanisms operating simultaneously. Because the *cis*- and *trans*-hydrocarbons give different ratios of tertiary alcohols it is possible to determine the relative reactivity of the tertiary positions of these hydrocarbons by using known mixtures of the hydrocarbons. From

the results in Table II one calculates that the tertiary positions on *cis*-1,2-dimethylcyclohexane are four times more reactive than those of *trans*-1,2-dimethylcyclohexane. Assuming that the axial tertiary hydrogen of the cis compound has the same reactivity as each of the axial tertiary hydrogens of the trans compound (*8*), one calculates that the equatorial tertiary hydrogen is seven times more reactive than axial ones. Similarly, the tertiary hydrogens of *cis*-Decalin are 5.6 times more reactive than those of *trans*-Decalin.

The effect of various additives on the isomer distribution of tertiary alcohols, obtained from *cis*-1,2-dimethylcyclohexane, was investigated to determine the reason for the lack of complete stereospecificity in the ozonation. The results are summarized in Table III. None of the addi-

Table III.   Isomer Distribution of Tertiary Alcohols from the Ozonation of *cis*-1,2-Dimethylcyclohexane at 22°C. in the Presence of Various Additives

	Solvent Composition, mole %		Isomer Distribution of Tertiary Alcohols from cis-DMC, %	
Additive	Additive	cis-DMC	cis	trans
None	0	100	85	15
Cumene	12	88	85	15
Chloroform	62	38	85	15
Nitrobenzene	56	44	85	15
Benzophenone	9	91	82	18
Ethyl acetate	57	43	79	21
2,4-Di-*tert*-butylphenol	9	91	73	27
Diphenylamine	8	92	70	30
Iodine	7	93	70	30
Bromotrichloromethane	16	84	80	20

tives has a dramatic effect. Some of the results may arise from a general solvent effect which requires further investigation. However, since none of the additives increases the stereospecificity of the ozonation, several mechanisms which might have explained the partial loss of stereospecificity can be eliminated (*see* Discussion).

Long (*17*) observed that ozonation of norbornane (bicyclo-2,2,1-heptane) in CCl$_4$ at 0°C. gives only *exo*-2-norbornanol and 2-norbornanone. We have confirmed this result using cyclohexane as solvent and gas chromatography for analysis; less than 2% of any other alcohol or ketone is formed. *Endo*-2-norbornanol could not have been formed initially and then rapidly oxidized to 2-norbornanone. In a control experiment 6 mg. of *endo*-2-norbornanol were added to 1.7 grams norbornane in 8 ml. of cyclohexane and ozonized for 95 minutes. Then, 75% of the *endo*-2-norbornanol was oxidized. Thus, it is oxidized under the reaction condi-

tions, but this reaction is slow enough that if 2% of the oxidation products were this compound, it could have been detected. By comparing the yields of norbornane oxidation products with those obtained from cyclohexane, and knowing the initial solvent composition, one can calculate that per hydrogen the exo hydrogens of norbornane are only 1.3 times more reactive than the hydrogens of cyclohexane.

Some peroxides are formed when saturated hydrocarbons are ozonized at room temperature. For example, when 1.07 mmoles of ozone are bubbled (during 2 hours) into 8 ml. of *cis*-1,2-dimethylcyclohexane, 0.26 mmoles of ozone passes through the solution, and 0.31 mmoles peroxide [determined by iodometric titration (25)] is formed in the hydrocarbon solvent. The identity of these peroxides has not yet been determined.

Discussion

Table IV compares some of the characteristics of the ozonation reaction with those of some other hydrocarbon reactions whose mechanisms have been studied extensively. The ozonation reaction resembles free radical reactions, such as the abstraction of hydrogen atoms by $\cdot O—C(CH_3)_3$ and the carbene-oxygen oxidation (12), in its selectivity

Table IV.   Comparison of Some Hydrocarbon Reactions

Reaction	Relative Reactivity per H			% Retention of Configuration	Deuterium Isotope Effect(k_H/k_D)	Reference
	prim	sec	tert			
Ozonation	1	13	110	70	4.5	This work
Chromate oxidation	1	110	7,000	70–100	2.5	16, 19, 28
Carbene insertions	1 (1)	1.0 (8)	1.2 (21)	100	1.3 to 2	15
Nitrene insertions	1	10	30	100	1.5	1, 5, 18
H abstraction by $\cdot O—C(CH_3)_3$	1	12	44	0	3.7	23, 26
Carbene-oxygen oxidation	1	15	140	0	4.6	12

toward various hydrogens and in its deuterium isotope effect. It is clear that the transition state for the ozonation reaction in alkane solvents cannot have much carbonium ion character; otherwise its selectivity would be much greater. The observation that the exo hydrogens of norbornane do not have any special reactivity agrees with this conclusion. Also, the transition state for the chromate oxidation of alkanes is believed

to have only partial carbonium ion character (*22*), and yet its selectivity is much greater.

The high degree of retention of configuration is different from that usually observed for free radical reactions. In the ozonation experiments, oxygen was present at approximately 1 atm., and alkyl radicals react with oxygen to give alcohols and ketones (*21*). However, only racemized alcohol is formed when such radicals are generated by other methods in the presence of an atmosphere of oxygen (*3, 12*). Thus, it is evident that most of the ozonation reaction cannot proceed through "free" free radical intermediates, and the alcohol with retention of configuration must be formed by some direct reaction of ozone with the hydrocarbon. The observed retention of configuration is similar to that obtained in carbene and nitrene insertion reactions. Therefore, an insertion reaction whose transition state has considerable radical character is the mechanism for the *initial* step of the ozonation which is in best agreement with the data. The details of the steps leading to the formation of racemized alcohol, ketone, peroxide, and fragmentation products are not completely clear at this time. However, some possibilities for the over-all mechanism are outlined in the reaction scheme below. It is suggested that the alkane and

$$R\text{—}H \;+\; O_3 \;\longrightarrow\; [I] \;\longleftarrow\; [II]$$

I

II

$$R\cdot \;+\; HO\cdot \;+\; O_2$$

$$ROH \;+\; O_2 \;\longleftarrow\; ROOOH$$

(retention of configuration)

$$\Big\downarrow O_2$$

$ROH\cdot$ (racemized) + ketone + peroxides + fragmentation products
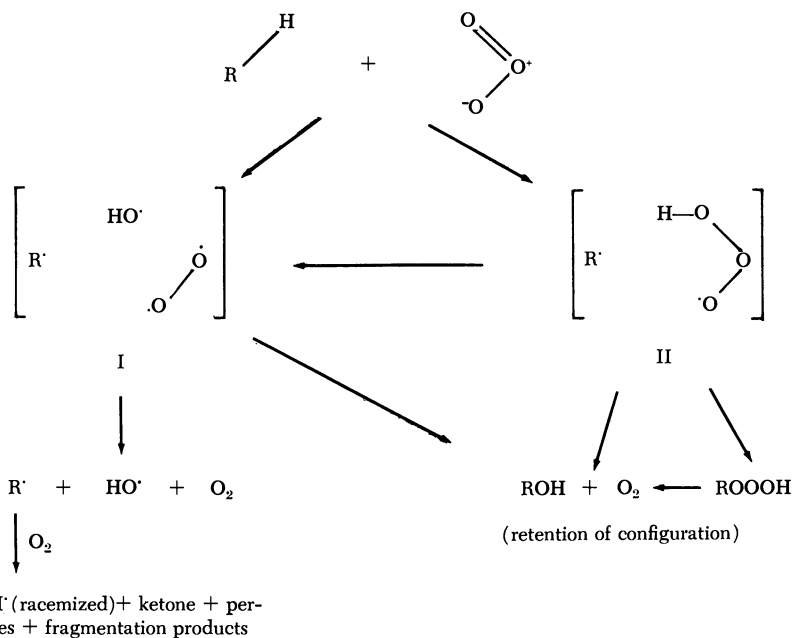
ozone react to give a transition state (or solvent caged intermediate), I or II, which has considerable radical character. If there is no partial bonding among the various radicals of I and II, then thermodynamic

considerations (*4*) indicate that I is more likely than II. However, if the R· radical is partially bonded to an oxygen species either I or II seem possible. Retention of configuration in the alcohol product would be expected if I or II collapsed directly to alcohol and oxygen (II possibly reacting with ROOOH as an intermediate (*27*)). To account for the formation of some racemized alcohol, ketone, peroxides, and fragmentation products, it is suggested that I and II can also separate into the radicals R· and HO·. Alkyl radicals are known to react with oxygen in a series of steps to give these other product (*21*).

Mechanisms for the formation of racemized alcohol, which involve the RO· radical's abstracting a hydrogen atom from the alkane as, for example, in the following sequence:

ROOOH → RO· + HOO·

RO· + RH → R· + ROH (retention)

R· + O$_2$ → ROH (racemized) + ketone + peroxides + fragmentation products
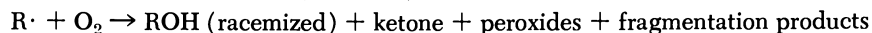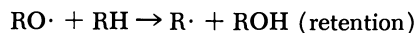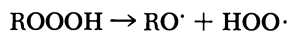
are not consistent with the stereospecificity experiments with various additives (Table III). Many of the additives would have trapped the RO· radicals, and thus no R· radicals would be formed and the percent retention of configuration would have increased. This is the opposite of that observed. If some of the additives could trap the R· radicals, then by either of the above mechanisms the percent retention of configuration should increase. However, oxygen would probably react too rapidly with R· for it to be trapped by other species.

The results reported here could also be explained if ozone or an intermediate such as I or II could exist in a singlet and a triplet form. The products with retention of configuration would then arise from the singlet species and the racemized products from the triplet. Some of the results with additives are consistent with this hypothesis: the decreased percent retention of configuration with some additives could be caused by catalysis of singlet to triplet interconversions. Clearly more experimental results are necessary to clarify this point.

Regardless of the nature of the subsequent steps in the reaction, it seems clear from the results here that the initial step in the oxidation is an insertion type reaction in which the transition state has radical character. Because the selectivity of ozone is greater than that of other insertion species (carbenes and nitrenes), it is possible to specify the characteristics of intermediates or transition states (such as I or II) to a greater extent. However, it should not be concluded that all ozone reactions necessarily proceed by such a mechanism. In other cases where ionic intermediates are more favored (*e.g.*, in more polar solvents or in cases where carbonium ions are more stable) it is possible that the transition state for the reaction has more polar character (*9, 10, 27*).

Enzymic hydroxylations of saturated hydrocarbons, which apparently involve the insertion of an oxygen to give alcohols with retention of configuration, could presumably occur by a mechanism similar to that proposed for the ozonation reaction. In the enzymic reactions oxygen is the oxidant, and the over-all mechanism is clearly more complicated than that for ozonation (11). However, in these reactions possibly some complexed form of oxygen is capable of abstracting hydrogen atoms and then donating a hydroxyl radical before the alkyl radical has an opportunity to invert. The over-all reaction would be an insertion reaction (11), but the transition state could have radical character, as observed for the ozonation reaction.

Acknowledgments

Literature Cited

(1) Anastassiou, A. G., Simmons, H. E., *J. Am. Chem. Soc.* **89,** 3177 (1967).
(2) Bailey, P. S., *Chem. Rev.* **58,** 925 (1958).
(3) Bartlett, P. D., Pincock, R. E., Rolston, J. H., Schindel, W. G., Singer, L. A., *J. Am. Chem. Soc.* **87,** 2590 (1965).
(4) Benson, S. W., *J. Am. Chem. Soc.* **86,** 3922 (1964).
(5) Breslow, D. S., Prosser, T. J., Marcantonio, A. F., Genge, C. A., *J. Am. Chem. Soc.* **89,** 2384 (1967).
(6) Chiurdoglu, G., *Bull. Soc. Chim. Belges.* **47,** 241 (1938).
(7) Durland, J. R., Adkins, H., *J. Am. Chem. Soc.* **61,** 429 (1939).
(8) Eliel, E. L., "Stereochemistry of Carbon Compounds," p. 211, McGraw-Hill, New York, 1962.
(9) Erickson, R. E., Bakalik, D., Richards, C., Scanlon, M., Huddleston, G., *J. Org. Chem.* **31,** 461 (1966).
(10) Erickson, R. E., Myszkiewicz, T. M., *J. Org. Chem.* **30,** 4326 (1965).
(11) Hamilton, G. A., *J. Am. Chem. Soc.* **86,** 3391 (1964).
(12) Hamilton, G. A., Giacin, J. R., *J. Am. Chem. Soc.* **88,** 1584 (1966).
(13) Hamilton, G. A., Workman, R. J., Woo, L., *J. Am. Chem. Soc.* **86,** 3390 (1964).
(14) Jones, R., Linstead, R., *J. Chem. Soc.* **1936,** 616.
(15) Kirmse, W., "Carbene Chemistry," Academic Press, New York, 1964.
(16) Lehr, R., Senior Thesis, Princeton University, Princeton, May, 1965.
(17) Long, Jr., W. P., Ph.D. Thesis, Harvard University, 1955.
(18) Lwowski, W., Maricich, T. J., *J. Am. Chem. Soc.* **87,** 3630 (1965).
(19) Mareš, F., Roček, J., *Collection Czech. Chem. Commun.* **26,** 2370 (1961).

(20) Nevitt, T., Hammond, G., *J. Am. Chem. Soc.* **76,** 4124 (1954).
(21) Pryor, W. A., "Free Radicals," McGraw-Hill, New York, 1966.
(22) Rocek, J., *Tetrahedron Letters* **1962,** 135.
(23) Russell, G. A., *J. Am. Chem. Soc.* **79,** 3871 (1957).
(24) Schubert, C. C., Pease, R. N., *J. Am. Chem. Soc.* **78,** 2044 (1956).
(25) Wagner, C. D., Smith, R. H., Peters, E. D., *J. Anal. Chem.* **19,** 976 (1947).
(26) Walling, C., Thaler, W., *J. Am. Chem. Soc.* **83,** 3877 (1961).
(27) White, H. M., Bailey, P. S., *J. Org. Chem.* **30,** 3037 (1965).
(28) Wiberg, K. B., Foster, G., *J. Am. Chem. Soc.* **83,** 423 (1961).

61

Substituent Effects in the Oxidative Cleavage of Organosilanes by Ozone

J. D. AUSTIN[1] and L. SPIALTER

Aerospace Research Laboratories, Wright-Patterson AFB, Ohio

Ozone reacts readily at room temperature with compounds of general formula R_3SiH to give the corresponding silanol R_3SiOH. No evidence of a peroxidic product—e.g., R_3SiOOH, was obtained. The effect of varying R on the rate of reaction was studied, and a plot of k_{rel} against Taft σ^* constants gave a reasonably straight line with a ρ^* of −0.40. The evidence is consistent with electrophilic attack by ozone involving the insertion of one oxygen only into the Si—H bond via *a three-centered transition state.*

Although the reaction of ozone with carbon compounds has been investigated extensively, little is known about the reaction of ozone with silicon compounds. Barry and Beck (*3*) reported that compounds containing an Si—H bond react with ozone, but they gave no further details.

Ozone has been found to cleave Si-X bonds, where X = silicon, alkyl, aryl, hydroxyl and alkoxyl, to give siloxanes as major products (*10, 11*).

We have now studied the cleavage of an SiH bond in R_3SiH, where R = alkyl or alkoxyl.

Experimental

Ozone was produced by a Welsbach T-23 Ozonizer, and the reagent referred to as ozone here was a 4% solution of ozone in oxygen.

Organosilanes were obtained from Pierce Chemical Co. or were prepared by conventional routes—*e.g.*, by coupling a Grignard or lithium reagent with a chlorosilane. Tris(1-perhydronaphthyl)silane was prepared as described below. All compounds were at least 98% pure as determined by vapor-phase chromatography (VPC).

Tris(1-perhydronaphthyl)silane. Tris(1-naphthyl)fluorosilane (5 grams) was hydrogenated by a procedure described earlier (*4*) using a 5% rhodium/charcoal catalyst. Methylcyclohexane (150 ml.) was used

[1] Present address: Research Department, Dow Corning Corp., Midland, Mich. 48640.

as a solvent, and the reaction was carried out at 125°C. for 48 hours under 2000 p.s.i.g. hydrogen to give tris(1-perhydronaphthyl)fluorosilane (4.8 grams) m.p., 190°–192°C. Analysis: calculated for $C_{30}H_{51}SiF$: C, 78.61; H, 11.13; F, 4.15. Found: C, 78.37; H, 11.04; F, 3.94.

Reduction of the fluorosilane by lithium aluminum hydride in refluxing butyl ether gave tris(1-perhydronaphthyl)silane (3.5 grams) m.p., 194°–196°C. Analysis: calculated for $C_{30}H_{52}Si$: C, 81.83; H, 11.81; Si, 6.36. Found: C, 81.59; H, 11.65; Si, 6.03.

Reaction between R_3SiH and Ozone. In a typical experiment ozone was bubbled into triethylsilane (5 grams) at room temperature. An exothermic reaction occurred, and after about 30 minutes, VPC indicated that no triethylsilane remained. The reaction product was distilled to give triethylsilanol (b.p., 153°–154°C.) in 95% yield.

Competition between Two Silanes Containing Si—H for Ozone. The silanes studied included triethylsilane, tri-*n*-butylsilane, tri-*n*-hexylsilane, tricyclohexylsilane, *tert*-butyldicyclohexylsilane, tris(1-perhydronaphthyl)-silane, dimethyl(3,3,3-trifluoropropyl)silane and tris(3,3,3-trifluoropropyl)silane.

The general procedure involved making a solution of two silanes (*e.g.*, triethylsilane and tri-*n*-butylsilane) in hexane, the hexane being unsaturate free. The quantity of each silane was *ca.* 1 mmole in 25 ml. of hexane. A saturated hydrocarbon which had a retention time on a gas chromatography column between the retention times of the two silanes involved in the competition reaction was used as a standard—*e.g.*, between triethylsilane and tri-*n*-butylsilane decane was used. All the hydrocarbon standards used were inert to ozone under the experimental conditions.

It was found that −10°C. was a suitable temperature for following the cleavage reaction kinetically. This relatively low temperature also minimized loss of silane by evaporation during the passage of the ozone stream through the reaction solution. The ozone stream was passed through hexane at −10°C. before passing into the reaction solution so as to eliminate any change in concentration of the silane in the reaction solution by loss of solvent.

Samples were taken from the reaction mixture at appropriate time intervals and analyzed by VPC. The amount of silane present was determined by taking the ratio of peak height (or area) of silane to that of the standard. For every sample, three measurements for the amount of silane in solution were taken and were generally accurate to within ±5%. The results obtained are discussed below.

Reaction of Tricyclohexylsilane with Ozone. A solution of tricyclohexylsilane in pentane reacted with ozone at room temperature to precipitate tricyclohexylsilanol in good yield (> 95%). The reaction was carried out at various temperatures ranging from 20° to −60°C. In each case the solvent was removed under reduced pressure at the reaction temperature, and the residue was treated with faintly acidic, aqueous alcoholic potassium iodide. No iodine was liberated, indicating the absence of peroxide.

Reaction with Oxygen. Under the experimental conditions, pure oxygen alone did not cause any of the above reactions to occur even after three- to fivefold reaction times.

Results and Discussion

The Si-H bond is readily cleaved at room temperature to give the corresponding silanol. If ozonization is continued, the dehydration product, a disiloxane, is obtained (*10*).

Tricyclohexylsilane reacted with ozone at temperatures ranging from 20° to −60°C., but in no case could any peroxide be detected after removing the solvent at the reaction temperature.

It has recently been reported (*5*) that triarylsilyl hydroperoxides and trialkyl hydroperoxides, such as tri-*n*-hexylsilane, are quite stable and may be stored indefinitely at room temperature. However, such hydroperoxides do tend to disproportionate to hydrogen peroxide and bis(trialkylsilyl)peroxide—*e.g.*, (*7*).

$$2 \, Me_3SiOOH \rightarrow (Me_3SiO)_2 + H_2O_2$$
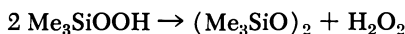
Since we could detect no peroxide as product in the ozonization of tricyclohexylsilane, it is reasonable to conclude that no tricyclohexylsilyl peroxide is formed either as a stable intermediate or as an intermediate which decomposes in a way analogous to the decomposition of trimethylsilyl hydroperoxide described above. The reaction is therefore more likely to proceed through a transition state of Type I rather than II since the former should lead to the observed product, tricyclohexylsilanol,
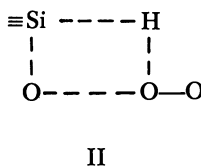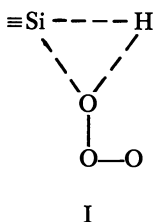
whereas II should produce tricyclohexyl silylperoxide. A similar three-centered transition state was proposed for the cleavage of a silicon-silicon bond by ozone (*11*). In this case only hexaalkyldisiloxane $(R_3Si)_2O$ and no bis(trialkylsilyl)peroxide $(R_3SiO)_2$ was observed as the reaction product.

A series of competition reactions was run to determine how the reactivity of the Si-H bond in R_3SiH toward ozone varied with R. The VPC of the crude reaction product indicated the presence of only the corresponding silanol and disiloxane. The latter could have been produced by dehydration of the silanol by ozone (*11*). In no case was any compound observed which could have been produced by the cleavage of a silicon-alkyl bond. Thus, the disappearance of silane is caused entirely by reaction of the Si-H bond. It is possible that various alcohols

and acidic products could be formed by the reaction of ozone with the hydrocarbon solvent, leading to acid-catalyzed solvolysis of the Si-H bond. This possibility would seem to be ruled out since the observed relative rates of reactivity of SiH with ozone are in the inverse order of the acid-catalyzed solvolysis (2).

If it is assumed that the reaction rate of all the silanes with ozone is first order in silane and that the order with respect to ozone is the same for all silanes, then the relative rates of reaction may be calculated from (8)

$$k_{rel} = \frac{k}{k'} = \frac{\ln a/a - x}{\ln \dfrac{a'}{a' - x'}}$$

where a and a' are the initial concentrations of the two silanes in competition and $(a - x)$ and $(a' - x')$ are the concentrations at the appropriate time interval. The value for k_{butyl} varied between 134 and 142 up to 76% reaction, indicating that the reaction is indeed first order in silane.

Competition reactions at −10°C. were run for various silanes, and the relative rates are given in Table I.

Table I.   Relative Rate Constants for Reactions of Silanes

R_3SiH	k_{rel}
$(C_2H_5)_3SiH$	100
$n\text{-}(C_4H_9)_3SiH$	119
$n\text{-}(C_6H_{13})_3SiH$	127
$(C_6H_{11})_3SiH$	270
$tert\text{-}C_4H_9(C_6H_{11})_2SiH$	261
$(C_{10}H_{17})_3SiH$	428
$(CF_3CH_2CH_2)_3SiH$	44
$(CF_3CH_2CH_2)(CH_3)_2SiH$	63
$(C_2H_5O)_3SiH$	24

For triethoxysilane the product was not identified, and it is likely that some silicon-ethoxy cleavage occurred (10, 11). Therefore, the value of 24 for triethoxysilane is a maximum, and the relative rate of cleavage of the silicon-hydrogen bond is probably even lower.

The accuracy of k_{rel} within a given run was about ±5%. The reproducibility of k_{rel} improved considerably when following reactions of higher boiling silanes and is probably caused by less silane being volatilized during the passage of ozone.

Table I shows that the reaction rate of R_3SiH decreases with the introduction of electron-withdrawing groups—*e.g.*, 3,3,3-trifluoropropyl and ethoxy, although the total variation in rate is small. There is a marked increase in going from the primary tri-*n*-hexylsilane to the secondary tricyclohexylsilane. This increase may be associated with the

greater electron-donating power of cyclohexyl (*13*) than *n*-hexyl. Steric factors are probably important also in view of the enhanced rate of the sterically crowded tris(1-perhydronaphthyl)silane. This requires, of course, some form of steric acceleration.

Although it is difficult to separate the steric and electronic effects of R in R_3SiH, it is noteworthy that the rate of cleavage of silicon-ethyl by ozone is faster in tetraethylsilane than in triethylmethylsilane (*11*). Thus, in R_3Si-alkyl, an increase in the rate of Si-alkyl cleavage is observed by increasing the electron-donating power of R and by increasing the size of R.

The variation in reactivity of the Si-H bond toward ozone is small, although this would seem to be characteristic of Si-H compounds—*e.g.*, in the acid-catalyzed hydrolysis k_{rel} for $Et_3SiH:n$-Bu_3SiH is 100:59 (*6*).

The relative reaction rates of R_3SiH are also consistent with electrophilic attack by ozone. Ozone has been regarded as an electrophile or a nucleophile (*1*), but the fact that electron-withdrawing groups decrease the rate of reaction would indicate that electrophilic attack is involved.

Figure 1 shows a plot of k_{rel} against Taft's σ^* constants (*13*); the slope (ρ^*) is −0.40. Such a low value might indicate that the reactions were run near the isokinetic temperature. However, k_{rel} for Et_3SiH:-$(CF_3CH_2CH_2)_3SiH$ at −60°C. was 100:55 compared with 100:63 at −10°C., which would indicate that genuine substituent effects are being observed and that the reaction involves electrophilic attack by ozone.

A possible reaction scheme is:

$$R_3SiH + O_3 \longrightarrow \overset{\delta+}{R_3Si} \text{———} \overset{\delta-}{H} \longrightarrow R_3SiOH + O_2$$
$$:O$$
$$|$$
$$O_2$$
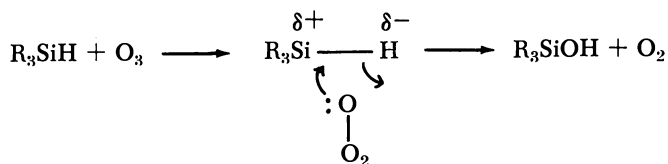
This is essentially an insertion reaction with the electrophilic attack by ozone on the hydridic hydrogen being assisted by coordination to the silicon, possibly using the silicon 3*d* orbitals.

Another scheme which would lead to the observed product R_3SiOH (and not R_3SiOOH) was suggested by a referee:

$$R_3SiH + O_3 \longrightarrow \overset{\delta+}{R_3Si}\text{- - - - -}\overset{\delta-}{H} \longrightarrow R_3Si\text{—O—O—O—H} \longrightarrow$$
$$\delta- \; O \qquad O \; \delta+$$
$$\diagdown O \diagup$$

$$\overset{+}{R_3Si}\text{- - -}O_2\text{- - - -}\overset{-}{OH} \text{ or } R_3Si\text{- - -}O_2\text{- - -}OH \longrightarrow R_3SiOH + O_2$$

LOG K_{REL}

TEMP. $-10°$C.

$\rho^* = -0.40$

$\Sigma\sigma^*$
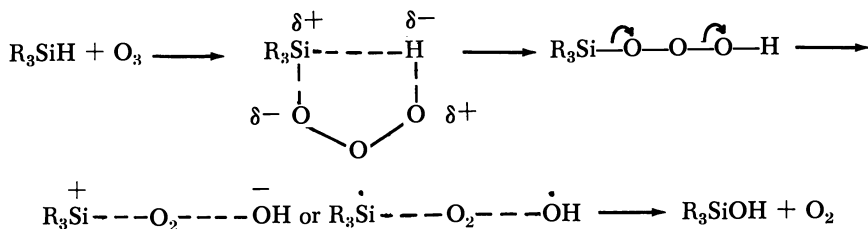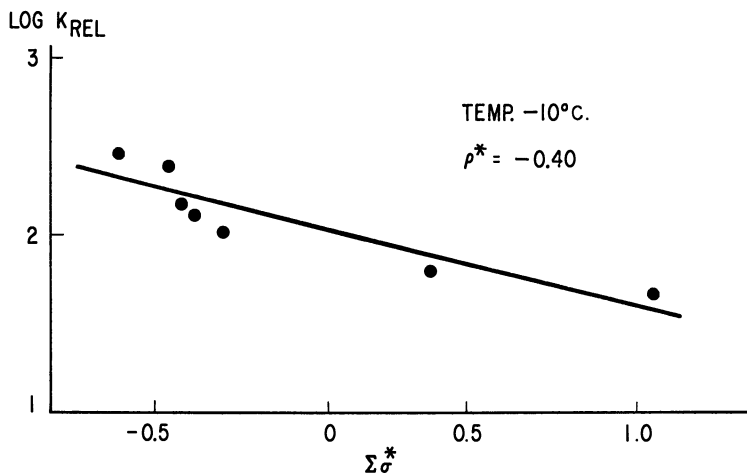
Figure 1. k_{rel} vs. $\Sigma\sigma^*$ *(Taft)*

Recent work (12) indicates that the reaction occurs stereospecifically with retention of configuration, indicating that a free radical process is not involved.

The reaction with ozone points out a difference between carbon and silicon chemistry. In the ozonization of hydrocarbons (9) peroxides are formed, and the reaction proceeds *via* a free radical process, whereas the cleavage of Si-H would appear to involve electrophilic attack, and the products do not include any peroxides.

Literature Cited

(1) Bailey, P. S., *Chem. Rev.* **58**, 925 (1958).
(2) Baines, J. E., Eaborn, C., *J. Chem. Soc.* **1956**, 1436.
(3) Barry, A. J., Beck, H. N., "Inorganic Polymers," F. G. A. Stone, W. A. G. Graham, Eds., Chap. 5, Academic Press, New York, 1962.
(4) Buell, G. R., Spialter, L., *J. Org. Chem.* **30**, 1662 (1965).
(5) Dannley, R. L., Jalics, G., *J. Org. Chem.* **30**, 2417 (1965).
(6) Eaborn, C., "Organosilicon Compounds," p. 206, Butterworth & Co., London, 1960.
(7) Hahn, W., Metzinger, L., *Makromol. Chem.* **21**, 113 (1956).
(8) Ingold, C. K., Stow, F. R., *J. Chem. Soc.* **1927**, 2918.
(9) Schubert, C. C., Pease, R. N., *J. Am. Chem. Soc.* **78**, 5553 (1956).
(10) Spialter, L., Austin, J. D., *J. Am. Chem. Soc.* **88**, 1828 (1966).
(11) Spialter, L., Austin, J. D., *Inorg. Chem.* **5**, 1975 (1966).
(12) Spialter, L., Buell, G. R., private communication.
(13) Taft, R. W., "Steric Effects in Organic Chemistry," M. S. Newman, Ed., Chap. 13, Wiley, New York, 1956.

62

Cross Ozonides from Pairs of Symmetrical Olefins

ROBERT W. MURRAY and GREGORY J. WILLIAMS

Bell Telephone Laboratories, Inc., Murray Hill, N. J.

3-Heptene ozonide has been produced by ozonizing mixtures of 3-hexene and 4-octene. The 3-heptene ozonide cis-trans ratio has been determined for a number of sources of this ozonide and found to depend on the stereochemistry of the olefin or pairs of olefins used to generate it. The effect of varying concentrations of added butyraldehyde on the ozonolysis of 3-hexene has been determined. The yields and cis-trans ratios of 3-hexene and 3-heptene ozonides depend on the butyraldehyde concentration.

The Criegee (2) mechanism of ozonolysis allows for the possibility of two zwitterions and two carbonyl moieties upon ozonolysis of an unsymmetrical olefin. This possibility leads to the prediction that such ozonolyses could lead to the production of three ozonide cis-trans pairs.
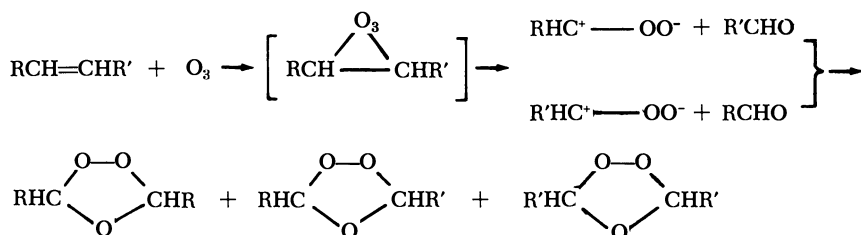
Failure to find the two symmetrical or cross ozonides for 3-heptene led Criegee to postulate a solvent cage (2) which prevented the cleavage fragments from participating in exchange or cross reactions. More recently a number of reports (5, 8, 9, 10, 11, 12, 13, 14) have indicated that cross ozonides can be produced for several unsymmetrical olefins. The fact that the percentage cross ozonide produced decreases with olefin concentration (8) possibly indicates that the earlier failures to find cross ozonides may simply have been caused by the olefin concentration used.

The observations of symmetrical cross ozonides from unsymmetrical olefins suggest that unsymmetrical cross ozonides ought to be produced from pairs of symmetrical olefins. Criegee had examined this point earlier (2) and found that no detectable amounts of 3-heptene ozonide were produced when a mixture of 3-hexene and 4-octene was ozonized. Again, this may have been a result of the particular olefin concentrations used. The recent observations that ozonide cis-trans ratios in both cross ozonides (5, 10, 11) and normal ozonides (4-14) can depend on olefin stereochemistry as well as steric factors in the olefin (11) prompted us to reinvestigate the possibility of obtaining unsymmetrical ozonides from pairs of symmetrical olefins. Such an investigation presents an opportunity to examine ozonide cis-trans ratios and yields where several new reaction variables are possible.

Experimental

Materials. The olefins were obtained from the Chemical Samples Co. and were from freshly-opened bottles. The aldehydes were distilled immediately before use.

Ozonolyses. The general procedure described earlier (11) was used. All ozonolyses were carried out at −70°C. and were continued to 75% of the theoretical amount of ozone required. The GLPC analyses were carried out on an Aerograph model A-700 gas chromatograph, using a 20-foot cyanosilicone column and equipped with an Aerograph model 471 digital integrator. The ozonide cis-trans ratios reported are the result of several integrations of the GLPC peak areas and have a maximum variation of ±0.5%.

The pure 3-heptene experiments were done on 1.0M solutions in pentane. The pure 3-hexene experiments were done on 0.5M solutions in pentane. The mixed hexene and octene experiments were done on pentane solutions which were 0.5M in each olefin. The added aldehyde experiments were done on pentane solutions which were 0.5M in olefin and of varying concentrations of the aldehydes. The ozonides were identified as previously described (11). Ozonide yields were obtained by calibrating the GLPC peak areas with known weights of the ozonides. The elemental analysis of hexene-3 ozonide was previously reported (11). Analyses for heptene-3 and octene-4 ozonide were obtained.

Analysis: Calculated for $C_7H_{14}O_3$: C, 57.51; H, 9.65; O, 32.84. Found: C, 57.67; H, 9.63; O, 32.91. Calculated for $C_8H_{16}O_3$: C, 59.98; H, 10.07; O, 29.96. Found: C, 60.24; H, 10.15; O, 30.20.

Results and Discussion

We have ozonized mixtures of 4-octene and 3-hexene as well as 3-heptene, and examined ozonide cis-trans ratios and yields. For mixtures all possible combinations of the cis and trans isomers of 3-hexene and 4-octene were used, and both the cis and trans isomers of 3-heptene were ozonized. 3-Heptene ozonide was prepared also by ozonizing the

cis and trans isomers of 3-hexene and 4-octene in the presence of the required aldehyde—*i.e.*, butyraldehyde or propionaldehyde.

The ozonolysis of mixtures of 3-hexene and 4-octene does indeed give 3-heptene ozonide, in addition to the ozonides of 3-hexene and 4-octene. Experiments were then designed to determine the effect of olefin geometry in the 3-hexene and 4-octene on the 3-heptene ozonide cis-trans ratio. The yields and cis-trans ratios of 3-heptene ozonide from 10 different sources are given in Table I. In these experiments the pure 3-heptene reactions were carried out at 1.0*M*, while the pure 3-hexene runs were made at 0.5*M*. Where mixtures of olefins were used, the solution was 0.5*M* in each olefin. In the olefin-aldehyde experiments the concentrations were 0.5 and 0.25*M* for olefin and aldehyde, respectively.

$$CH_3CH_2CH{=}CHCH_2CH_3 + CH_3CH_2CH_2CH{=}CHCH_2CH_2CH_3 + O_3$$
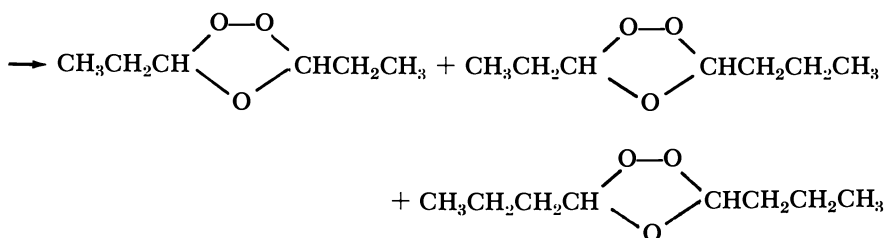
Clearly the 3-heptene ozonide cis-trans ratio depends on the origin of the ozonide. When both the 3-hexene and the 4-octene have the cis configuration, then the 3-heptene ozonide produced has a higher percentage cis ozonide than when both olefins are trans. When the 3-hexene and 4-octene are of different configurations, the 3-heptene ozonide cis-trans ratio falls between those for the all cis and all trans cases. The 3-heptene ozonide from the parent olefins shows the same trend seen earlier in a series of olefins—*i.e.*, the cis olefin gives a higher percentage cis ozonide than the trans isomer. It is significant that the combination of *cis*-3-hexene and *cis*-4-octene gives a higher percentage *cis*-3-heptene ozonide (58%) than does *cis*-3-heptene itself (52%).
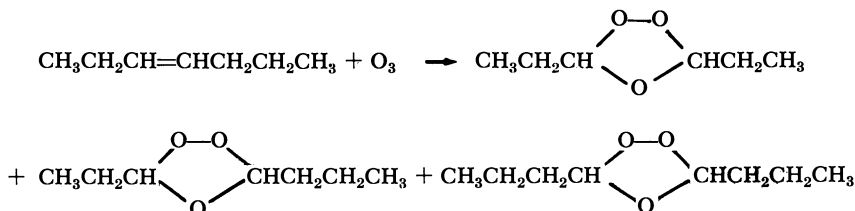
To determine what mechanistic pathways might be operating to account for the different cis-trans ratios, we have ozonized the olefin stereoisomers in the presence of the respective, necessary aldehydes.

$$CH_3CH_2CH{=}CHCH_2CH_3 + CH_3CH_2CH_2CHO + O_3 \rightarrow CH_3CH_2CH \begin{smallmatrix} O-O \\ \diagup \quad \diagdown \\ O \end{smallmatrix} CHCH_2CH_3$$

$$+ CH_3CH_2CH \begin{smallmatrix} O-O \\ \diagup \quad \diagdown \\ O \end{smallmatrix} CHCH_2CH_2CH_3$$

$$CH_3CH_2CH_2CH{=}CHCH_2CH_2CH_3 + CH_3CH_2CHO + O_3$$

$$\rightarrow CH_3CH_2CH_2CH \begin{smallmatrix} O-O \\ \diagup \quad \diagdown \\ O \end{smallmatrix} CHCH_2CH_2CH_3 + CH_3CH_2CH_2CH \begin{smallmatrix} O-O \\ \diagup \quad \diagdown \\ O \end{smallmatrix} CHCH_2CH_3$$
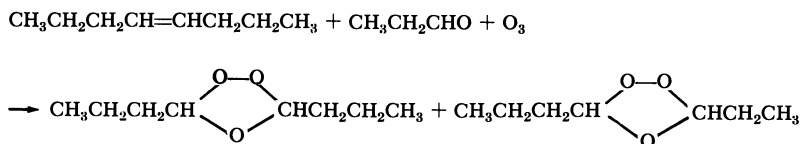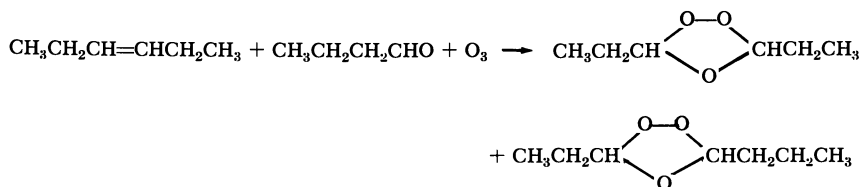
Table I shows that the olefin stereoisomers also give different 3-heptene ozonide cis-trans ratios when they react with the aldehyde only. The greatest difference is in the hexenes where the cis isomer gives 52% *cis*-3-heptene ozonide in this reaction, whereas the trans isomer gives only 40% *cis*-3-heptene ozonide.

When the 3-heptene ozonide cis-trans ratios from the all cis olefin pair and the cis olefins plus aldehyde experiments are compared, the all *cis* olefin pair gives a higher percentage *cis*-3-heptene ozonide. Thus, *cis*-3-hexene plus *cis*-4-octene gives 3-heptene ozonide with a 58:42 cis-trans ratio whereas *cis*-3-hexene plus butyraldehyde gives 3-heptene ozonide with a ratio of 52:48 (cis-trans), and *cis*-4-octene plus propionaldehyde gives a ratio of 49:51 (cis-trans). When a similar comparison is made for the same experiment using the trans olefin isomers, the symmetrical olefin pair gives a 3-heptene ozonide cis-trans ratio which is between that obtained in the two olefin-aldehyde experiments.

We have also examined the yields, and for 3-hexene the ozonide cis-trans ratio, in the symmetrical ozonides which result from the various reaction conditions used (Table II). Unfortunately, we were not able to get reliable cis-trans ratio determinations for the 4-octene ozonide because of the poor resolution of this pair on the GLPC column.

Here again, the 3-hexene ozonide cis-trans ratio depends on the origin of the ozonide. The same general observations that were found for 3-heptene ozonide also apply here. Thus, the all-cis olefin pair gives a higher percentage *cis*-3-hexene ozonide than the all-trans pair, while the two mixed isomer pairs give ratios which fall between those for the all-cis and all-trans cases.

Table I.   3-Heptene Ozonide cis-trans

Source

	+ CH₃CH₂CH₂CHO
	+ CH₃CH₂CH₂CHO
	+ CH₃CH₂CHO
	+ CH₃CH₂CHO
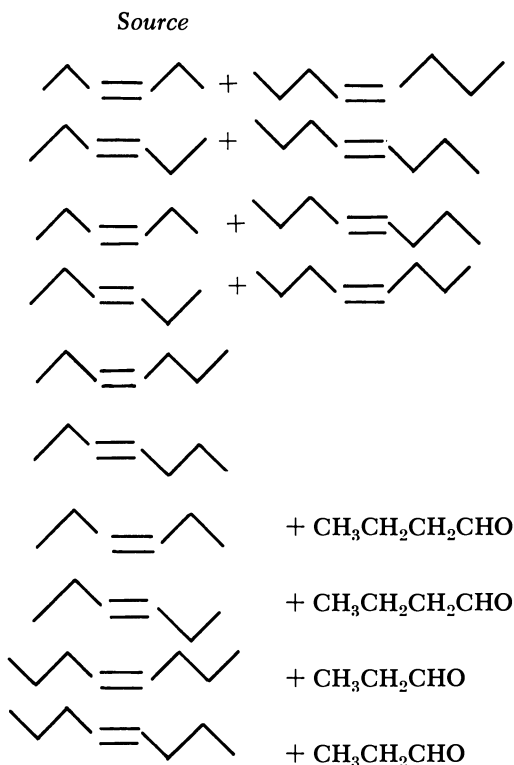
Some significant observations regarding the yields can be made. Tables I and II show that the cis isomers consistently give a higher total ozonide yield than the trans isomers. This is true for the individual olefins as well as for the pairs of like stereochemistry. It is even true when the individual olefins are ozonized in the presence of a foreign aldehyde. This observation is consistent with those made earlier (5, 9, 11, 14), all of which indicate that cis isomers invariably give a higher ozonide yield. This is only one of several factors which suggest that there is a fundamental difference in the mechanism of ozonolysis between many, if not all, cis and trans olefin isomers.

While the experiments with added foreign aldehyde in Table I were designed to test mechanistic possibilities, such an interpretation is complicated by the fact that these aldehydes cannot only enter into the chemistry of the ozonolysis process but may also exert a medium effect since they are considerably more polar than the pentane solvent. It is

Ratios and Yields from Various Sources

3-Heptene Ozonide			Total Ozonide, % Yield
% cis	% trans	% Total Ozonide	
58	42	23	97
44	56	20	43
51	49	16	97
51	49	20	66
52	48	81	82
42	58	80	39
52	48	32	89
40	60	30	65
49	51	40	90
46	54	42	60

possible, therefore, that the ozonolysis mechanism in the presence of *added* aldehyde is different from that where olefins alone are used. That this medium effect does in fact occur can be seen by examining the aldehyde experiments in Table II. Here, for 3-hexene plus butyraldehyde, for example, the 3-hexene ozonide cis-trans ratio obtained from *cis*-3-hexene is different from that obtained from this same olefin in pentane solution alone. A much lower percentage cis ozonide is obtained in the experiment with the added aldehyde. Since butyraldehyde cannot participate chemically in the 3-hexene ozonide formation, the change in the ozonide cis-trans ratio must be a medium effect of the aldehyde. The term medium effect is used here to describe all possible effects of the foreign aldehyde on the production of the normal ozonide of the olefin being ozonized. This would include polarity effects, solvation effects, perhaps assisted decomposition of ozone-olefin adducts, and selective diversion of the normal ozonide precursors in such a way that the ozonide cis-trans ratio is altered.

Table II.   3-Hexene Ozonide cis-trans Ratios and

Source

$+ CH_3CH_2CH_2CHO$

$+ CH_3CH_2CH_2CHO$

$+ CH_3CH_2CHO$

$+ CH_3CH_2CHO$
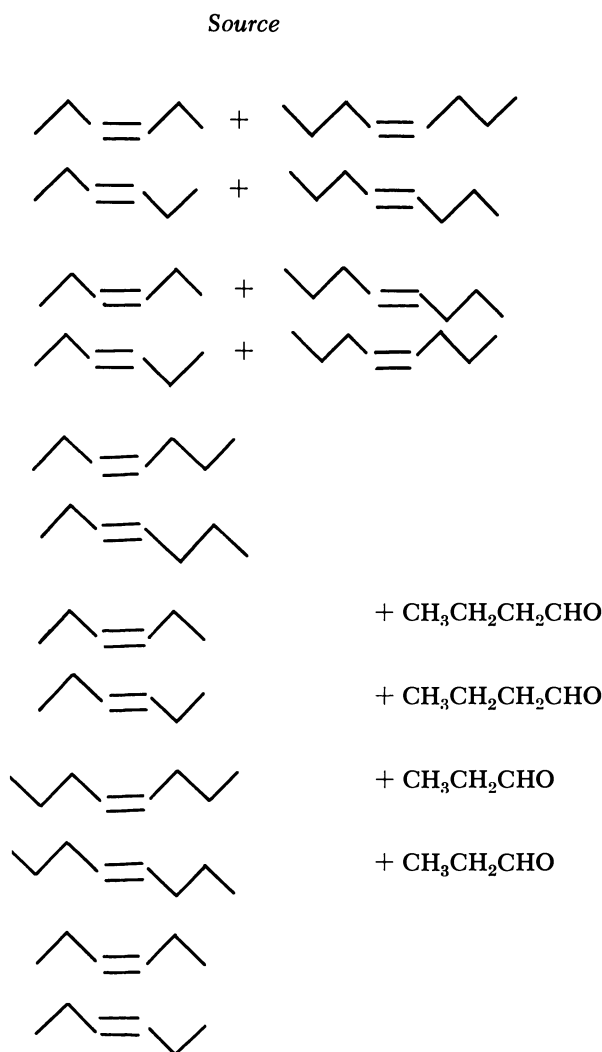
[a] Reliable ozonide cis-trans ratios for 4-octene ozonide not yet available.

Medium Effect of Added Aldehyde. To examine further the medium effect of added aldehyde we ozonized $0.5M$ solutions of *cis-* and *trans*-3-hexene containing varying concentrations of butyraldehyde and determined the ozonide cis-trans ratios and yields for both the 3-hexene and

3-Hexene and 4-Octene Ozonide Yields from Various Sources

3-Hexene Ozonide			4-Octene Ozonide,[a]	Total Ozonide,
% cis	% trans	% of Total Ozonide	% of Total Ozonide	% Yield
53	47	49	28	97
43	57	50	30	43
51	49	67	17	97
44	56	36	44	66
56	44	12	7	82
43	57	15	5	39
49	51	68	—	89
43	57	70	—	65
—	—	—	60	90
—	—	—	58	60
57	43	100	—	90
44	56	100	—	49

3-heptene ozonides produced. The effect of butyraldehyde concentration on the 3-hexene ozonide cis-trans ratio is shown in Figure 1. The added aldehyde has had a pronounced effect on the ozonide cis-trans ratio obtained from the cis olefin isomer and only a slight effect in the case of the trans isomer. For the cis isomer, increasing the concentration of

butyraldehyde causes an increase in the percentage *trans*-3-hexene ozonide until *ca.* 1.0M aldehyde concentration is reached, where the ratio stays fairly constant with increasing aldehyde concentration. In the trans case the 3-hexene ozonide cis-trans ratio stays fairly constant throughout the range of aldehyde concentrations although there is a slight increase in the percentage trans ozonide at aldehyde concentrations above 1.0M. The final ozonide cis-trans ratios reached at high aldehyde concentrations are approximately the same for the cis and trans olefin isomers.
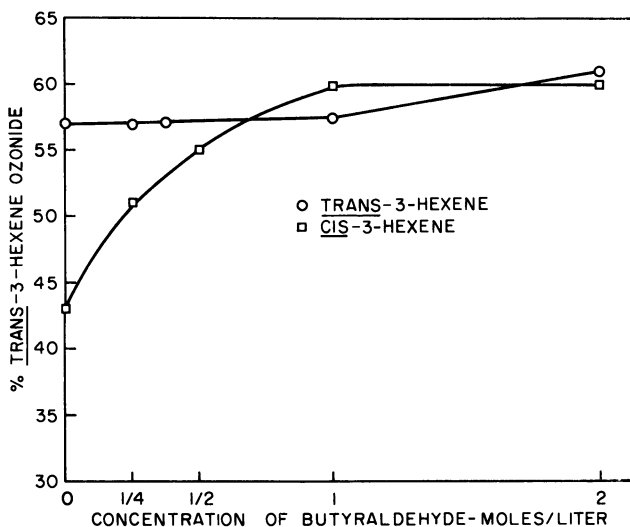
Figure 1.   3-Hexene ozonide cis-trans ratios as a function of added butyraldehyde concentration in the ozonolysis of cis- *and* trans-3-hexene

A somewhat similar effect occurs in the 3-heptene ozonide as shown in Figure 2. Here again the *trans*-3-hexene, ozonized in the presence of butyraldehyde, gives about the same 3-heptene ozonide cis-trans ratio at all butyraldehyde concentrations. A slight increase in the percentage trans ozonide does occur at aldehyde concentrations above 1.0M. The *cis*-3-hexene case shows an increasing percentage *trans*-3-heptene ozonide with increasing butyraldehyde concentration until the aldehyde concentration reaches about 2.0M, after which the ratio remains fairly constant. The final ozonide cis-trans ratios reached for the 3-heptene case, however, are different for the two 3-hexene stereoisomers with the cis isomer giving a higher percentage cis ozonide.

Similar differences for the olefin stereoisomers are seen in the yield data shown in Figures 3 and 4. For *cis*-3-hexene the total ozonide yield remains fairly constant and high throughout (Figure 3). In fact, the
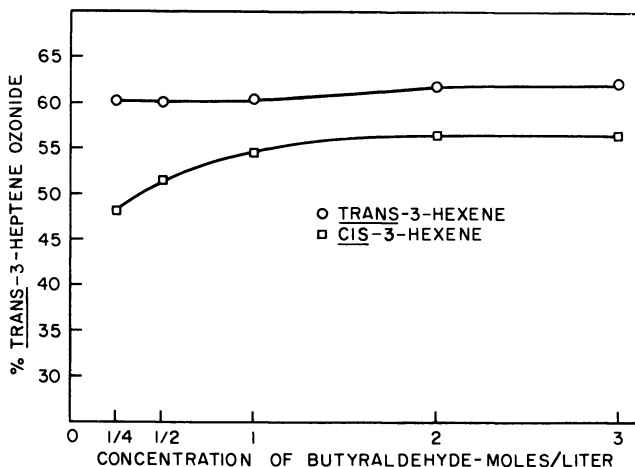
Figure 2.   3-Heptene ozonide cis-trans ratios as a function of added butyraldehyde concentration in the ozonolysis of cis- and trans-3-hexene

drop in yield of 3-hexene ozonide as butyraldehyde is added is almost perfectly matched by a concomitant increase in the yield of 3-heptene ozonide. At the higher aldehyde concentrations it becomes more and more difficult to divert 3-hexene ozonide precursors to 3-heptene ozonide, and the individual ozonide yield curves begin to level off. The situation for the trans isomer (Figure 4) is completely different. Here the added aldehyde actually increases the *total* yield of ozonide. This effect is particularly noticeable in the range 0-0.5M butyraldehyde. Over the same range the drop in 3-hexene ozonide yield is far less than the simultaneous increase in 3-heptene ozonide yield. Actually the increase in 3-heptene ozonide is about five times the corresponding loss in 3-hexene ozonide over this concentration range. As with the cis case a continued increase in butyraldehyde concentration leads to a leveling off in both the individual ozonide yield curves.

The mechanism of ozonolysis appears to be a very complex process. While the Criegee (2) mechanism has served as a unifying concept in this area, it seems clear that modifications to this basic scheme are required to account for the growing accumulation of data which seem to require a more complex mechanism. We have made some suggestions (11, 15) as to what additional pathways to ozonide ought to be considered. These suggestions are admittedly speculative and were made primarily to provide a working hypothesis for further experimentation. The results reported here are at least partly accounted for by the general features of these mechanistic proposals.
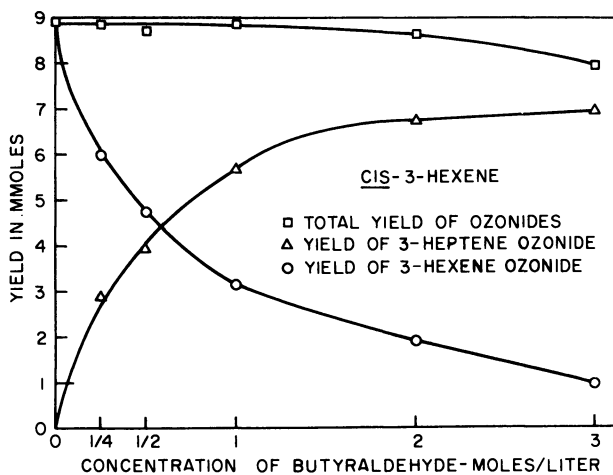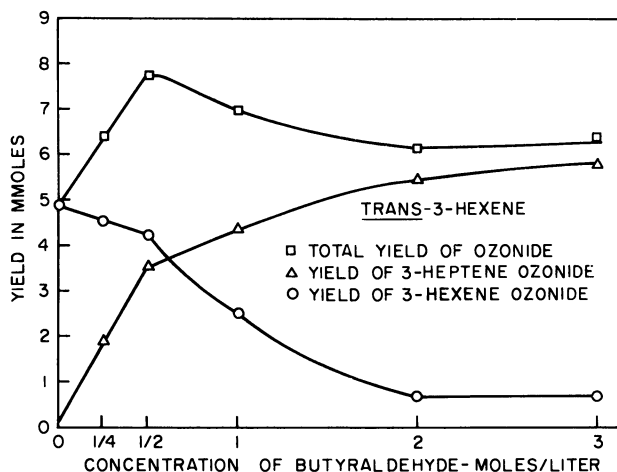
Figure 3. Variation of 3-hexene ozonide, 3-heptene ozonide, and total ozonide yields as a function of added butyraldehyde concentration in the ozonolysis of cis-3-hexene

We have suggested that trans olefins are in general more susceptible to an ozonolysis path involving fragmentation, after the initial olefin-ozone adduct is formed, than are cis olefins (*11, 15*). This presumably is one reason why cis olefins invariably give a higher yield of ozonide than do trans olefins. The extent of this difference is apparently also related to the steric requirements of the olefin substituents (*11*). The observed ozonide cis-trans ratios may be the resultants of several pathways with the percentage involvement of these pathways depending on several factors, including olefin stereochemistry, substituent size, solvent, etc. The data in Figure 1 suggest that for *trans*-3-hexene there is either a single dominant path to ozonide or a constant combination of more than one path, thus giving a constant ozonide cis-trans ratio. These paths could be the Criegee aldehyde-zwitterion recombination path (*2*) and/or the aldehyde-primary ozonide reaction path (*11, 15*), for example.

For *cis*-3-hexene a path giving a higher percentage cis ozonide seems to be present at low aldehyde concentrations, which path is overcome at higher aldehyde concentrations by one which gives a higher percentage trans ozonide. The higher solvent polarity accompanying higher butyraldehyde concentrations would be expected to enhance a fragmentation pathway thus making the cis case more like the trans. The path giving the higher percentage cis ozonide could be the intramolecular path from σ-complex described earlier (*11, 15*). Preferential diversion of this intermediate by the butyraldehyde would be expected to alter the 3-hexene ozonide cis-trans ratio in the observed manner.

The 3-heptene ozonide results shown in Figure 2 are more difficult to explain because here no intramolecular path to ozonide which favors cis ozonide formation can be invoked for the cis olefin. Perhaps increasing the aldehyde concentration and hence the polarity has altered a combination of pathways, each of which gives different ozonide cis-trans ratios, so that one which was dominant at low aldehyde concentrations is overcome by another at higher aldehyde concentrations. Again the difference between the pathways could be that the one at lower aldehyde concentration involves more intact 3-hexene-ozone adducts reacting with the butyraldehyde, while the higher aldehyde concentrations are more likely to involve fragmentation of the adduct, followed by reaction with the foreign aldehyde to give 3-heptene ozonide. Also the preferential diversion of ozone-3-hexene adducts by butyraldehyde which was invoked to explain the different 3-hexene ozonide cis-trans ratios at low aldehyde concentrations from *cis*-3-hexene might be expected to have a similar effect in the 3-heptene ozonide produced by this action. At any rate the final pathways or combination of pathways reached at the higher aldehyde concentrations give a different 3-heptene cis-trans ratio for the cis and trans 3-hexene olefin isomers.

The yield data in Figures 3 and 4 can be rationalized on similar grounds. In the cis case the initial olefin-ozone adduct can be diverted to 3-heptene ozonide by butyraldehyde, and by doing so can eliminate a precursor to 3-hexene ozonide. This process continues to operate throughout a wide range of aldehyde concentrations with the total ozonide

Figure 4.   Variation of 3-hexene ozonide yield, 3-heptene ozonide yield, and total ozonide yield as a function of added butyraldehyde concentration in the ozonolysis of trans-3-hexene

yield remaining fairly constant. At higher aldehyde concentrations it becomes more difficult to divert any more precursors perhaps because of tight cage reactions, and the 3-hexene ozonide yield curve has a reduced slope. The slightly reduced total ozonide yield at higher aldehyde concentrations could reflect the greater tendency to fragmentation reactions of the ozone-olefin adduct and the expected accompanying increase in side reactions.

In the trans case, however, it is clear from Figure 4 that something entirely different is happening. Here addition of the butyraldehyde has actually increased the total ozonide yield. The explanation for this probably lies in the suggestion made earlier that cis and trans olefins can have different ozonolysis mechanisms. It is interesting to recall that while there have been several reports (1, 3, 6) of the formation of a primary ozonide, which is stable at low temperatures, for trans olefins, cis olefins apparently give no such primary ozonide or one of completely different nature and stability.

As stated earlier, it is proposed that the trans case is more likely to involve fragmentation after formation of the initial olefin-ozone adduct. In the absence of added aldehyde, a certain percentage of these fragments combine in a cage, others wander out of the cage and then recombine, while still others wander to the extent that they stand a poorer chance of giving ozonide and may end up as non-ozonide products. In the presence of added aldehyde more of the fragments which have left the cage can be converted to ozonide, albeit a new ozonide, and the over-all ozonide-forming process is made more efficient. The fact that the yield of 3-hexene ozonide is reduced far less than the gain in yield of 3-heptene ozonide also suggests that many potential ozonide precursors would not have given ozonide in the absence of added aldehyde. As the butyraldehyde concentration increases, the yield of 3-hexene ozonide reaches a constant, non-zero value. This value may represent 3-hexene ozonide formation which occurs in a tight cage which the added aldehyde cannot penetrate even at fairly high concentrations.

We are still not able to discuss an over-all ozonolysis mechanism in any specific, detailed way. Instead we still must settle for broader generalizations and postulated intermediates which are given properties to rationalize the experimental results. Still as a result of continued experimentation there are clear differences appearing, such as the over-all differences between cis and trans olefins. Further work and new approaches may shed further light on this apparently complex process.

Literature Cited

(1) Bailey, P. S., Thompson, J. A., Shoulders, B. A., *J. Am. Chem. Soc.* **88**, 4098 (1966).
(2) Criegee, R., *Record Chem. Progr.* **18**, 111 (1957).

(3) Criegee, R., Schröder, *Chem. Ber.* **93,** 689 (1960).
(4) Criegee, R., Bath, S. S., Bornhaupt, B. V., *Chem. Ber.* **93,** 2891 (1960).
(5) Greenwood, F. L., *J. Am. Chem. Soc.* **88,** 3146 (1966).
(6) Greenwood, F. L., Haske, B. J., *Tetrahedron Letters* **1965,** 631.
(7) Kolsaker, P., *Acta. Chem. Scand.* **19,** 223 (1965).
(8) Loan, L. D., Murray, R. W., Story, P. R., *J. Am. Chem. Soc.* **87,** 737 (1965).
(9) Lorenz, O., Parks, C. R., *J. Org. Chem.* **30,** 1976 (1965).
(10) Murray, R. W., Youssefyeh, R. D., Story, P. R., *J. Am. Chem. Soc.* **88,** 3143 (1966).
(11) *Ibid.,* **89,** 2429 (1967).
(12) Privett, O. S., Nickell, E. C., *J. Am. Oil Chemists Soc.* **41,** 72 (1964).
(13) Riezebos, G., Grimmelikhuysen, J. C., Van Dorp, D. A., *Rec. Trav. Chim.* **82,** 1234 (1963).
(14) Schröder, G., *Chem. Ber.* **95,** 733 (1962).
(15) Story, P. R., Murray, R. W., Youssefyeh, R. D., *J. Am. Chem. Soc.* **88,** 3144 (1966).

63

Evidence for a New Mechanism of Ozonolysis

PAUL R. STORY, CLYDE E. BISHOP, JOHN R. BURGESS, and
JOHN B. OLSON

The University of Georgia, Athens, Ga. 30601

R. W. MURRAY and R. D. YOUSSEFYEH

Bell Telephone Laboratories, Inc., Murray Hill, N. J.

Generation of oxygen-18 labeled ozonides followed by location of the isotopic label using reductive techniques has served to substantiate a new mechanism of ozonolysis which was proposed to account for the dependence of ozonide cis/trans ratios on olefin geometry. The new mechanism requires fragmentation of the molozonide to produce some aldehyde and zwitterion but further requires that ozonide may also be formed by the reaction of molozonide and aldehyde.

Largely based on our finding that the cis/trans ratios of cross ozonides (10) formed from unsymmetrical olefins depended on olefin geometry (11, 12), we have proposed a new mechanism of ozonolysis which takes account of this effect (14). The new mechanism, which considers only a limited type of olefin, namely trans-disubstituted and relatively unhindered cis olefins, differs significantly from the generally accepted Criegee mechanism (1, 5).

In our view, cross ozonides may be formed by the typical sequence below in which aldehyde (4), produced in the reaction, reacts with molozonide (2) in an aldehyde interchange reaction to yield ozonide (5). As demonstrated previously, the molozonide-aldehyde interchange mechanism (12, 14), from consideration of steric interactions, correctly predicts that cis-olefin will generate relatively more cis-ozonide than will the corresponding trans-olefin. This interpretation does not refer to the absolute values of the cis/trans ratios.
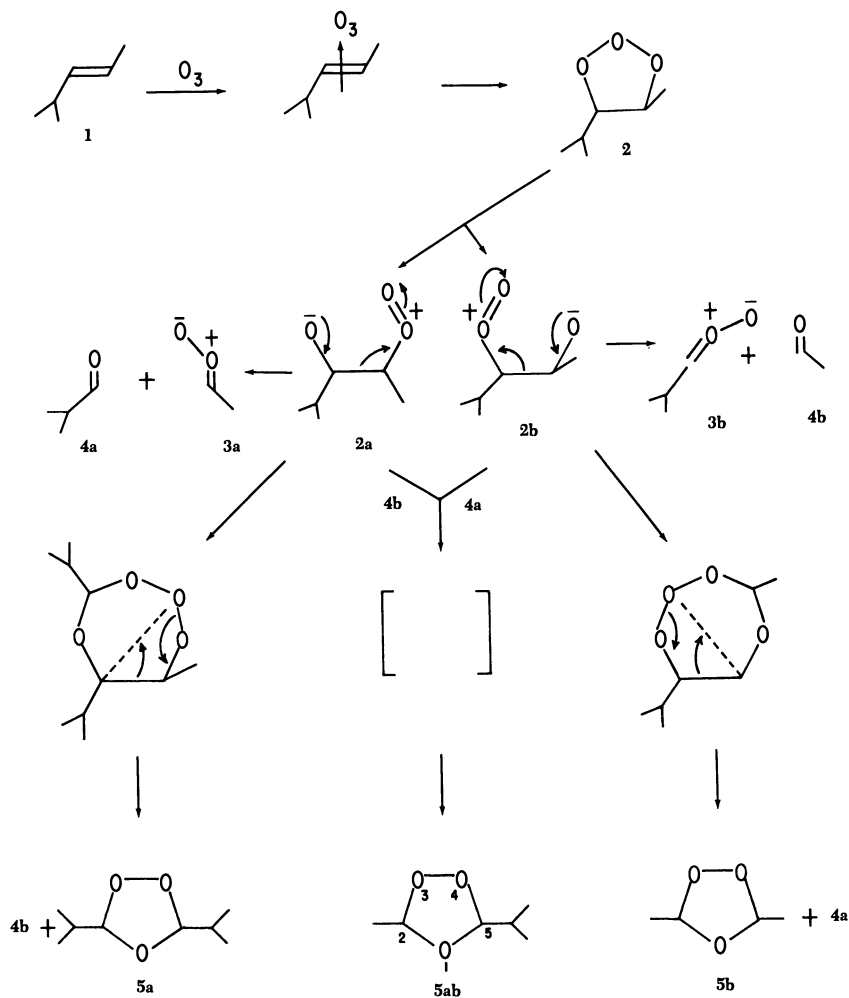
Figure 1.   Proposed mechanism of ozonolysis

According to the Criegee mechanism, ozonide is formed by combination of a zwitterion (3) and an aldehyde (4). Our mechanism does not discard the concept of the Criegee zwitterion.
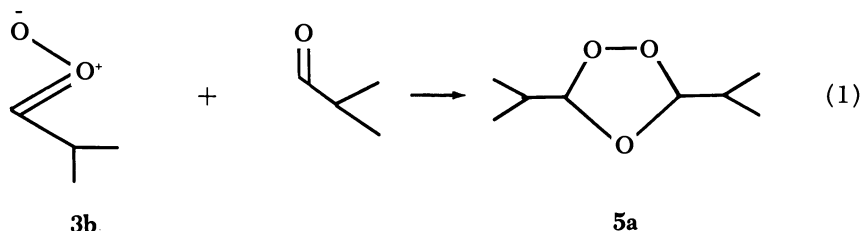
(1)

Essentially, we have proposed that ozonide (5) is formed not only by the Criegee mechanism but also by reaction of the molozonide with aldehyde. Thus, a competition exists between molozonide fragmentation and molozonide reaction with aldehyde. In addition, ozonide may also be formed by the reaction of molozonide with zwitterion followed by regeneration of a new zwitterion (Reaction 2). As yet we have no evi-

(2)

3a   **5a**
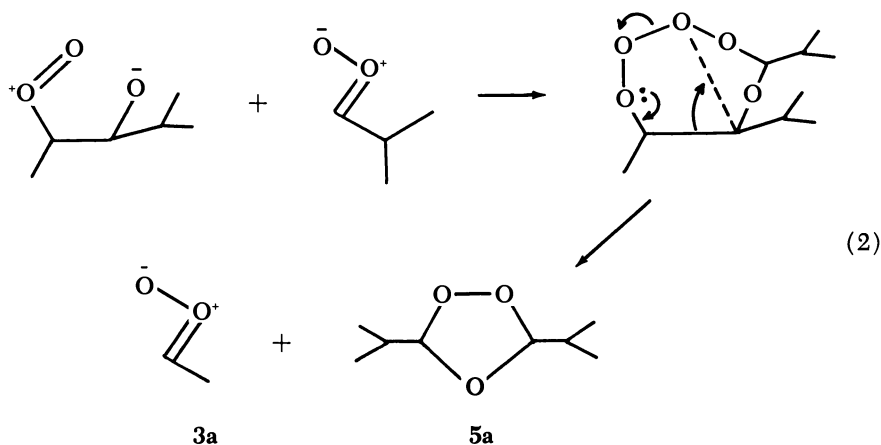
dence bearing on this possibility; this reaction does not result in incorporation of oxygen-18 label, and in this study it cannot be differentiated from combination of zwitterion with unlabeled aldehyde.

Experimental

Mass spectral analyses were performed by Gollub Analytical Labs., Berkeley Heights, N. J., and by Morgan-Schaffer Laboratories, Montreal, Quebec, Canada.

Acetaldehyde–^{18}O. Using standard vacuum line techniques, 4.4 grams (100 mmoles) of acetaldehyde (Eastman White Label) and 2.0 grams (100 mmoles) of 97.2% oxygen-18 water (YEDA Research) were transferred to a reaction vessel, which had been sealed to the vacuum system, and allowed to stand at room temperature for 36 hours. Assuming complete exchange after this time (4), the mixture was cooled to 0°C., and the acetaldehyde was distilled into a vessel containing about 2 grams of anhydrous sodium sulfate. After standing at room temperature for 1 hour, the acetaldehyde was redistilled through a 6 mm. × 8 inch column of anhydrous sodium sulfate into a removable container. Mass spectral analysis gave an oxygen-18 assay of 47.8%. Yield of labeled acetaldehyde was 4.1 grams (89%).

Cis/trans–Methyl Isopropyl Ozonide–^{18}O (5ab). A solution containing 4.04 grams (88 mmoles) of acetaldehyde–^{18}O, 14.5 grams (130 mmoles) of trans-diisopropylethylene (6) (Baker), and 75 ml. pentane

(Fisher Spectrograde) was ozonized in a dry ice–acetone bath to 90% completion. Following ozonolysis, the reaction vessel was stoppered and brought to room temperature. Part of the solvent was removed at low temperature on a rotary evaporator. The remaining liquids were separated and purified by GPC using an 8 ft. × 3/4 inch cyanosilicone (20%) column. Products isolated were 2.0 grams (15.2 mmoles, 17% based on acetaldehyde–^{18}O) of *cis-trans*-methyl isopropyl ozonide–^{18}O (5ab) and 6.4 grams (40 mmoles) of *cis/trans*-diisopropyl ozonide (5a). The GPC retention times and NMR spectra of both ozonides were identical to those of authentic samples (12). Ozonide (5ab) was also checked for purity using a 12 ft. × 1/4 inch fluorosilicone (10%) column. Care was taken not to fractionate the isotopically labeled product during GPC isolation.

Lithium Aluminum Hydride Reduction of *cis/trans*–Methyl Isopropyl Ozonide–^{18}O (5ab). A solution of 1.67 grams (12.7 mmoles) of 5ab in 25 ml. of anhydrous ether was added dropwise with stirring to a slurry consisting of 0.75 grams (19.7 mmoles) of lithium aluminum hydride and ether. Following addition, the reaction mixture was stirred for 30 minutes at room temperature and then heated under reflux for 15 minutes. Moist sodium sulfate was added after the excess hydride was destroyed by adding water cautiously. The clear ether layer was decanted, and the residual solids were washed several times with ether. The combined extracts were dried over sodium sulfate. Ether was removed carefully by distillation, and the remaining liquid was separated and purified by GPC using a 10 ft. × 3/8 inch UCON nonpolar (20%) column. Part of the ethyl alcohol (225 mg., 38%) and the isobutyl alcohol (450 mg., 48%) collected was transferred by vacuum line technique into breakseal ampules and sealed for mass spectral analysis. Ethyl alcohol–^{18}O assay: 25.4% oxygen-18; isobutyl alcohol assay: 7.6% oxygen-18.

Reaction of 5ab with Methyllithium. OZONIDE (5ab) FOR METHYL-LITHIUM REDUCTION. This substance was prepared using 40.61% ^{18}O–water (YEDA) to generate acetaldehyde containing 21.05% ^{18}O according to the procedure described above.

A solution of 110 mg. (0.83 mmoles) of 5ab in ether was added slowly to a solution of methyllithium (10% excess, Foote Chemical) in ether. The highly exothermic reaction was cooled in a room temperature water bath. Methane (39 ml.), ether vapor, and possibly carbon dioxide were collected [theoretical for proton abstraction reduction: 19 ml. of methane]. After addition of ozonide was complete, the reaction was worked up in the same manner as the lithium aluminum hydride reduction. GPC analysis of the crude mixture revealed isopropyl alcohol (9) (∼60% by GPC standard) and 3-methyl-2-butanol (10) (∼60%). Methanol is normally produced in approximately the same yield (∼60%) as 9 and 10. We were unable to collect a sufficient quantity from the labeling experiment for mass spectral analysis. Product identification was based on GPC retention times and by comparison of infrared spectra with those of authentic compounds. Mass spectral results were as follows: isopropyl alcohol–^{18}O assay: 11.88% oxygen-18; 3-methyl-2-butanol (10) assay: 2.45%.

Results and Discussion

Comparison of the two mechanisms under consideration reveals that the aldehyde oxygen is incorporated into ozonide in different ways; the Criegee mechanism yields ozonide which finds the aldehyde oxygen at the ether bridge (O-1), while our mechanism places the aldehyde oxygen in the peroxide bridge (O-3). This suggested, of course, that a critical test of the proposed mechanism would be provided by generating ozonide from oxygen-18 labeled aldehyde and determining the fate of the isotope. (The conclusion that the ozonide from the Criegee mechanism finds the aldehyde oxygen at the ether bridge is made assuming that the zwitterion cannot add to the aldehyde carbonyl 1,3 through the oxygens as though it possessed the structure:
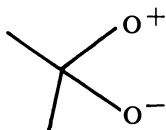
There is no evidence indicating that the zwitterion reacts in this fashion, and it would not account for the dependence of cross ozonide stereo-isomeric ratios on olefin geometry. We have experiments underway to check this possibility, however.)

The labeling experiment has been accomplished using the *trans*-diiso-propylethylene (6)—acetaldehyde—^{18}O (7) system outlined in Figure 2. Labeled ozonide (5ab) was prepared by ozonizing to 90% completion a pentane solution containing *trans*-diisopropylethylene (6) and acetaldehyde—^{18}O (7). The methyl isopropyl ozonide (5ab) was isolated as before (11, 12) as a cis/trans mixture in 17% yield based on acetaldehyde.

Location of the isotopic label in the product ozonide (5ab) was determined by two independent methods: (1) lithium aluminum hydride reduction of 5ab to ethyl alcohol and isobutyl alcohol, (2) reduction with methyllithium. Ozonide (5ab) for lithium aluminum hydride reduction was prepared using acetaldehyde containing 47.8% oxygen-18 by mass spectral analysis. Methyl isopropyl ozonide (5ab) was reduced cleanly and quantitatively to ethyl alcohol and isobutyl alcohol. Mass spectral analysis revealed that the ethyl alcohol contained 25.4% oxygen-18, and isobutyl alcohol contained 7.6%.

Unfortunately, the mechanism of hydride reduction of ozonides is not known. However, we can consider the most reasonable possibilities, all of which place the greatest portion of the label in the peroxide bridge at oxygen-3.

6   7

5ab   5ab
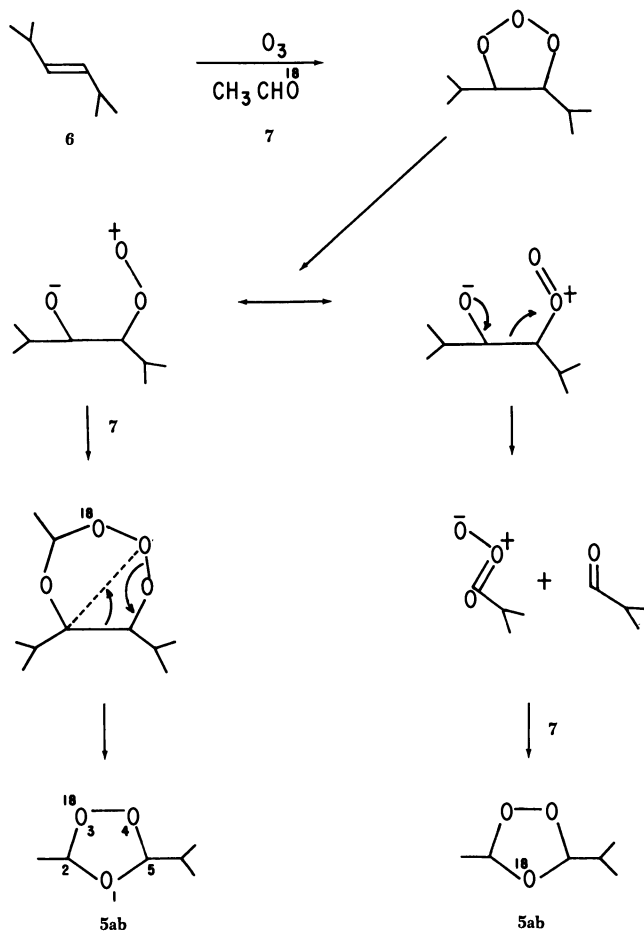
Figure 2. Isotopic labeling scheme

If we assume the mechanism usually written (7), by analogy to the reduction of peroxides, where the oxygen most likely to be lost is from the peroxide bridge [Mechanism A], we can conclude that 15.2% of the ozonide molecules contained oxygen-18 in the ether bridge (O-1) and that 32.6% contained label at oxygen-3. Under these circumstances and

$$(25.4\%) \quad (7.6\%)$$

$$\xrightarrow{\text{LiAlH}_4} CH_3CH_2{}^{18}OH \quad + \quad CH_2{}^{18}OH$$

$(47.8\%\ {}^{18}O)$

5ab
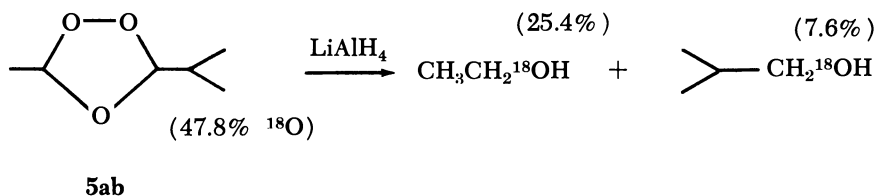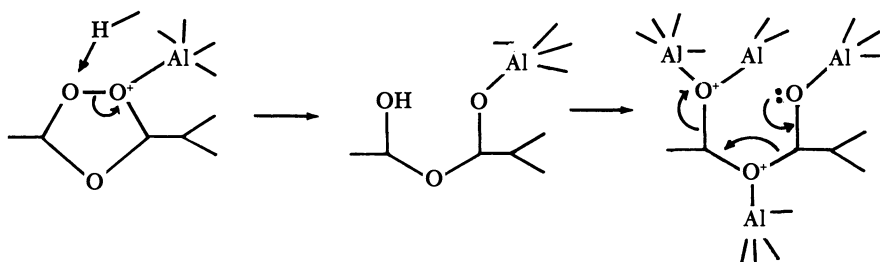
Mechanism A

presuming that the hydride reduction is not seriously affected sterically by the substituents, the ethyl alcohol should contain approximately 24% oxygen-18 regardless of the isotopic distribution between positions 1 and 3 in the ozonide (**5ab**). Our experimental value of 25.4% compares favorably and adds credence to this interpretation. [We have synthesized the ozonide of 1,2-dimethylcyclopentene (6) specifically labeled in the ether bridge, but containing only 0.3% oxygen-18. On lithium aluminum hydride reduction, all the label was retained in the diol. However, because of the very low incorporation of oxygen-18, considerable error could be involved (3)].

The same conclusion regarding isotopic distribution is reached if we assume a reduction mechanism similar to the scheme proposed by Rieche (13) for hydrolysis of ozonides [Mechanism B].
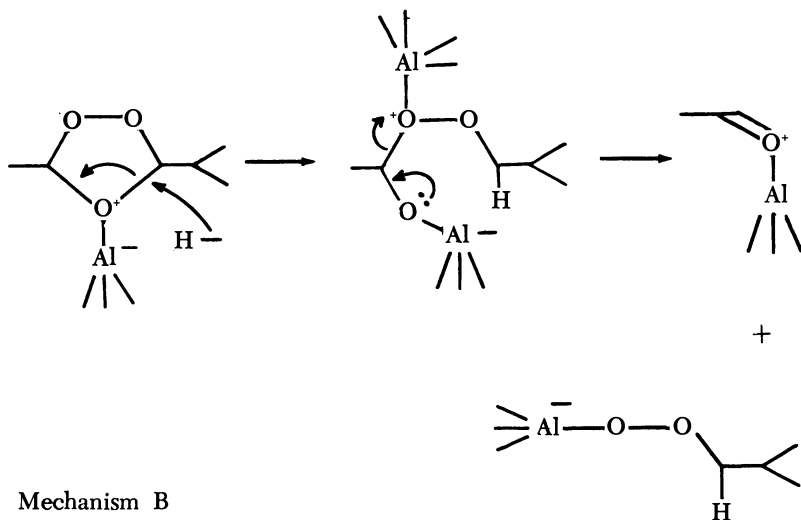
Mechanism B

If, however, oxygen loss on hydride reduction is purely statistical as illustrated by Mechanism C, the isotopic distribution would be altered but would still place more than half the isotopic label at oxygen-3. Under

5ab

Mechanism C
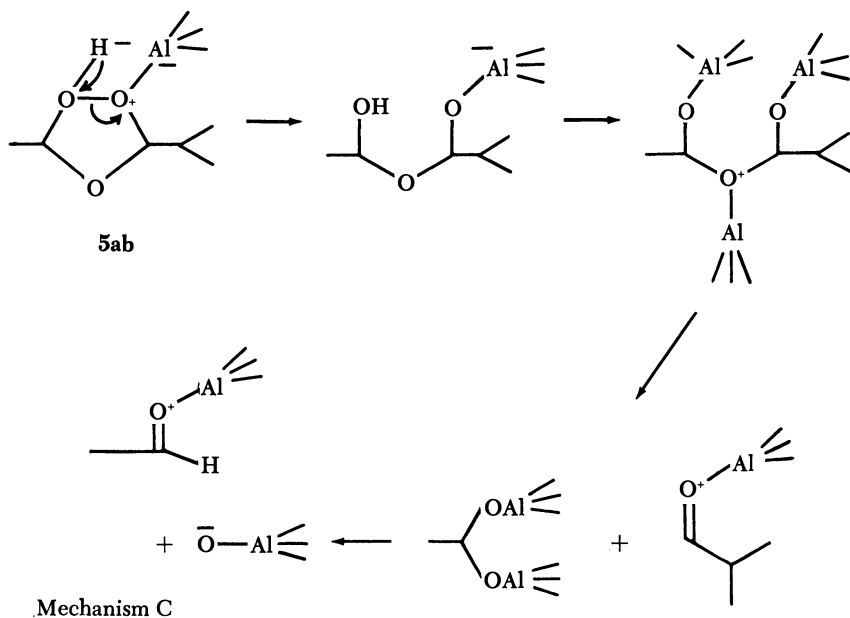
these conditions one-third of the oxygen in the isobutyl alcohol reduction product would arise from the ether bridge (O-1) indicating that 3 × 7.6% or 22.8% of the ozonide molecules must have contained label at this position; 25%, then, contained label at oxygen-3. The estimate of isotopic distribution provided by Mechanism C is considered the lower limit for isotopic label at oxygen-3.

Certainly, any conclusions drawn on the basis of the hydride reduction alone are somewhat tenuous. Two points are worth considering, however. (1) In the absence of large steric effects on the hydride reduction, the possibility that all of the label originated at oxygen-1 in the ozonide (5ab) is eliminated by the value obtained for the isotopic label in ethyl alcohol, 25.4%, and by the large difference in amount of isotope contained in the two alcohol products. (2) Any steric effect on the reduction should be small. In addition, the effect should be in the direction to remove an excess of oxygen-3; the cis ozonide should exhibit no measurable steric effect since attack would occur preferentially on the side of the ring away from the substituents. The trans isomer, on the other hand, should suffer hydride attack cis to the methyl substituent and as far away from the substituent as possible, thus leading to a predominant loss of oxygen-3 whether reduction takes place by addition of hydride to oxygen or to carbon.

We conclude, then, that the ozonide (5ab) is formed by two competing but complimentary reaction paths, and under the particular conditions [added aldehyde] of this experiment, translation of the data to

100% oxygen-18 [considering reduction Mechanisms A or B only] reveals that ∼ 30% of **5ab** is formed *via* the Criegee zwitterion mechanism and ∼ 70% of **5ab** according to the molozonide-aldehyde interchange mechanism (*14*).

This conclusion is confirmed by reduction of the same ozonide (**5ab**) using methyllithium (we thank R. Criegee for suggesting this type of reaction to locate the isotopic label). It was expected that reduction would occur by proton removal as illustrated in Figure 3. Hence, the fate of the ozonide oxygens would be unambiguous; analysis of the isopropyl alcohol would provide a measure of the oxygen-18 label at oxygen-3.
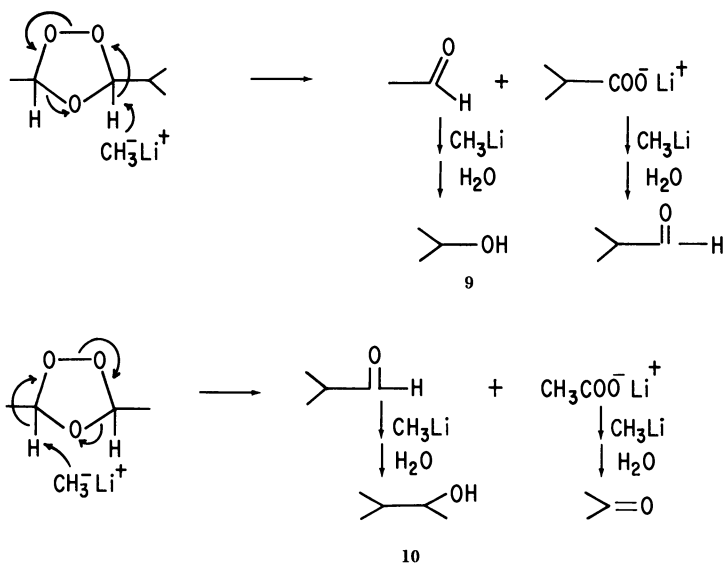
Figure 3.   Methyllithium reduction of ozonide by proton removal

The reaction of methyllithium with ozonide (**5ab**) was extremely rapid and exothermic, and although methane was evolved, the reaction appears to proceed principally by displacement on the oxygen-oxygen bond by methide to yield isopropyl alcohol (**9**), 3-methyl-2-butanol (**10**), and methyl alcohol. The source of the methane is unknown at present. However, the entire reaction is being investigated.

Methyllithium reduction of ozonides appears to follow a course similar to that of Grignard reduction. Greenwood treated diethyl ozonide with isopropyl Grignard and obtained 2-methyl-3-pentanol, isopropyl alcohol, and propane in good yield (*9*).

It is also conceivable that reduction occurs by methide displacement on carbon to yield hydroperoxide, which is subsequently reduced to alcohol (**9, 10**) and methanol. We cannot at present distinguish

these latter two possibilities either by product analysis or by isotope distribution.

If reduction of **5ab** occurs with displacement on oxygen as shown in Figure 4, one-half the oxygen contained in 3-methyl-2-butanol (**10**) originated at position 1. Therefore, the amount of label in the ether bridge is obtained by doubling the percentage oxygen-18 found in **10**.

Ozonide (**5ab**) prepared from acetaldehyde containing 21.05% oxygen-18 was treated with excess methyllithium in an apparatus which allowed collection of evolved gases. In every case, at least 1 mole of methane was collected (small traces of water accounted for some of the methane). Analysis of the product mixture by GPC revealed isopropyl alcohol (**9**) and 3-methyl-2-butanol (**10**) in approximately equimolar amounts and in high yield (*ca.* 60%, by GPC).

Mass spectral analysis of the GPC pure products revealed that isopropyl alcohol (**9**) contained 11.88% oxygen-18; 3-methyl-2-butanol (**10**) contained 2.45%. Interpreted in terms of methide displacement at oxygen (Figure 4) or at carbon [proton removal (Figure 3) is excluded as a major reaction pathway by product analysis and by the presence of label in **10**], the ether bridge (oxygen-1) must have contained 4.90% oxygen-18. The remainder, 16.15%, must have been at oxygen-3. If
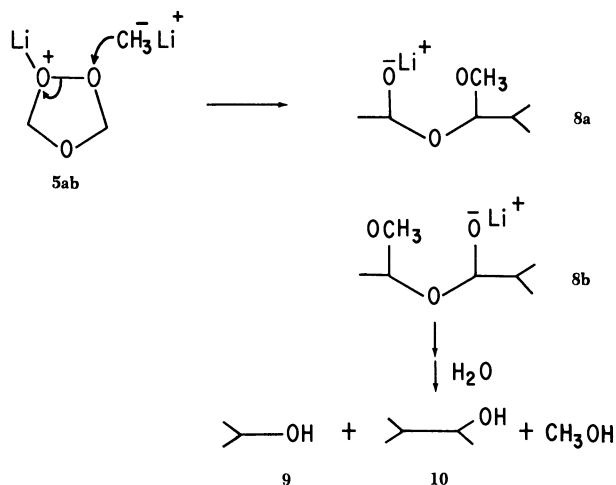
Figure 4. Apparent reaction path for the reaction of methyllithium with ozonide (5ab)

this scheme is correct, isopropyl alcohol should have been found to contain 8.07 + 2.45 or 10.52% oxygen-18. Our experimental value of 11.88% gives a discrepancy of 1.36% or about a 10% error which can probably be attributed to a slight steric effect. A steric effect argument

is reasonable since displacement at oxygen-4, which would produce iso-propyl alcohol rich in oxygen-3, would be favored. It is also possible that some of the alcohols were produced by proton abstraction, and in that way led to a high isotope content in 9. In fact, we obtained a small amount of a material with the same GPC retention time as authentic methyl isopropyl ketone which would be produced by hydrogen abstraction (Figure 3). We were unable to isolate sufficient methyl alcohol from the labeling experiment for mass spectral analysis.

From this experiment we would conclude that about 25% of the ozonide was formed according to the Criegee mechanism and that the remainder, 75%, was formed according to our molozonide-aldehyde mechanism. This result substantially agrees with that obtained by hydride reduction.

The labeling experiments, therefore, provide strong support for the mechanism we proposed to account for the dependence of ozonide cis/trans ratios on olefin geometry (14). In this particular case, under conditions of added aldehyde, approximately 70–75% of the ozonide (5ab) was, by all indications, formed through the molozonide–aldehyde reaction. However, in a normal ozonolysis aldehyde is not present initially, and before the molozonide–aldehyde mechanism can become important, a sufficient quantity of aldehyde must be produced, presumably by fission of the molozonide to zwitterion and aldehyde. Under these conditions it would not be surprising to find the new mechanism somewhat less important than in the present study. Once sufficient aldehyde is obtained in the normal ozonolysis, production of zwitterion may well nearly cease since the molozonide–aldehyde reaction does not deplete aldehyde concentration, and at sufficiently high aldehyde concentrations this reaction competes well with molozonide fission. Reaction temperature should be important in this competition.

While the oxygen-18 labeling results described here confirm the molozonide–aldehyde mechanism for the types of olefins considered, the ozonolysis reaction in general is quite complex and seems to vary widely depending especially upon the stereochemistry of the olefin. To sum up, the molozonide–aldehyde mechanism (14) considered here appears to be applicable to any important degree *only* to trans-disubstituted olefins, relatively unhindered cis olefins, and perhaps to unhindered terminal olefins. As pointed out, more hindered olefins seem to react by one or more different pathways, which differ most notably from the present system in the apparent absence of a molozonide intermediate (2, 8, 12, 14).

Acknowledgments

gation and the General Research Office, The University of Georgia, for purchase of the oxygen-18 water.

### Literature Cited

(1) Bailey, P. S., *Chem. Rev.* **58**, 925 (1958).
(2) Bailey, P. S., Thompson, J. A., Shoulders, B. A., *J. Am. Chem. Soc.* **88**, 4098 (1966).
(3) Bishop, C. E., unpublished work.
(4) Byrn, M., Calvin, M., *J. Am. Chem. Soc.* **88**, 1916 (1966).
(5) Criegee, R., *Rec. Chem. Progr. (Kresge-Hooker Sci. Lib.)* **18**, 111 (1957).
(6) Criegee, R., Lohaus, G., *Chem. Ber.* **86**, 1 (1953).
(7) Gaylord, N. G., "Reduction with Complex Metal Hydrides," p. 708, Interscience, New York, 1956.
(8) Greenwood, F. L., *J. Org. Chem.* **29**, 1321 (1964).
(9) Greenwood, F. L., Haske, B. J., *J. Org. Chem.* **30**, 1276 (1965).
(10) Loan, L. D., Murray, R. W., Story, P. R., *J. Am. Chem. Soc.* **87**, 737 (1965).
(11) Murray, R. W., Youssefyeh, R. D., Story, P. R., *J. Am. Chem. Soc.* **88**, 3143 (1966).
(12) *Ibid.,* **89**, 2429 (1967).
(13) Rieche, A., Meister, R., Sauthoff, H., *Ann.* **553**, 187 (1942).
(14) Story, P. R., Murray, R. W., Youssefyeh, R. H., *J. Am. Chem. Soc.* **88**, 3144 (1966).

Discussion

D. G. M. Diaper: Reaction of molozonide and zwitterion gives an eight-membered ring with four adjacent oxygens. No stable rings with four adjacent oxygens are known, and catenation of four oxygens has not often been invoked. Milas had such a system in peroxy radical dimer, but it lost O_2 at −30°C. Analogous O_2 loss would give a six-membered ring peroxide with that embarrassing C—C bond intact.
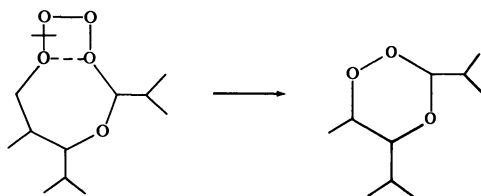
Paul R. Story: In the first place we cannot rule out some homolytic decomposition of the proposed intermediate. However, it is worth comparing our proposed seven-membered ring trioxide with the molozonide for which an ionic decomposition to zwitterion and carbonyl is readily envisioned; our intermediate and the proposed ionic decomposition are quite analogous to Criegee's molozonide or primary ozonide and its decomposition.

64

Ozonation of Amines

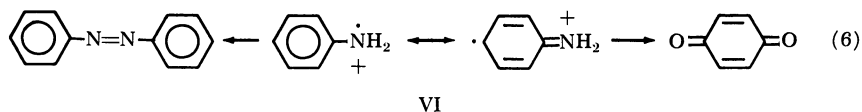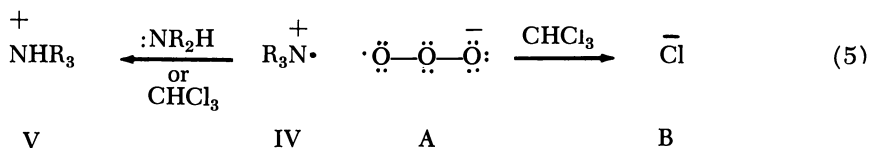PHILIP S. BAILEY, JOHN E. KELLER, DAVID A. MITCHARD, and
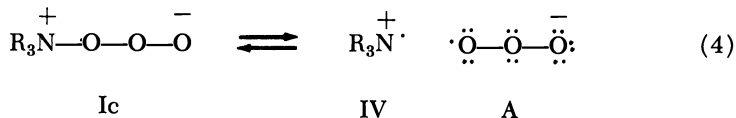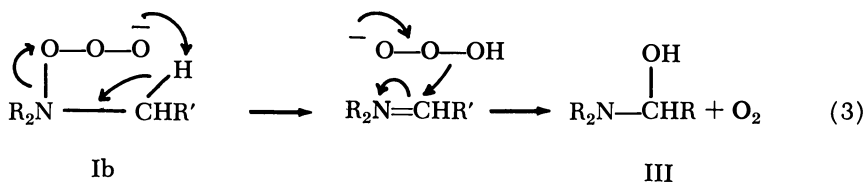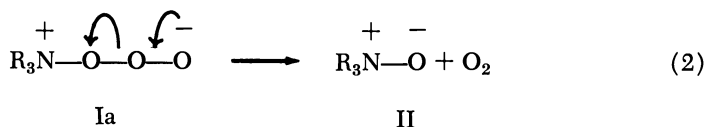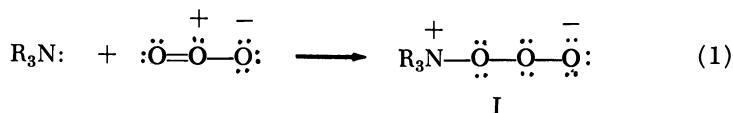HAROLD M. WHITE

University of Texas at Austin, Austin, Tex. 78712

A review of the literature concerning reactions of ozone with amines has given rise to the working hypothesis that these reactions all involve initially the electrophilic attack of ozone to give an adduct for which at least three different reaction routes are available: loss of molecular oxygen to give an amine oxide or further reaction products thereof, an intramolecular oxidation of a side chain, and dissociation to nitrogen cation radicals and the ozonate anion radical, followed by further reactions of these. Results from ozonations of tert-*butylamine and tri-n-butylamine, which furnish additional evidence for the above competitions, are described.*

The literature suggests several ways in which ozone reacts with amines. The best known of these is the ozonation of tertiary amines to amine oxides (II) (*1*). Henbest and Stratford (*11*) and Shulman (*17*) have shown that competing with this is an ozone attack on the alpha position of an alkyl side chain to produce various decomposition products of III. Henbest (*11*) showed that amine oxide formation is favored in chloroform and methanol, while side chain oxidation is predominant in hydrocarbon solvents. Also of considerable interest are the reported conversions, during ozonation, of phenylenediamines to Wurster's salts (VII) (*8, 14*), of liquid ammonia to ammonium ozonate (VA) at a low temperature (*18*), and of amines to amine hydrochlorides (VB) in chlorinated hydrocarbon solvents (*17, 19*). Finally, an early report states that azobenzene and quinone are obtained upon ozonation of aniline (*15*).

The expected initial reaction between ozone and amines would be an electrophilic ozone attack to give adduct I (Reaction 1) (*1*). A similar adduct has actually been observed in the reaction between the nucleophile triphenylphosphite and ozone (*20*). It occurred to us that all of the reactions described above could be explained by competing fates

of adduct I. Reaction 2 represents the generally accepted decomposition to an amine oxide and oxygen (*1*), and Reaction 3 is a possible course of the competing side chain oxidation (*12*). Reaction 4 involves the dissociation of the amine-ozone adduct to nitrogen cation radicals (IV) and the ozonate anion radical (A). The nitrogen cation radical from a phenylenediamine would be resonance stabilized (VII); that from an
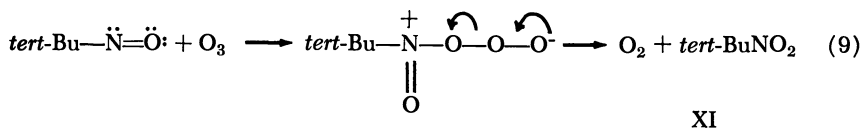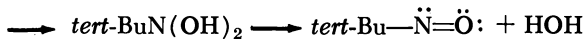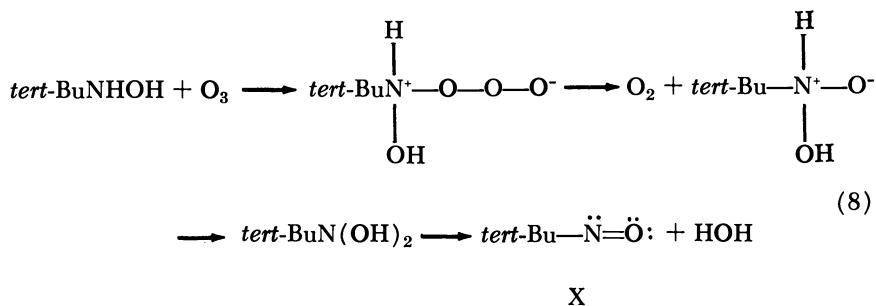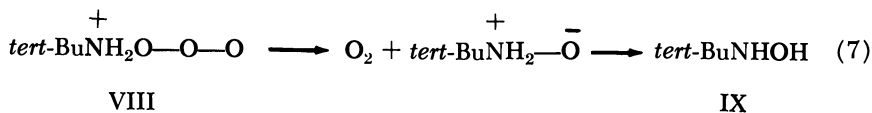
$$R_3N: \; + \; :\overset{+}{\ddot{O}}=\overset{\;}{\ddot{O}}-\overset{-}{\ddot{O}}: \longrightarrow R_3\overset{+}{N}-\overset{\;}{\ddot{O}}-\overset{\;}{\ddot{O}}-\overset{-}{\ddot{O}}: \qquad (1)$$

I

$$R_3\overset{+}{N}-O-O-\overset{-}{O} \longrightarrow R_3\overset{+}{N}-\overset{-}{O} + O_2 \qquad (2)$$

Ia II

$$\begin{array}{c} O-O-\overset{-}{O} \\ | \quad\quad H \\ R_2N - CHR' \end{array} \longrightarrow R_2N{=}CHR' \longrightarrow R_2N-CHR + O_2 \qquad (3)$$

Ib III

$$R_3\overset{+}{N}-O-O-\overset{-}{O} \rightleftharpoons R_3\overset{+}{N}\cdot \quad \cdot\overset{\;}{\ddot{O}}-\overset{\;}{\ddot{O}}-\overset{-}{\ddot{O}}: \qquad (4)$$

Ic IV A

$$\overset{+}{N}HR_3 \xleftarrow[\substack{\text{or} \\ CHCl_3}]{:NR_2H} R_3\overset{+}{N}\cdot \quad \cdot\overset{\;}{\ddot{O}}-\overset{\;}{\ddot{O}}-\overset{-}{\ddot{O}}: \xrightarrow{CHCl_3} \overset{-}{Cl} \qquad (5)$$

V IV A B

$$\text{(6)}$$

VI

VII

etc. X
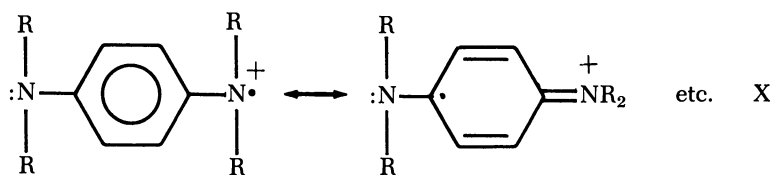
aliphatic amine or ammonia (IV), however, must stabilize itself by abstracting a hydrogen atom from another amine or ammonia molecule, or from the solvent (Reaction 5). A possible explanation for the reported aniline results involves competing reactions of the two canonical forms of the aniline cation radical (Reaction 6).

In order to obtain evidence for or against these ideas we have begun an intensive study of the reactions of ozone with a variety of amines. This paper summarizes results from the ozonation of *tert*-butylamine and of tri-*n*-butylamine, which furnish evidence for the competitions indicated by Reactions 2, 3, and 4. Additional details will be published elsewhere.

In a typical run, 5 mmoles of *tert*-butylamine in chloroform reacted with 4.1 mmoles of ozone in an ozone-nitrogen stream at about −60°C. to give 0.9 mmole (18%) of 2-methyl-2-nitropropane (XI), 0.9 mmole (18%) of *tert*-butyl isocyanate (XVI), and 3.0 mmoles (60%) of *tert*-butylammonium chloride (XIV). In a separate but similar run, 3.5 mmoles of molecular oxygen were determined as a product. Under the conditions of the reaction no significant reaction occurred between *tert*-butylamine and chloroform in the absence of ozone or between ozone and chloroform in the absence of the amine.

The probable reaction course to the nitroalkane (XI), after the formation of the amine-ozone adduct (Reaction 1), is shown by Reactions 7 to 9 and summed up in Reaction 10. A primary amine oxide would not be expected to be stable and should rearrange to the hydroxylamine (IX, Reaction 7). A similar set of reactions (Reaction 8) should result in the nitrosoalkane (X), which should then be converted to the nitroalkane (XI) as shown in Reaction 9. Evidence for this series of reactions was the observation of the blue color of the nitrosoalkane (X) throughout the ozonation and the demonstration, in separate experiments, that the hydroxylamine (IX) reacts with two mole equivalents of ozone and the nitrosoalkane (X) with one mole equivalent of ozone, each to give the nitroalkane (XI).

The most logical route from the initial ozone adduct (VIII) to *tert*-butylammonium chloride (XIV) is *via* nitrogen cation radical XII, produced in minute, equilibrium amounts through dissociation of VIII (Reaction 11). In the case of chloroform solvent, the proposed reaction course is shown by Reactions 11 to 15 and is summed up, with Reaction 1, in Reaction 16. Nitrogen cation radical XII apparently stabilizes itself by abstracting hydrogen from a solvent molecule to give ammonium cation XIVa and solvent radical XV (Reaction 12). The ozonate anion radical (XIII) and the solvent radical (XV) then interact to give the chloride anion (XIVb) and phosgene (Reaction 13). Phosgene and *tert*-butylamine produce *tert*-butyl isocyanate and additional salt (XIV)
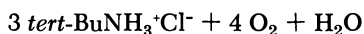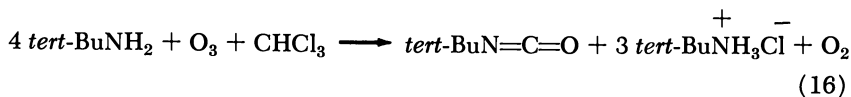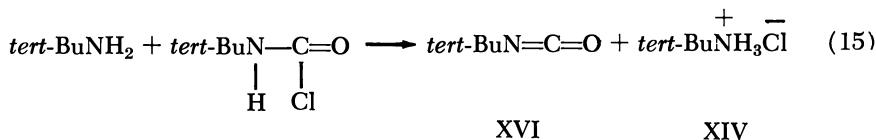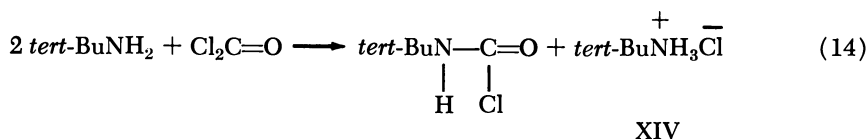
$$\underset{\text{VIII}}{\overset{+}{\text{tert-BuNH}_2\text{O—O—O}}} \longrightarrow O_2 + \underset{}{\overset{+ \quad -}{\text{tert-BuNH}_2\text{—O}}} \longrightarrow \underset{\text{IX}}{\text{tert-BuNHOH}} \quad (7)$$

$$\text{tert-BuNHOH} + O_3 \longrightarrow \text{tert-BuN}^+\underset{\overset{|}{\text{OH}}}{\overset{\overset{\text{H}}{|}}{\text{—O—O—O}^-}} \longrightarrow O_2 + \text{tert-Bu—N}^+\underset{\overset{|}{\text{OH}}}{\overset{\overset{\text{H}}{|}}{\text{—O}^-}}$$

$$\qquad\qquad\qquad\qquad\qquad\qquad\qquad\qquad\qquad\qquad\qquad\qquad (8)$$

$$\longrightarrow \text{tert-BuN(OH)}_2 \longrightarrow \underset{\text{X}}{\text{tert-Bu—}\ddot{\text{N}}\text{=}\ddot{\text{O}}:} + \text{HOH}$$

$$\text{tert-Bu—}\ddot{\text{N}}\text{=}\ddot{\text{O}}: + O_3 \longrightarrow \text{tert-Bu—}\underset{\overset{||}{\text{O}}}{\overset{+}{\text{N}}}\text{—O—O—O}^- \longrightarrow \underset{\text{XI}}{O_2 + \text{tert-BuNO}_2} \quad (9)$$

$$\text{tert-BuNH}_2 + 3\,O_3 \longrightarrow \underset{\text{XI}}{\text{tert-BuNO}_2} + 3\,O_2 + H_2O \qquad (10)$$

via Reactions 14 and 15. It was shown separately that phosgene and *tert*-butylamine interact to give the isocyanate at the ozonation temperature. Reaction 17 is a summation of Reactions 10 and 16, assuming that the two fates of amine-ozone adduct VIII occur equally. The fact that the experimental results described earlier agree well with the stoichiometry of Reaction 17 increases confidence in the validity of the proposed mechanisms.

In the ozonation of tri-*n*-butylamine at −40°C. with an ozone-nitrogen stream, 1.2 to 1.6 mole equivalents of ozone were absorbed, and the yields of tri-*n*-butylamine oxide were 53% from chloroform and 6% from pentane solvents. The other products were the side chain oxidation products described by Henbest and Stratford (*11*). These results eliminate the possibility that the side chain oxidation is an ozone-initiated autoxidation. The mechanism outlined by Reaction 3 explains nicely both the requirement of ozone itself as the oxidizing agent and the solvent effect observed. Solvents such as chloroform would be expected to solvate the ozone-amine adduct (Ib) and make the abstraction of the proton in Reaction 3 difficult. Thus, loss of molecular oxygen to give the amine oxide becomes the major reaction (Reaction 2). In pentane solu-

tion, no solvation of Ib occurs, and the major reaction course is as described by Reaction 3.

$$tert\text{-BuNH}_2\overset{+}{\text{OOO}^-} \rightleftharpoons tert\text{-Bu}\overset{+}{\overset{\cdot}{\text{NH}}_2} \quad \cdot\ddot{\text{O}}\text{—}\ddot{\text{O}}\text{—}\ddot{\text{O}}:^- \tag{11}$$

<div align="center">VIII   XII   XIII</div>

$$tert\text{-Bu}\overset{\cdot}{\overset{+}{\text{NH}}_2} + \text{CHCl}_3 \longrightarrow tert\text{-Bu}\overset{+}{\text{NH}_3} \quad + \quad \cdot\text{CCl}_3 \tag{12}$$

<div align="center">XII   XIVa   XV</div>

$$:\ddot{\text{O}}\text{—}\ddot{\text{O}}\text{—}\ddot{\text{O}}\cdot^- + \cdot\text{CCl}_3 \longrightarrow \overset{\text{Cl}}{\underset{\text{Cl}}{\text{O—O—O—}\overset{|}{\underset{|}{\text{C}}}\text{—Cl}}} \longrightarrow \overline{\text{Cl}} + \text{Cl}_2\text{C=O} + \text{O}_2 \tag{13}$$

<div align="center">XIII   XV   XIVb</div>

$$2\ tert\text{-BuNH}_2 + \text{Cl}_2\text{C=O} \longrightarrow tert\text{-Bu}\overset{|}{\underset{\text{H}}{\text{N}}}\text{—}\overset{}{\underset{\text{Cl}}{\text{C}}}\text{=O} + tert\text{-Bu}\overset{+}{\text{NH}}_3\overline{\text{Cl}} \tag{14}$$

<div align="center">XIV</div>

$$tert\text{-BuNH}_2 + tert\text{-Bu}\overset{|}{\underset{\text{H}}{\text{N}}}\text{—}\overset{}{\underset{\text{Cl}}{\text{C}}}\text{=O} \longrightarrow tert\text{-BuN=C=O} + tert\text{-Bu}\overset{+}{\text{NH}}_3\overline{\text{Cl}} \tag{15}$$

<div align="center">XVI   XIV</div>

$$4\ tert\text{-BuNH}_2 + \text{O}_3 + \text{CHCl}_3 \longrightarrow tert\text{-BuN=C=O} + 3\ tert\text{-Bu}\overset{+}{\text{NH}}_3\overline{\text{Cl}} + \text{O}_2 \tag{16}$$

$$5\ tert\text{-BuNH}_2 + 4\ \text{O}_3 + \text{CHCl}_3 \longrightarrow tert\text{-BuNO}_2 + tert\text{-BuN=C=O} + \tag{17}$$

$$3\ tert\text{-BuNH}_3^+\text{Cl}^- + 4\ \text{O}_2 + \text{H}_2\text{O}$$

Experimental

The ozonation setup and procedures and the method of determining molecular oxygen yields are described in earlier publications (2, 3, 4, 5, 16). The tert-butylamine, tri-n-butylamine, and solvents were the best

grades available commercially; the amines were further purified by distillation. *tert*-Butylhydroxylamine (IX) (*9*), 2-methyl-2-nitrosopropane (X) (*10*), 2-methyl-2-nitropropane (XI) (*13*), and *tert*-butyl isocyanate (XVI) (*6*) were prepared by known literature procedures.

Ozonation of *tert*-Butylamine. In a typical experiment, a solution of 5.0 mmoles of *tert*-butylamine in 50 ml. of chloroform was cooled to −60°C. and treated with an ozone-nitrogen stream containing 6 mmoles of ozone; the exit gases were analyzed for molecular oxygen (*4, 5, 16*). From the beginning of the ozonation a slight blue color arising from the presence of 2-methyl-2-nitrosopropane (X) appeared, but it was replaced at the end by the purple color of unreacted ozone. A precipitate of *tert*-butylammonium chloride formed during the ozonation. Excess ozone was purged with nitrogen, and it was found, by titrating the iodide trip, that 4.1 mmoles of ozone had reacted. The solution above the precipitate was analyzed for all products except the *tert*-butylammonium chloride by an F and M gas chromatograph, using a 1/4-inch × 20 foot column containing Carbowax 20M on Chromosorb P. The column temperature was 125°C. for all products except *tert*-butyl isocyanate, for which it was 75°C. The *tert*-butylammonium chloride yield was determined by dissolving the precipitate in water and titrating for chloride ion. Ozonations of *tert*-butylhydroxylamine (IX) and 2-methyl-2-nitrosopropane (X) were carried out similarly.

A quantity of 10 mmoles of ozone was passed into 50 ml. of chloroform at −60°C., and the exit gases were passed into 10% sodium carbonate solution. The chloroform was also washed with the carbonate solution, which was then acidified with nitric acid and treated with silver nitrate. Only a faint turbidity was produced. When a solution of 50 ml. of chloroform and 20 mmoles of *tert*-butylamine was allowed to stand at room temperature for 3 hours, only 5 mg. of *tert*-butylammonium chloride were produced.

Ozonation of Tri-*n*-butylamine. In a typical experiment, solutions of 4.0 grams (21.6 mmoles) of tributylamine in 40 ml. of pure pentane or chloroform were treated with 21.6 mmoles of ozone at −45°C. The ozone absorption was quantitative. For pentane solvent, the reaction mixture was extracted with water (3 × 15 ml.) at room temperature and an aliquot of the water extract was used to determine the amine oxide by the titanium chloride method (*7*). For the chloroform reaction mixture, the solvent was removed under reduced pressure, the residue was dissolved in pentane, and the amine oxide was determined as just described. The unreacted starting material and side chain oxidation products were determined with an Aerograph Model 1520B gas chromatograph, equipped with a hydrogen flame detector and a disk integrator. A 1/8-inch × 10-foot column of 30% silicone gum rubber SE-30 on Chromosorb W was used with temperature programming from 75° to 250°C. The principal side chain oxidation products were, in decreasing order of importance, di-*n*-butylamine, 1-di-*n*-butylamino-1-butene, *N,N*-dibutylbutyramide, and *N,N*-dibutylformamide. The ratio of ozone reacting to amine reacting was 1.2 to 1.6.

Acknowledgment

Literature Cited

(1) Bailey, P. S., *Chem. Rev.* **58**, 925 (1958).
(2) Bailey, P. S., *J. Am. Chem. Soc.* **78**, 3811 (1956).
(3) Bailey, P. S., *J. Org. Chem.* **22**, 1548 (1957).
(4) Bailey, P. S., Reader, A. M., *Chem. Ind. (London)* **1961**, 1063.
(5) Bailey, P. S., Kolsaker, P., Sinha, B., Ashton, J. B., Dobinson, F., Batterbee, J. E., *J. Org. Chem.* **29**, 1400 (1964).
(6) Brauner, B., *Ber.* **12**, 1874 (1879).
(7) Brooks, R. T., Sternglanz, P. D., *Anal. Chem.* **31**, 561 (1959).
(8) Delman, A. D., Ruff, A. E., Simms, B. B., Allison, A. R., ADVAN. CHEM. SER. **21**, 119 (1959).
(9) Emmons, W. D., *J. Am. Chem. Soc.* **79**, 5739 (1957).
(10) *Ibid.*, p. 6522.
(11) Henbest, H. B., Stratford, M. J. W., *J. Chem. Soc.* **1964**, 711.
(12) Kolsaker, P., Meth-Cohn, O., *Chem. Commun.* **18**, 423 (1965).
(13) Kornblum, N., Clutter, R. J., Jones, W. J., *J. Am. Chem. Soc.* **78**, 4003 (1956).
(14) Layer, R. W., *Rubber Chem. Technol.* **39**, 1584 (1966).
(15) Otto, M., *Ann. Chim. Phys.* (7) **13**, 106 (1898).
(16) Reader, A. M., Bailey, P. S., White, H. M., *J. Org. Chem.* **30**, 784 (1965).
(17) Shulman, G. P., *Can. J. Chem.* **43**, 3069 (1965).
(18) Solomon, I. J., Hattori, K., Kacmarek, A. J., Platz, G. M., Klein, M. J., *J. Am. Chem. Soc.* **84**, 34 (1962).
(19) Strecker, W., Baltes, M., *Ber.* **54**, 2693 (1921).
(20) Thompson, Q. E., *J. Am. Chem. Soc.* **83**, 845 (1961).

Ozonation of Polycyclic Aromatics

XV. Carcinogenicity and K- and/or L-Region Additivity towards Ozone

EMIL J. MORICONI and LUDWIG SALCE

Fordham University, Bronx, N. Y.

Ozonation of benzo[r,s,t]pentaphene (7) followed by oxidative workup led to benzo[r,s,t]pentaphene-5,8-dione (12) (14%), phthalic acid (13) (4%), p-terphenyl-2,2',3',2''-tetracarboxylic acid-2',3'-anhydride (14) (10%), and 2-(o-carboxyphenyl)-1,10-phenanthrenedicarboxylic acid anhydride (15) (3%), with a 56% recovery of unreacted 7. Ozonation of pentaphene (11) led to a peroxidic mixture which on oxidative workup led to 2,2'-binaphthyl-3,3'-dicarboxaldehyde (16) (16%), 2,2'-binaphthyl-3,3'-dicarboxylic acid (17) (16%), and 13 (2%), with a 28% recovery of unreacted 11. A comparison of the reactivity to ozone of carcinogenic polycyclic aromatics benzo[c]phenanthrene (1), 7,12-dimethylbenz[a]anthracene (2), 3-methylcholanthrene (3), dibenz[a,j]- (4), and dibenz[a,h]anthracene (5), benzo[a]pyrene (6) and 7, and the noncarcinogen 11, all determined in our laboratory, leads us to conclude that there is no simple, consistent correlation between carcinogenicity, K- and L-region additivity towards ozone and the Pullmans' electronic theory of carcinogenesis.

One of the most stimulating theories advanced to relate structure with carcinogenic activity of polycyclic aromatics has been the "electronic theory of carcinogenesis" proposed by the French school of theoretical chemists led by A. Pullman and B. Pullman (*30, 32*) and P. Daudel and R. Daudel (*13*). This quantum mechanical study of the electronic structure of polycyclic aromatics has disclosed two regions of high electron density which are of particular significance in their

chemical behavior. These sites correspond to the 9,10-bond in phenan-
threne (K-region) and the 9,10-positions in anthracene (L-region). A
third site (M-region) involves the positions reactive in metabolic per-
hydroxylation.
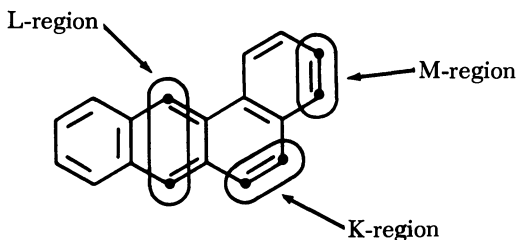
The two most recently expressed fundamental, quantitative propo-
sitions of the theory are (*30*):

(1) The appearance of carcinogenic activity in aromatic hydrocar-
bons is determined by the existence of a K-region, whose complex index
is equal to or smaller than 3.31β. (These complex indices are defined by
Pullman and Pullman (*30*); β is expressed in terms of resonance integral
($\sim$20 kcal./mole); the numerical limits listed (3.31β and 5.66β) are
those calculated for the K- and L-regions of dibenz[*a,j*]anthracene (*4*),
considered as the weakest polycyclic carcinogen.

(2) If, however, the molecule contains also an L-region, its complex
index should be equal to or greater than 5.66β (*see above*).

Simply stated, one of the essential steps in carcinogenesis is the
"reaction" between the carcinogenic polycyclic aromatic and the "cellular
receiver," at or through the K-region of the carcinogen. A necessary but
not sufficient condition for "reactivity" is an active K-region (calcd.
complex index: $= /> 3.31\beta$). A too-reactive L-region, however, (calcd.
complex index: $< 5.66\beta$) may divert the polycyclic carcinogen to a
noncarcinogenic reaction.

Verification of these propositions has taken two different pathways:

(1) Theoretical: quantitative calculations which, for example, pre-
dicted (*30*) the carcinogenicity of benzo[*r,s,t*]pentaphene (*7*) whose
measured potency ($++++$) ranks it between 3-methylcholanthrene
(*3*) and benzo[*a*]pyrene (*6*) (*18, 35*).

(2) Chemical: comparison of cycloaddition reactions occurring
either at the K-region (osmium tetroxide) (*1, 2*) or L-region (maleic
anhydride and photo-oxidation) (*29, 31*).

The inadequacies of this chemical proof seemed to us twofold: the
cycloaddition reactions were unrelated chemically, each occurring at
either the K-/L-regions, whereas the theory considered both regions simul-
taneously; further, these reactions did not occur, or at least had not been
tried with a sufficient number of carcinogenic and noncarcinogenic poly-
cyclic aromatics.

For a chemical reaction to have relevance, it seemed necessary that the reaction occur simultaneously at both K- and L-regions and with all carcinogenic and noncarcinogenic polycyclic aromatics. In our view, this competitive response to the chemical reactant at the two sites within the substrate molecule could lead, intramolecularly, to a conclusion on the relative reactivity of the K- and L-regions. Further, since the chemical reaction could be studied under identical reaction conditions, the results could also lead, intermolecularly, to valid comparisons of relative reactivity.

When this research began, the ozonation reaction seemed ideally suited. Ozone was known to react at both the K-region [in phenanthrene (8)] (4, 5, 34, 37) and L-region (in anthracene) (6, 7, 33). During the decade since, we have investigated the reaction between ozone and some 11 polycyclic aromatics (1–11). Other laboratories have reported

CARCINOGENS
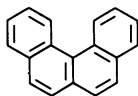
Benzo[c]phenanthrene (19)
1
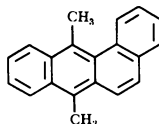
7, 12-Dimethylbenz[a]anthracene (20)
2
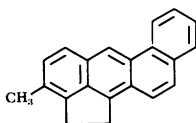
3-Methylcholanthrene (21)
3
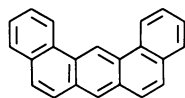
Dibenz[a,j]anthracene (20)
4
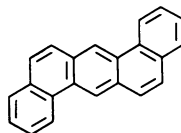
Dibenz[a,h]anthracene (24)
5
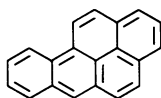
Benzo[a]pyrene (25)
6
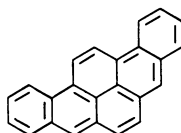
Benzo[r,s,t]pentaphene (26)
7

NONCARCINOGENS
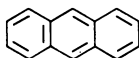
Phenanthrene (34)
8
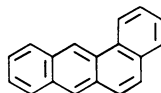
Benz[a]anthracene (27)
9
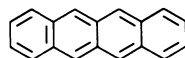
Napthacene (28)
10
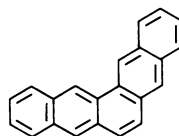
Pentaphene (26)
11

on eight more (naphthalene (8), triphenylene (11), pyrene (36), chrysene (11), benzo[g]chrysene (11), picene (11), dibenz[c,g]phenanthrene (11), and perylene (12). All react with ozone, and reaction occurs uniquely at one or more of the three relevant sites, the K-, L-, and M-regions.

Here, we report on the ozonation of two symmetrically structured polycyclic aromatics at opposite ends of the carcinogenic spectrum—the highly carcinogenic (18, 35) benzo[r,s,t]pentaphene (7) and the inactive (10) pentaphene (11)—and summarize the results of our study of 1–7 and 11. The preparation of 7 and 11 and the isolation and identification of ozonation products 12–18 have been reported previously (26).

Ozonation of Benzo[r,s,t]pentaphene (7) and Pentaphene (11)

Ozonation of 7 in methylene chloride at −78°C. with 3.5 mole equivalents of ozone (requiring passage of 5–6 mole equivalents), followed by oxidative workup (1:1 10% sodium hydroxide: 30% hydrogen peroxide) led to benzo[r,s,t]pentaphene-5,8-dione (12) (14%), phthalic acid (13) (4%), p-terphenyl-2,2′,3′,2″-tetracarboxylic acid-2′,3′-anhydride (14) (10%), and 2-(o-carboxyphenyl)-1,10-phenanthrenedicarboxylic acid anhydride (15) (3%), with a 56% recovery of unreacted 7, as shown below.
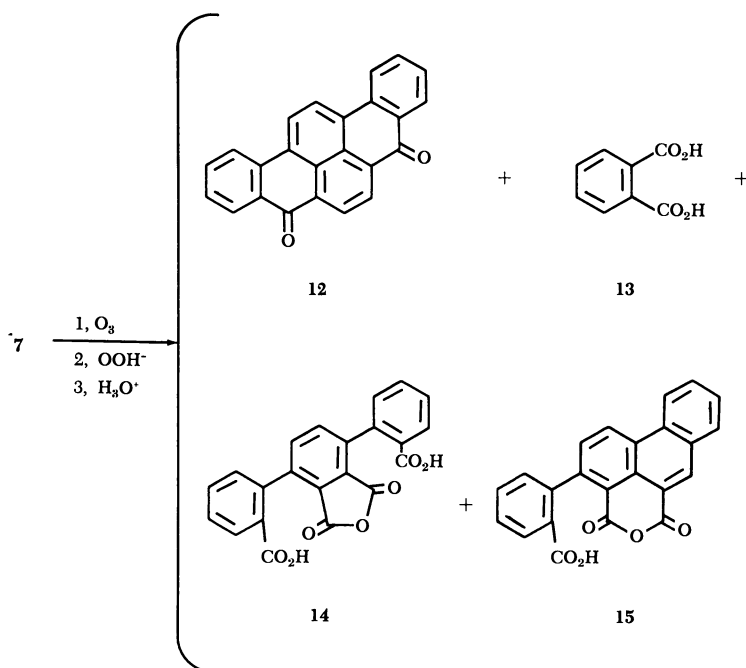
Ozonation of pentaphene (11) (shown below) in methylene chloride at −78°C. with one mole equivalent of ozone led to a peroxidic mixture which on oxidative workup led to 2,2′-binaphthyl-3,3′-dicarboxaldehyde (16) (16%), 2,2′-binaphthyl-3,3′-dicarboxylic acid (17) (16%), and phthalic acid (13) (2%); reductive workup (sodium iodide in acetic acid) gave 16 (25%). In both cases, 28% of unreacted 11 was recovered. Ozonation of 11 with 4 mole equivalents of ozone followed by oxidative workup gave 2,2′,4,4′,5,5′-hexacarboxybiphenyl (18) (53%) and phthalic acid (13) (9%).
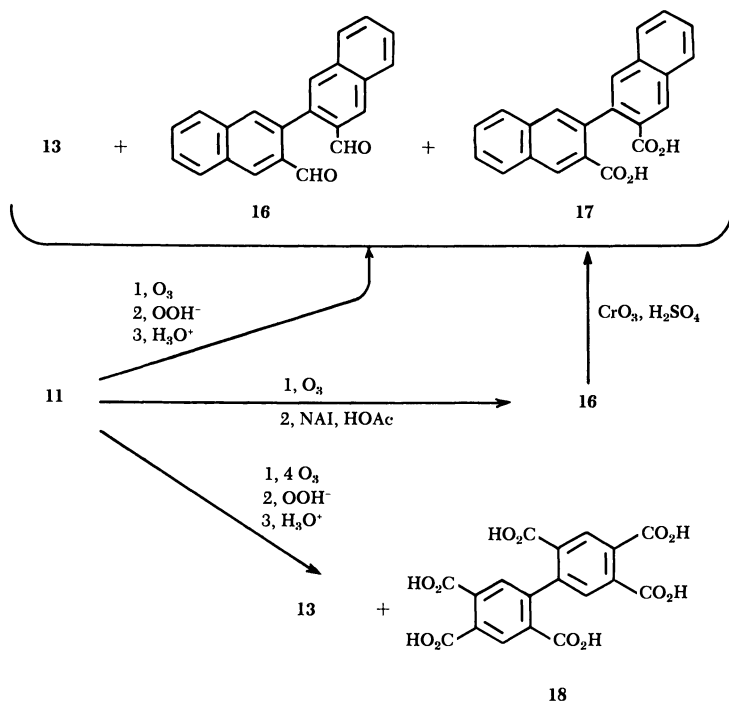
Summary and Conclusions

Table I summarizes the data now available from our laboratory on the ozonation of carcinogenic polycyclic aromatic hydrocarbons 1–7 and the noncarcinogen, 11. All the compounds have at least one K-region (with similar electronic indices, 3.16–3.41β).

Despite some initially encouraging results which suggested that unsubstituted polycyclic aromatics of increasing carcinogenic activity did react more strongly with ozone at the K-region and to a correspondingly lesser degree at the L-region (*20, 23, 28*), we have observed several exceptions.

In their study of protein binding as a necessary, but not sufficient, prerequisite for hydrocarbon carcinogenesis, Heidelberger and Moldenhauer (16) have experimentally demonstrated that 2, 3, and 6 were bound to skin protein to a large and approximately equal extent. A portion of this tissue interaction most probably occurs at the K-region (9), in accordance with the theoretical speculation of the Pullmans (30, 32). Thus, any direct correlation between carcinogenicity and reactivity to ozone would result in predominant electrophilic ozone attack at the K-region of these three ++++ carcinogens. Compounds 2, 3, and 6, however, reacted with ozone exclusively at the L- and M-regions. Certainly 3 was not a privileged compound (30) in which the L-region was protected from attack by ozone.

The lesser carcinogens benzo[c]phenanthrene (1) (19) (+), dibenz[a,j]anthracene (4) (20) (+), and dibenz[a,h]anthracene (5) (24) (++) reacted with ozone predominantly at the K-region. Relative to 6, this response to ozone is the reversal of what would have been predicted by the electronic theory of carcinogenesis.

Both benzo[r,s,t]pentaphene (7) and 6 are ++++ carcinogens, and some identity of response to electrophilic ozone would be predicted. Yet the fusion of a benzene ring to the 1,2-bond in 6 has enhanced the K-region activity of 7 to ozone (13% total of 14 and 15), lowered the

Table I.   Ozonation of Polycyclic

Polycyclic Aromatic	Pullman-Pullman Electronic Indices[a]		Ozone-Polycyclic Mole Ratio
	K-Region	L-Region	
Pentaphene (11)	3.23	5.56	1.0
Benzo[c]phenanthrene (1)	3.41	—	0.6
Dibenz[a,j]anthracene (4)	3.31	5.66	1.0
Dibenz[a,h]anthracene (5)	3.30	5.69	1.0
7,12-Dimethylbenz[a]anthracene (2)			1.0
3-Methylcholanthrene (3)			1.5
Benzo[a]pyrene (6)	3.16	—	1.0
Benzo[r,s,t]pentaphene (7)	3.16	—	3.5

[a] See Ref. 2.
[b] Reaction conditions: ozonation at −78°C. in methylene chloride or 3:1 methylene chloride : methanol, followed by alkaline hydrogen peroxide workup (unless otherwise stated). Ozonation of 7 and 11 also produced 13 (4% and 2%, respectively). These yields are not included in either K- or L- region product totals since the site of ozone attack to produce 13 is unknown.
[c] 1-(o-Carboxyphenyl)-2-naphthoic acid.
[d] 1,4-Dimethyl-3-hydroxymethyl-2-phenylnaphthalene-2'-carboxylic acid.
[e] Yield of biphenyl from the presumed primary ozonation product, 2,2',3,4,5-pentacarboxybiphenyl.

reactivity of the L-region (14% of **12**), and decreased the over-all ease of ozonation of **7** relative to **6**.

The yields of K-region cleavage products, under the same conditions of ozonation vary from 0–45% (Table I). Even considering the experimental errors involved in ozonation and oxidative workup, there is no simple, observable correlation between the Pullmans' theoretical K-region values and the reactivity of these sites to electrophilic ozone.

Although three of the compounds listed in Table I have formal L-regions, the most potent carcinogens (**2, 3, 6,** and **7**) do not. Two (**6** and **7**) can be considered to have such sites whose activity has been suppressed by a fused ring, and two (**2** and **3**) are essentially substituted at the L-region. Thus, the ozonation results for these four compounds, summarized in Table I, cannot truly be considered L-region quinoid products. Despite this, the relative yields of such quinones clearly show an inverse relationship between the theoretical, predicted low L-region activity and the course of the ozone reaction.

To sum up, a comparison of the observed relative reactivity of **7** and **11** to ozone with that predicted by Pullmans' theoretical calculations (*30, 32*), and an analysis of all the available ozonation data lead us to conclude that there is no simple, consistent correlation between carcino-

Aromatic Hydrocarbons

Actual % Yields of K- and L-Region Ozonation Products[b]		% Recovery	
Total K-Region Cleavage Products	L-Region Quinoid Products	Unreacted Polycyclic Aromatic	Carcinogen Potency
32	0	28	0
30[c]	0	40	+
42	10	32.5	+
45	0	0	++
14[d]	29[g]	0	+++
4[e]	32[h]	0	+++
0	27-30[i]	60-65	+++
13[f]	14[j]	56	+++

[f] Total yield of **14** and **15**.
[g] Composed of 23% of benz[*a*]anthracene-7,12-dione and 6% of 1,2-anthraquinone-dicarboxylic acid.
[h] Composed of 15% of 8,9-dimethylbenz[*a*]anthracene-7,12-dione and 18% of 1,2-dimethylanthraquinone. Undoubtedly the yields of primary ozonization products, 9-methylbenz[*a*]anthracene-7,12-dion-8-acetic acid, and 2-methyl-5,6-dicarboxyanthraquinon-1-acetic acid are higher.
[i] No alkaline hydrogen peroxide workup required.
[j] Compound **12**.

genicity, K- and L-region additivity towards ozone, and the Pullmans' electronic theory of carcinogenesis.

Finally, even the observation (14, 21) that the metabolic reactions likely to be related to the course of these ozone reactions are those of detoxification rather than of carcinogenic responsibility is not without exception—cf., e.g., the seven metabolic oxidation products of 5 (22) to the single ozonation product (24).

Acknowledgment

Literature Cited

(1) Badger, G. M., *J. Chem. Soc.* **1949**, 456.
(2) *Ibid.*, **1950**, 1809.
(3) Badger, G. M., Campbell, J. E., Cook, J. W., Raphael, R. A., Scott, A. I., *J. Chem. Soc.* **1950**, 2326.
(4) Bailey, P. S., *J. Am. Chem. Soc.* **78**, 3811 (1956).
(5) Bailey, P. S., Mainthia, S. B., *J. Org. Chem.* **23**, 1089 (1958).
(6) Bailey, P. S., Ashton, J. B., *J. Org. Chem.* **22**, 98 (1957).
(7) Bailey, P. S., Kolsaker, P., Sinha, B., Ashton, J. B., Dobinson, F., Batterbee, J. E., *J. Org. Chem.* **29**, 1400 (1964).
(8) Bailey, P. S., Bath, S. S., Dobinson, F., Garcia-Sharp, F. J., Johnson, C. D., *J. Org. Chem.* **29**, 697 (1964).
(9) Bhargava, P. M., Heidelberger, C., *J. Am. Chem. Soc.* **78**, 3671 (1956).
(10) Cook, J. W., Hieger, I., Kennaway, E. L., Mayneord, W. J., *Proc. Roy. Soc. (London)* **B111**, 455 (1932).
(11) Copeland, P. G., Dean, R. E., McNeil, D., *J. Chem. Soc.* **1961**, 1232.
(12) Copeland, P. G., Dean, R. E., McNeil, D., *Chem. Ind.* **1959**, 329.
(13) Coulson, C. A., *Advan. Cancer Res.* **1**, 1 (1953).
(14) Cromwell, N. H., *Am. Scientist* **53**, 213 (1965).
(15) Danheux, C., Hanoteau, L., Martin, R. H., Van Binst, G., *Bull. Soc. Chim. Belges* **72**, 2891 (1963).
(16) Heidelberger, C., Moldenhauer, M. G., *Cancer Res.* **16**, 442 (1956).
(17) Johnson, C. D., Bailey, P. S., *J. Org. Chem.* **29**, 703 (1964).
(18) Lacassagne, A., Zajdela, F., Buu-Hoi, N. P., Chalvet, O., *Compt. Rend.* **244**, 273 (1957).
(19) Moriconi, E. J., Salce, L., Taranko, L. B., *J. Org. Chem.* **29**, 3297 (1964).
(20) Moriconi, E. J., Taranko, L. B., *J. Org. Chem.* **28**, 1831 (1963).
(21) *Ibid.*, p. 2526.
(22) *Ibid.*, p. 2526, footnote 4.
(23) Moriconi, E. J., O'Connor, W. F., Rakoczy, B., *J. Org. Chem.* **27**, 3618 (1962).
(24) Moriconi, E. J., O'Connor, W. F., Schmitt, W. J., Cogswell, G. W., Furer, B. P., *J. Am. Chem. Soc.* **82**, 3441 (1960).
(25) Moriconi, E. J., O'Connor, W. F., Rakoczy, B., *J. Am. Chem. Soc.* **83**, 4618 (1961).

(26) Moriconi, E. J., Salce, L., *J. Org. Chem.* **32,** 2829 (1967).
(27) Moriconi, E. J., O'Connor, W. F., Wallenberger, F. T., *J. Am. Chem. Soc.* **81,** 6466 (1959).
(28) Moriconi, E. J., O'Connor, W. F., Taranko, L. B., *Arch. Biochem. Biophys.* **83,** 283 (1959).
(29) Newman, M. S., Otsuka, S., *J. Nat. Cancer Inst.* **21,** 721 (1958).
(30) Pullman, A., Pullman, B., *Advan. Cancer Res.* **3,** 117 (1955).
(31) *Ibid.*, pp. 141-144.
(32) Pullman, A., Pullman, B., "La Cancerisation par les Substances Chimiques et la Structure Moléculaire," Masson et Cie, Paris, 1955.
(33) Roitt, I. M., Waters, W. A., *J. Chem. Soc.* **1949,** 3060.
(34) Schmitt, W. J., Moriconi, E. J., O'Connor, W. F., *J. Am. Chem. Soc.* **77,** 5640 (1955).
(35) Unseren, E., Fieser, L. F., *J. Org. Chem.* **27,** 1386 (1962).
(36) Vollmann, H., Becker, H., Correll, M., Streeck, H., *Ann.* **531,** 1 (1937).
(37) Wibaut, J. P., DeBoer, Th. J., *Konikl. Ned. Akad. Wetenschap.* **59,** 421 (1956).
(38) Wibaut, J. P., DeBoer, Th. J., *Rec. Trav. Chim.* **78,** 183 (1959).

66

Comments on the Mechanism of Ozone Rate Action with Hydrocarbons and Alcohols

SIDNEY W. BENSON

Department of Thermochemistry and Chemical Kinetics, Stanford Research Institute, Menlo Park, Calif. 94025

The ozone molecule has a bond dissociation energy of 24 kcal. for decomposition into an oxygen molecule and a ground state oxygen atom. Almost all of the gas-phase work I know of concerning ozone and organic materials (for $T > 25°C.$) can be explained in terms of an initiation step, producing oxygen atoms from the ozone, followed by chain-propagation steps, as follows:

$$M + O_3 \underset{t}{\overset{i}{\rightleftarrows}} O_2 + O + M$$

$$O + RH \overset{1}{\rightarrow} R\cdot + \cdot OH$$

$$R\cdot + O_3 \overset{2}{\rightarrow} RO\cdot + O_2$$

$$RO\cdot + RH \overset{3}{\rightarrow} ROH + R\cdot$$
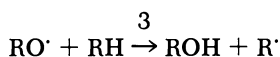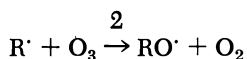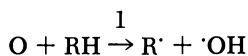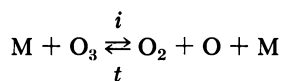
Step 2 in this sequence is exothermic by about 66 kcal. If any significant share of this is left as excitation energy of the alkoxy radical, it will probably dissociate further into a simple aldehyde or ketone, plus a smaller alkyl group. However, at dry ice temperatures or lower, the initiation step, i, is almost certainly too slow to account for the reaction rates which have been reported here. The suggestion—that ozone attacks alcohols and hydrocarbons by abstracting hydrogen to form the HO_3 radical—appears equally unlikely.

$$O_3 + RH \overset{4}{\rightarrow} HO_3\cdot + R\cdot$$
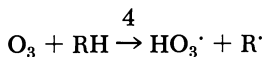
The H—O bond in the HO_3 radical can be calculated to have a bond strength of about 61 ± 2 kcal. (1). If the R—H bond is taken as 91, as

reported for 2-propanol or in isobutane, then Reaction 4 is endothermic by some 30 kcal. At dry ice temperatures this is even slower by many powers of 10 than the initiation step, *i*, above. Step 4 in alcohol solution may benefit by a heat of solution of the $HO_3\cdot$ radicals to the extent of possibly 10 or perhaps 12 kcal. This would make the over-all reaction endothermic by only 18 or 19 kcal., if we ignore any possible solvation of ozone, which may amount actually to a few kcalories.

This is still too high an activation energy to account for a simple one-step reaction, which has been reported. On the other hand, if the net increment in solvation energy is as large as 12 kcal., then Step 4 could conceivably be an initiation step in a reasonably long chain mechanism. If, however, a chain reaction is involved, the most likely next steps would be the attack of $R\cdot$ radicals on either oxygen or on ozone. The oxygen reaction is likely to be diffusion controlled and would lead to peroxy-type products. However, attack on ozone is more likely to lead to formation of free acid and smaller alkyl radicals, and these are not observed as major products.

It thus appears as if a radical mechanism cannot satisfy the observations. The alternative has been suggested that Step 4 occurs as a hydride ion abstraction with the formation of a dissociated ion pair, HO_3^- and R^+. If this is the case, it would require unusually large electron affinities for the $HO_3\cdot$ radical or unusually small ionization potentials for the $R\cdot$ radical to account for the data. I don't believe that independent measurements of these quantities can be adduced to support such a contention. Nevertheless, an intimate ion pair mechanism cannot be completely ruled out at the moment.

The thermochemistry of polyoxide radicals and molecules can also be used to comment on the mechanism of olefin ozonization. One can ask if addition of ozone to the double bond occurs *via* a biradical with the formation of one bond at a time or through a concerted process to produce cyclic trioxide. If it produces one bond at a time, it must go through the formation of an $RO_3\cdot$ type biradical as shown in Reaction 5. However, the energetics of Reaction 5 (*1*) show that the activation energy would be much too high for this reaction to be appreciable at dry ice temperatures, where it has been observed. We must then conclude that addition of ozone to olefin at low temperatures, or probably also at higher temperature, is a concerted process leading to the direct formation of a cyclic trioxide, Reaction 5′, and this is pretty much in accord with the data recently reported. However, the other data reported on the stability of these cyclic peroxides is in accord with our own estimates of the bond strength of the O—O bond in such trioxides. Normally, it would be of the order of 21 kcal. In the case of the strained five-membered ring with strain energies around 6 kcal., it should have a bond strength of

$$O_3 + \text{olefin} \xrightarrow{5} \text{biradical} \xrightarrow{8}$$
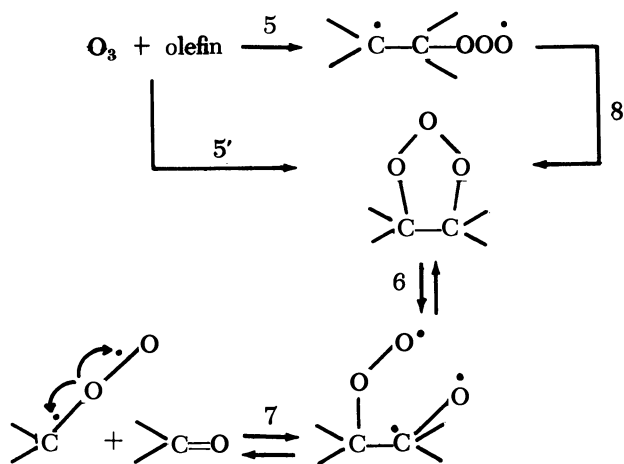
some 15 kcal. Thus the opening of this ring to produce the oxyperoxy biradical, as shown by Reaction 6, would be expected to be reasonably rapid at dry ice temperatures. One might expect this biradical to be the precursor of the products which are seen in the subsequent displacement reaction with carbonyl and aldehyde species or in the secondary decomposition of ozonides.

Literature Cited

(1) Benson, S. W., Shaw, R., ADVAN. CHEM. SER. 75, 288 (1968).

67

Type II Photosensitized Oxygenation Reactions

KLAUS GOLLNICK

University of Arizona, Tucson, Ariz.[a]

In Type II photo-oxygenation reactions, singlet oxygen is produced by an energy transfer process from the electronically excited light absorber. Various classes of compounds, such as polycyclic aromatic hydrocarbons, cyclic 1,3-dienes, and furans as well as olefins containing allylic hydrogens are suitable substrates for the reaction with singlet oxygen. Stereoelectronic effects exerted by olefins on the reactions with $^1O_2$ are dealt with, and the mechanism of $^1O_2$ formation is discussed. Preliminary results on $^1O_2$ production and its reaction with 2,5-dimethylfuran as a function of the triplet energy of (π,π^*)- and (n,π^*)-sensitizers are reported.

Photo-oxygenation reactions of organic compounds, A, in solution,

$$A + O_2 \xrightarrow{\quad h\nu/(\text{sensitizer}) \quad} AO_2$$
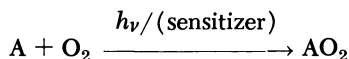
affording addition products (AO_2), may occur as direct or indirect (sensitized) photo-oxygenation reactions, depending on whether A or a molecule other than A—*i.e.*, a photosensitizer—absorbs the light. (Only when the exciting photons possess wavelengths shorter than 2000 A. must absorption by O_2 be considered.) Furthermore, depending on whether free radicals or only electronically excited molecules are involved as intermediates, Type I processes may be distinguished from Type II processes (*17*).

The benzophenone-sensitized photo-oxygenation of 2-propanol (*53*) may be considered as a typical example of a Type I process, in which the electronically excited benzophenone initiates a free radical oxidation by abstracting a hydrogen atom from 2-propanol. The initiation is then followed by O_2 addition to the 2-hydroxyisopropyl radical and reaction

---

[a] On leave of absence from the Max-Planck-Institut für Kohlenforschung, Abteilung Strahlenchemie, Mülheim an der Ruhr, Germany.

with a hydrogen donor, which may be either another 2-propanol molecule in a chain-propagating step or the benzophenone ketyl radical in a termination step. Thus, the over-all reaction is

$$CH_3CHOHCH_3 + O_2 \xrightarrow{h\nu/\text{benzophenone}} CH_3C(OH)CH_3$$
$$|$$
$$OOH$$
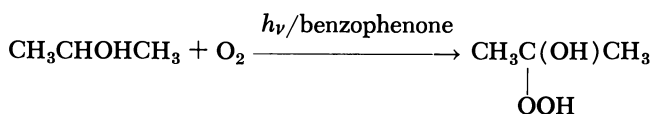
The Type II photo-oxygenation reactions with which we are concerned occur by a completely different mechanism. The main feature of these reactions is that an "activated oxygen" is formed during the reaction, which can react stereoselectively with certain substrates to give the addition products. Today, we have reason to believe that the "activated oxygen" is the excited singlet oxygen, $^1O_2$.

Polycyclic aromatic hydrocarbons such as anthracenes, tetracenes, and pentacenes, as well as cyclopentadienes, cyclohexa-1,3-dienes, cyclohepta-1,3-dienes, and furans, have been found to be suitable diene systems to which the singlet oxygen adds as a dienophile in a 1,4-cycloaddition reaction. Thus, endoperoxides (transannular peroxides) and, in the case of furans, ozonides of the corresponding cyclobutadienes are the primarily produced, more or less stable addition products (*2, 21, 22*).

Olefins containing at least one allylic hydrogen are suitable substrates and are of special importance and interest with regard to the intrinsic mechanism involved in their reactions with singlet oxygen. Allylic hydroperoxides are formed, but the mechanism of their formation is clearly distinct from that by which allylic hydroperoxides are produced in thermal or photochemically initiated (*see* example above for a Type I process) autoxidation reactions. This has unequivocally been shown with optically active limonene as a substrate, which gives rise to different products in free radical and Type II photo-oxygenation reactions (*22, 57, 61*).

While, for example, the thermal autoxidation reaction of (+)-limonene (1) proceeds as a free radical chain reaction (*61*), the photosensitized oxygenation of 1 occurs according to the scheme shown at the top of the next page (*51, 52*).

Phenomenologically, this reaction may be described as occurring in three steps:

(1) Attachment of oxygen to one of the carbon atoms of the double bond (in the scheme to C_1).
(2) Shift of the double bond to the allylic position (C_2, C_3)
(3) Migration of the allylic hydrogen to the terminus of the peroxy group.

Mechanistically, however, the reaction probably takes place in a concerted fashion involving a cyclic six-membered transition state (*13, 22, 45, 56, 57*).

$$-\!\!-\overset{|}{C_1}\!\!=\!\!\overset{|}{\underset{\underset{H}{|}}{C_2}}\!\!-\!\!\overset{|}{C_3}\!\!-\!\!- \qquad \xrightarrow{h\nu/\text{sensitizer}/O_2} \qquad -\!\!-\overset{|}{\underset{\underset{OOH}{|}}{C_1}}\!\!-\!\!\overset{|}{C_2}\!\!=\!\!\overset{|}{C_3}\!\!-\!\!-$$

11% 12% 22% racemate 19% racemate 13% 13% + unidentified product 10%

(1) free radical autoxidation
(2) reduction

1   1a

(1) sens./hν/O$_2$. (2) reduction

2 3 4 5 6 7
34% 10% 5% 10% 21% 20%
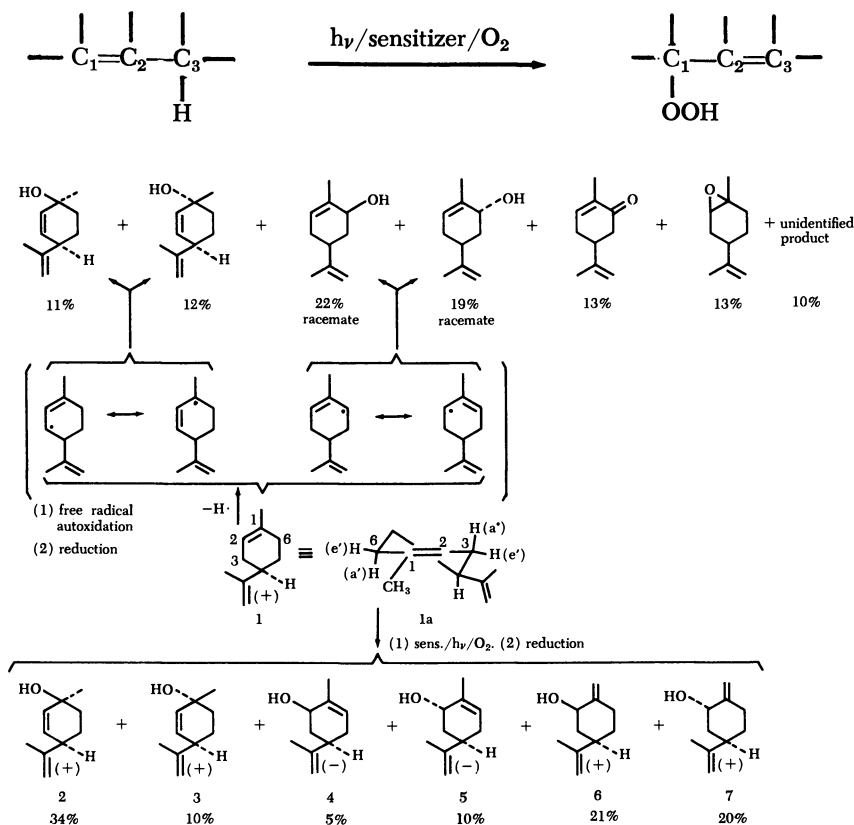
The following results are in favor of the assumed concerted reaction:

(1) Only those allylic hydrogens are used in the reaction which are cis-oriented with respect to the oxygen attack on the double bond carbons, as was demonstrated with 7α-D- and 7β-D-cholesterol (45) affording 5α-hydroperoxy-Δ⁶-cholesten-3β-ol (58).

(2) Trialkylsubstituted ethylenes such as limonene (57) and 1-methylcyclohexene (50) give rise to ratios of tertiary-secondary hydroperoxides of about 44 to 56, while open-chain olefins such as trimethylethylene, 1,1-dimethyl-2-ethylethylene, 2,6-dimethyl-2-octene, myrcene, β-citronellol, linalool, and 1,1-dimethyl-2-benzylethylene give ratios of tertiary-secondary hydroperoxides between 54 to 46 and 60 to 40 (31, 43, 47, 60, 63, 66). Since there is no hydrogen abstraction prior to oxygen addition to one of the double bond carbons, this addition must be the first step if a multistep reaction takes place. Whatever the so-formed intermediates may be, however, diradical species such as 8a or 8b, or ionic species such as 9a or 9b [the latter has been suggested by some authors (37, 67)], secondary hydroperoxides should be produced almost exclusively from the nonsterically hindered olefins since in the case of the peroxy intermediates, 8a and 9a, the most stable (tertiary) alkyl radical or carbonium ion, respectively, should be formed, and in the case of the

perepoxy intermediates, **8b** and **9b**, the attacking radical or cation is more strongly bonded to the carbon with the smallest number of alkyl substituents (*94*). Obviously, there is not much discrimination between the two double bond carbon atoms, and the slight deviations from 1 to 1 ratios in all these cases are probably due to stereochemical rather than electronic effects exerted by the olefins on the reaction with singlet oxygen.


8a

8b

9a

9b
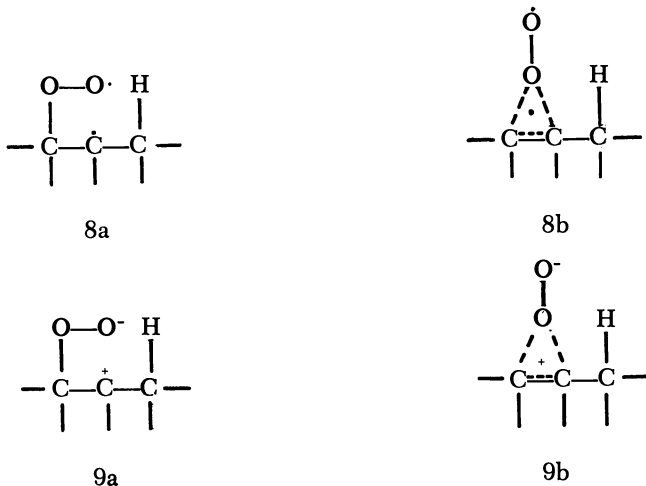
(3) According to the results obtained in conformational analysis, limonene (in solution at room temperature) assumes a half-chair conformation with the isopropenyl group in an equatorial position (*6, 34*) (*see* Formula **1a**). As the enhanced formation of **2** as compared with **3** and the 1 to 1 ratio of **6** and **7** show, there is no steric hindrance exerted by the equatorial side chain on an oxygen attack at C_1 or C_2. Therefore, the stereoselective reaction of limonene with singlet oxygen as revealed by the product distribution must be caused by an enhanced reactivity of the quasi-axial (*a'*) hydrogens at C_3 and C_6 as compared with the corresponding quasi-equatorial (*e'*) hydrogens. Furthermore, the 1 to 1 ratio of **6** and **7** and their enhanced production as compared with the formation of **4** and **5** must be caused by the fact that the C—H bond of the methyl group can approach (on both sides of the limonene molecule) the perpendicular arrangement with respect to the double bond plane, necessary for developing the new double bond, even better than a quasi-axial ring-allyl hydrogen. The increased reactivity of allylic hydrogens, —CH₃ > quasi-axial > quasi-equatorial, has been found to be a general phenomenon (*17, 45, 57*).

(4) The tertiary hydroperoxides formed from the open-chain olefins mentioned above all contain trans-substituted double bonds (*63, 66*). As one can see from models, the most stable conformations of these olefins (general formula **10**) are those in which one of the allylic hydrogens at C_3 is eclipsed with the double bond (**10a,b**). Reaction with the other allylic hydrogen must therefore give rise to trans-substituted double bonds. The conformational isomer **10c**, which would give rise to cis-substituted double bonds by a concerted reaction, is expected to be highly

unfavored because of strong steric repulsion between the R group and the methyl group at C_1 which is cis to this R group. The formation of intermediates such as **8** or **9** in a multistep reaction would also explain the occurrence of the thermodynamically more stable trans-substituted double bonds in the tertiary hydroperoxides. However, the nearly exclusive formation of the secondary hydroperoxide, **15**, from 1,1-dimethyl-2-isopropylethylene, **13** (*22, 63, 66*), supports the assumption of a concerted reaction: The most stable conformation of **13** is **13a**, in which the allylic hydrogen at C_3 needed for the formation of the tertiary hydroperoxide, **14**, is eclipsed with the double bond, the most unfavorable position an allylic hydrogen can assume for a concerted reaction with oxygen. Therefore, the production of **14** should be almost suppressed. On the other hand, if the tertiary hydroperoxides (**11**) were formed by a multistep reaction, one would expect a reasonable amount of **14** to be formed from **13** by the same mechanism.

(5) Methyl groups such as the C_8-methyl groups of α-pinene, **16** (*54*), Δ^3-carene, **18** (*23, 62*), Δ^4-carene, **22**, and the Δ^2-carenes, **25** and **27** (*19*), or the angular methyl groups attached to C_{10} in certain steroids (*10, 45, 46, 55, 58*) may completely shield the double bond against an attack of the singlet oxygen. Thus, steric shielding effects in addition to conformational effects exerted by the allylic hydrogens cause the stereoselectivity


10   10a   10b

10c

11   12

54-60%   46-40%

13

13a

14

< 5%

15

> 95%

16

16a

17
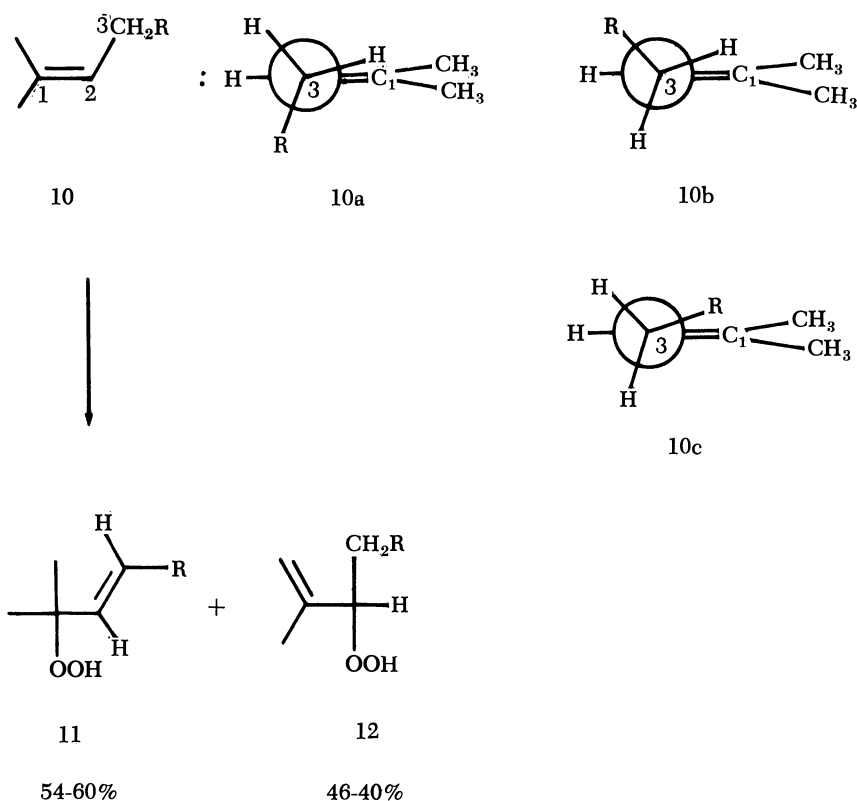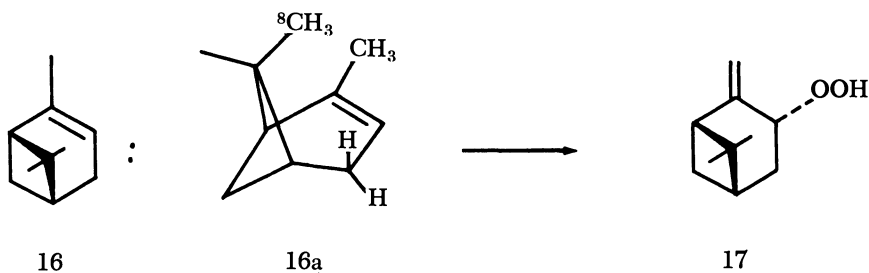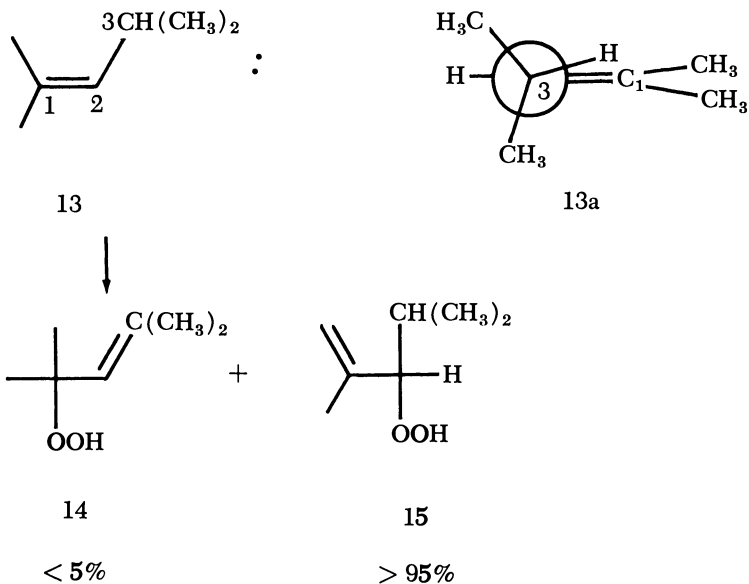
of Type II photo-oxygenation reactions. Interestingly enough, the ob-
served product distribution from Δ^3-carene was explained (*23*) by assum-
ing that of the two boat conformations, **18a** and **18b**, only the closed-boat
form, **18b**, takes part in the hydroperoxidation reaction since only if this
is the case, the product ratios of **19** to (**20** + **21**) and of **20** to **21** should
be 1 to 1. The attack of oxygen on the α-side of **18** at C_3 and C_4 should
follow a statistical pattern and the α-hydrogens at C_2 and C_5 should be
as available as the allylic hydrogens of the C_{10}-methyl group. On the
other hand, a β-attack on **18b** should be completely prevented by the
C_8-methyl group. Recently, it was shown that Δ^3-carene exists to about
93% in the closed-boat conformation (**18b**) at 20°C. (*1*) at which the
photo-oxygenation reaction was carried out.

In preparative organic chemistry, much use has been made of the
stereoselective Type II photo-oxygenation reaction since the primarily
produced allylic hydroperoxides can be reduced under retention of con-
figuration. However, depending on the nature of the allylic hydroper-

oxides and the particular reaction conditions applied (temperature, concentrations of the substrates, solvents, etc.), secondary reactions may occur—*e.g.*, rearrangements of allylic tertiary hydroperoxides to secondary allylic hydroperoxides, elimination of water from secondary allylic hydroperoxides to yield α,β-unsaturated ketones, and fragmentation of allylic hydroperoxides to carbonyl compounds. Furthermore, Type I processes (free radical chain autoxidation reactions) may accompany Type II reactions, especially when relatively unreactive olefins (mono- or disubstituted olefins) serve as substrates (*17*).

25   26

27
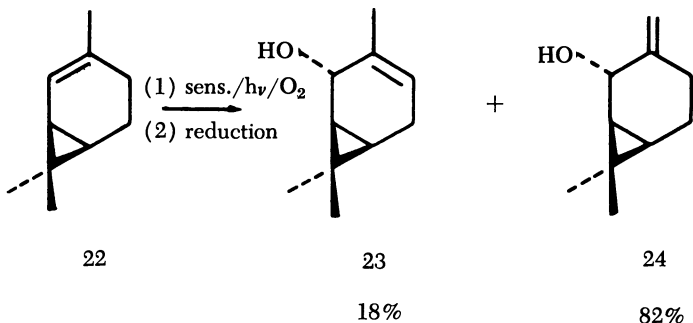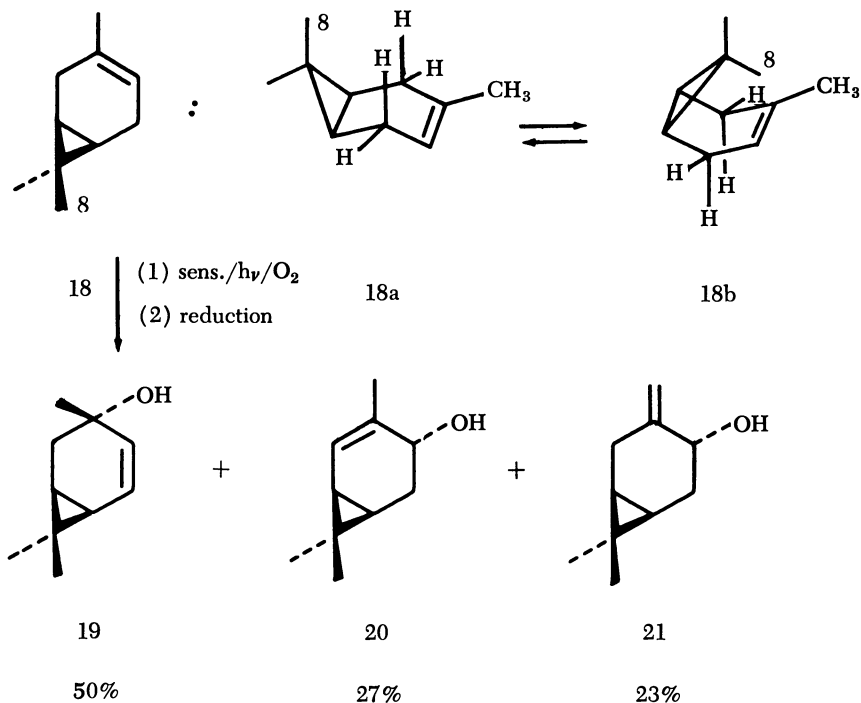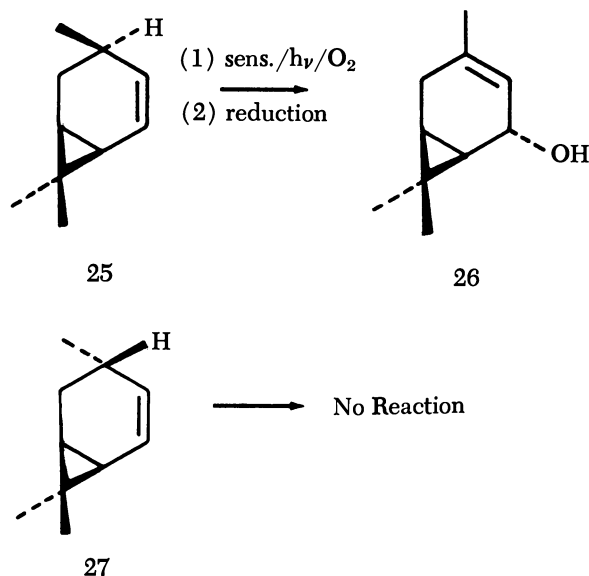
Generally, tetraalkyl-substituted double bonds react with singlet oxygen at faster rates than do trialkyl-substituted double bonds, which in turn react faster than dialkyl-substituted ones (*22, 50, 63, 66*). According to the reaction sequence of Type II photo-oxygenation reactions given below, the reaction of a substrate with singlet oxygen (Step 9) competes with the spontaneous deactivation of singlet oxygen (Step 8). From the variation of the rate of oxygen consumption with the concentration of the substrate, k_8/k_9 can be determined for various substrates. Since k_8 remains constant under similar reaction conditions, relative reactivities of the substrates towards singlet oxygen can be obtained (*56*). In Table I, relative free energies of activation, $\Delta\Delta F^\ddagger$, for the reaction of singlet oxygen at C_1 and C_2 of different olefins are given, calculated from experimental k_8/k_9 values with tetramethylethylene (TME) (**28**) as the reference compound:
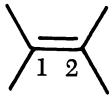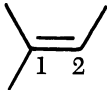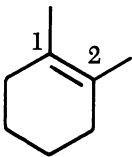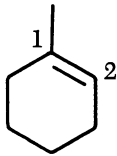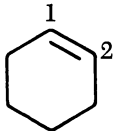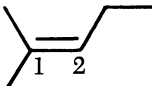
$$\Delta\Delta F^\ddagger = RT \ln k_{rel} \ (T = 293°K., \text{ reaction temperature}) \tag{1}$$

with

$$k_{rel} = \frac{(k_8/k_{9,TME})}{(k_8/k_{9,substr.})} \cdot \frac{p_{substr.}}{p_{TME}} \cdot \frac{n_{TME}}{n_{substr.}} \tag{2}$$

in which p is the factor which accounts for the product distribution and n is the number of equivalent transition states leading to a particular product. In order to determine n, the equivalence of one ring-allylic hydrogen to three CH$_3$-allylic hydrogens in a concerted reaction has been assumed. Furthermore, no distinction between quasi-axial and quasi-equatorial hydrogens was made.
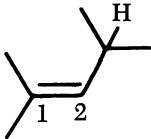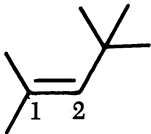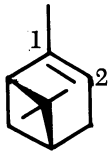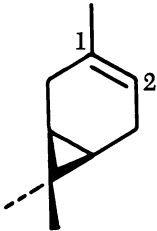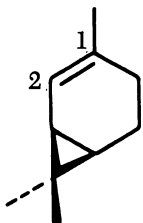
Table I.   Relative Free

Compound	$k_8/k_{9,substr.}$, Moles/L.	$\dfrac{k_8/k_{9,TME}}{k_8/k_{9,substr.}}$
(structure) 28	0.003	1.00
(structure) 30	0.055	0.055 0.045[a] 0.07[b]
(structure) 33	0.030	0.100
(structure) 36	1.20	0.0025 0.0020[a] 0.002[b] 0.0082[c]
(structure) 40	26.0	0.00012
(structure) 42	0.18	0.0166

Energies of Activation

Reaction at				$\Delta\Delta F^{\ddagger}$, *Kcal./Mole*, Reaction at	
C-1		C-2			
p_1	n_1	p_2	n_2	C-1	C-2
0.50	4	0.50	4	0	0
0.54	2	0.46	4	1.25	1.75
0.44(M)	2	0.44(M)	2	1.01(M)	1.01(M)
0.06(R)	2	0.06(R)	2	2.17(R)	2.17(R)
0.45	2	0.40(M)	2	3.15	3.20(M)
		0.15(R)	2		3.79(R)
0.50	2	0.50	2	4.86	4.86
0.55	2	0.45	4	1.93	2.44
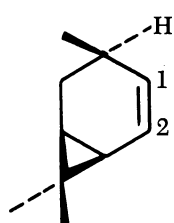
Table I.

Compound		$k_8/k_{9,substr.},$ Moles/L.	$\dfrac{k_8/k_{9,TME}}{k_8/k_{9,substr.}}$
	13	1.30	0.0023
	45	4.20	0.00071
	16	8.20	0.00037
	18	0.40 [d]	0.0075
	22	0.21 [d]	0.0153

Continued

Reaction at				$\Delta\Delta F^{\ddagger}$, Kcal./Mole, Reaction at	
C-1		C-2		C-1	C-2
p_1	n_1	p_2	n_2		
0.05	2	0.95	4	4.48	3.17
—	–	1.00	4	—	3.83
—	–	0.94	1	—	3.43
0.50	1	0.25(M)	1	2.04	2.45(M)
		0.25(R)	1		2.45(R)
—	–	0.80(M)	2	—	1.75(M)
		0.20(R)	1		2.16(R)

Table I.

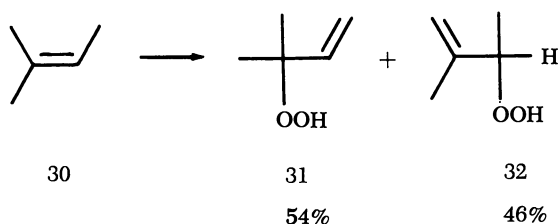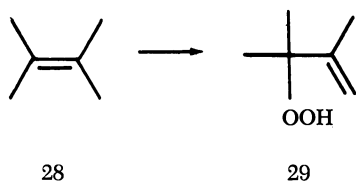| Compound	$k_8/k_{9,substr.,}$ Moles/L.	$\dfrac{k_8/k_{9,TME}}{k_8/k_{9,substr.}}$
25	$0.17^{\,d}$	0.0177

$\Delta\Delta F^{\ddagger}$ calculated from experimental data taken from Schenck and Gollnick (56).
[a] Obtained from photosensitized oxygenation (11, 25).
[b] Obtained from H_2O_2/NaOCl experiments (11, 25).
[c] Calculated from data given by Kopecky and Reich (37).

Since only relative rate constants could be measured so far and no activation energies for the compounds of Table I have been determined yet, the contributions of $\Delta\Delta H^{\ddagger}$ and $\Delta\Delta S^{\ddagger}$ to a particular $\Delta\Delta F^{\ddagger}$ cannot be separated. However, differences in $\Delta\Delta F^{\ddagger}$ obtained for **28** and **30** as well as for an oxygen attack on C-1 of **33**, **36**, and **40** forming the cyclohexene derivatives **34**, **37**, and **41**, respectively, are probably mainly due to differences in $\Delta H^{\ddagger}$. On the other hand, differences in $\Delta\Delta F^{\ddagger}$ obtained for the formation of **34** and **35** from **33** and of **37**, **38**, and **39** from **36** seem to be due mainly to differences in $\Delta S^{\ddagger}$. Thus, there seems to be a marked decrease in $\Delta H^{\ddagger}$ with an increasing number of methyl groups directly attached to a double bond carbon, indicating the electrophilicity of
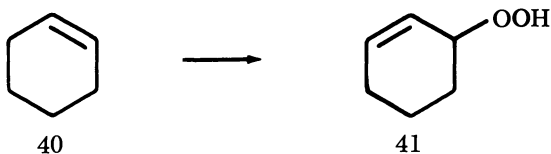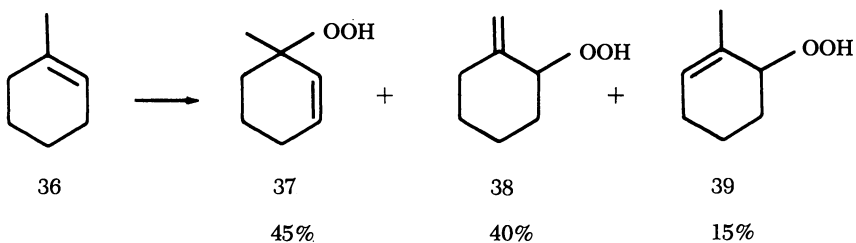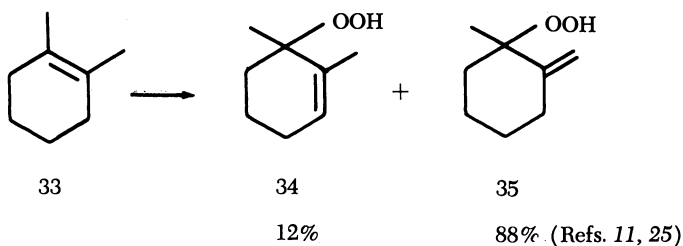

28   29

30   31   32

54%   46%

Continued

Reaction at				$\Delta\Delta F^{\ddagger}$, Kcal./Mole, Reaction at	
C-1		C-2			
p_1	n_1	p_2	n_2	C-1	C-2
—	-	1.00	1	—	1.14

[a] From (20).
M. Reaction occurring with CH_3-allylic hydrogen.
R. Reaction occurring with ring-allylic hydrogen.

33   34   35

12%   88% (Refs. 11, 25)

36   37   38   39

45%   40%   15%

40   41

singlet oxygen. The increase in $\Delta\Delta F^{\ddagger}$ for ring-allylic hydrogens as compared with CH_3-allylic hydrogens reflects the conformational effects of the two different hydrogens on the reaction with oxygen. [No distinction

between the two different ring-allylic hydrogens, quasi-axial and quasi-equatorial, has been made in these calculations. However, from the foregoing discussion it should be obvious that the quasi-equatorial allylic hydrogens are much less suitable for the reaction than the quasi-axial allylic hydrogens.]

Differences in $\Delta\Delta F^{\ddagger}$ for an oxygen attack on C-2 of 30, 42, 13, and 45 are probably mainly caused by steric shielding of C-2 by the increasing bulkiness of the alkyl groups attached to this carbon.

42	43		44
	55%		45%

45	46
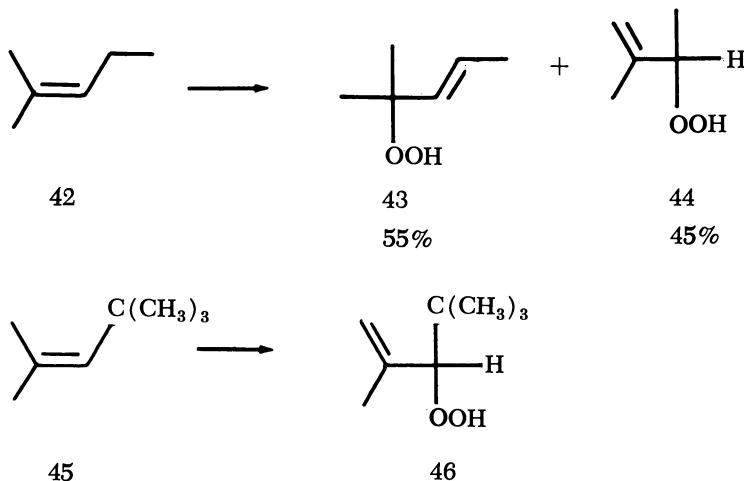
The comparison of $\Delta\Delta F^{\ddagger}$ values of compounds 36, 16, 18, and 22 for the oxygen attack at C-2 reveals a remarkable difference in the effect of an isopropylidene group when attached to 1-methylcyclohexene in a 1,3- and a 1,2- manner. Thus, while this group in α-pinene, 16, exerts only a small effect on the reactivity of the double bond, a clearly enhanced reactivity of the double bond of 18 and especially of 22 is observed. The reactivity-increasing effect of the dimethylcyclopropane ring conjugated to a double bond becomes even more obvious when one compares the $\Delta\Delta F^{\ddagger}$ values of cis-Δ²-carene, 25, and of cyclohexene, 40.

Carbonyl groups conjugated to a double bond and allyl OH- and OOH-groups decrease the reactivity of the double bond considerably, at least by about 1 kcal. per mole (56). Thus, if the photo-oxygenation leads to hydroperoxides with double bonds substituted to the same or a lower degree than those of the initial olefins, overoxidation (consumption of more than one molecule of oxygen per molecule of olefin) is easily avoided by stopping the reaction after one mole of oxygen per mole of olefin is taken up. Consumption of two molecules of oxygen takes place with olefins like iso-Tetralin, 47 (36, 59) or neoabietic acid, 50 (65), since the reactivity-decreasing effect of the OOH group is compensated
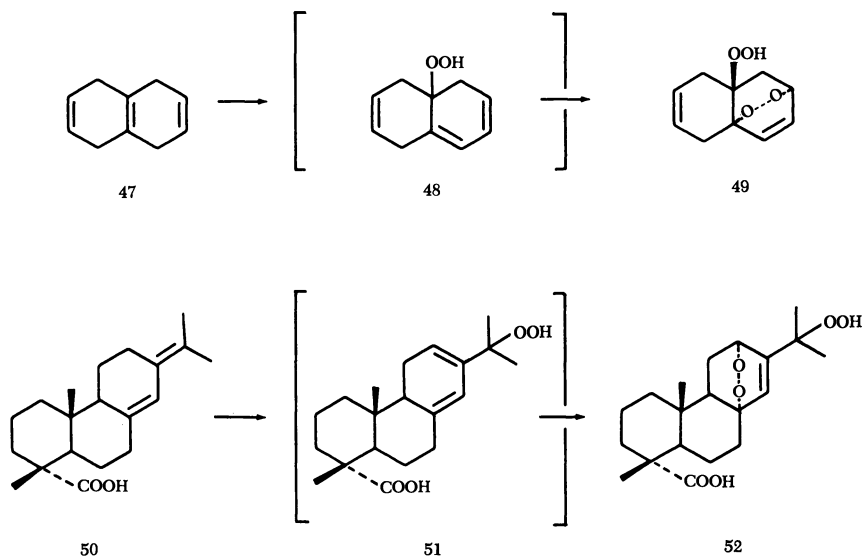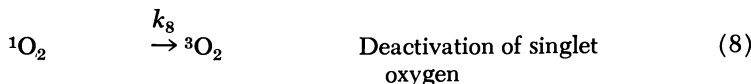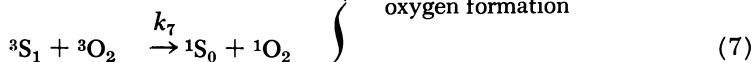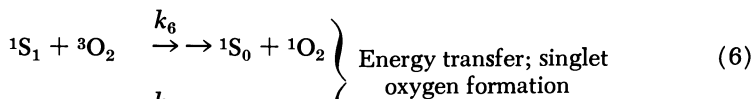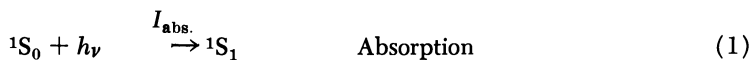
by the highly reactive 1,3-cyclohexadiene system of **48** and **51**, respectively (*17*).

Finally, it may be mentioned that certain hydrazones, thiosemicarbazones, sulfides, sulfoxides, and amines have been found to be suitable substrates in photosensitized oxygenation reactions (*17*).

For a long time, the question of whether the oxygenating species in Type II photo-oxygenation reactions is the electronically excited singlet oxygen (*27, 28, 29*) or a complex composed of the electronically excited light absorber and oxygen (*5, 22, 35, 39, 52, 64*) remained open. Based on recent results that electronically excited singlet oxygen, generated by nonphotochemical means, reacts with certain substrates to form the same products (*9, 12, 42, 71*), and displays the same stereoselectivity (*13*) and the same kinetics (*11, 25*) as the "activated oxygen" in photo-oxygenation reactions (*56, 57*), there is but little doubt that singlet oxygen is the oxygenating species in Type II photo-oxygenation reactions. Furthermore, the relative reactivities of different substrates towards the oxygenating species were found to be independent of the nature of the sensitizers applied (*37, 56, 70*), which supports the idea of a common intermediate in all these reactions.

Elaborate kinetic analyses of the photo-oxygenation of 2,5-dimethylfuran (*22, 56*) and allylthiourea (*40*) sensitized by xanthene dyes and chlorophyll, respectively, and of the direct photo-oxygenation of anthracene and 9,10-diphenylanthracene (*41*) have revealed that Type II direct and indirect (sensitized) photo-oxygenation reactions proceed with

essentially the same mechanism according to the following reaction sequence:

$$^1S_0 + h\nu \xrightarrow{I_{abs.}} {}^1S_1 \qquad \text{Absorption} \qquad (1)$$

$$^1S_1 \xrightarrow{k_2} {}^1S_0 + h\nu' \qquad \text{Fluorescence} \qquad (2)$$

$$^1S_1 \xrightarrow{k_3} {}^1S_0 \qquad \text{Internal conversion} \qquad (3)$$

$$^1S_1 \xrightarrow{k_4} {}^3S_1 \qquad \text{Intersystem crossing} \qquad (4)$$

$$^3S_1 \xrightarrow{k_5} {}^1S_0 \qquad \text{Intersystem crossing} \qquad (5)$$

$$^1S_1 + {}^3O_2 \xrightarrow{k_6} \rightarrow {}^1S_0 + {}^1O_2 \qquad \left.\begin{array}{l}\\\\\end{array}\right\} \begin{array}{l}\text{Energy transfer; singlet} \\ \text{oxygen formation}\end{array} \qquad (6)$$

$$^3S_1 + {}^3O_2 \xrightarrow{k_7} {}^1S_0 + {}^1O_2 \qquad (7)$$

$$^1O_2 \xrightarrow{k_8} {}^3O_2 \qquad \begin{array}{l}\text{Deactivation of singlet} \\ \text{oxygen}\end{array} \qquad (8)$$

$$^1O_2 + {}^1A_0 \xrightarrow{k_9} {}^1(AO_2)_0 \qquad \text{Product formation} \qquad (9)$$

with $S = A$ in direct, $S =$ photosensitizer, different from A, in indirect photo-oxygenation reactions; $^1S_0$, $^1S_1$, and $^3S_1 =$ singlet ground state, first excited singlet and triplet state of S, respectively, $^1A_0$ and $^1(AO_2)_0 =$ singlet ground states of substrate A and product AO_2, respectively; $^3O_2 =$ triplet ground state oxygen $(^3\Sigma_g^-)$; $^1O_2 =$ excited singlet oxygen $(^1\Sigma_g^+$ and/or $^1\Delta_g)$. Singlet oxygen replaces the light absorber-oxygen complex given in the original papers.

Omitting the state symbols for simplicity, the quantum yield of product formation is given by

$$\phi_{AO_2} = \frac{[O_2]}{k_2 + k_3 + k_4 + k_6[O_2]} \left(k_6 + k_4 \frac{k_7}{k_5 + k_7[O_2]} \right) \frac{k_9[A]}{k_8 + k_9[A]}$$

or

$$\phi_{AO_2} = \phi_{{}^1O_2} \frac{[A]}{[A] + k_8/k_9}$$

with

$$\phi_{{}^1O_2} = \phi^s{}_{{}^1O_2} + \phi^T{}_{{}^1O_2} = \frac{k_6[O_2]}{k_2 + k_3 + k_4 + k_6[O_2]}$$

$$+ \frac{k_4}{k_2 + k_3 + k_4 + k_6[O_2]} \cdot \frac{k_7[O_2]}{k_5 + k_7[O_2]}$$

$\phi^s{}_{1O_2}$ and $\phi^T{}_{1O_2}$ being the quantum yields of singlet oxygen formation by energy transfer from the excited singlet or triplet state light absorber, respectively. Generally, $\phi^T{}_{1O_2}$ equals the quantum yield of $^3S_1$-formation, ϕ_T (at $[O_2] \geqslant 10^{-5}$ mole per liter) since $^3S_1$ is normally long-lived (10^{-4} seconds and longer) and quenching of triplet state molecules by oxygen occurs at approximately diffusion-controlled rates. Thus, if ϕ_{1O_2} exceeds ϕ_T, singlet oxygen formation must occur partly by an energy transfer from the excited singlet light absorber, a process which simultaneously must give rise to fluorescence quenching.

Such observations were made with chlorophyll and anthracenes in oxygen-saturated methanolic and benzene solutions (*40, 41*). This, however, raises the question of the mechanism involved in the energy transfer process. Assuming that the spin conservation rules must be obeyed, the energy transfer reaction requires the formation of a triplet light absorber:

$$^1S_1 + {}^3O_2 \rightarrow {}^3S_1 + {}^1O_2. \tag{10}$$
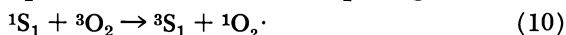
This process can occur only if the energy separation between $^1S_1$ and $^3S_1$ is at least 22.6 kcal. per mole necessary to excite triplet oxygen into its lowest excited singlet state, $^1\Delta_g$. However, in the case of chlorophyll, this separation is only 10.2 kcal. per mole (*68*). Furthermore, the triplet sensitizer produced by Reaction 10 should react with another $^3O_2$ to give $^1O_2$ and $^1S_0$ according to Reaction 7. Thus, the limiting quantum yield of $^1O_2$ formation should approach a value of 2 with increasing oxygen concentrations, in disagreement with experimental results obtained (—*e.g.*, for 9,10-diphenylanthracene and rubrene in benzene solutions). The fluorescence quantum yield of rubrene in oxygen-free benzene solutions was determined to be unity (*5*), showing that no triplet rubrene is formed. In oxygen-containing benzene solutions rubrene is oxygenated to an endoperoxide, whose quantum yield approaches unity with increasing oxygen concentration. Once this value is reached, a further increase in oxygen concentration does not change the quantum yield (*15, 16*).

The following mechanism for the energy transfer to oxygen was therefore proposed (*17*): according to Tsubomura and Mulliken (*69, see also 26, 44*), the interaction between ground state triplet oxygen, $^3O_2$, and the light absorber, S, in its singlet ground state, excited singlet, and triplet state leads to contact pairs, $^3(S \ldots O_2)_0$, $^3G(S \ldots O_2)$, and $^1F,^3F,^5F(S \ldots O_2)$, respectively, in addition to the formation of a singlet and triplet charge transfer complex, ^1CT and ^3CT, which arise by an electron transfer from the highest filled molecular orbital of S to the π-system of oxygen, and which energetically are placed between the ^3G- and F-states. While the ground state contact pair, $^3(S \ldots O_2)_0$, is considered to be almost completely dissociated into its components, $^1S_0$ and $^3O_2$ (*69*), this may not be so with the ^3G- and F-states. Porter and Wright (*48*), for example, deduced a stability of several kilocalories for a contact pair formed by an

interaction of $^3O_2$ with triplet state molecules. The assumption of a minimum in the potential energy curves of the ^3G- and F-states would also agree with the diffusion-controlled rate of quenching of $^1S_1$ and $^3S_1$ by oxygen since these minima may prevent the contact pairs from dissociating into their original components, $^1S_1 + {}^3O_2$ and $^3S_1 + {}^3O_2$, respectively, which should decrease the values of the rate constants of the quenching processes considerably.

Introducing now another contact pair, ^1X, which arises from interaction of the singlet ground state light absorber, $^1S_0$, with either $^1\Sigma_g^+O_2$ or $^1\Delta_g O_2$, we get what one may call an extended Tsubomura-Mulliken diagram (Figure 1).
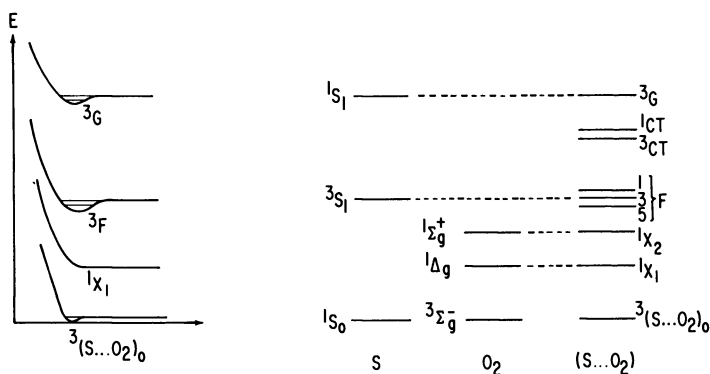

Figure 1.   Energy level and potential energy curve diagrams for a sensitizer, oxygen, and a sensitizer-oxygen contact pair

In the potential energy curve diagram, the charge transfer, ^1CT and ^3CT, and the ^1F- and ^5F-contact pairs are not shown for simplicity reasons, and also only one of the two possible ^1X-contact pairs is drawn. Furthermore, the ^1X-contact pair is assumed to be completely dissociative, which may be correct only for those light absorber-oxygen pairs for which no quenching of $^1O_2$ by $^1S_0$ [to $^3O_2$ or product formation, $^1(SO_2)_0$] has been observed. However, even if the latter reaction occurs—for example, in the direct photo-oxygenation of anthracene where $^1O_2$ + anthracene $\rightarrow$ anthracene-endoperoxide—there seems to be no direct path from ^1X to the stable endoperoxide, since all kinetic results have revealed the participation of two molecules of anthracene in this reaction. This also indicates that the excess energy, contained in ^1X after transition from the F-state, is used as kinetic energy with which $^1S_0$ and $^1O_2$ fly apart.

If there exists an effective pathway for the internal conversion process, $^3G \rightarrow {}^3F$, reactions between excited singlet light absorbers, $^1S_1$, and oxygen, $^3O_2$, result in the formation of the ^3F-contact pair (as does the reaction between $^3S_1$ and $^3O_2$), from which either intersystem crossing to ^1X or internal conversion to the ground state contact pair, $^3(S \ldots O_2)_0$,

may occur. Such an energy transfer mechanism, which assumes a step-wise degradation of excitation energy through contact pairs, allows the reaction $^1S_1 + {}^3O_2 \rightarrow {}^1S_0 + {}^1O_2$ to occur, which is independent of the energy separation between $^1S_1$ and $^3S_1$, and it reduces the limiting quantum yield of $^1O_2$ formation as well as of product formation to unity.

Singlet oxygen generated by mixing H_2O_2 with NaOCl consists mainly of $^1\Delta_g O_2$ (*3, 4, 7, 32, 33*). Since singlet oxygen produced by this method and by energy transfer from xanthene dyes in their triplet states displays the same chemical behavior toward substrates, the energy transfer process may predominantly lead to $^1\Delta_g O_2$. However, since xanthene dyes possess triplet energies well above 37.7 kcal. per mole (*17*), energy transfer from these dyes to oxygen may also lead to $^1\Sigma_g^+ O_2$, which may either react independently of its higher energy content in the same manner as $^1\Delta_g O_2$, which may rapidly decay to this lower singlet oxygen state before it reacts with the substrate, or which may decay directly to the ground state $^3\Sigma_g^- O_2$ with a faster rate than does $^1\Delta_g O_2$, so that only the reaction of the latter is observed under the conditions used. Furthermore, $^1X_2$ originated from $^1S_0 + {}^1\Sigma_g^+ O_2$, may undergo a rapid internal conversion to the lower $^1X_1$ state (which is composed of $^1S_0 + {}^1\Delta_g O_2$) before it dissociates into ground state sensitizer and singlet oxygen. Another question is, whether the probabilities of the two competing processes, $^3F \rightarrow {}^1X$

Table II.   Triplet Energy of Sensitizers

(π,π^*)-Sensitizers	Triplet Energy,[a] Kcal./Mole	(n,π^*)-Sensitizers	Triplet Energy,[a] Kcal./Mole
Benzene	84.5	Acetone	—
Fluorene	67.6	Propiophenone	74.6
Triphenylene	66.6	Xanthone	74.2
Biphenyl	65.7	Acetophenone	73.6
Phenanthrene	62.2	Carbazole	70.1
Naphthalene	60.9	Benzophenone	68.5
1-Bromonaphthalene	59.0	Thioxanthone	65.5
1-Iodonaphthalene	58.6	Flavone	62.0
Pyrene	48.7	2-Naphthylphenyl ketone[b]	59.6
1,2-Benzanthracene	47.2	1-Naphthylphenyl ketone[b]	57.5
Anthracene	42.0	Fluorenone[b]	53.3
Acenaphthylene			
Eosin	42.4[c]		
Erythrosin	42.0[c]		
Rose Bengal	39.4[c]		
Azulene	Between 31 and 38[d]		
Tetracene	29.4		

[a] Triplet energies of (π,π^*)- and (n,π^*)-sensitizers [taken from (*8*)].
[b] Reacting triplets are probably $^3(\pi,\pi^*)$ (*24*).
[c] From (*17*).
[d] From (*38*).

→ $^1S_0$ + $^1O_2$ and ^3F → $^3(S \ldots O_2)_0$ → $^1S_0$ + $^3O_2$, are functions of the triplet energies of the sensitizers or not; because of the mechanism given above singlet oxygen formation should not depend on the singlet energy but may depend on the triplet energy of the light absorber. [Recently, a quantum mechanical treatment of the mechanism of quenching of triplet state molecules by oxygen was carried out (30). The authors, also considering the interaction of singlet oxygen with singlet ground state light absorbers, conclude that the ratio of rates for the two competing processes is of the order of 100 to 1000—*i.e.*, triplet quenching by oxygen should almost exclusively be accompanied by singlet oxygen formation.]

Since all the direct and sensitized photo-oxygenation reactions have been carried out with "low-energy light absorbers" (triplet energies lower than about 45 kcal. per mole), we examined a series of sensitizers with triplet energies from about 30 to 85 kcal. per mole (18). 2,5-Dimethylfuran, 53, which reacts with singlet oxygen to the ozonide (54) that is immediately converted to a methoxy hydroperoxide, 55, in the presence of methanol (14, 21), was used as a substrate. In the presence of the (π,π^*)- and (n,π^*)-sensitizers given in Table II, the dimethylfuran in methanolic solution took up 1 mole of O_2 per mole of dimethylfuran,
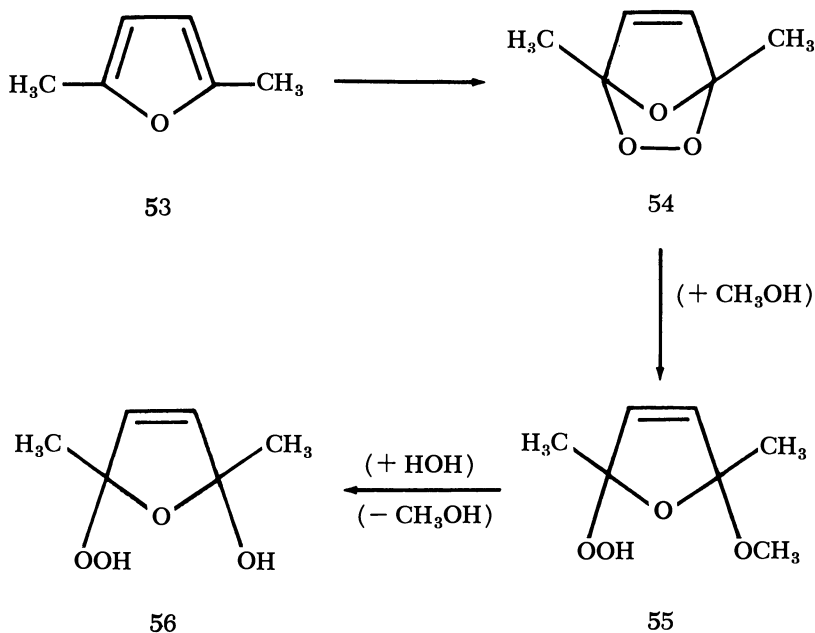
and the only product formed was the methoxy hydroperoxide which was identified by its melting point, infrared spectrum, and hydrolysis product, 56. Furthermore, in all cases the unchanged sensitizer was recovered in

about 90% yield, except for anthracene, which was dimerized to about 75% during the irradiation period, 1-iodonaphthalene which was photolyzed, and azulene, about 10% of which was destroyed. In addition, we carried out the thermal autoxidation of 2,5-dimethylfuran in refluxing methanol and isolated only a brownish, viscous oil that possesses a different infrared spectrum from that of 55. (The methoxy hydroperoxide, 55, is stable under these conditions.)

These results clearly show that all the (π,π^*)- as well as the (n,π^*)-sensitizers independent of their triplet energies transfer their energy to $^3O_2$, thereby forming $^1O_2$. These experiments do not answer, however, the question of which singlet oxygen is involved and if the two singlet oxygens exert different chemical behavior. At present, quantum yield of $^1O_2$-formation as well as product formation and product distributions with various olefinic substrates as a function of the sensitizers applied are being studied.

Literature Cited

(1) Acharya, S. P., *Tetrahedron Letters* **1966**, 4117.
(2) Arbuzov, Y. A., *Russ. Chem. Rev.* **34**, 558 (1965).
(3) Arnold, S. J., Ogryzlo, E. A., Witzke, H., *J. Chem. Phys.* **40**, 1769 (1964).
(4) Bader, L. W., Ogryzlo, E. A., *Discussions Faraday Soc.* **37**, 46 (1964).
(5) Bowen, E. J., "The Photochemistry of Aromatic Hydrocarbon Solutions," in "Advances in Photochemistry," W. A. Noyes, Jr., G. S. Hammond, and J. N. Pitts, Jr., eds., Vol. I, p. 23, Interscience, Wiley, New York, London, Sidney, 1963.
(6) Brewster, J. H., *J. Am. Chem. Soc.* **81**, 5493 (1959).
(7) Browne, R. J., Ogryzlo, E. A., *Proc. Chem. Soc. London* **1964**, 177.
(8) Calvert, J. G., Pitts, J. N., Jr., "Photochemistry," Wiley, New York, London, Sidney, 1966.
(9) Corey, E. J., Taylor, W. C., *J. Am. Chem. Soc.* **86**, 3881 (1964).
(10) Eisfeld, W., Dissertation, University of Göttingen, 1965.
(11) Foote, C. S., Cheng, H., private communication.
(12) Foote, C. S., Wexler, S., *J. Am. Chem. Soc.* **86**, 3879, 3880 (1964).
(13) Foote, C. S., Wexler, S., Ando, W., *Tetrahedron Letters* **1965**, 4111.
(14) Foote, C. S., Wuesthoff, M. T., Wexler, S., Burstain, I. G., Denny, R., Schenck, G. O., Schulte-Elte, K. H., *Tetrahedron* **23**, 2583 (1967).
(15) Gaffron, H., *Biochem. Z.* **264**, 251 (1933).
(16) Gaffron, H., *Z. Physik. Chem.* **B37**, 437 (1937).
(17) Gollnick, K., *Advan. Photochem.*, in press.
(18) Gollnick, K., Dörhöfer, G., unpublished manuscript.
(19) Gollnick, K., Schade, G., *Tetrahedron Letters* **1966**, 2335.
(20) Gollnick, K., Schade, G., unpublished manuscript.
(21) Gollnick, K., Schenck, G. O., "1,4-Cycloaddition Reactions: the Diels-Alder Reaction in Heterocyclic Syntheses," J. Hamer, ed., Chap. X, p. 255, Academic Press, New York, 1967.
(22) Gollnick, K., Schenck, G. O., *Pure Appl. Chem.* **9**, 507 (1964).
(23) Gollnick, K., Schroeter, S., Ohloff, G., Schade, G., Schenck, G. O., *Liebigs Ann. Chem.* **687**, 14 (1965).
(24) Hammond, G. S., Leermakers, P. A., *J. Am. Chem. Soc.* **84**, 207 (1962).
(25) Higgins, R., Foote, C. S., Cheng, H., ADVAN. CHEM. SER. **77**, 102 (1968).

(26) Hoijtink, G. J., *Mol. Phys.* **3**, 67 (1960).
(27) Kautsky, H., *Biochem. Z.* **291**, 271 (1937).
(28) Kautsky, H., deBruijn, H., *Naturwissenschaften* **19**, 1403 (1931).
(29) Kautsky, H., deBruijn, H., Neuwirth, R., Baumeister, W., *Ber. deut. Chem. Ges.* **66**, 1588 (1933).
(30) Kawaoka, K., Khan, A. U., Kearns, D. R., *J. Chem. Phys.* **46**, 1842 (1967).
(31) Kenney, R. L., Fisher, G. S., *J. Am. Chem. Soc.* **81**, 4288 (1959).
(32) Khan, A. U., Kasha, M., *Ibid.*, **88**, 1574 (1966).
(33) Khan, A. U., Kasha, M., *J. Chem. Phys.* **39**, 2105 (1963).
(34) Klyne, W., "Progress in Stereochemistry," Vol. I, p. 81, Butterworths, London, 1954.
(35) Koblitz, W., Schumacher, H. J., *Z. Physik. Chem.* **B35**, 11 (1937).
(36) Köller, H., Diplomarbeit, University of Göttingen, 1958.
(37) Kopecky, K. R., Reich, H. J., *Can. J. Chem.* **43**, 2265 (1965).
(38) Lamola, A. A., Herkstroeter, W. G., Dalton, J. C., Hammond, G. S., *J. Chem. Phys.* **42**, 1715 (1965).
(39) Livingston, R., "Photochemical Autoxidation," in "Autoxidation and Anti-oxidants," W. O. Lundberg, ed., Vol. I, p. 249, Interscience, Wiley, New York, London, Sidney, 1961.
(40) Livingston, R., Owens, K. E., *J. Am. Chem. Soc.* **78**, 3301 (1956).
(41) Livingston, R., Rao, V. S., *J. Phys. Chem.* **63**, 794 (1959).
(42) McKeown, E., Waters, W. A., *J. Chem. Soc. London* **B 1966**, 1040.
(43) Mertz, C., Diplomarbeit, University of Göttingen, 1958.
(44) Murrell, J. N., *Mol. Phys.* **3**, 319 (1960).
(45) Nickon, A., Bagli, F., *J. Am. Chem. Soc.* **83**, 1498 (1961).
(46) Nickon, A., Mendelson, W. L., *Can. J. Chem.* **43**, 1419 (1965).
(47) Ohloff, G., Klein, E., Schenck, G. O., *Angew. Chem.* **73**, 578 (1961).
(48) Porter, G., Wright, M. R., *Discussions Faraday Soc.* **27**, 18 (1959).
(49) Roberts, J. D., Caserio, M. C., "Basic Principles of Organic Chemistry," Chaps. 7-5, 7-6, W. A. Benjamin, New York, N. Y., 1965.
(50) Schenck, G. O., *Angew. Chem.* **64**, 12 (1952).
(51) Schenck, G. O., German Pat. **933925** (Dec. 24, 1943).
(52) Schenck, G. O., *Naturwissenschaften* **35**, 28 (1948).
(53) Schenck, G. O., Becker, H. D., Schulte-Elte, K. H., Krauch, C. H., *Chem. Ber.* **96**, 509 (1963).
(54) Schenck, G. O., Eggert, H., Denk, W., *Liebigs Ann. Chem.* **584**, 177 (1953).
(55) Schenck, G. O., Eisfeld, W., unpublished manuscript.
(56) Schenck, G. O., Gollnick, K., *Forschungsber. Land Nordrhein-Westfalen,* No. **1256**, Westdeutscher Verlag, Köln, Opladen, 1963.
(57) Schenck, G. O., Gollnick, K., Buchwald, G., Schroeter, S., Ohloff, G., *Liebigs Ann. Chem.* **674**, 93 (1964).
(58) Schenck, G. O., Gollnick, K., Neumüller, O. A., *Ibid.*, **603**, 46 (1957).
(59) Schenck, G. O., Köller, H., unpublished manuscript.
(60) Schenck, G. O., Mertz, C., unpublished manuscript.
(61) Schenck, G. O., Neumüller, O. A., Ohloff, G., Schroeter, S., *Liebigs Ann. Chem.* **687**, 26 (1965).
(62) Schenck, G. O., Schroeter, S., Ohloff, G., *Chem. Ind. (London)* **1962**, 459.
(63) Schenck, G. O., Schulte-Elte, K. H., unpublished manuscript.
(64) Schönberg, A., *Liebigs Ann. Chem.* **518**, 299 (1935).
(65) Schuller, W. H., Lawrence, R. V., *J. Am. Chem. Soc.* **83**, 2563 (1961).
(66) Schulte-Elte, K. H., Dissertation, University of Göttingen, 1961.
(67) Sharp, D. B., "Abstracts of Papers," 138th Meeting, ACS, Sept. 1960, p. 79P.
(68) Singh, I. S., Becker, R. S., *J. Am. Chem. Soc.* **82**, 2083 (1960).

(69) Tsubomura, H., Mulliken, R. S., *J. Am. Chem. Soc.* **82,** 5966 (1960).
(70) Wilson, T., *J. Am. Chem. Soc.* **88,** 2898 (1966).
(71) Winer, A. M., Bayes, K. B., *J. Phys. Chem.* **70,** 302 (1966).

68

Chemistry of Singlet Oxygen

V. Reactivity and Kinetic Characterization

RAYMOND HIGGINS, CHRISTOPHER S. FOOTE, and HELEN CHENG

University of California, Los Angeles, Calif. 90024

Reactivities of olefinic and other acceptors are determined for oxygenation, both dye-photosensitized and with singlet oxygen (generated by reaction of metal hypochlorites with hydrogen peroxide). The ratio of the rate constant for reaction with acceptor to that for decay is the same for the intermediate in both reactions. Relative reactivities of various acceptors (from competition experiments) are the same in both reactions and indicate that the intermediate is electrophilic and quite discriminating. In addition, product distributions in the two reactions are identical. The reactive intermediate in the dye-sensitized photo-oxygenation of these substrates cannot be distinguished by any criterion yet devised from chemically generated $^1\Delta_g$ oxygen.

The dye-sensitized photo-oxygenation of olefins and dienoid compounds has been the subject of much recent interest (*3, 13, 14, 15, 16, 32, 34*). Other papers in this volume provide a good introduction to the background and scope of the reaction (*17, 23, 27, 33*). Previous work has shown that singlet oxygen (*1, 24*), produced by the reaction of sodium hypochlorite and hydrogen peroxide (*8, 9, 10, 29*) or by electrodeless discharge (*6*), reacts with typical photo-oxygenation acceptors to give products which are indistinguishable from those of photosensitized oxygenation. In particular, the stereoselectivities of the reactive species in the photo-oxygenation and of chemically produced singlet oxygen are identical (*9*). In this paper, the reactivity of the photochemical intermediate is compared with that of chemically produced singlet oxygen.

The kinetics of the dye-sensitized photo-oxygenation have been studied by several groups (*3, 4, 5, 13, 14, 15, 16, 28, 32, 34, 35*). With

Rose Bengal and many other sensitizers, the reaction proceeds by way of the triplet dye (^{3}Sens); at oxygen concentrations above $2 \times 10^{-5}M$ (exceeded for methanol solutions in equilibrium with air or oxygen), all of the triplet dye reacts with oxygen to give a reactive species (RS) which is the actual oxygenating agent (*13, 14, 15, 34*). This reactive species has often been assumed to be a complex of sensitizer and oxygen (Sens-O$_2$), but singlet oxygen (^{1}O$_2$), formed by energy transfer from the dye triplet to oxygen, is kinetically equivalent (*11, 19*). The reactive species either decays, regenerating ground state oxygen (Reaction 1) or reacts with acceptor (A) to give the product (AO$_2$, Reaction 2).

$$^3\text{Sens} + {}^3\text{O}_2 \rightarrow \text{RS (Sens-O}_2 \text{ or } {}^1\text{O}_2)$$

$$\text{RS} \xrightarrow{k_1} {}^3\text{O}_2 \tag{1}$$

$$\text{RS} + \text{A} \xrightarrow{k_2} \text{AO}_2 \tag{2}$$

The instantaneous quantum yield for product formation (Φ_{AO_2}) is given by the following expression.

$$\Phi_{\text{AO}_2} = \Phi_{3\,\text{Sens}} \frac{k_2[\text{A}]}{k_1 + k_2[\text{A}]}$$

Thus, the limiting quantum yield of product formation at high acceptor concentration ($k_2[\text{A}] \gg k_1$) is the quantum yield of triplet dye formation ($\Phi_{3_{\text{Sens}}}$); at limiting low acceptor concentration ($k_2[\text{A}] \ll k_1$), Φ_{AO_2} is proportional to [A]. The constant β is defined as k_1/k_2 and is characteristic for a given acceptor. The numerical value of β gives the acceptor concentration at which half the reactive species gives product. Values of β for a few compounds have been reported (*4, 5, 13, 14, 16, 34, 36, 37*).

The instantaneous yield of product (Y_{AO_2}) in the hypochlorite–H$_2$O$_2$ oxygenations would be expected to be given by an expression very similar to that for Φ_{AO_2} in the photo-oxygenation:

$$Y_{\text{AO}_2} = Y_{{}^1\text{O}_2} \frac{k_2[\text{A}]}{k_1 + k_2[\text{A}]}$$

In this expression, $Y_{{}^1\text{O}_2}$ is the yield of singlet oxygen produced from a given amount of hypochlorite, and the other terms have the same meaning as stated previously.

For both the photochemical and chemical oxygenation, a plot of $1/\Phi_{\text{AO}_2}$ or $1/Y_{\text{AO}_2}$ against $1/[\text{A}]$ should be a straight line and can be used to determine β for a given acceptor.

and

$$\frac{1}{\Phi_{AO_2}} = \frac{1}{\Phi_{3\,Sens}} \left(1 + \frac{\beta}{[A]}\right)$$

$$\frac{1}{Y_{AO_2}} = \frac{1}{Y_{{}^1O_2}} \left(1 + \frac{\beta}{[A]}\right)$$

The ratio of slope to intercept is β in both expressions.

These relationships are valid only if [A] does not change during the reaction (negligible conversions). This point has been overlooked at times. In practice, instead of Φ_{AO_2}, the amount of product formed in a given time of irradiation will be used since it is proportional to Φ_{AO_2} if the light flux is constant within a series of reactions.

Reaction 3 is an important mode of decomposition of $^1O_2$ in the vapor phase (1, 24).

$$^1O_2 + {}^1O_2 \xrightarrow{k_3} 2\,{}^3O_2 \tag{3}$$

The expressions derived above assume all decay of the reactive species is first order. If Reaction 3 is significant under these conditions, the expression for the chemical oxygenation would have to be modified as follows:

$$Y_{AO_2} = Y_{{}^1O_2} \frac{k_2[A]}{k_1 + k_2[A] + 2\,k_3[{}^1O_2]}$$

and a similar correction would be necessary for the photochemical process. The fraction of intermediate giving product would depend on the concentration of intermediate. Even though in photochemical experiments the rate of production of intermediate is constant (for a given apparatus), its steady state concentration would depend on acceptor concentration, and curved plots should result. In the chemical reaction, nothing resembling a constant rate of $^1O_2$ formation is obtained in our experiments because hypochlorite is not introduced at a steady rate. Since excellent linear plots are observed (see Results), $2k_3[{}^1O_2] << k_1$ in solution.

From the ratio of $\beta(k_1/k_2)$ values for different acceptors, the relative rate constant (k_2) for the reaction of each with the reactive species can be obtained. However, it is much easier to use a competition method. This method has been used by Kopecky and Reich (26) and by Wilson (39) for the photo-oxygenation, using different sensitizers and acceptors. It has been shown that the relative value of k_2 does not depend on sensitizer (26, 39), and a ratio of k_2 values obtained using $^1O_2$ generated by electrodeless discharge was found to be compatible with that obtained in photosensitized oxygenation (39). These results were used to support the suggestion (11, 19) that singlet oxygen is intermediate in the photosensitized oxygenations (26, 39).

For the photochemical reaction, the expression shown below governs competition reactions with two acceptors (A and B).

$$\frac{-d[A]}{-d[B]} = \frac{d[AO_2]}{d[BO_2]} = \frac{\Phi_{AO_2}}{\Phi_{BO_2}} = \frac{\dfrac{k_2{}^A[A]}{k_1 + k_2{}^A[A] + k_2{}^B[B]}}{\dfrac{k_2{}^B[B]}{k_1 + k_2{}^A[A] + k_2{}^B[B]}} = \frac{k_2{}^A[A]}{k_2{}^B[B]}$$

This differential expression can be used directly for small conversions. Since the denominators cancel, the expression can also be integrated easily to give the equations necessary for higher conversions:

$$\frac{k_2{}^A}{k_2{}^B} = \frac{\log(1 - [AO_2]/[A]_o)}{\log(1 - [BO_2]/[B]_o)} = \frac{\log([A]_f/[A]_o)}{\log([B]_f/[B]_o)}$$

These expressions are for measurement of product (AO_2, BO_2) appearance or acceptor disappearance, respectively. Initial and final concentrations are indicated by the subscript o or f, respectively. This result is equivalent to the method of Ingold and Shaw (*18*), derived for the less complex case of aromatic nitration, where no decay term (k_1) for the intermediate interferes, and was used by Kopecky and Reich for the photo-oxidation, apparently without derivation (*26*). Previous authors followed acceptor disappearance, which is very difficult to measure accurately, particularly for unreactive acceptors, and is subject to severe errors if starting material is consumed by side reactions (*26, 39*). However, the technique has the advantage that gas-chromatograph detector calibration is not required since only concentration ratios are measured. We have used this technique also, but we found it far more accurate to measure product appearance since highly characteristic products are formed, which in many cases distinguish the desired reaction from all side reactions. However, this method presents the difficulty that the product peroxides must be quantitatively reduced for gas chromatography, and all products must be isolated and characterized and detector response carefully calibrated.

Experimental

Materials. *cis*-4-Methyl-2-pentene, 2-methyl-2-butene, 1-methylcyclohexene and 2,3-dimethyl-2-butene were Phillips Petroleum Co. 99% grade. Sodium hypochlorite was Purex 14 (Purex Corp.). Other reagents were from standard sources.

Since the olefins used for product appearance studies always contained sufficient oxygen-containing impurities to interfere with analyses, they were purified immediately before use by repeated passage through silica gel until shown to be sufficiently pure.

Preparative Photo-Oxygenations. The apparatus used has been described (*8, 16*). Peroxides were reduced with a fourfold excess of sodium

borohydride, with cooling. After workup by partial solvent removal and ether–water partition, the crude alcohol mixtures were separated by preparative GLC. Structures were unambiguously determined by infrared, nuclear magnetic resonance, and high resolution mass spectra, which will be reported in more detail later.

Kinetic Measurements. PHOTO-OXYGENATIONS. The reaction vessel was a small immersion irradiation apparatus similar to that used for preparative work (8, 16). It was immersed in a constant temperature bath (30°C.) and cooled internally by circulating 0.2M Cu_2Cl_2 solution (also held at 30°C.) through the water jacket; the coolant also served as an infrared filter. To ensure stability, the light source (Sylvania DWY) was operated from a constant voltage transformer; to avoid overheating and to ensure convenient reaction times (5.00 min.), the voltage was reduced to 50 volts. The temperature in the solution rose less than 2°C. when the lamp was in operation.

Stock solutions of Rose Bengal were prepared in the appropriate solvent, filtered, and stored in the dark. Weighed quantities of 2-methyl-2-pentene were dissolved in the solvent, an aliquot of sensitizer solution was added, and the solution diluted volumetrically (solutions were handled in subdued light after addition of sensitizer). After reaction, the solutions were immediately reduced by adding excess trimethylphosphite (7, 25). They were left overnight, and an aliquot of isoamyl alcohol internal standard was added. The solutions were analyzed on a Perkin-Elmer Model 800 flame-ionization gas chromatograph (N_2 carrier) using an 8-foot × 1/8-inch copper column with 10% UCON WS on 80/100 mesh Anakrom ABS at 80°C. Peak areas were evaluated by triangulation and by the peak height-half height width method. Absolute yields were calculated by calibrating the detector by injecting weighed mixtures of pure product alcohols and the internal standard in the appropriate solvent. The data are summarized in Tables I and II.

Table I.   Effect of Acceptor Concentration on Product Yield for Photo-Oxygenation of 2-Methyl-2-pentene (A) in *tert*-Butyl Alcohol

[A], M	[AO$_2$],[a] mM	Conversion, %
0.0109	0.88	8.1
0.0131	1.01	7.7
0.0199	1.43	7.2
0.0313	1.92	6.1
0.0504	2.40	4.8
0.1003	3.22	3.2
0.1989	4.69	2.4

[a] Sum of yields of two products; mean of three or more analyses.

CHEMICAL OXYGENATIONS. Weighed amounts of 2-methyl-2-pentene were dissolved in 50:50 (by volume) methanol–*tert*-butyl alcohol. Hydrogen peroxide (1 ml. of 9.08M) was added, and the solution was diluted to 100 ml. To 50.0 ml. of this solution was added 0.50 ml. of 1.05M aqueous NaOCl over 10 min. with stirring at 25°C. NaOCl was

Table II. Effect of Acceptor Concentration on Product Yield for the Photo-Oxygenation of 2-Methyl-2-pentene (A) in Methanol–*tert*-butyl Alcohol

[A], M	$[AO_2]$,[a] mM	Conversion, %
0.0098	0.422	4.3
0.0118	0.479	4.1
0.0141	0.616	4.3
0.0203	0.840	4.1
0.0270	0.995	3.7
0.0325	1.250	3.8
0.0401	1.513	3.8
0.0518	1.680	3.2
0.0988	2.520	2.5
0.2067	3.510	1.7

[a] Sum of yields of two products; mean of three or more analyses.

Table III. Effect of Acceptor Concentration on Product Yield for the Chemical Oxygenation of 2-Methyl-2-pentene (A)

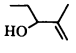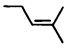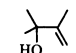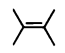| [A], M	$[AO_2]$,[a] mM	Conversion, %
0.0121	0.310	2.6
0.0220	0.552	2.5
0.0284	0.737	2.6
0.0490	0.972	2.0
0.0933	1.680	1.8
0.1995	2.280	1.1
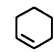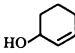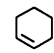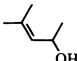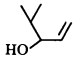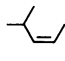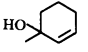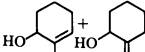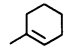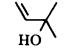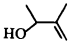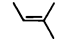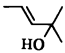
[a] Sum of yields of two products; mean of three or more analyses.

introduced through a capillary below the solution surface. The capillary was fed with a syringe driven by a thumbscrew. After addition, the peroxides were reduced overnight with excess trimethyl phosphite, and the solutions were analyzed by gas chromatography, as above. The results are summarized in Table III.

COMPETITION REACTIONS: PRODUCT ANALYSIS METHOD. The procedures used were identical to those described above, except that pairs of olefins were present in the solutions. In some cases trimethyl phosphite had a retention time near that of a product, and triphenyl phosphite was used as the reducing agent. In chemical oxygenation of the less reactive olefins, products other than those found in photo-oxygenation reactions were detected. These side products could be suppressed by adding free-radical inhibitors such as 2,6-di-*tert*-butylphenol and conducting the reaction near 0°C. The products from these olefins are listed in Table IV. The results are listed in Table V.

COMPETITION REACTIONS; ACCEPTOR DISAPPEARANCE METHOD. *Photo-Oxygenation.* Weighed quantities of the two olefins (such that the final solution was approximately 0.24M in each) and an internal standard

Table IV. Products of Olefin Oxygenations[a]

Olefin	Alcohol A	Alcohol B	Photo-Oxygenation % A	% B	OCl⁻/H₂O₂ % A	% B
(structure)	*(structure)*	*(structure)*	100		100	
(structure)	*(structure)*	*(structure)*	49	51	51	49
(structure)	*(structure)*	*(structure)*	48	52	49	51
(structure)	*(structure)*	*(structure)*	51	49	52	48
(structure)	*(structure)*	*(structure)*	96	4	94	6
	(structure)	*(structure)*	100		[b]	

[a] After reduction of the peroxides to the corresponding alcohols: mean of four or more analyses.
[b] Free radical products could not be suppressed sufficiently to permit analysis.

Table V. Relative Reactivities of Olefins by Product Analysis[a]

Olefin A	Olefin B	Photo-Oxygenation[b] k_2^A/k_2^B	OCl⁻/H₂O₂[c] k_2^A/k_2^B
2,3-Dimethyl-2-butene	2-Methyl-2-butene[d]	41	35
2-Methyl-2-butene	2-Methyl-2-pentene[d]	1.32	1.28
2-Methyl-2-pentene	1-Methylcyclohexene[d]	4.5[e]	3.9[e, f]
cis-4-Methyl-2-pentene	Cyclohexene[g]	5.4[e]	[h]
cis-4-Methyl-2-pentene	2-Methyl-2-pentene[i]	0.014	0.011[j]
trans-4-Methyl-2-pentene	2-Methyl-2-pentene[i]	0.0025	0.0020[j]

[a] Mean of two or more experiments in methanol–*tert*-butyl alcohol (50:50); reduced with trimethyl phosphite unless otherwise stated.
[b] Sensitized by Rose Bengal, 30°C.
[c] At 25°C. unless otherwise stated; solution volume 50 ml.
[d] Internal standard, isoamyl alcohol.
[e] Reduced with triphenyl phosphite.
[f] 0.024M in 2,6-di-*tert*-butylphenol; reaction temperature 3–4°C.
[g] Internal standard, n-amyl alcohol.
[h] Free radical products could not be suppressed sufficiently to permit analysis.
[i] Internal standard, isobutyl alcohol.
[j] 0.097M in 2,6-di-*tert*-butylphenol; reaction temperature 3–4°C.

were dissolved in methanol–*tert*-butyl alcohol (50:50 by volume) containing Rose Bengal, and a small quantity of this solution was removed for analysis. The remaining solution was then irradiated under oxygen, and the reaction was followed by oxygen consumption. Irradiation was continued until the extent of reaction was approximately equal that used in the chemical oxygenation of the same pair of olefins (*see below*). Analyses were performed on a Perkin-Elmer Model 154 gas chromato-

graph. Peak heights of the two olefins relative to the internal standard in the final solution were compared with the same quantities in the unreacted solution to calculate the fractions of each of the olefins converted. The columns and internal standards used are given in Table VI. In some reactions, a free radical inhibitor was also present to make conditions strictly parallel to those used in the calcium hypochlorite experiments. Addition of this compound had no detectable influence on the results, which are summarized in Table VI.

Chemical Oxygenations. These were carried out using the reaction of either sodium or calcium hypochlorite with hydrogen peroxide. In the sodium hypochlorite experiments, solutions of the two olefins and internal standard (again 0.24M in the three compounds) and hydrogen peroxide (in excess of the quantity of hypochlorite to be added) in methanol–*tert*-butyl alcohol (50:50 by volume) were prepared, a small quantity removed for analysis, and the remaining solution cooled to below −20°C. Aqueous sodium hypochlorite solution was then added dropwise to this solution under stirring, and the progress of the reaction was followed by measuring the oxygen evolved. The initial and final solutions were then analyzed as in the photo-oxygenation. The experiments using calcium hypochlorite were essentially identical, except that the solutions also

Table VI. Relative Reactivities of Acceptors by Acceptor Disappearance[a]

Compound A	Compound B	Photo-Oxygenation[b] k_2^A/k_2^B	NaOCl/ H_2O_2 k_2^A/k_2^B	Ca(OCl)$_2$/ H_2O_2 k_2^A/k_2^B
2,5-Dimethylfuran	2,3-Dimethyl-2-butene[c, e]	2.4	5.2	1.5
Cyclopentadiene	2,3-Dimethyl-2-butene[d, f]	1.2	2.0	0.7
2,3-Dimethyl-2-butene	1,3-Cyclohexadiene[d, f]	13[j]		3
	2-Methyl-2-butene[c, g]	22	15	23
	cis-3-Methyl-2-pentene[c, h]	36	25	
2-Methyl-2-butene	cis-3-Methyl-2-pentene[c, h]	1.8		2.5
	trans-3-Methyl-2-pentene[c, h]	1.2		1.4
	1-Methylcyclopentene[c, g]	1.0		1.6
	1-Methylcyclohexene[d, i]	23		20
trans-3-Methyl-2-pentene	1-Methylcyclohexene[d, i]	22		7

[a] Mean of two or more determinations in methanol–*tert*-butyl alcohol (50:50).
[b] Sensitized by Rose Bengal.
[c] Analyzed on a 6-foot × 1/4-inch aluminum column packed with 20% UCON WS on 60/80 Chromosorb W.
[d] Analyzed on a 6-foot × 1/4-inch aluminum column packed with 10% 3,3'-thiodipropionitrile on 70/80 Anakrom ABS.
[e] Internal standard, toluene.
[f] Internal standard, carbon tetrachloride.
[g] Internal standard, hexane.
[h] Internal standard, heptane.
[i] Internal standard, octane.
[j] Result of a single determination.

contained 2,4,6-tri-*tert*-butylphenol (5-10% of the olefin concentration), and the calcium hypochlorite was added as a solid. The results are summarized in Table VI.

Results

Determination of $\beta(k_1/k_2)$. The previous discussion shows that the amount of product formed changes most rapidly with changes in acceptor concentration when the range of [A] brackets β. Since the convenient experimental range of [A] is 0.01-0.2M, 2-methyl-2-pentene, [reported $\beta = 0.18M$ in methanol (*13, 14, 34*)], was selected.

Initial experiments were run in *tert*-butyl alcohol, which dictated a reaction temperature of 30°C., but since methanol–*tert*-butyl alcohol (50:50 by volume) was found to be the best solvent for the chemical oxygenation, the photo-oxygenation experiments were rerun in this solvent.

Solutions of 2-methyl-2-pentene of concentrations in the range 0.01 to 0.2M containing identical quantities of Rose Bengal were prepared and irradiated under identical conditions for 5 minutes. Figure 1 is a plot of $1/[AO_2]$, the amount of product formed in photo-oxygenations in the two solvents against $1/[A]_{mean}$, the mean concentration of acceptor during a reaction. Since conversions were purposely kept low (in no case exceeding 8%), $[A]_{mean}$ differs only slightly from $[A]_{initial}$, and the equation discussed in the introduction is valid. The least-square line through the points gives a value of β equal to $0.13 \pm 0.02M$ for methanol–*tert*-butyl alcohol, and $0.051 \pm 0.003M$ for *tert*-butyl alcohol. The results of the chemical oxygenation in methanol–*tert*-butyl alcohol are plotted in Figure 2 with the least-square line giving β equal to $0.16 \pm 0.04M$.

Relative Reactivities. BY PRODUCT ANALYSIS. Solutions of pairs of olefins in methanol–*tert*-butyl alcohol were irradiated using Rose Bengal as sensitizer. The peroxides were reduced to the corresponding alcohols, and the products were analyzed by gas chromatography. Methods similar to those described above were used for the chemical oxygenations. With unreactive olefins, large amounts of reagents had to be used to give sufficient conversions, and side reactions became important in some cases. The side reactions could be suppressed by adding free radical inhibitors and lowering the temperature.

BY ACCEPTOR DISAPPEARANCE. Weighed quantities of two compounds, chosen to be similar in reactivity, were dissolved along with an unreactive internal standard in methanol–*tert*-butyl alcohol containing Rose Bengal. Analyses of the solution before and after irradiation were carried out, and the data were treated as described in the introduction. Similar methods were used for the chemical oxygenations, which were carried out at −20°C. Radical inhibitors were added in some of the runs. Severe
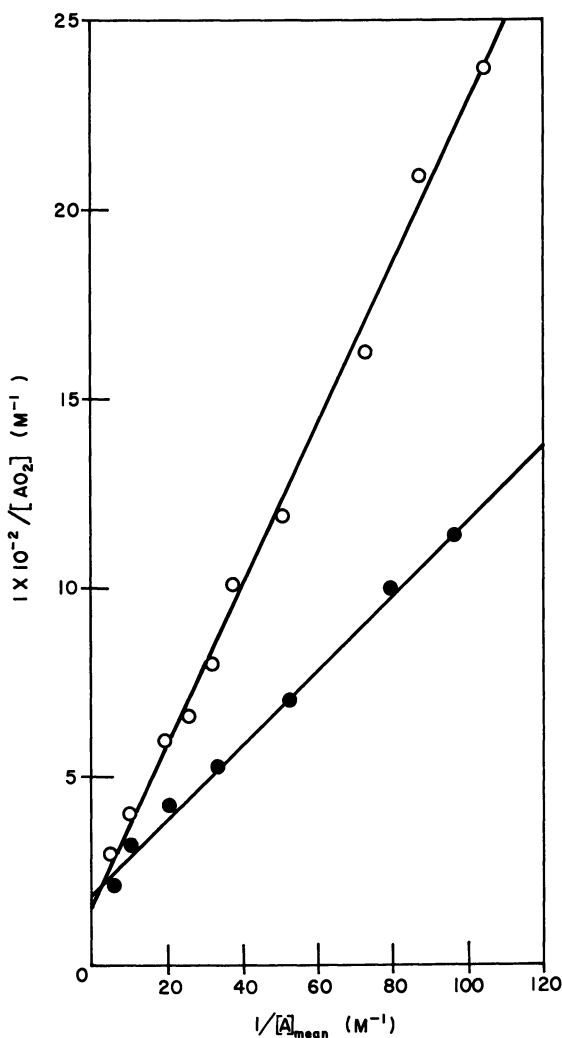
Figure 1. Photo-oxygenation of 2-methyl-2-pentene at 30°C.

○: *in methanol–tert-butyl alcohol ($\beta = 0.13$M $\pm$ 0.02)*
●: *in tert-butyl alcohol ($\beta = 0.051$M $\pm$ 0.003)*

difficulties were encountered in using this technique with unreactive acceptors because large amounts of aqueous hypochlorite had to be added to convert enough acceptor for accurate measurement.

Reactivities of various acceptors (values of k_2 relative to k_2 for 2,3-dimethyl-2-butene), calculated by the method of Ingold and Shaw (*18*) (as discussed in the introduction) are assembled in Table VII. Values

determined by previous workers for photo-oxygenation are included for comparison. Those of Gollnick and Schenck (*13, 14, 34*) are calculated from β values obtained from oxygen uptake measurements, whereas those of Kopecky and Reich (*26*) were determined by acceptor disappearance studies.

Discussion

The excellent linear plot (Figure 2) obtained for the chemical oxygenation of 2-methyl-2-pentene demonstrates that a transient reactive intermediate is formed in this reaction and that the fraction of the intermediate which is trapped depends on acceptor concentration in the expected way. [From the intercept of this plot, it can be determined that the yield of $^1O_2$, based on hypochlorite is 43% under these conditions. At lower temperatures, yields as high as 65% can be obtained reproducibly (*8*)].
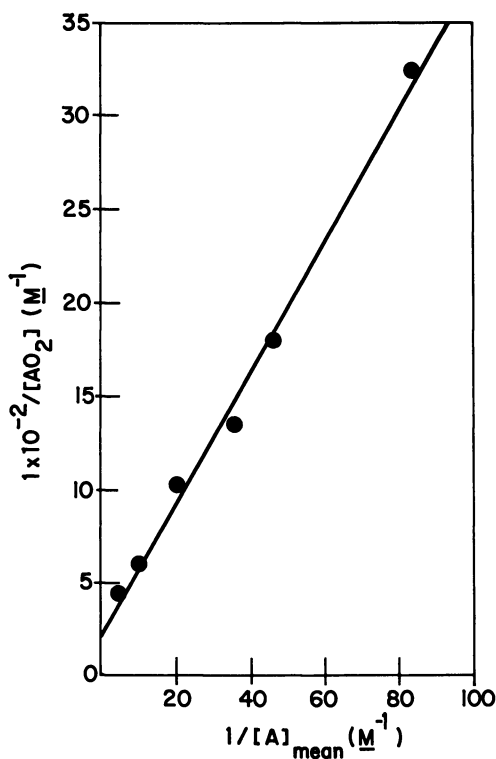
Figure 2.   Chemical oxygenation (NaOCl/ H₂O₂) of 2-methyl-2-pentene in methanol– tert-butyl alcohol (β = 0.16M ± 0.04)

The value of β (k_1/k_2) obtained from Figure 2 is 0.16 ± 0.04M, in excellent agreement with that obtained for the photochemical oxygenation (0.13 ± 0.02M). These values (for methanol–*tert*-butyl alcohol) are in good agreement with that obtained for 2-methyl-2-pentene in methanol (0.18M) by oxygen absorption methods (*13, 14, 34*). [The small discrepancy is probably caused by a solvent effect, as shown by the fact that the photochemical value in pure *tert*-butyl alcohol is 0.051 ± 0.003M. No large solvent effect on β is observed; values in solvents as different as methanol and benzene differ by less than a factor of 2 (*12*).] That the values for the two reactions are so similar provides strong support for the suggestion (*11, 19*) that singlet oxygen is the reactive intermediate in both reactions. It would be a remarkable coincidence if the ratio of the two rate constants were the same for Sens-O_2 and for $^1O_2$; complexing with sensitizer would have to affect both the reaction rate of oxygen with acceptor and the decay rate by the same fraction.

Relative reactivities (Table VII) determined in this study are in excellent agreement with previous photo-oxygenation values (*13, 14, 26, 34*), considering that the reactivity spread is 10^5. Results of the product appearance studies are highly reproducible, and the values for photosensitized and chemical oxygenation agree within the experimental error. The results of the acceptor disappearance studies are more erratic; results of chemical oxygenation are reproducible from run to run only within about a factor of two (most of the values in Table VII are the average of many determinations). The lack of reproducibility is probably caused by the fact that low conversions had to be used to avoid solubility problems caused by adding aqueous hypochlorite. In addition, even small amounts of acceptor lost by evaporation or side reactions cause a large error in results obtained by this method, particularly with unreactive acceptors. Nevertheless, the results obtained for the two reactions are in good agreement. The worst agreement is found for 1,3-cyclohexadiene, where the results for the two reactions differ by a factor of 4; only one run was carried out in the photo-oxygenation of this substrate, and the value may well be in error.

The reactivity of cyclohexene determined is lower by a factor of 3–5 than that found in previous studies. Particularly with this very unreactive acceptor, product appearance studies are more reliable since acceptor disappearance methods (*26*) or oxygen uptake studies (*13, 14, 34*) can lead to a deceptively high reactivity for the reasons mentioned above. However, side reactions occurred to such an extent in the chemical oxygenation that the desired product could not be distinguished reliably from side products.

If the reactive intermediate in the photo-oxygenations were a complex of sensitizer and oxygen, the sensitizer should influence the electron

Table VII. Relative Reactivities of Acceptors

	Product Analysis[a]		Olefin Disappearance[a]		Photo-Oxygen-ation[c]	Photo-Oxygen-ation[d]
	Photo-Oxygen-ation	NaOCl/ H_2O_2	Photo-Oxygen-ation	OCl^-/ H_2O_2[b]		
2,5-Dimethylfuran			2.4	3.8		
Cyclopentadiene			1.2	1.1		
2,3-Dimethyl-2-butene	(1.00)	(1.00)	(1.00)	(1.00)	(1.00)	(1.00)
1,3-Cyclohexadiene			0.08[e]	0.3		
2-Methyl-2-butene	0.024	0.028	0.05	0.06	0.055	
1-Methylcyclopentene			0.05	0.03		0.070
2-Methyl-2-pentene	0.019	0.022				0.017
Trans-3-methyl-2-pentene			0.04	0.03		
Cis-3-methyl-2-pentene			0.03	0.03		
1-Methylcyclohexene	0.0041	0.0056	0.002	0.003	0.0025	0.0082
Cyclohexene	0.000048				0.00012	0.00018
Cis-4-methyl-2-pentene	0.00026	0.00024				
Trans-4-methyl-2-pentene	0.000047	0.000044				

[a] Present work.
[b] Combined results from NaOCl and Ca(OCl)$_2$ experiments.
[c] Calculated from β values reported in Refs. 13, 14, 34.
[d] From Ref. 26.
[e] Result of a single determination.

demand of the oxygen (and presumably reduce it). The complex should also be bulkier than singlet oxygen. Hence, it would be expected to differ from singlet oxygen in sensitivity to both electron density and steric effects. However, the relative reactivities of acceptors are the same in both reactions.

As already pointed out (9), the stereoselectivity of the reactive intermediate should be altered if a bulky sensitizer were attached to the oxygen, but no differences in stereoselectivity between photosensitized and chemical oxygenation were observed (9). The results in Table IV provide further strong evidence that no differences in stereoselectivity exist since the product distributions in the two reactions are identical with these acceptors also.

Thus, by the criteria of reactivity, decay rate, and stereoselectivity the chemically generated reactive species is indistinguishable from the

reactive intermediate in the photo-oxygenation. Strong arguments based on lifetime and chemistry have been advanced that the intermediate in the chemical oxygenation is $^1\Delta_g$ O_2 (rather than $^1\Sigma_g^+$ or vibrationally excited ground state O_2) (8). The reactive intermediate in the photo-oxygenations is thus probably also $^1\Delta_g$ O_2.

The results of Litt and Nickon (27) show small but reportedly significant differences in isotope effects with different photosensitizers and in chemical oxygenation. Further study is obviously desirable. The formation of a sensitizer–oxygen complex which dissociates before reacting (13, 14, 17, 23, 34) would be entirely consistent with our results.

A recent study indicates that with sensitizers of triplet energy above 37 kcal./mole, $^1\Sigma_g^+$ O_2 is the principal primary product of oxygen quenching of the dye triplet (20-23). Rose Bengal has a triplet energy of 45.4 kcal./mole and should give substantial amounts of $^1\Sigma_g^+$ O_2 (20-23). The results reported here show that $^1\Sigma_g^+$ O_2 either does not react appreciably with these substrates, or else (much less likely) it has an identical ratio of reaction to decay rates and gives an identical product distribution. If this were not the case, curvature of the plots in Figures 1 and 2 would be expected, and the product distribution would depend on acceptor concentration since the lifetime of $^1\Sigma_g^+$ O_2 is less than that of $^1\Delta_g$ O_2 (1, 2, 33). Similar conclusions were reached by Wilson on the basis of more limited evidence (39). Probably $^1\Sigma_g^+$ O_2, if formed, decays to $^1\Delta_g$ O_2 rather than directly to ground state O_2, since the maximum quantum yield for product formation in the photo-oxygenation is equal to the quantum yield of Rose Bengal triplet formation (13, 14, 15, 34) so that no intermediate is lost. The results reported by Ogryzlo (33) show that the lifetime of $^1\Sigma_g^+$ O_2 is so short that the reaction rate of an acceptor must be 10^5–10^8 times faster with $^1\Sigma_g^+$ than with $^1\Delta_g$ O_2 for the $^1\Sigma_g^+$ reaction to be detected.

The factors influencing the reactivity of various substrates in the photo-oxygenation have been discussed by Kopecky and Reich (26) and by Gollnick and Schenck (13, 14, 15, 34). The results reported here confirm that electron-rich olefins are particularly reactive and that cyclohexenes are comparatively unreactive compared with acyclic compounds. Kopecky and Reich (26) rationalized this reactivity sequence by using an extreme resonance form of singlet oxygen, reacting *via* a perepoxide, as originally proposed by Sharp (38).
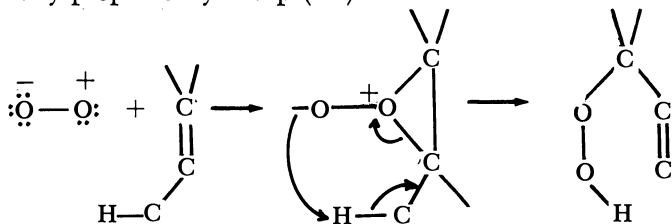
While it is very difficult to rule out such a mechanism positively, it seems far more likely that the reaction is a nearly concerted cycloaddition, as previously suggested by Gollnick and Schenck (*13, 14, 15, 34*) and by Nickon (*27, 30, 31, 32*) on stereochemical grounds. Singlet oxygen ($^1\Delta_g$) has an electronic structure similar to ethylene (*8*), and the electronegativity of the oxygen atoms is quite adequate to rationalize the electrophilic character of the reaction without recourse to the perepoxide mechanism. Litt and Nickon have presented additional arguments against the perepoxide mechanism (*27*). Singlet oxygen can be visualized as a dienophile, undergoing the Diels-Alder reaction with dienes, and the ene reaction with olefins (*9*). (It should be emphasized that it is a reagent of remarkable selectivity and undergoes no reaction at all with most compounds.)

The concerted nature of the reaction is indicated by the fact that a Markovnikoff-type directing effect is essentially absent. Secondary and tertiary products are formed in nearly equal amounts from unsymmetrically substituted olefins (*9, 13, 14, 15, 17, 27, 34*). In addition, substituents on the phenyl group of trimethylstyrene exert no effect on the product distributions (*12*). Furthermore, β values for 2-methyl-2-pentene show only a very small solvent effect (*12*). All these facts suggest that little polarity is developed at the transition state and are consistent with a concerted reaction.

J. H. Knox has asked whether singlet oxygen might not be implicated in spontaneous initiation processes at elevated temperatures since the activation energy would be fairly low. However, $^1\Delta_g$ O_2, even if spontaneously formed (a fairly slow process, even at 300°C. because of the forbiddenness) would not react appreciably with ethylene or propylene; more highly substituted olefins might in principle react, but the over-all rate would probably be too low. However, little is known about gas-phase reactions of singlet O_2.

Acknowledgments

Literature Cited

(1) Arnold, J. S., Browne, R. J., Ogryzlo, E. A., *Photochem. Photobiol.* **4**, 963 (1965).
(2) Bader, L. W., Ogryzlo, E. A., *Discussions Faraday Soc.* **37**, 46 (1964).
(3) Bowen, E. J., *Advan. Photochem.* **1**, 23 (1963).

(4) Bowen, E. J., *Discussions Faraday Soc.* **14**, 143 (1953).
(5) Bowen, E. J., Tanner, D. W., *Trans. Faraday Soc.* **51**, 475 (1955).
(6) Corey, E. J., Taylor, W. C., *J. Am. Chem. Soc.* **86**, 3881 (1964).
(7) Denny, D. B., Goodyear, W. F., Goldstein, B., *J. Am. Chem. Soc.* **82**, 1393 (1960).
(8) Foote, C. S., Wexler, S., Ando, W., Higgins, R., *J. Am. Chem. Soc.* **90**, 975 (1968).
(9) Foote, C. S., Wexler, S., Ando, W., *Tetrahedron Letters* **1965**, 4111.
(10) Foote, C. S., Wexler, S., *J. Am. Chem. Soc.* **86**, 3879 (1964).
(11) *Ibid.*, p. 3880.
(12) Foote, C. S., Denny, R., unpublished observations.
(13) Gollnick, K., Ph.D. Dissertation, University of Göttingen, Germany, 1962.
(14) Gollnick, K., *Advan. Photochem.*, in press.
(15) Gollnick, K., Schenck, G. O., *Pure Appl. Chem.* **9**, 507 (1964).
(16) Gollnick, K., Schenck, G. O., "1,4-Cycloaddition Reactions," J. Hamer, Ed., p. 255, Academic Press, New York, 1967.
(17) Gollnick, K., ADVAN. CHEM. SER. **77**, 78 (1968).
(18) Ingold, C. K., Shaw, F. R., *J. Chem. Soc.* **1927**, 2918.
(19) Kautsky, H., *Biochem. Z.* **291**, 271 (1937).
(20) Kawaoka, K., Khan, A. U., Kearns, D. R., *J. Chem. Phys.* **46**, 1842 (1967).
(21) Kearns, D. R., Hollins, R. A., Khan, A. U., Chambers, R. W., Radlick, P., *J. Am. Chem. Soc.* **89**, 5455 (1967).
(22) Kearns, D. R., Hollins, R. A., Khan, A. U., Radlick, P., *J. Am. Chem. Soc.* **89**, 5456 (1967).
(23) Khan, A. U., Kearns, D. R., ADVAN. CHEM. SER. **77**, 143 (1968).
(24) Khan, A. U., Kasha, M., *J. Am. Chem. Soc.* **88**, 1574 (1966).
(25) Kharasch, M. S., Mosher, R. A., Bengelsdorf, I. S., *J. Org. Chem.* **25**, 1000 (1960).
(26) Kopecky, K. R., Reich, H. J., *Can. J. Chem.* **43**, 2265 (1965).
(27) Litt, F. A., Nickon, A., ADVAN. CHEM. SER. **77**, 118 (1968).
(28) Livingston, R., Subba Rao, V., *J. Phys. Chem.* **63**, 794 (1959).
(29) McKeown, E., Waters, W. A., *J. Chem. Soc.* **1966**, B1040.
(30) Nickon, A., Bagli, J. F., *J. Am. Chem. Soc.* **83**, 1498 (1961).
(31) Nickon, A., Mendelson, W. L., *Can. J. Chem.* **43**, 1419 (1965).
(32) Nickon, A., Schwartz, N., DiGorgio, J. B., Widdowson, D. A., *J. Org. Chem.* **30**, 1711 (1965).
(33) Ogryzlo, E. A., ADVAN. CHEM. SER. **77**, 133 (1968).
(34) Schenck, G. O., Gollnick, K., *Forschung. Landes Nordrhein-Westfalen* No. **1256** (1963).
(35) Schenck, G. O., Koch, E., Z. *Elektrochem.* **64**, 170 (1960).
(36) Schenck, G. O., Schulte-Elte, K.-H., *Ann.* **618**, 185 (1958).
(37) Schenck, G. O., *Angew. Chem.* **69**, 579 (1957).
(38) Sharp, D. B., "Abstracts of Papers," 138th Meeting, ACS, Sept. 1960, 79P.
(39) Wilson, T., *J. Am. Chem. Soc.* **88**, 2898 (1966).

69

Photo-Oxygenation of Mono-Olefins

Reaction Steps Involving the Olefin

FRED A. LITT and ALEX NICKON

Enjay Additives Laboratory, Linden, N. J., and The Johns Hopkins University, Baltimore, Md.

Early studies on photosensitized oxygenation of mono-olefins have shown the non-involvement of mesomeric allylic intermediates, based on the shifting of the position of the double bond during reaction. In this work, six other intermediates, all involving preliminary formation of the C—O bond are considered. Data from the literature are used to disprove formation of some of these, and data are presented ruling out the others. The reaction steps involving the olefin are thus shown to be concerted.

All primary products isolated from olefin photo-oxygenations contain the unsaturation in a position adjacent to the original position, as illus-


Figure 1. Primary products from olefin photo-oxygenations, showing unsaturation in position adjacent to original position

trated in Figure 1. Mesomeric allylic intermediates, such as **1**, are there-

1
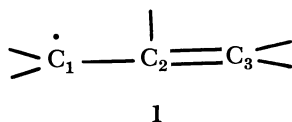
fore precluded. A particularly elegant example of this rule is the photo-oxygenation of optically active limonene (**2**). One product of this

reaction, after reduction, is *trans*-carveol (3), which has the absolute

2   **3**
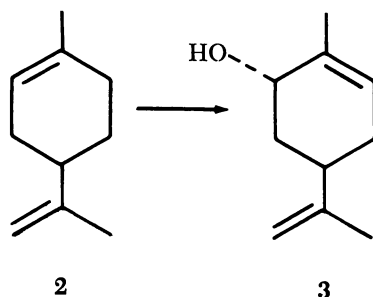
stereochemistry indicated, ruling out intermediacy of species such as the allylic free radical, 4 (*8, 9*).

4
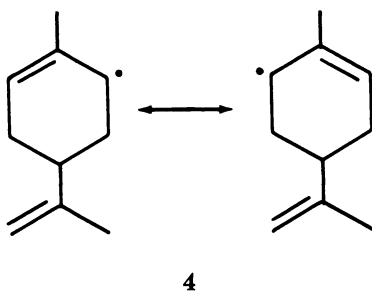
The photosensitized oxygenation of the cholesterol-7-d_1 molecules containing epimeric isotopic labels (5a and 5b) has demonstrated the cyclic nature of the reaction; the C—H or C—D bond broken was always
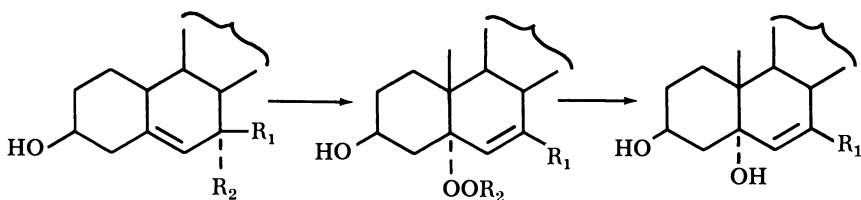
5a: R_1 = H, R_2 = D   **6a:** R_1 = H
5b: R_1 = D, R_2 = H   **6b:** R_1 = D

the bond on the α side of the steroid skeleton, cis to the C—O bond formed (*11*). At the time, however, no conclusions regarding the timing of the formation of the C—O and O—H bonds could be drawn.

The species that reacts with the olefin has been variously cited as singlet oxygen and as a complex between oxygen and sensitizer. We find only six reasonable ways to combine an olefin with singlet oxygen. These

possible intermediates are shown in Figure 2. The sensitizer, if still present, could be considered bound to the oxygen in some manner.

While the first five intermediates, 7 through 11, could be considered extreme forms of a resonance hybrid, we are obliged to consider these structures separately, lacking *a priori* information on the relative contributions of these forms.
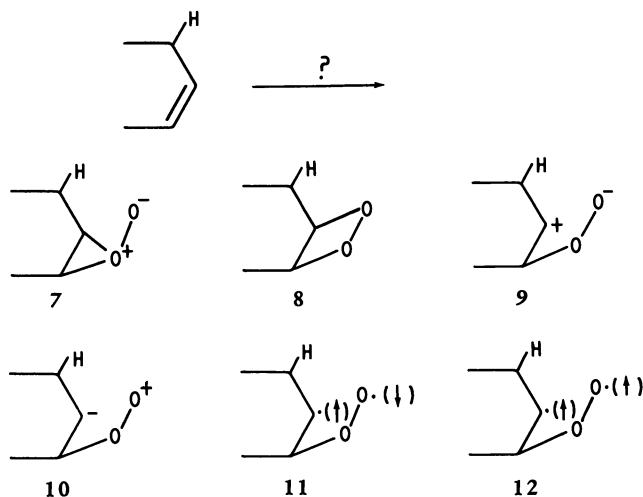

Figure 2. Possible intermediates in photo-oxygenation of olefin

Intermediate 7 was first proposed by D. B. Sharp (*14*) and named by him a "perepoxide." The following discussion, regarding the photo-oxygenation of a simple trisubstituted olefin, shows that the likelihood of involvement of this intermediate is small.

In the photo-oxygenation of a trisubstituted olefin, such as trimethyl-ethylene (13), two perepoxides are possible—a *syn*-perepoxide (14), and an *anti*-perepoxide (15)—as shown in Figure 3. While 14 could give either the tertiary hydroperoxide 16 or the secondary hydroperoxide 17, perepoxide 15 could only yield 17. Statistically, therefore, only one-fourth of the olefin undergoing reaction would give 16. In reaction of 13, the predominating perepoxide should be 15, for steric reasons. Furthermore, in the reaction of 14, if there is any partial positive charge on the oxirane carbon, 17 would predominate since the partial positive charge would be at a tertiary center rather than a secondary one, as for the formation of 16. Therefore the statistical result above is the upper limit required by this mechanism. The observed result was that the two hydroperoxides were formed in equal yields (8, 9). The photo-oxygenation of trisubstituted olefins other than 13 typically also gives nearly
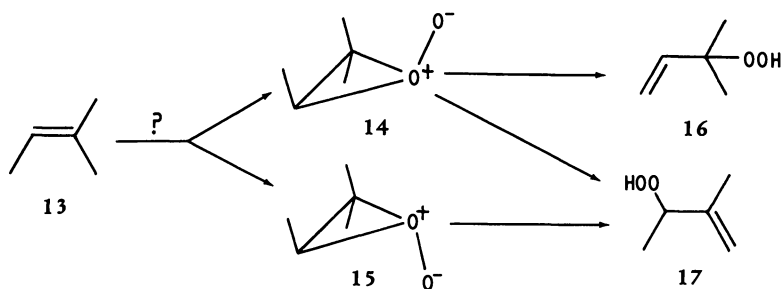
Figure 3.   Mechanism for photo-oxygenation of a trisubstituted olefin

equal yields of secondary and tertiary hydroperoxides (*1*). Involvement of perepoxide intermediates is not, therefore, likely.

A number of studies have shown that increasing alkyl substitution of the double bond facilitates the reaction (*9, 10, 14*). Intermediacy of **10** is, therefore, precluded since it requires the opposite substituent effect.

Norbornene (**18**) proved to be a useful substrate in testing for intermediates **8** and **9**. The bridgehead hydrogens are kept from participating by the consequent introduction of a bridgehead double bond (Bredt's rule) (*7*). The olefinic linkage in norbornene has been shown to be at least as reactive to a variety of reagents as that of an acyclic or monocyclic olefins (*6*). The dioxetane intermediate, **19,** if formed would be capable of giving *cis*-1,3-diformylcyclopentane, **20.** The zwitterion intermediate, **21,** if formed, would be capable of giving any of a host of ultimate products, through skeletal rearrangements customarily associated with the 2-norbornonium ion system (*12*). These reaction paths are shown in Figure 4.

With these possibilities in mind we attempted the photo-oxygenation of norbornene. With either methylene blue or hematoporphyrin as sensitizer and methanol or pyridine as solvent, we obtained no evidence of any reaction by infrared or NMR spectrum, by gas chromatography, or by spot test for hydroperoxide (potassium iodide/starch in 2-propanol/ acetic acid) or peroxide (hydriodic acid/starch in 2-propanol). While the half-life of reaction of cyclohexene was only about one day under our reaction conditions, no evidence of reaction of norbornene was obtained in a period of one month. Assay of norbornene by gas chromatography with benzene as internal standard failed to show any depletion of norbornene over the attempted reaction interval.

While we found no evidence of any reactivity of norbornene, the relevant point is that the reactivity, if existent, is at least four orders of magnitude lower than that of cyclohexene, a similarly substituted olefin containing reactive allylic hydrogens. We therefore find that the di-
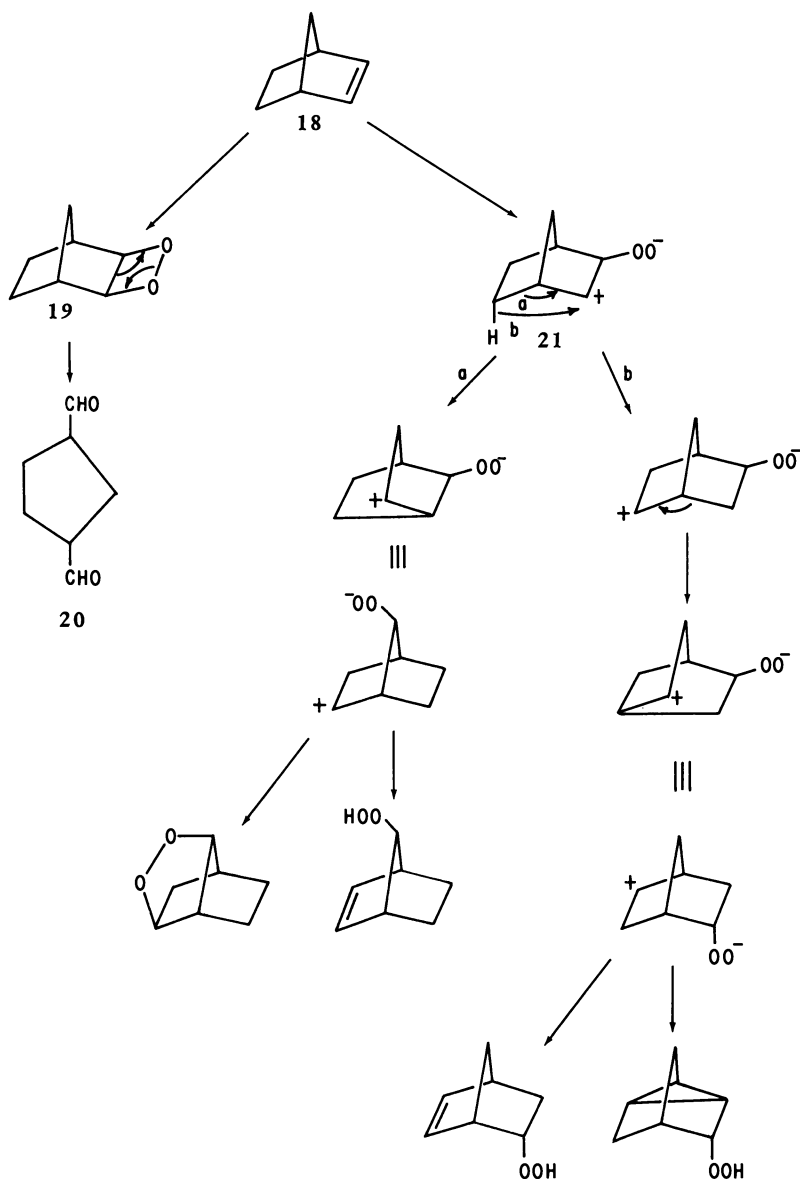
Figure 4.   Reaction paths in the photo-oxygenation of norbornene

oxetane and zwitterion intermediates 8 and 9, do not contribute signifi-
cantly to the photo-oxygenation path of "reactive" olefins.

The possible involvement of singlet diradical 11 or triplet diradical
12 was tested by studying the photo-oxygenation of various cis-trans
olefin pairs as follows. Figure 5 indicates a potential scheme for photo-

oxygenation of a 1,2-disubstituted olefin. (The scheme would apply to reaction of an unsymmetrical tri- or tetrasubstituted olefin as well.) The important feature of this sequence is the presence of a single bond in the position of the original double bond. Rotation around this single bond converts diradical **22**, produced by addition of oxygen to the cis olefin, to **23**, that produced from the trans olefin. If these intermediates were formed reversibly, the geometric isomers of the olefin would inter-convert during reaction.

We felt it best to select an unreactive olefin pair for this study since the reduced reactivity could reflect the slowness of the final step and maximize the isomerization possibility. The cyclododecene isomers were
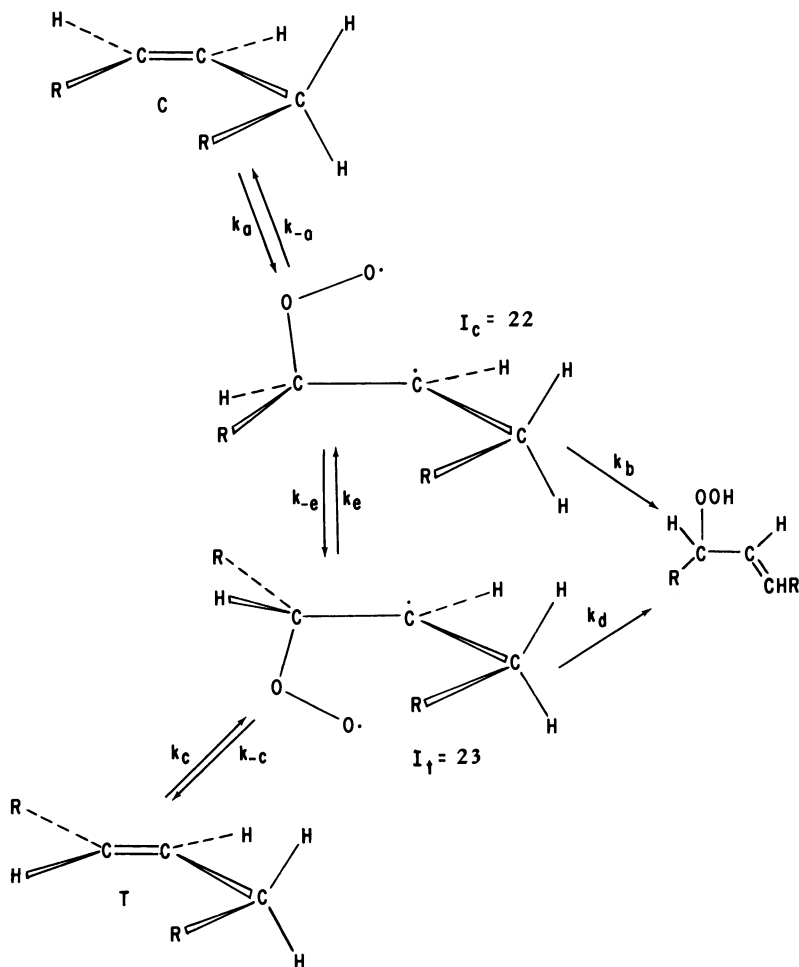

Figure 5.   Potential scheme for photo-oxygenation of a 1,2-disubstituted olefin

found suitable. Under the conditions in which cyclohexene reacted with a one-day half-life, the half-life of *trans*-cyclododecene photo-oxygenation was about 3 weeks. The trans isomer, **24**, was about three times as reactive as the cis isomer **25**. Samples of the cyclododecenes, separated from a


24   25
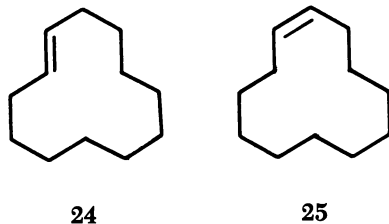
commercial mixture by preparative gas chromatography, were separately photo-oxygenated with methylene blue as sensitizer. Although the detection limit of the isomer of the starting olefin was less than 1%, relative to the starting isomer, in no case was isomerization detected.

Since it was desirable to include an olefin with a particularly large driving force toward isomerization we chose caryophyllene (**26**). The *trans*-cyclononene linkage of caryophyllene is readily isomerized by radicals such as the nitrogen oxides (*4*). Even in this case, however, no isomerization was apparent. We confirmed that isocaryophyllene (**27**) would have been detected under the reaction conditions had it been

26   27
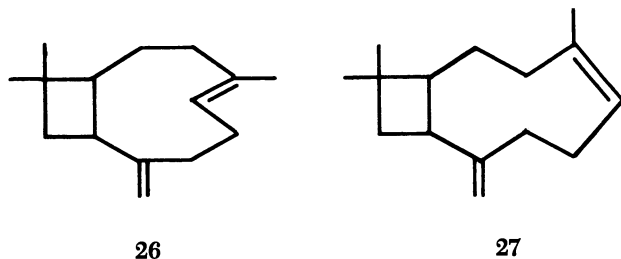
formed. We further found that caryophyllene was about five times as reactive as isocaryophyllene, and therefore, if isocaryophyllene had been formed, it would have persisted for detection.

To extend the generality of these results, we examined the photo-oxygenation of *trans, trans, trans*-1,5,9-cyclododecatriene (**28**). The

28   29
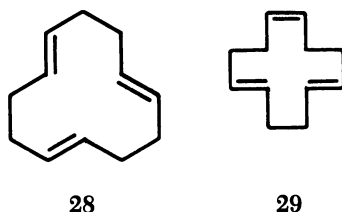
monoisomerized material (**29**) failed to appear during reactions. Examination of the photo-oxygenation of both geometrical isomers of 4-methyl-2-pentene and 2-octene (**30** through **33**) failed to show isomerization in these cases.

| **30** | **31** | **32** | **33** |
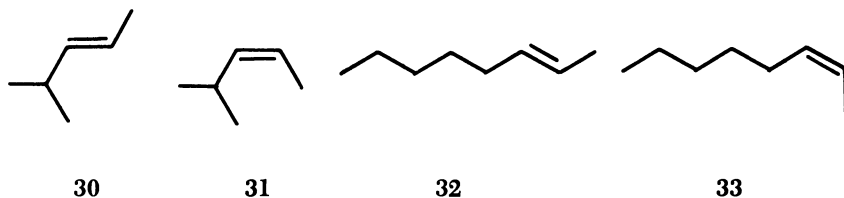
Quantitatively, unless the photo-oxygenation rate of the isomer not initially present is negligible compared with the photo-oxygenation rate of the starting isomer, the detection limit of the isomerization rate constant (as a fraction of the rate constant for product formation) is greater than that for the isomer initially absent since, if formed, some of the latter would react before detection. To evaluate the detection limit of the isomerization rate constant, the detailed scheme of Figure 5 is simplified to give the scheme of Figure 6.
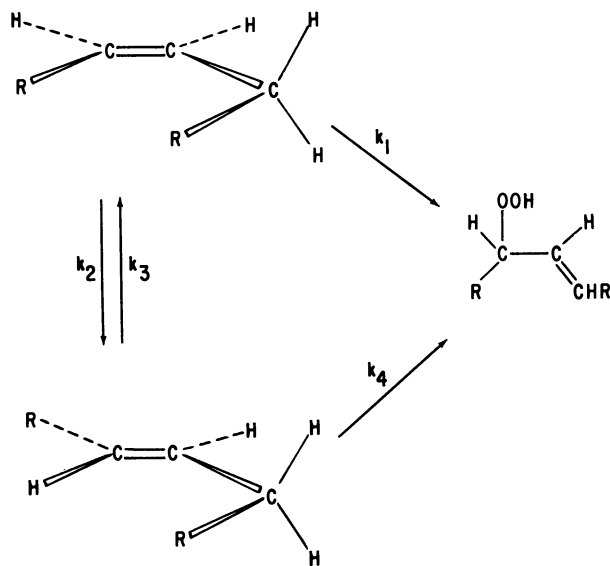

Figure 6.   Simplified scheme for photo-oxygenation of a 1,2-disubstituted olefin

Rate constants in Figure 6 are related to those in Figure 5 by the following equations:

$$k_1 = \left[\frac{1}{D}\right][k_a k_b(k_e + k_{-c} + k_d) + k_a k_{-e} k_d] \tag{1}$$

$$k_2 = \left[\frac{1}{D}\right][k_a k_{-e} k_{-c}] \tag{2}$$

$$k_3 = \left[\frac{1}{D}\right][k_c k_e k_{-a}] \tag{3}$$

$$k_4 = \left[\frac{1}{D}\right][k_c k_d(k_{-e} + k_b) + k_c k_e k_b] \tag{4}$$

where

$$D = [k_{-a} + k_{-e} + k_b)(k_{-c} + k_e + k_d) - k_e k_{-e}]$$

The details of this derivation, based on the steady-state approximation for the diradical intermediates, are found in the Appendix.

The derivation of the isomerization rate constant upper limit expression is as follows. For definiteness, assume the starting isomer to have the trans configuration. Under the high dilution conditions with these relatively unreactive disubstituted olefins we found the photo-oxygenation to proceed by pseudo-first-order kinetics. The rates of change of the concentrations of the two isomers are given by Equations 5 and 6.

$$dT/dt = -(k_3 + k_4)T + k_2 C \tag{5}$$

$$dC/dt = -(k_1 + k_2)C + k_3 T \tag{6}$$

where C and T represent the concentrations of the cis and trans isomers, respectively, and t is time.

Since the experiment shows that $k_4 >> k_3$, $k_1 >> k_2$, and k_1 is comparable with k_4, it follows that $k_2 C << k_4 T$ since $C << T$, and Equation 5 reduces to Equation 7, which integrates to Equation 8, in which the subscript o indicates the initial value.

$$dT/dt = -k_4 T \tag{7}$$

$$T = T_o \exp(-k_4 t) \tag{8}$$

Equation 8 is substituted into Equation 6, and with $k_1 >> k_2$, the latter differential equation is solved with the initial condition $C_o = 0$ to give Equation 9.

$$C = \frac{k_3 T_o}{k_1 - k_4}[\exp(-k_4 t) - \exp(-k_1 t)] \tag{9}$$

One unfortunate aspect of these long-duration photo-oxygenations is that the sensitizer bleached at a significant rate during the reaction and had to be replenished at intervals. It was desirable, therefore, to elimi-

nate time as a variable in Equation 9. Inversion of Equation 8 expresses the time as a function of the concentration of the trans olefin, and Equation 10 results from thus substituting Equation 8 into Equation 9.

$$C = \frac{k_3 T_o}{k_1 k_4} \left[(T/T_o) - (T/T_o)^{(k_1/k_4)} \right] \tag{10}$$

Equation 10 is then rearranged to yield an expression for k_3/k_4, Equation 11.

$$k_3/k_4 = mC/T_o \tag{11}$$

where $m = [(k_1/k_4) - 1][(T/T_o) - (T/T_o)^{k_1/k_4}]^{-1}$

If none of the *cis* isomer appeared during reaction, the upper limit of k_3, $k_{3\,lim}$ corresponds to the detection limit of the cis isomer, $C_{det.}$, as indicated in Equation 12.

$$k_{3lim}/k_4 = mC_{det}/T_o \tag{12}$$

The parameter m should be evaluated at the particular conversion analyzed. The best sample is the one that minimizes $k_{3\,lim}$; if the expression for m is differentiated with respect to T, the optimum conversion is found to be that of Equation 13. Experimentally, the relative photo-

$$(T/T_o)_{m_{min}} = (k_4/k_1)[(k_1/k_4) - 1]^{-1} \tag{13}$$

oxygenation rate, k_1/k_4, was determined, the optimum conversion calculated, and the single olefin photo-oxygenation performed, with aliquots taken until the conversion was near optimal. The detection limit was determined for this optimal aliquot, and the upper limit of the isomerization rate constant, k_2 or k_3, was calculated. The results of these experiments constitute Table I. Significant reversible formation of diradical intermediates, therefore, does not occur.

Table I. Upper Limits of Isomerization Rate Constants

Starting Isomer	Sought Isomer	Percent Unreacted	$\dfrac{k_{Sought}}{k_{Start}}$	M (Eq. 11)	Isomer Det. Lim.[a]	$k_{Isom.}$ Det. Lim.[b]
24	25	18[c]	0.34	1.7	0.2	0.4
25	24	60[c]	3.1	5.4	0.2	1.1
26	27	36	0.17	1.9	2.0	4.
28	29	48[c]	1.8	3.8	0.4	1.5
30	31	45	0.53	2.3	0.2	0.5
31	30	62	1.8	5.2	0.2	1.0
32	33	60	1.2	3.5	0.2	0.7
33	32	50	0.85	2.8	0.2	0.6

[a] Percent of initial concentration of starting isomer by gas chromatography.
[b] Percent of photo-oxygenation rate constant, Equation 12.
[c] Optimum point—aliquots taken over entire reaction.

The question of irreversible diradical formation can be answered by the following thermochemical argument. In Figure 7, irreversible diradical formation requires either $k_3 >> k_2$ or $k_6 >> k_7$ as a necessary condition. While, except for k_1, none of these rate constants have been measured for any olefin, we can examine the plausibility of the necessary condition for irreversible diradical formation through theoretical considerations.
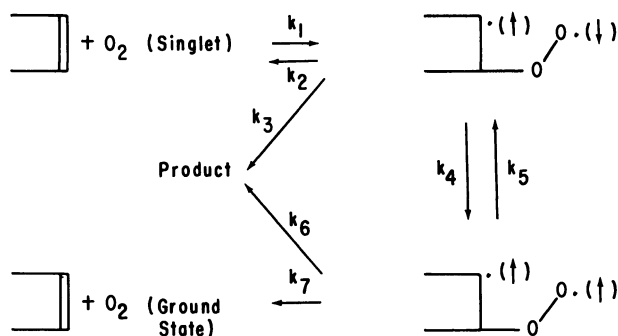

Figure 7.   Scheme for irreversible diradical formation

We would expect $k_7 > k_2$ since the entropies of Reactions 2 and 7 should be comparable, and Reaction 7 is the more exothermic. Since Reaction 6 requires intersystem crossing during reaction while Reaction 3 does not, we would expect $k_3 > k_6$. Therefore, disproof of $k_3 >> k_2$ is a condition sufficient to disprove irreversible diradical formation since this condition would also rule against $k_6 >> k_7$.

We estimate equilibrium constant k_1/k_2 as follows. Since ΔH and ΔG are differences between state functions of reactants and products, their values are independent of the path. We therefore use the experimentally infeasible but mathematically tractable path shown in Figure 8.

The actual triplet energies of olefins other than ethylene have not been reported; ethylene has a triplet energy of about 83 kcal./mole. An
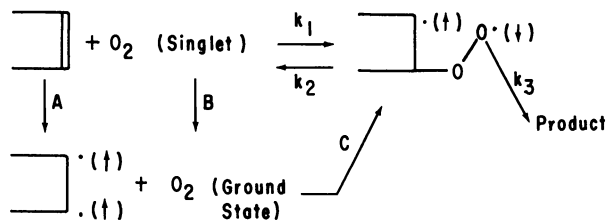

Figure 8.   Scheme showing mathematically tractable path for evaluating irreversible diradical formation

order of magnitude estimate of the effect of alkyl substitution may be obtained by using the "Woodwards rule" wavelength shift for dienes, converted to energy units. The shift of 5 mμ at the order of magnitude of 217 mμ is equivalent to 2.3% of the diene singlet energy or about 3 kcal./mole per alkyl group. We therefore take 75 kcal./mole as an approximate value for ΔH_A.

The value of ΔH_B is simply the excited state energy of oxygen— —22 kcal./mole for the $^1\Delta_g$ state and —38 kcal./mole for the $^1\Sigma_g^+$ state (the value is negative since the reaction is exothermic).

The value of ΔH_C can be estimated as the energy of the reaction

$$R\cdot + O_2 \text{ (ground state)} \rightarrow R\text{—O—O}\cdot,$$

the oxygenation of a simple alkyl free radical. Benson has reported this to be about —28 kcal./mole (exothermic) (*1*). This absolute value should be considered a lower limit for the oxygenation of the diradical, since the C—O bond formed in the latter case is somewhat weakened by the odd electron on the adjacent carbon.

Reaction 1, therefore, has a ΔH of about +25 kcal./mole for $O_2(^1\Delta_g)$ and about +9 kcal./mole for $O_2(^1\Sigma_g^+)$, both being highly endothermic. Since Reaction 1 involves the loss of three translational degrees of free-dom, $\Delta S_1 \cong -3R = -6$ cal./mole, °K., and $T\Delta S_1 \cong -1.8$ kcal./mole at room temperature. We therefore approximate ΔG_1 as +27 kcal./mole for $O_2(^1\Delta_g)$ and +11 kcal./mole for $O_2(^1\Sigma_g^+)$. Equilibrium constant k_1/k_2 is therefore approximately 10^{-19} for $O_2(^1\Delta_g)$ and 10^{-9} for $O_2(^1\Sigma_g^+)$, using the activities of reactants and products. Because of the high dilu-tion, we can assume unit activity coefficients. Rate constant ratio k_1/k_2 is, therefore, 10^{-19} (mole/liter)$^{-1}$ for $O_2(^1\Delta_g^+)$ and 10^{-9} (mole/liter)$^{-1}$ for $O_2(^1\Sigma_g^+)$.

The failure of the olefin to isomerize during reaction at the limits indicated in Table I indicate the necessity of hypothesizing $k_3/k_2 \geqslant$ ~10^2. Combining this result with the previous one, $k_3/k_1 \geqslant 10^{21}$ mole/liter for $O_2(^1\Delta_g)$ and $k_3/k_1 \geqslant 10^{11}$ for $O_2(^1\Sigma_g^+)$.

For *trans*-cyclododecene (**24**), the order of magnitude of the quan-tum yield may be estimated as follows. Cholesterol, under identical conditions, photo-oxygenates 100-200 times as fast as **24**. Eisfeld has shown that cholesterol photo-oxygenates at about 1/40 the rate of 2,5-dimethylfuran (**5**), which in turn has been shown to photo-oxygenate with a quantum yield of the order of 0.5 (*9*). The quantum yield of *trans*-cyclododecene photo-oxygenation is thus about 10^{-4} at the concen-tration studied, about 10^{-2} moles/liter. Schenck and Koch have shown that the species that reacts with the olefins decays with a rate constant of about 10^8 sec.$^{-1}$ (*13*). The value of k_1 for **24** therefore is about 10^6 liters/mole-sec. Therefore, for the $^1\Delta_g$ and $^1\Sigma_g^+$ states of oxygen, $k_3 \geqslant$

10^{27} and 10^{18} sec.$^{-1}$, respectively. These are, of course, greater than Eyring's transition-state vibrational frequency kT/h. Irreversible formation of diradicals is, therefore, impossible. We therefore conclude that the reaction of the olefin is concerted.

Supporting evidence against irreversible intermediate formation is found in some unpublished studies by H. G. Vilhuber (15), E. Werstiuk (16), and V. Chuang (3) on the primary deuterium isotope effect. Primary isotope effects of 1.2 to 2.1 were determined for deuterated olefins **34-36.**

34   **35**   **36**
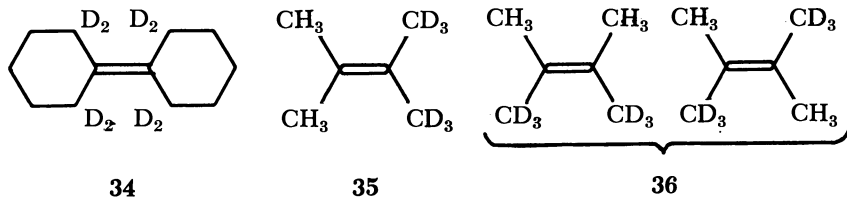
Participation of the hydrogen (or deuterium) during the rate-determining reaction is thus indicated since, as shown earlier, the O—H bond could not be formed prior to formation of the C—O bond.

Experimental

Photo-oxygenations were performed in a tubular apparatus previously reported (4). In the photo-oxygenation of the more volatile olefins (**30** through **33**), the solvent was saturated with oxygen before dissolution of the olefin, and no oxygen was admitted during irradiation. In the photo-oxygenation of the slower olefins (**24, 25, 28**) a 500-watt slide projector was used in conjunction with a flat-sided cell and a capillary bubbler.

Preparative gas chromatography was used to separate the cyclodo-decene isomers. An Aerograph A-700 instrument with a 20-foot × 3/8 inch diethylene glycol succinate polyester column at 160°C. was used. The crude fractions were rechromatographed to obtain samples of *ca.* 99.8% purity.

cis-2-Octene (**33**) was purified by preparative gas chromatography in the same instrument with a 12 foot × 1/4 inch silver nitrate/diethylene glycol column at room temperature. The purity of the product was *ca.* 99.9%.

trans, trans, trans-1,5,9-Cyclododecatriene (**28**) was isolated by partial freezing of the commercial mixture of isomers and recrystallizing the solid product from methanol.

The caryophyllene (**26**) used contained about 3% isocaryophyllene (**27**) (we are indebted to Dr. J. Roberts for supplying this sample). Attempts to remove this impurity by preparative gas chromatography led to no improvement. Other olefins were commercial samples of > 99% purity.

Reactions were monitored by gas chromatography. Cyclododecane was used as internal standard for olefins **24** through **29** on a Perkin-Elmer model 226 instrument with a 9 foot ×1/8 inch diethylene glycol succinate

polyester column at 150°C. Benzene was used as internal standard in the photo-oxygenation of **18** and **30** through **33** on an Aerograph instrument with a 10 foot × 1/8 inch silver nitrate/diethylene glycol column at room temperature.

Acknowledgments

Literature Cited

(1) Benson, S. W., *J. Am. Chem. Soc.* **87**, 972 (1965).
(2) Calvett, J. G., Pitts, Jr., J. N., "Photochemistry," p. 91, Wiley, New York, 1966.
(3) Chuang, V., Nickon, A., unpublished results.
(4) Deussen, E., Lewinsohn, A., *Ann.* **356**, 20 (1907).
(5) Eisfeld, W., Ph.D. Dissertation, Göttingen, 1965.
(6) Eliel, E. L., "Stereochemistry of Carbon Compounds," p. 303, McGraw-Hill, New York, 1962.
(7) Fawcett, F. S., *Chem. Rev.* **47**, 219 (1950).
(8) Foote, C. S., Wexler, R., Ando, W., *Tetrahedron Letters* **46**, 4111 (1965).
(9) Gollnick, K., Schenck, G. O., *Pure Appl. Chem.* **9**, 507 (1964).
(10) Kopecky, K. R., Reich, H. J., *Can. J. Chem.* **43**, 2265 (1965).
(11) Nickon, A., Bagli, J. F., *J. Am. Chem. Soc.* **83**, 1498 (1961).
(12) Sargent, G. D., *Quart. Rev.* **20**, 301 (1966).
(13) Schenck, G. O., Koch, E., *Z. Electrochem.* **64**, 170 (1960).
(14) Sharp, D. B., "Abstracts of Papers," 138th Meeting, ACS, Sept. 1960, 79P.
(15) Vilhuber, H. G., Nickon, A., unpublished results.
(16) Werstiuk, E., Nickon, A., unpublished results.

Appendix

Simplification of isomerization kinetics:
The complete kinetic scheme for isomerization and reaction is shown in Figure 5.
Assuming I_o and I_t are at steady-state concentrations:

$$d(I_c)/dt = 0 = k_a C + k_e I_t - k_{-a} I_c - k_{-c} I_c - k_b I_c \qquad \text{(A-1)}$$

$$d(I_t)/dt = 0 = k_c T + k_{-e} I_c - k_{-c} I_t - k_e I_t - k_d I_t, \qquad \text{(A-2)}$$

where t is time, C and T represent cis and trans olefins, I_c and I_t represent the intermediates, and all k's are pseudo-first-order rate constants.

Rearranging Equations A-1 and A-2

$$I_c(k_{-a} + k_{-e} + k_b) + (-k_e)I_t = k_a C. \qquad (A\text{-}3)$$

$$I_t(k_{-c} + k_e + k_d) + (-k_{-e})I_c = k_c T. \qquad (A\text{-}4)$$

Solving Equations A-3 and A-4 simultaneously for I_c and I_t

$$I_c = \frac{k_a C(k_{-c} + k_e + k_d) + k_c k_e T}{(k_{-a} + k_{-e} + k_b)(k_e + k_{-c} + k_d) - k_e k_{-e}} \qquad (A\text{-}5)$$

$$I_t = \frac{k_c T(k_{-a} + k_{-e} + k_b) + k_a k_{-e} C}{(k_{-a} + k_{-e} + k_b)(k_e + k_{-c} + k_d) - k_e k_{-e}} \qquad (A\text{-}6)$$

Defining

$$k_1 = \frac{k_a k_b(k_e + k_{-c} + k_d) + (k_a k_{-e} k_d)}{(k_{-a} + k_{-e} + k_b)(k_{-c} + k_e + k_d) - k_e k_{-e}} \qquad (A\text{-}7)$$

$$k_2 = \frac{k_a k_{-c} k_{-c}}{(k_{-a} + k_{-e} + k_b)(k_{-c} + k_e + k_d) - k_e k_{-e}} \qquad (A\text{-}8)$$

$$k_3 = \frac{k_c k_e k_{-a}}{(k_{-a} + k_{-e} + k_b)(k_{-c} + k_e + k_d) - k_e k_{-e}} \qquad (A\text{-}9)$$

$$k_4 = \frac{k_c k_d(k_{-e} + k_{-a} + k_b) + (k_c k_e k_b)}{(k_{-a} + k_{-e} + k_b)(k_{-c} + k_e + k_d) - k_e k_{-e}} \qquad (A\text{-}10)$$

The detailed system is kinetically equivalent to the simplified system of Figure 6,

$$dC/dt = -(k_1 + k_2)C + k_3 T \qquad (A\text{-}11)$$

$$dT/dt = -(k_3 + k_4)T + k_2 C \qquad (A\text{-}12)$$

as may be verified by substituting Equations A-5 through A-10 into the kinetic law for Figure 5, which is

$$dC/dt = -k_a C + k_a I_c$$

$$dT/dt = -k_c T + k_c I_t$$

Relaxation and Reactivity of Singlet Oxygen

S. J. ARNOLD, M. KUBO, and E. A. OGRYZLO

University of British Columbia, Vancouver 8, B. C., Canada

Measurements of some energy transfer, physical quenching, and chemical reaction processes of singlet oxygen are presented. The results of these measurements and those obtained previously are analyzed in an attempt to assess the fate of $O_2(^1\Delta_g)$ and $O_2(^1\Sigma_g^+)$ in oxidation systems.
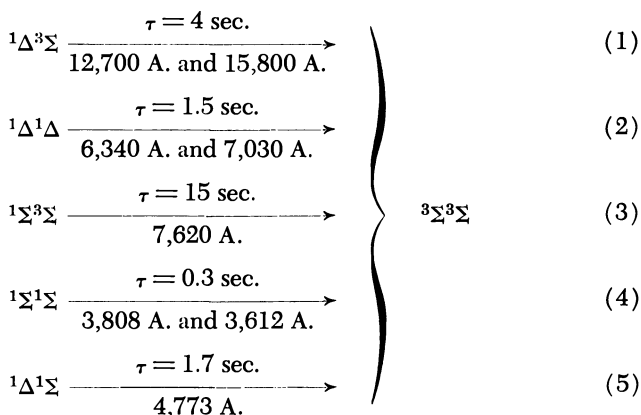
Two electronically excited singlet states of oxygen are located 22.5 and 37.5 kcal. above the triplet ground state. The one at 22.5 kcal. is commonly designated $a^1\Delta_g$ and will be abbreviated $^1\Delta$. The higher one has the term symbol $b^1\Sigma_g^+$ and will be referred to as $^1\Sigma$. The ground state $X^3\Sigma_g^-$ will be abbreviated $^3\Sigma$. Because their relative importance in chemical reactions has not yet been determined, these two excited states are referred to as singlet oxygen. This paper considers the various physical and chemical processes which the two species can undergo, and an attempt is made to assess their relative importance in oxidation processes.

Experimental

A typical flow system used to prepare $^1\Delta$ molecules for kinetic studies is shown in Figure 1. Oxygen at a pressure between 1 and 10 torr is passed through a microwave discharge. The atoms are removed with a mercuric oxide ring immediately after the discharge. The concentration is measured at one point in the tube by the heat liberated when the molecules are deactivated on a cobalt wire. Relative concentrations of excited molecules along the observation tube can be measured with a movable interference filter and photomultiplier. The details of these methods have been described (1, 3, 4). Tank oxygen is normally selected for low nitrogen content and used without further purification. Quenching gases were treated only to remove higher boiling impurities, especially water.

Radiative Relaxation

In the absence of any external perturbation both $^1\Delta$ and $^1\Sigma$ oxygen do not emit any measurable electric dipole radiation. However, with a lifetime of 7 sec., $^1\Sigma$ can give rise to magnetic dipole radiation at 7619 A., and $^1\Delta$ can give rise to magnetic dipole radiation at 12,683 A. with a lifetime of 45 minutes. In a collision with another molecule electric dipole transitions between these states are made more probable, and the radiative lifetime can be shortened. The exact radiative lifetime of singlet oxygen in a collision complex is difficult to estimate because the duration of a collision is uncertain. However, with a reasonable estimate of about 10^{-13} sec. for this collision time, the following radiative lifetimes for a number of collision complexes can be calculated from the integrated absorption coefficients.

$$^1\Delta{}^3\Sigma \xrightarrow[\text{12,700 A. and 15,800 A.}]{\tau = 4 \text{ sec.}} \qquad (1)$$

$$^1\Delta{}^1\Delta \xrightarrow[\text{6,340 A. and 7,030 A.}]{\tau = 1.5 \text{ sec.}} \qquad (2)$$

$$^1\Sigma{}^3\Sigma \xrightarrow[\text{7,620 A.}]{\tau = 15 \text{ sec.}} \qquad {}^3\Sigma{}^3\Sigma \qquad (3)$$

$$^1\Sigma{}^1\Sigma \xrightarrow[\text{3,808 A. and 3,612 A.}]{\tau = 0.3 \text{ sec.}} \qquad (4)$$

$$^1\Delta{}^1\Sigma \xrightarrow[\text{4,773 A.}]{\tau = 1.7 \text{ sec.}} \qquad (5)$$

When the collision complex is made up of two excited molecules, a novel energy pooling process occurs in which the energy of two molecules appears in a single photon. The above list shows that the probability of such a cooperative event can be comparable with that for a one-electron transition. However, because the fraction of molecules in a state of collision is small, radiative relaxation is not responsible for the decay of a significant number of excited molecules under the usual experimental conditions. For example, the strongest induced radiation for $^1\Delta$ occurs at 6340 and 7030 A. If this were the only mode of decay, the observed lifetime at 1 atm. would be 10^3 sec., whereas the observed lifetime is much less than 1 sec. The 6340-A. band is, however, a convenient and sensitive emission for monitoring the singlet delta concentration since the emission intensity is proportional to the square of its concentration.
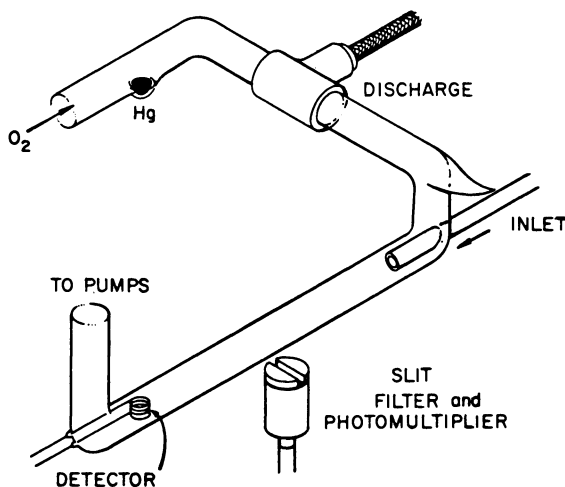
Figure 1. Core of flow system used for quenching studies

Energy Transfer

For efficient transfer of electronic excitation to another molecule, the acceptor must possess an excited electronic state at or not too far below that of the donor. Not many molecules can meet this requirement when the donor is singlet oxygen. We have observed energy transfer to the following species, (a) another $^1\Delta$ molecule, (b) violanthrone (dibenzanthrone), (c) nitrogen dioxide, and (d) iodine atoms. The mechanism of energy transfer to (b) is not well understood and will be described elsewhere (7). Since (c) and (d) are not directly related to the subject of hydrocarbon oxidation, they will not be discussed in any detail. The transfer to iodine atoms is undoubtedly the most efficient process which we have observed (2), and this can be attributed to the fact that the $^2P_{1/2}$ state of iodine lies 22 kcal. above the $^2P_{3/2}$ ground state—in almost perfect resonance with $^1\Delta$ oxygen. The transfer to nitrogen dioxide is much less efficient and appears to involve energy transfer from $^1\Sigma$ and $^1\Delta$ to raise the acceptor to a radiating state which lies about 60 kcal. above the ground state (2).

$^1\Delta$–$^1\Delta$ **Transfer.** Since the $^1\Sigma$ state lies 15 kcal. above the $^1\Delta$, the latter can act as an acceptor as well as a donor in an energy disproportionation process:

$$^1\Delta + {}^1\Delta \xrightarrow{k_D} {}^1\Sigma + {}^3\Sigma \tag{6}$$

Two laboratories have reported rate constants for this reaction. A value of 1.8×10^7 liters/mole/sec. was reported by Young and Black (8),

and a value of 1.3 $\times$ 10³ liters/mole/sec. was more recently reported by Arnold and Ogryzlo (3). Because of the large discrepancy between these two values we have attempted a third determination by measuring the rate of ¹Δ removal directly. The results of these measurements are shown in Figure 2. The ¹Δ concentration was varied by changing the power fed into the discharge. Assuming that in addition to Reaction 6, which is
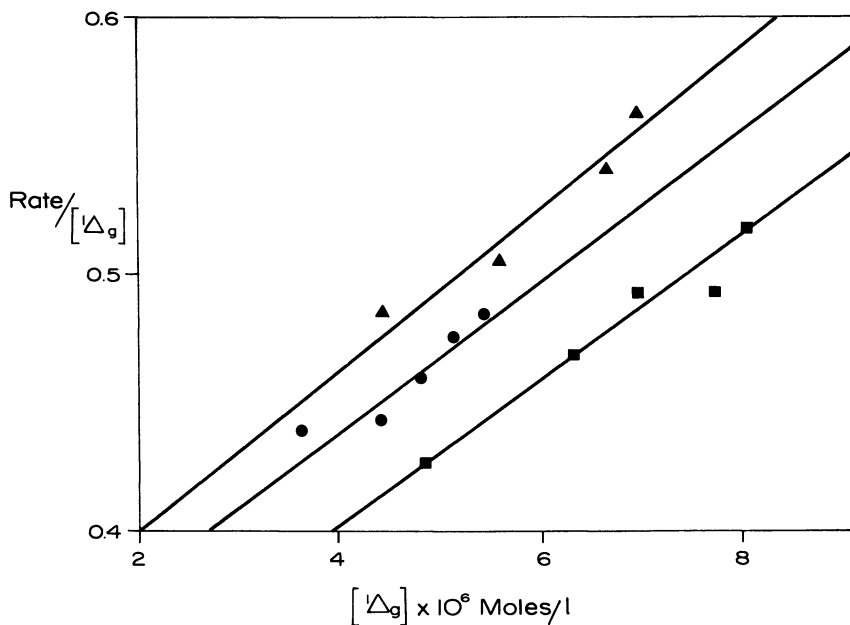
Figure 2.   Rate of singlet delta decay ($R = d[^1\Delta]/dt$) divided by singlet delta concentration as a function of the singlet delta concentration

second order in ¹Δ, we can have wall and gas-phase quenching that is first order in ¹Δ, the rate equation becomes:

$$R = \frac{d[^1\Delta]}{dt} = k_Q[^1\Delta] + k_D[^1\Delta]^2$$

$$R/[^1\Delta] = k_Q + k_D[^1\Delta_g]$$

The slopes of the lines in Figure 2 are then equal to k_D. The average value we obtain is 3 $\times$ 10⁴ liters/mole/sec. This value can be compared with 1.3 $\times$ 10³ liters/mole/sec., previously reported by Arnold and Ogryzlo (3) for Reaction 6. The technique used in the earlier measurement is quite difficult, and possibly the value is somewhat low. However, it is also conceivable that the process we have measured is not the slower,

spin-forbidden Reaction 6, but the more rapid spin-allowed process, Reaction 7.

$$^1\Delta + {}^1\Delta \rightarrow {}^3\Sigma + {}^3\Sigma \tag{7}$$

A decision between these possibilities must await further measurements. We can only conclude that the value of k_6 lies between 1.3×10^3 and 3×10^4 liters/mole/sec.

An important consequence of the occurrence of Reaction 6 is that $^1\Sigma$ is constantly being formed in any system which contains $^1\Delta$. We shall see later that the reverse is probably also true.

Radiationless Non-Resonance Relaxation

When an external perturbation such as that caused by a colliding molecule is sufficiently great, the electronic excitation may be degraded into nuclear motion within the collision complex. However, very little information is available about the efficiency of such processes, and consequently no complete theoretical model exists which we could use to predict quenching rates.

The experimental determination of $^1\Delta$ quenching is difficult because of its great stability. In most flow systems the decay is largely on the walls of the vessel where it can suffer about 2×10^5 collisions before deactivation. Collisions with most other molecules are even less effective. At the moment it can only be said that more than 10^8 collision with $O_2(^3\Sigma)$ are necessary to deactivate $^1\Delta$. Other, nonreactive gases cannot be tested simply because so much must be added that it radically affects the flow system and discharge, making the measurements difficult to interpret.

The quenching of $^1\Sigma$ oxygen is somewhat easier to study because it is more easily deactivated. In the absence of any quenching gas, a steady-state concentration of $^1\Sigma$ is maintained in the flow system by the following reactions.

$$^1\Delta + {}^1\Delta \xrightarrow{k_D} {}^1\Sigma + {}^3\Sigma \tag{8}$$

$$^1\Sigma + \text{wall} \xrightarrow{k_w} \text{products} \tag{9}$$

hence,

$$^1\Sigma = \frac{k_D}{k_w} [^1\Delta]^2 \tag{10}$$

and the emission intensity from $^1\Sigma$ is given by

$$I = k[^1\Sigma] = k \frac{k_D}{k_w} [^1\Delta]^2$$

In the presence of a quenching gas (Q) we must add Reaction 11:

$$^1\Sigma + Q \xrightarrow{k_Q} \text{products} \tag{11}$$

and therefore the steady state concentration is given by

$$[^1\Sigma] = \frac{k_D[^1\Delta]^2}{k_W + k_Q[Q]} \tag{12}$$

and the emission intensity in the presence of Q:

$$I_Q = \frac{kk_D[^1\Delta]^2}{k_w + k_Q[Q]} \tag{13}$$

The ratio of the emission with and without the quencher is therefore given by:

$$\frac{I_o}{I_Q} = 1 + \frac{k_Q}{k_w}[Q] \tag{14}$$

A plot of I_o/I_Q against Q should yield a straight line with a slope of k_Q/k_w. Such a plot is given in Figure 3 for 15 different gases.
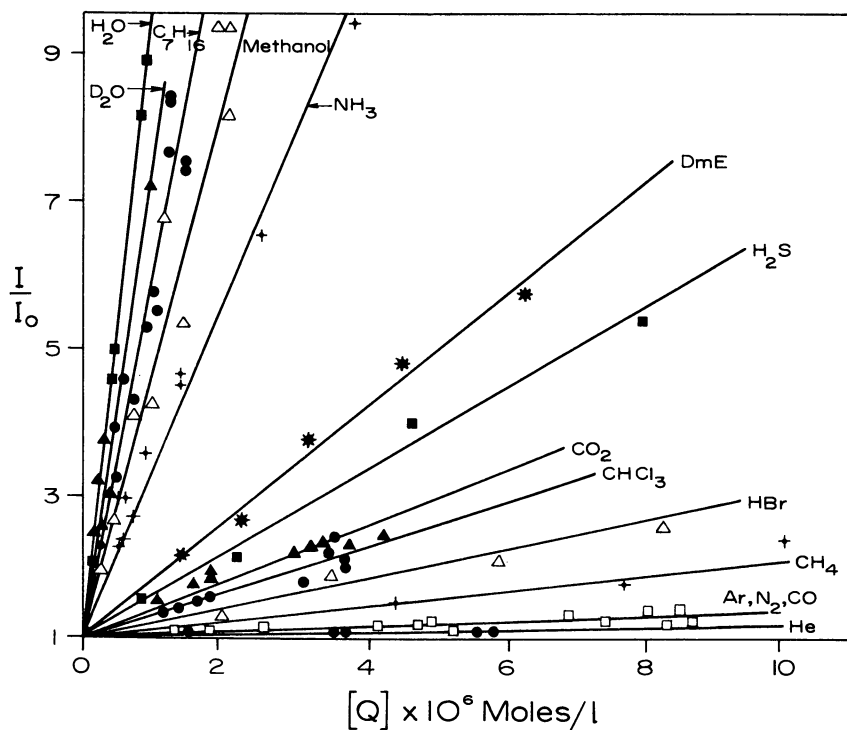

Figure 3.   *Stern-Volmer plot of 7619-A. emission intensity for a series of quenching gases*

Table I. k_Q/k_w from I_o/I_Q vs. Q

	$k_Q/k_w \times 10^{-6}$	$k_Q \times 10^{-7}$ if $k_w = 1,300$	if $k_w = 65$
He	0.01	1.5	0.07
N_2, Ar, CO	0.02	3	0.15
CH_4	0.11	16	0.8
HBr	0.21	30	1.5
$CHCl_3$	0.31	45	8.8
CO_2	0.39	56	2.8
H_2S	0.56	81	4.0
DME	0.78	110	10
NH_3	2.3	330	16
Methanol	3.7	530	26
Heptane	5.0	720	36
D_2O	6.8	980	49
H_2O	8.5	1200	60

The values of k_Q/k_w obtained from the slopes of these lines are given in Table I. To obtain k_Q, we require k_w. This can be obtained from measurements of the steady-state $^1\Sigma$ and $^1\Delta$ concentrations in the absence of any quencher. From Equation 10,

$$\frac{k_D}{k_w} = \frac{^1\Sigma}{[^1\Delta]^2}$$

Values of $[^1\Delta]$ and $[^1\Sigma]$ are listed in Table II together with values of k_D/k_w. From the value of $k_D = 3 \times 10^4$ calculated earlier we obtain $k_w = 1.3 \times 10^3$ on a clean borosilicate glass surface. Combining this value of k_w with the values of k_Q/k_w in Table I, we obtained the values of k_Q listed in the second column of the same table. The third column gives the values of k_Q calculated with the previously determined (3) value of $k_w = 65$.

Table II.   Values of $[^1\Delta]$ and $[^1\Sigma]$

P, torr	$[O_2(^1\Sigma_g^+)] \times 10^9$, Moles/Liter	$[O_2(^1\Delta_g)] \times 10^6$, Moles/Liter	k_D/k_w, Liters/Mole
2.4	1.75	9.0	20.5
3.1	2.54	11.0	21.5
3.8	4.20	14.2	20.8
5.1	6.24	17.5	20.3

In this process $^1\Sigma$ may be relaxed into either the $^1\Delta$ or $^3\Sigma$ state. Since the transition to the $^3\Sigma$ state requires the conversion of more electronic energy into nuclear motion and also requires a "spin flip," we would expect the transition to the $^1\Delta$ state to be much more probable. This is confirmed by the observation that the quenching by paramagnetic O_2 is,

if anything, less effective than species like Ar and N_2. None of the molecules included in this study display any special resonance effect. There is, however, a rough correlation between quenching efficiency and boiling point. This is a reasonable correlation since one might expect the probability of such an induced transition to be related to the magnitude and duration of the perturbation. We will not attempt a detailed analysis of this correlation here and will simply observe that boiling points reflect both these quantities in a somewhat indirect manner and can therefore be used to estimate quenching rates.

Physical Quenching Processes

From Equation 16 it follows that in the presence of a quenching species Q the ratio of $^1\Sigma$ to $^1\Delta$ concentrations is given by

$$\frac{[^1\Sigma]}{[^1\Delta]} = \frac{k_D[^1\Delta]}{k_Q[Q]}$$

When Q is water or a hydrocarbon with a similar boiling point, the equation becomes:

$$\frac{[^1\Sigma]}{[^1\Delta]} = 2 \times 10^{-6} \frac{[^1\Delta]}{[Q]}$$

In most chemical and photochemical oxidation systems the ratio of $[^1\Delta]$ to $[Q]$ is extremely small, and therefore the $^1\Sigma/^1\Delta$ ratio is very much smaller than 10^{-6}. The only such system in which this ratio might be approached is the Cl_2–H_2O_2 reaction where the partial pressure of $^1\Delta$ probably exceeds 70 torr (6). However, we must also consider the quenching of $^1\Delta$. The relevant processes are then the following in the presence of quenchers such as water:

$$^1\Sigma \left\{ \begin{array}{c} \xrightarrow[\text{[Q]}]{k \simeq 10^9} \\ \xleftarrow[{[^1\Delta]}]{k = 1.3 \times 10^3} \end{array} \right\} {}^1\Delta \xrightarrow[\text{[Q]}]{k \approx 10^1 - 10^2} {}^3\Sigma$$
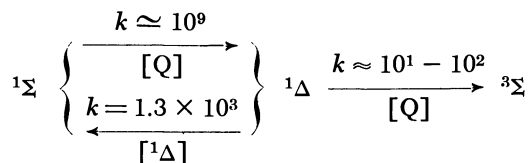
(Since we are most interested in the possibility that $^1\Sigma$ contributes to the reactivity of singlet oxygen, we have used the lower quenching constants for $^1\Sigma$ calculated from Arnold and Ogryzlo's value of k_w (3).) In about one collision in 100 ($\sim 10^{-9}$ sec. in solution) $^1\Sigma$ is relaxed to $^1\Delta$ by Q. Only if $^1\Delta$ is $\approx 0.1\%$ of Q is $^1\Sigma$ efficiently reformed from $^1\Delta$. Otherwise, it is relaxed to $^3\Sigma$ in about one collision in 10^9–10^{10} (1-10 msec. in solution) with Q. Under these conditions we obtain a $^1\Delta/^1\Sigma$ ratio of about 10^8. Consequently, in such systems when a steady state is established, the rate constant for reaction with $^1\Sigma$ would have to be about 10^8 faster than that for $^1\Delta$ to be competitive.

Chemical Reactions

No technique for measuring the absolute values of rate constants for singlet oxygen reactions in solution has yet been reported. However, such a measurement is possible in the gas phase with the technique described here, provided the species is volatile and highly reactive. We have studied the reaction of singlet oxygen with tetramethylethylene (TME), whose reaction with singlet oxygen in the gas phase was first described by Bayes and Winer (5). The reaction was followed by monitoring the $^1\Delta$ and $^1\Sigma$ concentrations under various conditions. We have found, however, that kinetically the process is not as simple as the preliminary studies suggested. It is possible that this may be a characteristic of exothermic association processes in low density systems where there are an insufficient number of collisions which unreactive molecules to prevent chain reactions from developing. In contrast to the situation in condensed media, it is highly probable that the energy-rich product of the initial reaction will collide with another energetic molecule rather than with an inert species which could relax it to a stable product. We are attempting to study the reaction under conditions which are more comparable with those in the solution reaction, with the hope that the kinetics will become somewhat simpler. Ignoring the complexity of the system we can make a preliminary estimate of 10^8 liters/mole/sec. for this rate constant (TME-$^1\Delta$) from the initial slope of the decay curve.

We have no evidence for a direct reaction between TME and $^1\Sigma$. The effect of TME on the steady-state $^1\Sigma$ concentration is consistent with its boiling point—*i.e.*, it quenches (or reacts with) it with a rate constant somewhat smaller than 10^9 liters/mole/sec. In the last section we concluded that in order to make a significant contribution to the reactions of singlet oxygen in systems where steady-state concentrations of $^1\Sigma$ and $^1\Delta$ are established, the rate constant for the $^1\Sigma$ reaction would have to be between 10^5 and 10^8 times faster than that for $^1\Delta$. This clearly cannot be the case for the TME since collision frequency would be exceeded. However, in "non-steady-state" systems where the initial concentration of $^1\Sigma$ is comparable with $^1\Delta$, the direct importance of the former species depends on the ratio of quenching species to reactive species. However, $^1\Sigma$ is probably relaxed to $^1\Delta$, and even if it does not react directly can indirectly lead to oxidation.

Acknowledgment

Literature Cited

(1) Arnold, S. J., Browne, R. J., Ogryzlo, E. A., *Photochem. Photobiol.* 4, 963 (1965).
(2) Arnold, S. T., Finlayson, N., Ogryzlo, E. A., *J. Chem. Phys.* **44,** 2529 (1966).
(3) Arnold, S. T., Ogryzlo, E. A., *Can. J. Phys.* **45,** 2053 (1967).
(4) Bader, L. W., Ogryzlo, E. A., *Discussions Faraday Soc.* **37,** 46 (1964).
(5) Bayes, K. D., Winer, A. M., *J. Phys. Chem.* **70,** 302 (1966).
(6) Browne, R. J., Ogryzlo, E. A., *Can. J. Chem.* **43,** 2915 (1965).
(7) Ogryzlo, E. A., Pearson, A. E., *J. Phys. Chem.* **72,** 2913 (1968).
(8) Young, R. A., Black, G., *J. Chem. Phys.* **42,** 3740 (1965).

Generation and Reactions of ${}^1\Sigma_g^+$ and ${}^1\Delta_g$ Oxygen Molecules in Sensitized Photo-Oxygenations

AHSAN U. KHAN and DAVID R. KEARNS

University of California, Riverside, Calif.

In the oxygen-induced quenching of triplet state molecules, ${}^3M_1$, ${}^1\Sigma_g^+$ and ${}^1\Delta_g$ oxygen molecules can be generated by energy transfer from ${}^3M_1$; the ${}^1\Sigma_g^+$ and ${}^1\Delta_g$ generation rates are predicted to be a function of E_t, the triplet state energy of the donor. Experimental evidence for the formation and reaction of ${}^1\Sigma_g^+$ and ${}^1\Delta_g$ is presented. The energetics of the $M \ldots O_2$ complex indicate that the $[{}^3M_1 \ldots {}^3O_2]$ complex may be stable, whereas the $[{}^1M_0 \ldots {}^1O_2]$ complexes are not. These results allow us to resolve some current controversies. The reaction of O_2 with dienes to form endoperoxides and the decomposition of peroxides were investigated theoretically. A procedure, using state correlation diagrams, can be used to predict the reactivities of ${}^1\Delta_g$ and ${}^1\Sigma_g^+$ oxygen toward organic acceptors.

It has become clear recently that the metastable excited singlet states of molecular oxygen ${}^1\Sigma_g^+$ and ${}^1\Delta_g$ play an unsuspected but important role in numerous physical and chemical transformations which involve the interaction of electronically excited organic molecules with oxygen (5, 11, 12, 20, 21, 31, 42, 43, 53, 54). The basis for much of the current thinking is apparently derived from suggestions by Kautsky (20) regarding the mechanism of dye sensitized photo-oxygenations. He proposed that excited oxygen molecules (${}^1\Sigma_g^+$ or ${}^1\Delta_g$), generated by transfer of electronic excitation energy from the triplet state of a sensitizer, are the reactive intermediates in sensitized photo-oxygenation reactions. Although the Kautsky mechanism appears to account satisfactorily for much of the data regarding sensitized photo-oxygenation reactions, it raises interesting questions regarding the mechanism by which molecular oxygen

quenches triplet state molecules, the relation between the quenching mechanism and the oxygenation reactions, and perhaps most interestingly, the nature of the reactivity of singlet state excited oxygen molecules.

Here we summarize the results of our previous investigation of the quenching of triplet state molecules by oxygen (*21*) and present some new results on the energetics of the interaction of O_2 with organic molecules. We then show how these results provide new insight into the nature of the intermediates involved in sensitized photo-oxygenation reactions. Finally, we consider the problem of predicting the course of reactions of ground and singlet excited state oxygen molecules with organic acceptors such as dienes.

Quenching of Triplet State Molecules by Oxygen

Mechanisms. Molecular oxygen is known to quench reversibly the emission from triplet state molecules in what appears to be a diffusion controlled process (*1, 42, 43*). During the past 30 years a number of different mechanisms have been suggested to account for this quenching.

ELECTRON TRANSFER. Since many inorganic ions quench the fluorescence and phosphorescence of organic molecules in solutions by electron transfer, Weiss proposed that the quenching action of molecular oxygen might similarly be caused by an electron transfer of the type (*55*):

$$^3M_1 + {}^3O_2 \rightarrow M^+ + O_2^-$$
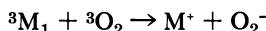
where $^3M_1$ is a triplet state donor molecule, $^3O_2$ is a ground state oxygen molecule, and M^+ and O_2^- are the respective ions. It would appear that this mechanism for O_2 quenching can be eliminated simply by energetic considerations (*51*), and many observations on dye sensitized photo-oxygenation (*5, 11, 12, 13, 31, 53, 54*). It is possible that with a very good electron donor in a polar solvent, the electron transfer mechanism might be operative, but even then other mechanisms should be more important (*21*).

INHOMOGENEOUS MAGNETIC FIELD EFFECT. Since an inhomogeneous magnetic field mixes singlet and triplet states, it is possible for an inhomogeneous field, generated by molecular oxygen, to enhance intersystem crossing between the triplet state and the ground singlet state of a molecule (*56*). This mechanism is, however, inconsistent with the observation that the efficiency with which various paramagnetic ions quench triplet state molecules is not correlated with the magnetic moments of the ions (*33, 41*). Further, a theoretical evaluation of the magnitude of this effect showed that it was of negligible importance (*51*).

ENHANCED INTERSYSTEM CROSSING. O_2 is known to enhance reversibly radiative $S_0 \rightarrow T_1$ transitions in organic molecules (*8, 9*). As this enhancement requires some sort of oxygen-induced mixing of singlet and

triplet states, we wondered whether such mixing might not also enhance the non-radiative $T_1 \rightarrow S_0$ transition. If, for example, the interaction with molecular oxygen mixed the lowest triplet state of the molecule with the ground state, intersystem crossing would definitely be enhanced. Because of the known O_2 effect on the $S_0 \rightarrow T_1$ absorption, we felt this quenching mechanism deserved careful evaluation.

ENERGY TRANSFER. In the Kautsky mechanism for quenching triplet state molecules, electronic excitation energy is transferred from $^3M_1$ to the oxygen molecules, as follows (*20*):

$$^3M_1 + {}^3O_2 \rightarrow {}^1M_0 + {}^1O_2$$
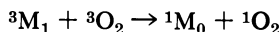
where $^1O_2$ represents an oxygen molecule in either its $^1\Delta_g$ state (22 kcal.) or $^1\Sigma_g^+$ state (37 kcal.). The studies on sensitized photo-oxygenation reactions require that we give this mechanism serious consideration.

Of the four mechanisms mentioned above, only the enhanced intersystem crossing and the energy transfer mechanisms appeared to merit further detailed consideration. In our study we were interested in the following aspects of the quenching process:

(a) What is the importance of quenching by energy transfer relative to enhanced intersystem crossing?

(b) What factors control the relative importance of these two mechanisms?

(c) Are the absolute magnitudes of the theoretical quenching rates sufficient to account for the experimental observations?

Below, we outline our theoretical treatment of the quenching mechanisms (*21*), and summarize some of the most important results. Some new results on calculating the energetics of the M . . . O_2 interaction are given later in the text.

Theory and Results. To discuss the actual calculation of the quenching rate constants, consider first the various states which arise when molecular oxygen is weakly complexed with an organic molecule, M. Since the organic molecules of interest are presumed to have ground singlet states and since the ground state of oxygen is a $^3\Sigma_g^-$ state, the ground state of the M–O_2 complex is necessarily a triplet state. A number of excited states of the complex can be formed by exciting either M or O_2, and these various possibilities are indicated in Figure 1 (*51*). In addition to those states of the complex which arise from excitation of only one of the components, there are also charge transfer states produced by transfer of an electron from M to O_2. For the benzene–O_2 complex, for example, this charge transfer state is believed to lie about 100 kcal. above the ground state (*32*).

The various states of the complex which we have just described are strictly valid only when M and O_2 are completely separated from each other, and it is only under this condition that they would represent "sta-

tionary states." We call these the zero-order states. When M and O_2 are brought together to form a weak complex, the intermolecular interaction will cause these zero-order states to become nonstationary with respect to radiationless transitions to nearly degenerate states of the same multiplicity. In this sense, complex formation may be viewed as introducing a time-dependent perturbation, which causes the initial, zero-order states to become nonstationary.

In terms of the states indicated in Figure 1, enhanced intersystem crossing actually involves a radiationless transition between the initial state $^3\Gamma_3$ and some nearly degenerate, vibrationally excited state of $^3\Gamma_0$. Energy transfer, on the other hand, involves a transition from $^1\Gamma_3$ to either $^1\Gamma_2$ or $^1\Gamma_1$, again with the conversion of the requisite amount of electronic energy, $\Delta\epsilon$, into vibrational excitation of the complex.

If the initial state of the complex is described by a wavefunction Ψ_i and the final state of interest by Ψ_f, then the rate at which a radiationless transition from Ψ_i to Ψ_f occurs is given by (45, 46):

$$k = \frac{2\pi\rho}{\hbar N} \, |<\Psi_f|\mathcal{H}|\Psi_i>|^2 \qquad (1)$$

where $\mathcal{H}$ is the complete Hamiltonian for the system, ρ is the density of final states which are nearly degenerate with Ψ_i, and N is the number of molecules per cc. In the Born-Oppenheimer approximation, Ψ can be expressed as a product of two functions ψ and Ξ such that $\Psi = \psi\Xi$, where ψ is a function of all electronic coordinates and depends only parametrically on the nuclear coordinates, and Ξ is the vibrational wave-
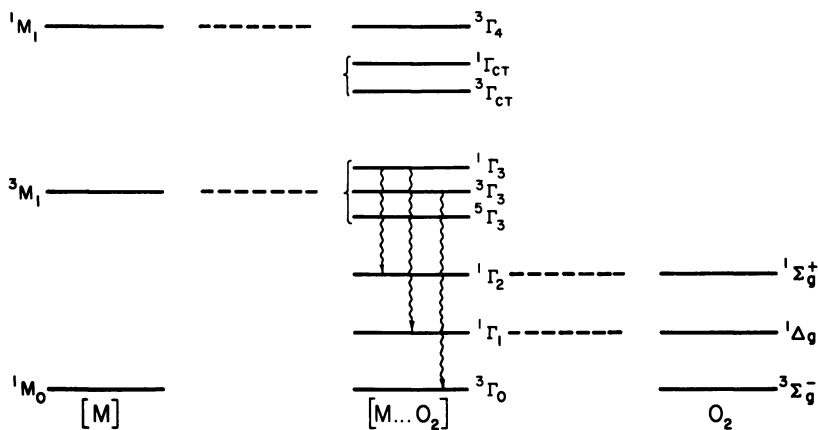
Figure 1. Low-lying electronic states of 1:1 complex (M . . . O$_2$) between the electronic states of the free molecules and those of the complex. [This figure is similar to one given by Tsubomura and Mulliken (51)]

function and depends on the electronic state of the complex and the nuclear coordinates. With this approximation, the rate expression becomes:

$$k = \frac{2\pi\rho}{\hbar N} |<\psi_f|\mathcal{H}|\psi_i>|^2 \cdot \sum_n <\Xi_f{}^n|\Xi_i{}^o>^2 = \frac{2\pi\rho}{\hbar N} \beta_{el}{}^2 F_{if} \tag{2}$$

where $\beta_{el} = <\psi_f|\mathcal{H}|\psi_i>$, $F_{if} = <\Xi_f{}^n|\Xi_i{}^o>^2$ and where n runs over all vibrational states of the complex which permit the total energy (electronic + vibrational) of the final state to be nearly degenerate in energy with the initial electronic state. F_{if} is the Franck-Condon factor for the complex.

The above expression is appropriate for the case where there is direct mixing of a particular pair of initial and final states (zero order) of the complex (18). It may happen, however, that direct mixing of ψ_i and ψ_f is quite small, in which case indirect mixing resulting from strong mixing of these two states with a common third state, ψ_k, may be more important (35, 51). When indirect mixing is important, the expression for quenching rate constant is formally as that given in Equation 2, except that β_{el} is replaced by β'_{el}, where

$$\beta_{el}' = \frac{<\psi_f|\mathcal{H}|\psi_k> \; <\psi_k|\mathcal{H}|\psi_i>}{(E_i - E_k)} \tag{3}$$

where $(E_i - E_k)$ is the difference between the electronic energies of the initial state ψ_i and the intermediate state ψ_k.

With this formulation of the problem the calculation of quenching rate constants is reduced to evaluating various matrix elements of the type $<\psi_i|\mathcal{H}|\psi_k>$, of Franck-Condon factors for the complex, and of the density of states factor ρ.

EVALUATION OF β_{el} AND β'_{el}. The procedure used to evaluate the electronic matrix elements has been described (21). Before presenting the results, we note the various complex geometries considered, and these are indicated in Figure 2. The results are summarized in Table I.

From these results, several important conclusions can be drawn. First, direct mixing matrix elements are small compared with those for indirect mixing, involving an intermediate charge transfer state. Secondly, and perhaps more importantly, the matrix elements for indirect mixing are the same for all three quenching mechanisms. Since we expect the density of final states to be the same for all three cases (45, 46), it is primarily the Franck-Condon factor which ultimately determines the relative importance of the three quenching mechanisms. It is this factor which we now consider.
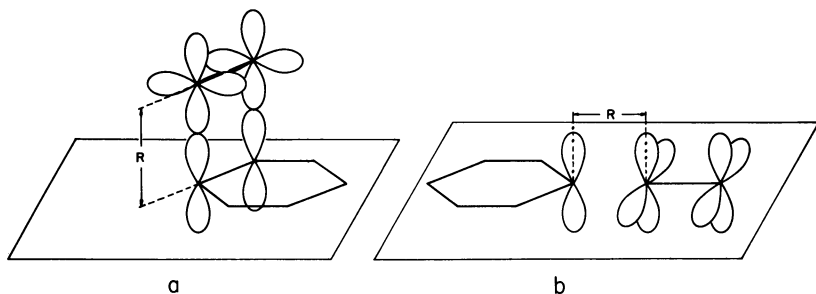
Figure 2. Schematic representation of two possible geometries for the $M \ldots O_2$ complex

(a): The atomic orbitals of O_2 and the two adjacent orbitals of carbon atoms in M are shown approaching each other face-to-face. R is the distance between the planes containing the molecular axis of M and O_2
(b): Orbitals of O_2 and M are shown for an end-on approach of the molecules. Here R is distance between carbon and oxygen atoms

FRANCK-CONDON FACTORS. In the limit of weak coupling of M and O_2 the vibrational wavefunction for the complex may be written as a product of the vibrational wavefunctions for the two components:

$$\Xi_k{}^n = \chi_M(k,n)\chi_{O_2}(k,n) \tag{4}$$

where $\chi_M(k,n)$ is the vibrational wavefunction for M when the M $\ldots O_2$ complex is in some vibronic state specified by k and n and $\chi_{O_2}(k,n)$ is the corresponding vibrational wavefunction for O_2. With this approximation, the Franck-Condon factor for the complex becomes

$$F_{if} = \Sigma_n <\chi_M(i,o)|\chi_M(f,n)>^2 <\chi_{O_2}(i,o)|\chi_{O_2}(f,n)>^2 \tag{5}$$

In the various quenching mechanisms which we are considering, the total energy of the system is conserved by converting the proper amount of electronic excitation energy into vibrational excitation of M

Table I. Electronic Matrix Elements for Direct and Indirect Mixing[a]

Direct Mixing

$\beta(^3\Gamma_3 - {}^3\Gamma_0)$	2 cm.$^{-1}$
$\beta(^1\Gamma_3 - {}^1\Gamma_2)$	0
$\beta(^1\Gamma_3 - {}^1\Gamma_1)$	2

Indirect Mixing via a Charge Transfer State

$\beta'(^3\Gamma_3 - {}^3\Gamma_0)$	20 cm.$^{-1}$
$\beta'(^1\Gamma_3 - {}^1\Gamma_2)$	20
$\beta'(^1\Gamma_3 - {}^1\Gamma_1)$	20

[a] Values calculated for complex geometry a with $R = 4A$ or with geometry b but with $R = 3A$ (*see* Figure 2).

and O_2. Actually to determine F_{if}, we must decide just how a given amount of vibrational energy $\Delta\epsilon$ will be partitioned between M and O_2.

From studies of emission from electronically excited oxygen molecules, we know that the oxygen Franck-Condon factor rapidly diminishes (factor of > 100) when there is a change of 1 or 2 quanta in the vibrational state of O_2 (*26, 36*).

We, therefore, anticipate that most of the vibrational excitation will be deposited in M rather than in O_2 (formation of a strong M–O_2 complex might somewhat relax this "selection rule"). Consequently, the variation of F_{if} with $\Delta\epsilon$ will be almost entirely conditioned by variations in f_m, the Franck-Condon factor for the molecule. Fortunately, semi-empirical formulas for evaluating f_m have been developed (*19, 24, 48*), and one such expression is given in Equation 6.

$$f_m = 0.15 \exp[-(\Delta\epsilon - 4000)/11{,}500] \tag{6}$$

where $\Delta\epsilon$ is now the amount of electronic energy (in cm.$^{-1}$) which is converted into vibrational excitation of M. Regardless of exact magnitudes of f_M and f_{O_2}, it is evident from the above discussion that the process which involves the conversion of the least amount of electronic energy into vibrational energy will be the dominant one. Since intersystem crossing always involves the conversion of the largest amount of electronic excitation energy into vibrational energy, we conclude that energy transfer to oxygen is the major quenching process. These conclusions do not depend upon exact numerical evaluation of matrix elements and other factors, and, therefore, may be considered to be strong predictions.

MAGNITUDES OF THE RATE CONSTANTS. The electronic factors and the Franck-Condon factors have already been evaluated above, and all that remains is to obtain a value for the density of final states. As in our earlier paper, we use Robinson's value of $\rho/N = 1$ cm. (*45*). For the quenching of a triplet state molecule with an energy $E_t = 60$ kcal., we obtain the following unimolecular rate constants:

$$(^1\Gamma_3 \rightarrow {}^1\Gamma_2) \; 10^{12}/\text{sec. (energy transfer to } {}^1\Sigma_g{}^+)$$

$$(^1\Gamma_3 \rightarrow {}^1\Gamma_1) \; 10^{11}/\text{sec. (energy transfer to } {}^1\Delta_g)$$

$$(^3\Gamma_3 \rightarrow {}^3\Gamma_0) \; 10^9/\text{sec. (enhanced intrasystem crossing).}$$

While the exact magnitudes of these rate constants are not expected to be particularly accurate, the relative magnitudes should be reliable.

Since the rate constants for energy transfer are on the order of 10^{11}–10^{12}/sec., our calculations easily account for the experimental observation that the O_2 quenching of triplet states is diffusion controlled. (If M and O_2 only form collision complexes, the rate constant for dissociation would be on the order of 10^{10}/sec., much smaller than 10^{11}–10^{12}/sec.) The above results answer the three questions we posed earlier. We now

consider other aspects of our results which seem to be relevant to interpreting sensitized photo-oxygenations.

Variation in the $^1\Sigma_g^+/^1\Delta_g$ Ratio with Triplet State Energy of the Sensitizer. The calculations indicate that quenching of high energy triplet state molecules ($E_t > 50$ kcal.) generates more $^1\Sigma_g^+$ than $^1\Delta_g$ by roughly a factor of 10. This large $^1\Sigma_g^+/^1\Delta_g$ ratio arises simply from the fact that less electronic energy is converted into vibrational energy when the $^1\Sigma_g^+$ state is produced than when the $^1\Delta_g$ state is generated. With molecules that have triplet energies less than 37 kcal., the minimum energy required to produce the $^1\Sigma_g^+$ state, naturally only $^1\Delta_g$ molecules can be generated. With intermediate energy triplet state molecules ($50 > E_t > 37$ kcal.) the expression used to evaluate f_M breaks down, and to obtain some idea of the behavior of the $^1\Sigma_g^+/^1\Delta_g$ ratio with sensitizers in this range we have used experimental observations on triplet-triplet energy transfer. Porter and Wilkinson found that as the triplet state energy of a sensitizer approaches (say, within 5 kcal.) the energy of the acceptor, the transfer probability is significantly reduced (40). If a similar result were obtained with molecular oxygen as the acceptor, the rate of $^1\Sigma_g^+$ generation would actually decrease as E_t approaches 37 kcal. The rate of generating $^1\Delta_g$, on the other hand, is expected to increase. The net result of these two effects is that the $^1\Sigma_g^+/^1\Delta_g$ ratio would decrease smoothly to zero as the sensitizer triplet state energy is decreased from 45 to 37 kcal. The curve in Figure 3a shows the expected variation in the $^1\Sigma_g^+/^1\Delta_g$ ratio with E_t.

Energetics of Interaction of Organic Molecules with O_2

In the theory outlined above we assumed a weak collision complex between the triplet state of the organic molecule and the triplet state of oxygen, and we were able to account for the rate of quenching of triplet states by O_2 on this basis. Further investigation into the nature of this interaction indicates that it is not necessarily weak (7).

The calculation of the rate of quenching of triplet states by O_2 was essentially an evaluation of the magnitude of interaction between two different states of the complex. Determination of potential energy curves for the M–O_2 interaction, requires an evaluation of the total energy of the complex as a function of R, the intermolecular distance.

A consideration of the various states of the complex at relatively large intermolecular distances ($R > 4A$), as given above, is the starting point of the present investigation. The energies of these states are well known and are indicated, in order of increasing energy, on the right side of Figure 4 (21).

Since we have experimental information regarding the ground state of the complex (3, 6, 7), and since it would be impossible to calculate
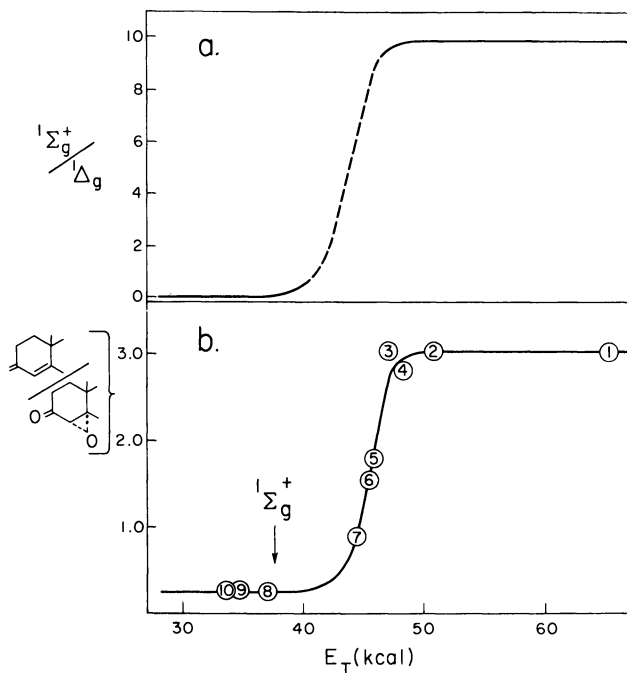
Figure 3.   (a) Predicted variation in the $^1\Sigma_g^+/^1\Delta_g$ ratio with sensitizer triplet state energy

(b) Observed variation in the product distribution from the dye sensitized photo-oxygenation of cholest-4-en-3β-ol with the triplet state energy of the sensitizer (37, 38). 1, Triphenylene; 2, Fluorescein; 3, Eosin Y; 4, Acridine Orange; 5, Sulfurhodamine B; 6, Erythrosin B; 7, Rose Bengal; 8, Hematoporphyrin; 9, Chlorine$_6$; 10, Methylene blue

reliably the steeply rising repulsive portion of the potential energy curve, we have evaluated the potential energy curves for the excited states with reference to the ground states. In doing so we have assumed that the strongly repulsive intermolecular interactions at small R are the same for all states of the complex.

We now indicate in more detail the procedure for constructing the potential energy curves for the states of the complex shown in Figure 4.

Ground State. The heat of formation of a complex between a non-ionic, ground state organic molecule and a ground state oxygen is very small, and these complexes are dissociative at room temperature (3, 6, 7). This implies that as M and O_2 approach each other, or $R[M \ldots O_2]$ decreases, the potential energy curve goes through a small or negligible minimum before it starts to rise, and the ground state curve in Figure 4 is drawn accordingly.
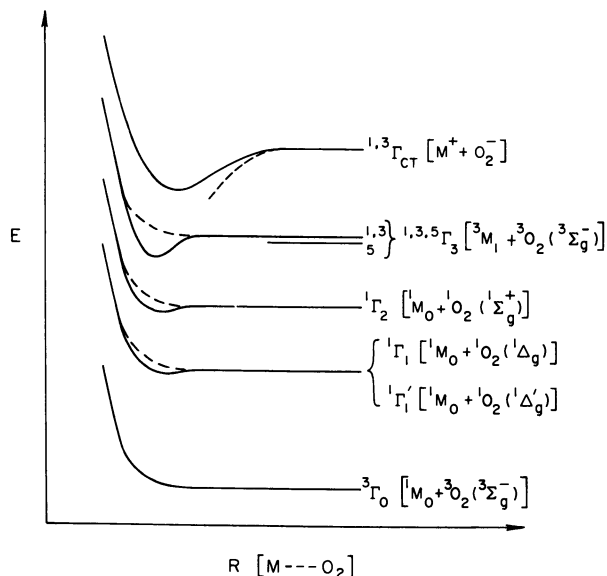
Figure 4. Potential energy curves for the different states of the (M . . . O₂) complex. Dashed curves represent the energy of the respective states of the complex in the absence of configuration interaction. Continuous curves indicate the result of including configuration interaction

Excited States. If we neglect configuration interaction, the excited states Γ_1, Γ_2, and Γ_3 behave essentially like the ground state and are shifted relative to one another only by a repulsive intermolecular exchange integral. Since typical values for these exchange integrals are of the order of 1–10 cm.$^{-1}$ for intermolecular separations down to 3 A (21), their effect on the potential energy curves is negligible. We also neglect the lifting of the degeneracy of the two $^1\Delta_g$ states of oxygen, $^1\Gamma_1$ and $^1\Gamma'_1$ which occurs as R becomes smaller since we expect the $^1\Delta_g$–$^1\Delta'_g$ splitting to be small (16).

The charge transfer (CT) states, Γ_{CT}, behave quite differently from the nonpolar states. Because of the strong coulombic interaction between the negatively charged oxygen and the positive M ion, the energy of CT state varies approximately as $1/R$. This is indicated in the Figure 4 by dotted curves. As the Γ_{ct} state closely approaches the Γ_3 state, configuration interaction between the singlet components, and between the triplet components of Γ_{ct} and Γ_3 can no longer be ignored.

As a result of this configuration interaction, $^1\Gamma_{ct}$ is destabilized, but the singlet component of Γ_3 is stabilized by at least 1 kcal., and probably

more. A similar interaction occurs between the respective triplet components of Γ_{ct} and Γ_3 and results in a destabilization of the $^3\Gamma_{ct}$ state and a stabilization of $^3\Gamma_3$ (solid lines in Figure 4). Configuration interaction is also present between $^1\Gamma_{ct}$ and $^1\Gamma_2$ and between $^1\Gamma_{ct}$ and $^1\Gamma_1$ but with decreased effectiveness because of the increased energy differences between the interacting states. The stabilization of $^{1,3}\Gamma_3$ is, therefore, expected to be larger than the stabilization of either $^1\Gamma_2$ or $^1\Gamma_1$ (compare the difference between the solid and dotted curves in Figure 4). Because of the absence of any nearby quintet state, the $^5\Gamma_3$ state is unperturbed by configuration interaction and will probably behave like the ground state.

To summarize, the $^1\Gamma_2$ and $^1\Gamma_1$ states and the ground state are essentially dissociative, whereas $^{1,3}\Gamma_3$ exhibit significant potential minima.

The complex $^{1,3}(^3M \ldots {}^3O_2)$ may actually be more stable than we originally assumed, in which case the Franck-Condon factors for the complex may have to be modified to include vibrational excitation of O_2 as indicated previously. Although these considerations regarding the nature of the $[M \ldots O_2]$ complex do not alter any of the major conclusions regarding the quenching mechanism, they are important in interpreting sensitized photo-oxidation reactions.

Relation of Theoretical Quenching Results to Interpretation of Sensitized Photo-Oxygenations

We now discuss sensitized photo-oxygenation reactions and show how some of our theoretical results clarify some current controversies and give us new insight into the reaction mechanisms.

Comparison of Terenin-Schenck Mechanism and the Singlet Oxygen Mechanism. Terenin (*49, 50*), and later Schenck (*47*), proposed the following mechanism for dye sensitized photo-oxygenation reactions:

$$^1M_0 \xrightarrow{h\nu} {}^1M_1$$

$$^1M_1 \rightarrow {}^3M_1$$

$$^3M_1 + {}^3O_2 \rightarrow [M \ldots O_2]$$

$$[M \ldots O_2] + A \rightarrow {}^1M_0 + AO_2$$
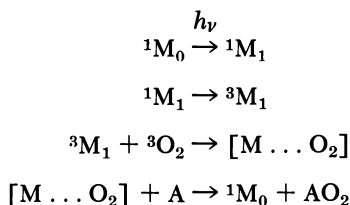
Where the moloxide, $[M \ldots O_2]$, is the reactive intermediate which transfers oxygen to the acceptor, A, to form products AO_2. This mechanism, which was given strong support by the extensive work of Schenck and co-workers (*15*), was until recently the generally accepted mechanism for sensitized photo-oxygenation reactions.

An alternative scheme, which we mentioned earlier, is that proposed by Kautsky and can be written as follows (20):

$$^{1}M_0 \xrightarrow{h\nu} {}^{1}M_1$$

$$^{1}M_1 \rightarrow {}^{3}M_1$$

$$^{3}M_1 + {}^{3}O_2 \rightarrow {}^{1}M_0 + {}^{1}O_2 \; ({}^{1}\Sigma_g{}^{+} \text{ or } {}^{1}\Delta_g)$$

$$^{1}O_2 + A \rightarrow AO_2$$
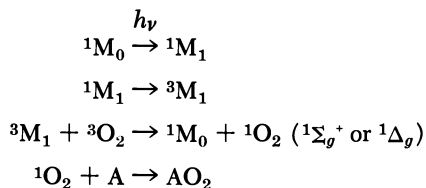
In the Kautsky scheme the reactive intermediate is an excited singlet state oxygen molecule ($^{1}\Sigma_g{}^{+}$ or $^{1}\Delta_g$) instead of the moloxide. Although much of the recent work in this field has concentrated on determining which of these, apparently mutually exclusive, mechanisms is correct, our calculation on the energetics of the [M . . . O_2] interaction, suggest that the Terenin-Schenck mechanism can actually be viewed as an incomplete version of the singlet oxygen mechanism. The moloxide of Terenin-Schenck can be identified with the complex $^{1,3}(^{3}M \ldots {}^{3}O_2)$ which we discussed previously. This excited state of the complex is expected to be very short lived ($<10^{-10}$ sec.) because of radiationless transitions to the lower lying dissociative states of the complex $^{1}\Gamma_2$ and $^{1}\Gamma_1$, yielding $^{1}\Sigma_g{}^{+}$ or $^{1}\Delta_g$ oxygen. It is these species which go on to react with acceptors as proposed by Kautsky.

Evidence for the Participation of Both $^{1}\Sigma_g{}^{+}$ and $^{1}\Delta_g$ Oxygen. One of the conclusions of our investigation was that both $^{1}\Sigma_g{}^{+}$ and $^{1}\Delta_g$ oxygen could be generated in the quenching of triplet state molecules and that the $^{1}\Sigma_g{}^{+}/^{1}\Delta_g$ ratio depends upon E_t. The importance of this in interpreting triplet sensitized photo-oxygenation reactions lies in the possibility that $^{1}\Sigma_g{}^{+}$ and $^{1}\Delta_g$ might exhibit different chemical reactivities. If this is true, the distribution of products from a sensitized photo-oxygenation might vary significantly with the triplet state energy of the sensitizer.

Until now it has usually been assumed that most singlet oxygen reactions could be attributed to reactions of $^{1}\Delta_g$ (11, 12, 13, 39, 54). As far as we are aware, the only published attempt to find experimental evidence for a difference in the reactivity of $^{1}\Sigma_g{}^{+}$ and $^{1}\Delta_g$ gave negative results (10). We now discuss some data on the sensitized photo-oxygenation of cholesterol, which we believe provides evidence for involvement of both $^{1}\Sigma_g{}^{+}$ and $^{1}\Delta_g$.

The dye sensitized photo-oxygenation of cholest-4-en-3β-ol yields only two products (37, 38), an enone (III) and an epoxy ketone (II) as illustrated. The anomalous aspect of these results is that the enone/epoxy ketone ratio varies by a factor of 150 depending upon the choice of sensitizer. In light of our prediction regarding the variation in the $^{1}\Sigma_g{}^{+}/^{1}\Delta_g$ ratio with E_t, we were interested in whether there was a
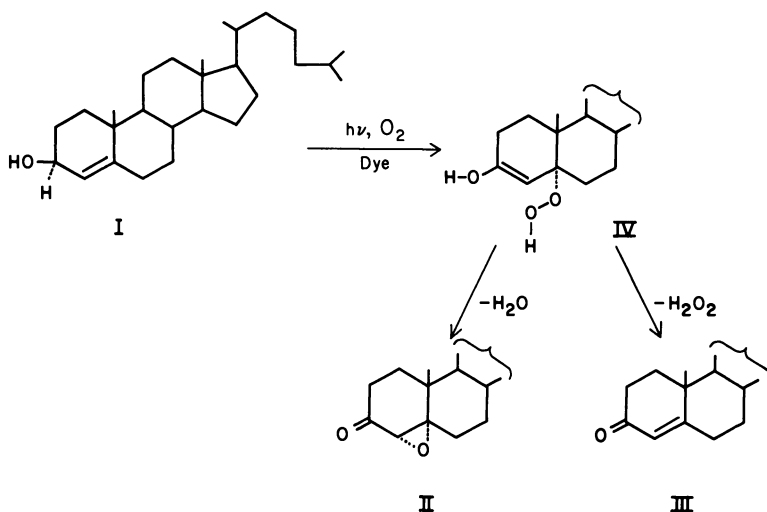
similar correlation between the product distribution and E_t (*22, 23*). The results are presented in Figure 3b. Comparison of Curves a and b shows that the variation in the III/II ratio can be accounted for in terms of a variation in the $^1\Sigma_g^+/^1\Delta_g$ ratio with E_t. With high energy sensitizers $^1\Sigma_g^+$ is the major species initially generated, and this species apparently reacts to produce mainly enone (perhaps by a hydrogen atom abstraction). Since some $^1\Delta_g$ is also generated by high energy sensitizer, it is possible that $^1\Sigma_g^+$ reacts to produce exclusively enone. Low energy sensitizers generate only $^1\Delta_g$ oxygen, and this species apparently reacts with I to form an intermediate of type IV, which then decomposes to give mainly the epoxy ketone.

Most of the sensitizers we used are known to abstract hydrogen atoms from good donors like phenol, and it was possible that some of the enone production might arise from hydrogen atom abstraction by the excited dye. This possibility appears to be eliminated by the observation that with eosin, for example, there was no change in the product distribution when the oxygen pressure was varied from 0.2 to 10 atm. The results obtained using triphenylene ($E_t = 67$ kcal.) as a sensitizer also support this conclusion. Of all the sensitizers used, triphenylene is least susceptible to photoreduction, and yet when used as a sensitizer it still gave the 3:1 enone/epoxy ketone ratio expected for a high energy sensitizer.

Since the lifetime of $^1\Sigma_g^+$ in solution is much shorter than $^1\Delta_g$, one might expect that a reduction in the concentration of the acceptor (I) would favor reactions involving $^1\Delta_g$. The results of an experimental test of this possibility are presented in Table II. Since methylene blue is a

low energy sensitizer capable of generating only $^1\Delta_g$ oxygen, no concentration effect on the product distribution is expected, and little, if any, is observed experimentally. However, with the high energy sensitizers fluorescein and eosin, a reduction in the concentration of I from 10^{-2} to $10^{-4}M$ causes a decrease in the enone/epoxy ketone ratio from 3/1 to about 1/4. If we assume a simple reaction mechanism in which $^1\Sigma_g^+$ molecules are lost, either by decay to $^1\Delta_g$ or by a diffusion-controlled reaction with I, our concentration data would require a $^1\Sigma_g^+$ lifetime in solution which is greater than 10^{-6} sec. This appears to be inconsistent with the recent observations of Ogryzlo on the quenching of $^1\Sigma_g^+$ in the gas phase (39). Without further investigation of the kinetics of the reactions of I we can only suggest that the actual reaction mechanism is more complicated than the simple one suggested above.

Table II. Product Variation with Concentration of Substrate in the Photosensitized Photo-Oxygenation of Cholest-4-en-3β-ol (I) [a]

Sensitizer	Concentration of I [b]	Ratio of III/II [c]
Methylene	1.3×10^{-2}	$1/3$ [d]
	1.0×10^{-4}	$1/4$-$1/5$
Fluorescein	1.3×10^{-2}	$3/1$ [e]
	1.0×10^{-4}	$1/3$
Eosin Y	1.3×10^{-2}	$3/1$ [d]
	8.2×10^{-4}	$1/1$
	4.0×10^{-4}	$1/4$
	2.5×10^{-4}	$1/4$
	1.6×10^{-4}	$1/4$
	8.3×10^{-5}	$1/5$
Lumichrome [f]	1.0×10^{-2}	$6/1$
Riboflavin	1.3×10^{-2}	$30/1$ [d]
	5.0×10^{-4}	$6/1$
	1.0×10^{-4}	$1/2$
	7.5×10^{-5}	$1/5$

[a] Photo-oxygenation conditions were essentially the same as those used by Nickon, except that a 500-watt tungsten lamp was used, and typical runs were 24 hours long.
[b] Concentration in moles/liter.
[c] Ratios determined by chromatography and infrared spectroscopy.
[d] This value also reported by Nickon (37, 38).
[e] Data of Nickon (37, 38).
[f] Three-day irradiation.

Prediction of the Reactivity of Ground State and Singlet Excited Molecular Oxygen with Organic Molecules

The validity of the Kautsky singlet oxygen mechanism seems to be confirmed both theoretically (21) and experimentally (5, 11, 12, 13, 31,

53, 54), and we have now been able to incorporate certain aspects of the "Terenin-Schenck" mechanism within the framework of the singlet oxygen mechanism (*27*). In view of these interesting results we thought it worthwhile to explore theoretically the reactions between organic molecules and ground and excited state oxygen molecules and the reverse process, decomposition of the oxygenation product. For this investigation we utilize the information inherent in the symmetry properties of the orbitals and states of the "reactant" and "product" molecules to construct correlation diagrams for the system. By using such diagrams we are able to make predictions regarding nature and course of reactions (*28, 29*).

Reactions of Singlet Oxygen with Conjugated Dienes. Thermochemical and spectroscopic data can be combined with orbital correlation diagrams (*17*) to construct state correlation diagrams (*34*) for reactions of singlet oxygen with conjugated dienes. With these state correlation diagrams we can account for the experimental observations and derive information on the factors which control the relative reactives of $^1\Sigma_g^+$ and $^1\Delta_g$ in other concerted addition reactions. We illustrate the essential features of our approach by considering the concerted addition of molecular oxygen to a conjugated diene (*e.g.*, cyclopentadiene, 1,3-cyclohexadiene, furan) to form an endoperoxide (geometry of the transition state indicated in Figures 5 and 6) (*15*). The state correlation diagram which forms the basis for understanding this reaction is shown in Figure 6 and was constructed as follows. First, thermochemical data (bond strengths, resonance, energies, etc.) were used to scale the ground state energy of the reactants relative to the ground state of the product. Spectroscopic data were then used to locate the excited states of the reactants (oxygen + diene) with respect to their ground state, and likewise for the product. Finally, symmetry and spin selection rules were used to correlate states of the reactants with those of the product and thereby construct a "primitive" state correlation diagram (dotted curves, Figure 6). Although this shows which initial state of the reactants ultimately correlate with a particular state of the product, it does not indicate exactly *how* the states correlate. Barriers arising from intended crossing of levels are, for example, not indicated (*17*). To obtain this detailed information, we used the orbital correlation diagram presented schematically in Figure 5.

The molecular orbitals on the left side of the diagram are those of the weakly complexed diene and O_2. The σ_{oo}, σ_{oo}^*, π_x, π_y, π_x^*, and π_y^* are the molecular orbitals of O_2 and ψ_1, ψ_2, ψ_3, and ψ_4 are the pi-molecular orbitals of the diene, and the nodal pattern of each orbital is schematically indicated in the figure. S, S', and A, and A' indicate whether the orbitals are symmetric or antisymmetric with respect to the assumed plane of symmetry.
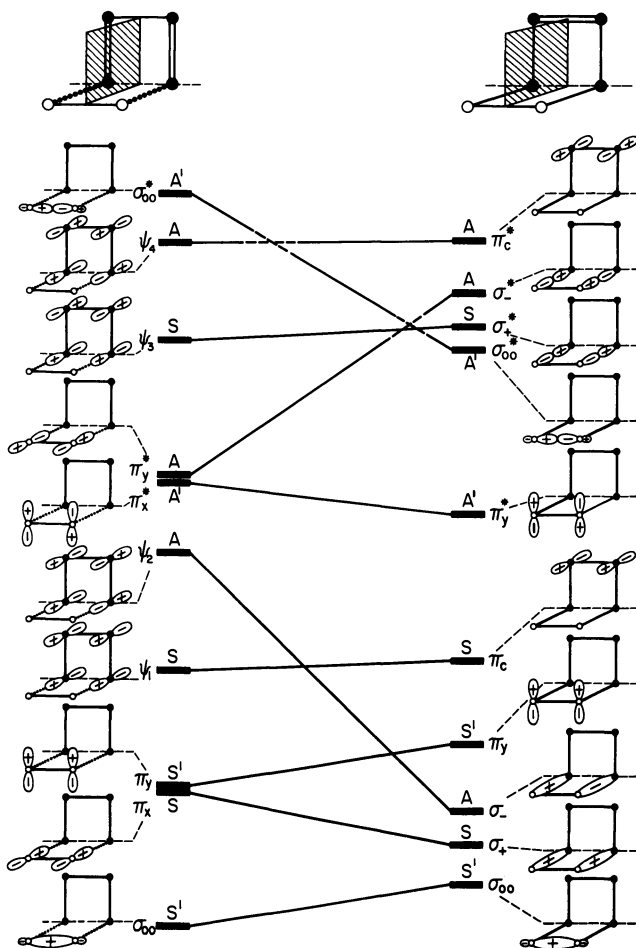
Figure 5. Orbital correlation diagram for the concerted addition of molecular oxygen to a diene. The molecular orbitals of O_2 (σ_{oo}, π_x, π_y, π_x^*, π_y^*, and σ_{oo}^*) and of the diene (ψ_1, ψ_2, ψ_3, and ψ_4) are given on the left, and the molecular orbitals of the product peroxide are on the right. The orbitals are arranged vertically in order of increasing energy, and nodal patterns of the orbitals are indicated schematically

The molecular orbitals of the endoperoxide are indicated on the right side of Figure 5, with the orbitals arranged in the order of energy and again classified as symmetric or antisymmetric.

Because of the degeneracy of the π^* orbitals in the oxygen molecule, it is simpler, for purposes of discussion, to consider first the regeneration of the diene and molecular oxygen from the peroxide rather than the

reverse process. According to the orbital correlation diagram the ground state configuration $(\sigma_{oo}{}^2\sigma_+{}^2\sigma_-{}^2\pi_y{}^2\pi_c{}^2\pi_y{}^{*2})$ is expected to increase significantly in energy as the C—O bonds are broken because of the increase in the energy of $\sigma_\pm$ orbitals. It is primarily this same factor which causes the states arising from the configuration $(\sigma_{oo}{}^2\sigma_+{}^2\sigma_-{}^2\pi_y{}^2\pi_c{}^2\pi_y{}^{*1}\sigma_{oo}{}^{*1})$ to increase initially in energy. Because of interaction with other higher energy states, these states and higher lying states ultimately pass through a maximum in energy and finally correlate with the $^1\Sigma_g{}^+$ and $^1\Delta_g{}^*$ states, respectively. Incorporating the orbital information into the "primitive" state correlation yields the improved state correlation diagrams given by the solid curves in Figure 6.
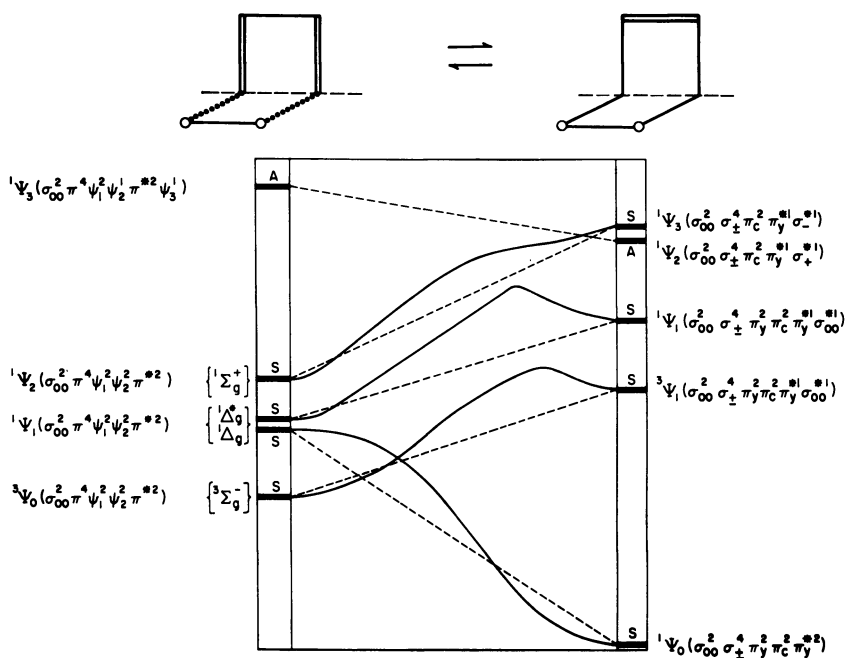
Figure 6. Schematic of the state correlation diagram for the concerted addition of molecular oxygen to a diene. The electronic configurations for states of the (O_2 + diene) complex are indicated on the left (state of O_2 in the complex given in brackets). States of the cyclic peroxides with their appropriate electronic configurations are on the right in order of increasing energy. Dashed curves indicate the "primitive" correlations obtained by straightforward application of symmetry and spin restrictions. Solid curves indicate final correlations obtained by using the additional information contained in the orbital correlation diagram

Although construction of this diagram was discussed in terms of decomposition of the peroxide, we can use it to make several important

predictions regarding the reverse reaction in which molecular oxygen adds to a ground state diene.

(a) Under normal conditions $^3\Sigma_g^-$ oxygen is not expected to be reactive since this initial state of the reactants (a triplet) correlates endothermically with an *excited* triplet state of the peroxide.

(b) $^1\Delta_g$ oxygen is predicted to be reactive since this state of the complex correlates smoothly and exothermically with the ground singlet state of the peroxide.

(c) The low lying excited states of the complex arising from interaction of O_2 in its $^1\Delta_g^*$ of $^1\Sigma_g^+$ state with the ground state of the diene both correlate with high energy *excited* singlet states of the peroxide; hence, $^1\Delta_g^*$ and $^1\Sigma_g^+$ oxygen are predicted to be unreactive in this mode.

The extension of these considerations to other *concerted* addition reactions is straightforward. In general we find:

(1) Both the ground $^3\Sigma_g^-$ and excited $^1\Sigma_g^+$ states of oxygen are unreactive because the states of the complex associated with these states of oxygen correlate endothermically with excited states of the product. Exceptions are expected only if a very stable peroxide or hydroperoxide is formed.

(2) $^1\Delta_g$ is in general predicted to be reactive since this state of the complex correlates smoothly with the ground state of the peroxide or hydroperoxide.

In the formation of an endoperoxide the exothermicity is determined primarily by the difference between the extra energy gained in forming two σ_{oo} bonds at the expense of a C=C double bond and accompanying resonance energy. From this analysis of the energetics we can understand easily why molecules like anthracene, tetracene, and pentacene readily form photoperoxides. The puzzling nonreactivity of naphthalene and phenanthrene (*15*) can correspondingly be understood in terms of the very large loss of resonance energy which accompanies the formation of *trans*-annular peroxides of these molecules.

The above considerations apply specifically to concerted addition reactions where the oxygen adduct is presumed to have a singlet ground state. When radicals are produced, however, a somewhat different picture emerges. Since the ground state of a pair of radicals (R· + HOO·, for example) will be a triplet state, the ground state of the reactants (ground state acceptor + $^3\Sigma_g^-$ oxygen) can now correlate with the *ground* state rather than with an excited state of the products. If the energetics are not too unfavorable, we may now expect to find reactions of this type which involve $^3\Sigma_g^-$ ground state oxygen.

We may also expect to find $^1\Sigma_g^+$ reacting in this mode (radical formation), provided the radical products have low lying excited singlet states. This is an interesting contrast to the predicted nonreactivity of $^1\Sigma_g^+$ in concerted addition reactions.

Decomposition of Endoperoxides. An intriguing property of some endoperoxides is their ability to dissociate upon heating into molecular oxygen and the parent hydrocarbon (*2, 15*). Perhaps even more intriguing are the experimental observations which suggest that the O_2 is formed in an excited electronic state (presumably $^1\Delta_g$) (*25, 52*). To understand how and under what conditions this might occur, we have used orbital and state correlation diagrams to explore possible modes of endoperoxide decomposition. Following procedures outlined above, we have constructed the state correlation diagram for the decomposition of a simple endoperoxide (I) either by cleavage of the O—O bond to form a diradical (II) or by loss of molecular oxygen with formation of the parent hydrocarbon (III). The state and orbital correlation diagrams for the latter reaction were given in Figures 5 and 6, and the orbital correlation diagram for formation of the diradical from the endoperoxide is shown in Figure 7.

In constructing the complete state correlation diagram, the ground state electronic configuration of the diradical was taken to be $(\sigma_\pm{}^4\pi_c{}^2P^6)$. [In the absence of configuration interaction the following electronic configurations (for simplicity these are all denoted as $(\sigma_\pm{}^4\pi_c{}^2P^6)$) are assumed to be nearly degenerate in energy: $^{1,3}(\sigma_\pm{}^4\pi_c{}^2P_{x_1}{}^2P_{y_1}{}^1P_{x_2}{}^2P_{y_2}{}^1)$, $^{1,3}(\sigma_\pm{}^4\pi_c{}^2P_{x_1}{}^2P_{y_1}{}^1P_{x_2}{}^2P_{y_2}{}^2)$, $^{1,3}(\sigma_\pm{}^4\pi_c{}^2P_{x_2}{}^2P_{y_1}{}^1P_{x_2}{}^2P_{y_2}{}^1)$, $^{1,3}(\sigma_\pm{}^4\pi_c{}^2P_{x_2}{}^1P_{y_1}{}^2P_{x_2}{}^1P_{y_2}{}^1)$, where for example P_{x_1} is an x-directed 2P-orbital on oxygen center 1.] While it might at first seem strange to suggest this electronic configuration for the ground state of the diradical (oxygen orbitals only partially filled), it must be remembered that the ordering of these orbital energies presented in Figure 7 is only appropriate to a situation in which all atoms remain essentially neutral. If electrons were removed from what appears to be a higher energy π_c-orbital, and placed in the partially filled oxygen p-orbitals, the oxygen atoms would develop a net negative charge, and the electronegativity of the oxygen atoms would be greatly decreased (perhaps by as much as 13 e.v. per added extra electron) (*44*). The electronegativity of the positively charged carbon atoms would correspondingly be increased, and the relative ordering of the oxygen p- and ethylenic π-orbitals would be inverted (*30*). As a consequence of our choice of this electronic configuration the ground state of the diradical (probably a triplet state) is expected to be nearly degenerate in energy with a number of excited singlet and triplet states, as indicated in the state correlation diagram in Figure 8.

The completed state correlation diagram given in Figure 8 now provides us with the information needed to examine the two modes by which endoperoxides generally decompose (*15*). On the basis of this diagram we predict the following.
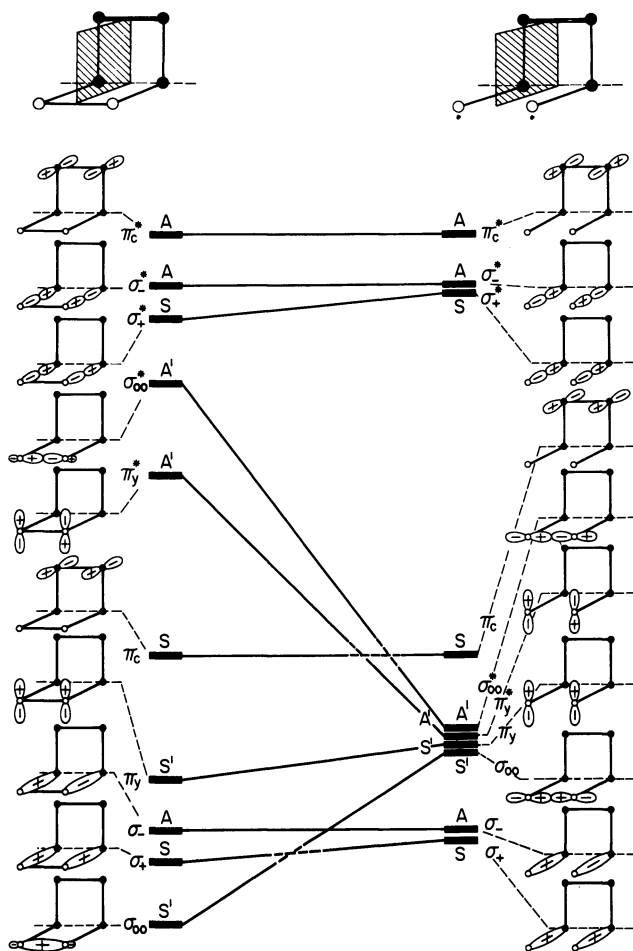
Figure 7. Schematic of the orbital correlation diagram for the formation of a diradical (II) from a cyclic peroxide (I). Orbitals (nodal patterns indicated schematically) are arranged vertically in order of increasing energy and classified with respect to an assumed plane of symmetry

(a) Thermal decomposition leading to diradical formation will be favored over thermal dissociation into parent hydrocarbon and molecular oxygen because of the lower activation energy (ΔE_3 as compared with ΔE_1 or ΔE_2).

(b) The first excited singlet and triplet states of the endoperoxide will decompose by cleavage of O—O bond since these states correlate smoothly and exothermically with low lying states of the diradical. Decomposition into parent hydrocarbon and molecular oxygen is prevented by the appearance of energy barriers in the excited state potential curves.

(c) The third excited singlet state, however, is expected to dissociate into parent hydrocarbon and $^1\Sigma_g{}^+$ oxygen.

In accord with these theoretical predictions most simple endoperoxides are experimentally found to be thermally unstable with respect to diradical formation (15). Furthermore, photochemical studies indicate that upon excitation to low lying excited singlet states, simple peroxides dissociate into radicals, whereas higher energy excitation apparently leads to the formation of molecular oxygen ($^1\Sigma_g{}^+$?) (4).

Although the above discussion deals with a specific endoperoxide, the results can be extended to the preferred mode of decomposition of polyacenes endoperoxide. In the polyacene series, the energy necessary to form the diradical from the endoperoxide will remain essentially constant (roughly equal to the strength of the O—O bond in the peroxide). The energy required to regenerate the parent hydrocarbon and molecular oxygen from the endoperoxide will, however, be determined primarily
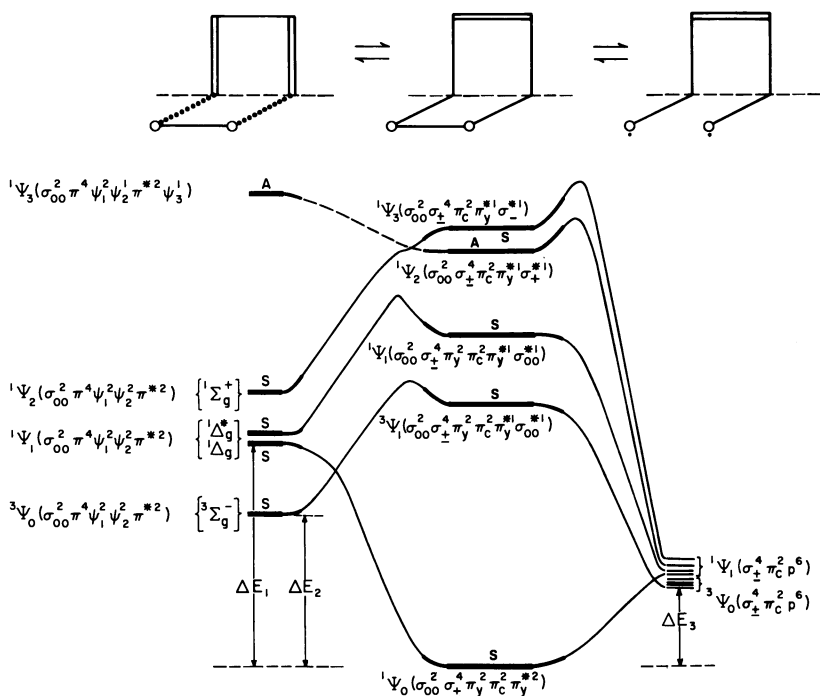
Figure 8.   Schematic of the state correlation diagram for the (diene + O_2) ⇌ peroxide ⇌ diradical interconversions. States of the diene-O_2 complex are on the left [state of molecular oxygen is specifically noted for each state]. States of the peroxide are depicted in the middle. The nearly degenerate set of low lying singlet and triplet states of the diradical are shown on the right. The states are arranged in order of increasing energy, and the electronic configuration for each state is indicated

by the amount of resonance energy gained in formation of the parent hydrocarbon—*i.e.*, the larger the resonance energy gained by the parent hydrocarbon, the easier it becomes for the peroxide to decompose by this mode. On the basis of these energetic considerations we predict that anthracene 9,10-endoperoxide should decompose thermally to the diradical. On the other hand, decomposition of 9-phenyl-, 9,10-diphenylanthracene and tetraphenyltetracene (rubrene) peroxide should generate molecular oxygen since the resulting gain in resonance energy by the hydrocarbon ($\sim$30 kcal.) is sufficiently large to make this the preferred mode of decomposition. The state correlation diagram further suggests that the molecular oxygen produced by this decomposition should be in an electronically excited $^1\Delta_g$ state. In apparent confirmation of these theoretical predictions we note that the thermal decomposition of 9,10-diphenylanthracene peroxide, in the presence of tetramethylethylene, yields products characteristic of reactions of tetramethylethylene with $^1\Delta_g$ oxygen (52); further, the thermal decomposition of rubrene endoperoxide is accompanied by a bright chemiluminescence, which, according to the Khan and Kasha theory of chemiluminescence, suggests the involvement of $^1\Delta_g$ oxygen (25).

The results of this preliminary theoretical investigation are sufficiently encouraging to justify a more detailed study of the reactions of oxygen with organic acceptors, and work along these lines is in progress.

Acknowledgment

Literature Cited

(1)   Backstrom, H. L. J., Sandros, K., *Acta Chem. Scand.* **12**, 823 (1958).
(2)   Bergmann, W., McLean, M. J., *Chem. Rev.* **28**, 367 (1941).
(3)   Bradley, H., King, A. D., *J. Chem. Phys.* **47**, 1189 (1967).
(4)   Calvert, J. G., Pitts, J. N., "Photochemistry," Chap. 5, Wiley, New York, 1966.
(5)   Corey, E. J., Taylor, W. C., *J. Am. Chem. Soc.* **86**, 3881 (1964).
(6)   Dijkgraaf, C., Ph.D. Thesis, Amsterdam, 1962.
(7)   Evans, D. F., *J. Chem. Soc.* **1961**, 1987.
(8)   *Ibid.*, **1957**, 1351, 3885.
(9)   *Ibid.*, **1959**, 2753.
(10) Fisher, E. R., McCarty, M., *J. Chem. Phys.* **45**, 781 (1966).
(11) Foote, C. S., Wexler, S., *J. Am. Chem. Soc.* **86**, 3879, 3880 (1964).
(12) Foote, C. S., Wexler, S., Ando, W., *Tetrahedron Letters* **46**, 4111 (1965).
(13) Foote, C. S., *Accounts Chem. Res.* **1**, 104 (1968).
(14) Gollnick, K., *Advan. Photochem.*, in press.
(15) Gollnick, K., Schenck, G. O., "1,4-Cycloaddition Reactions," J. Hamer, Ed., p. 255, Academic Press, New York, 1967.

(16) Griffith, J. S., "Oxygen in the Animal Organisms," F. Dickens, E. Neil, Eds., p. 481, Pergamon, Oxford, 1964.

(17) Hoffman, R., Woodward, R. B., *Accounts Chem. Res.* **1**, 17 (1968).

(18) Hoijtink, G. J., *Mol. Phys.* **3**, 67 (1960).

(19) Hunt, G. R., McCoy, E. F., Ross, I. G., *Australian J. Chem.* **15**, 591 (1962).

(20) Kautsky, H., *Trans. Faraday Soc.* **35**, 216 (1939).

(21) Kawaoka, K., Khan, A. U., Kearns, D. R., *J. Chem. Phys.* **46**, 1842 (1967).

(22) Kearns, D. R., Khan, A. U., Radlick, P., Hollins, R., Chambers, R., *J. Am. Chem. Soc.* **89**, 5455 (1967).

(23) Kearns, D. R., Hollins, R. A., Khan, A. U., Radlick, P., *J. Am. Chem. Soc.* **89**, 5456 (1967).

(24) Kellogg, R. E., Wyeth, N. C., *J. Chem. Phys.* **45**, 3156 (1966).

(25) Khan, A. U., Kasha, M., *J. Am. Chem. Soc.* **88**, 1574 (1966).

(26) Khan, A. U., Kasha, M., *J. Chem. Phys.* **39**, 2105 (1963).

(27) Khan, A. U., Kearns, D., *J. Chem. Phys.* **48**, 3272 (1968).

(28) Khan, A. U., Kearns, D. R., *J. Am. Chem. Soc.* **90**, 000 (1968).

(29) *Ibid.*, p. 000.

(30) Khan, A. U., Kearns, D. R., unpublished SCF extended Hückel calculations.

(31) Kopecky, Karl R., Reich, H. J., *Can. J. Chem.* **43**, 2265 (1965).

(32) Lim, E. C., Kowalski, V. L., *J. Chem. Phys.* **36**, 1729 (1962).

(33) Linschitz, H., Pekkarinen, L., *J. Am. Chem. Soc.* **82**, 2411 (1960).

(34) Longuet-Higgins, H. C., Abrahamson, E. W., *J. Am. Chem. Soc.* **87**, 2045 (1965).

(35) Murrell, J. N., *Mol. Phys.* **3**, 319 (1960).

(36) Nicholls, R. W., Fraser, P. A., Jarmain, W. R., McEachran, R. P., *Astrophys. J.* **13**, 399 (1960).

(37) Nickon, A., Mendelson, W. L., *J. Am. Chem. Soc.* **85**, 1894 (1963).

(38) *Ibid.*, **87**, 3921 (1965).

(39) Ogryzlo, E. A., ADVAN. CHEM. SER. **77**, 133 (1968).

(40) Porter, G., Wilkinson, F., *Proc. Roy. Soc. (London)* **A264**, 1 (1961).

(41) Porter, G., Wright, M. R., *J. Chem. Phys.* **55**, 705 (1958).

(42) Pringsheim, P., "Fluorescence and Phosphorescence," p. 333, Interscience, New York, 1965.

(43) Reid, C., "Excited States in Chemistry and Biology," p. 98, Butterworth Scientific Publications, London, 1957.

(44) Rein, R., Fukuda, N., Win, H., Clarke, G. A., Harris, F. E., *J. Chem. Phys.* **45**, 4743 (1966).

(45) Robinson, G. W., Frosch, R. P., *J. Chem. Phys.* **37**, 1962 (1962).

(46) *Ibid.*, **38**, 1187 (1963).

(47) Schenck, G. O., *Naturwiss.* **35**, 28 (1948).

(48) Siebrand, W., *J. Chem. Phys.* **44**, 4055 (1966).

(49) Terenin, A. N., *Acta Physicochim. USSR* **18**, 210 (1943).

(50) Terenin, A. N., "Photochemistry of Dyes and Related Organic Compounds," Chap. 7, Academy of Sciences Press, Moscow, 1947 (transl. by Kresge-Hooker Scientific Library).

(51) Tsubomura, H., Mulliken, R. S., *J. Am. Chem. Soc.* **82**, 5966 (1960).

(52) Wasserman, H. W., Scheffer, J. R., *J. Am. Chem. Soc.* **89**, 3073 (1967).

(53) Waters, W., *J. Chem. Soc.* **1966B**, 1040.

(54) Wilson, Therese, *J. Am. Chem. Soc.* **88**, 2898 (1966).

(55) Weiss, J., *Trans. Faraday Soc.* **35**, 48 (1939).

(56) Yuster, P., Weissman, S., *J. Chem. Phys.* **17**, 1182 (1949).

Discussion

K. Wei, A. D. Broadbent, K. Ervin, W. S. Gleason, J. C. Mani, and J. N. Pitts, Jr. (University of California, Riverside, Calif.):
The photo-oxidation of dry liquid benzene has been shown to give *trans-trans*-2,4-hexadiene-1,6-dial (mucondialdehyde) and 2,4,6,8,10-dodecapentaene-1,12-dial (probably in the all-trans configuration) (*10*). In addition, phenol has now been identified as a major product of this reaction.

The dependence of the quantum yield of the dodecapentaenedial on the concentration of oxygen dissolved in the benzene and on the wavelength of the incident radiation indicate that a triplet state of benzene is largely responsible at least for the formation of this compound. On irradiation at 2537 A. the initial rate of formation of dodecapentaenedial rapidly increases as the initial oxygen concentration increases but soon reaches a maximum (at $8 \times 10^{-4}M$ O_2) and then gradually decreases. This result can only arise if a triplet state of benzene is the main excited state leading to the product. The formation of dodecapentaenedial occurs readily on irradiation of oxygen-saturated benzene at 3130 A., thus supporting the proposal that a triplet state of benzene is an active intermediate. Oxygen is known to extend the long wave absorption of benzene because of enhancement of the spin-forbidden $T_1 \leftarrow S_0$ transition (*2, 9*).

Low concentrations of acetone, 2-pentene, and cyclohexene cause a substantial decrease in the quantum yield of dodecapentaenedial. A linear relationship was found between $1/\Phi$ and acetone concentration, suggesting that acetone quenches only singlet benzene or triplet benzene. If the latter is assumed to be quenched by acetone because of its longer lifetime, it must be the excited state responsible for the oxidation to the dodecapentaenedial.

Direct reaction of triplet benzene and oxygen, energy transfer between triplet benzene and oxygen giving excited singlet oxygen molecules, and isomerization of benzene followed by reaction with oxygen are all processes which give similar relationships for the rate of formation of dodecapentaenedial but different mechanisms. The quantum yield studies provide no information of the actual mechanisms.

The reactive species in sensitized photo-oxidations appears to be molecular oxygen in an excited singlet state (*3, 4, 5, 6*). To test whether singlet oxygen reacts with benzene, it has been generated by the action of bromine on alkaline hydrogen peroxide (*8*). It is necessary to isolate the benzene from the aqueous peroxide since these react at $0°-10°$C. to give phenol and other products similar to those from the photo-oxidation. Initial qualitative results indicate that benzene is not readily oxidized by

singlet oxygen. To demonstrate that singlet oxygen is produced and to obtain some quantitative data for benzene, model compounds are currently being examined. 2,5-Diphenyl-3,4-benzofuran has been used for this purpose (*1*), but despite its high reactivity (*11*) the reaction with ground state oxygen in the dark renders it unsuitable (*7*). On passing oxygen from the bromine/peroxide reaction through a methanolic solution of 2,5-dimethylfuran, both 2-methoxy- and 2-hydroxy-2,5-dimethyl-5-hydroperoxydihydrofuran are produced. Ordinary oxygen has no effect. The lack of reaction in benzene may be caused by poor mixing of gas and liquid.

Literature Cited

(1) Corey, E. J., Taylor, W. C., *J. Am. Chem. Soc.* **86**, 3881 (1964).
(2) Evans, D. F., *J. Chem. Soc.* **1957**, 1351, 3885; **1959**, 2753; **1961**, 1987.
(3) Foote, C. S., Wexler, S., *J. Am. Chem. Soc.* **86**, 3879, 3880 (1964).
(4) Foote, C. S., Wexler, S., Ando, W., *Tetrahedron Letters* **1965**, 4111.
(5) Kautsky, H., Hirsch, A., Flesch, W., *Chem. Ber.* **68**, 152 (1935).
(6) Kearns, D. R. *et al.*, *J. Am. Chem. Soc.* **89**, 5455, 5456 (1967).
(7) LeBerre, A., Ratsimbazafy, R., *Bull. Chim. Soc. France* **1963**, 229.
(8) McKeown, E., Waters, W., *J. Chem. Soc.* **B1966**, 1040.
(9) Tsubomura, H., Mulliken, R. S., *J. Am. Chem. Soc.* **82**, 5966 (1960).
(10) Wei, K., Mani, J. C., Pitts, J. N., Jr., *J. Am. Chem. Soc.* **89**, 4225 (1967).
(11) Wilson, T., *J. Am. Chem Soc.* **88**, 2898 (1966).

A. M. Trozzolo (Bell Telephone Laboratories): The benzil-sensitized photo-oxygenation of 1,3-cyclohexadiene in pentane–ether solution, with 3500-A. light gave the endoperoxide, 5,6-dioxabicyclo[2,2,2]2-octene. Benzophenone was also used as the sensitizer in this study.
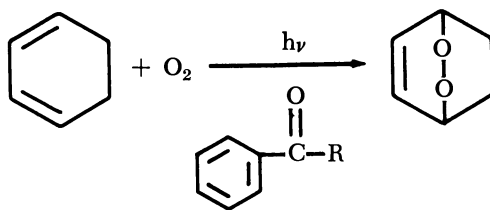
No dimers of cyclohexadiene were detected as products, although under the same conditions in the absence of oxygen, dimer formation is the main reaction process. The formation of endoperoxide is interpreted as indicating that singlet oxygen is being formed by quenching of the n-π^* triplet state of the sensitizer. The absence of dimers suggests that singlet oxygen formation competes effectively with energy transfer from sensitizer to the olefin. Previous sensitized photo-oxygenations used π-π^*

triplets. The results of this study show that also n-π^* carbonyl triplets, even though short lived, can produce singlet oxygen in sensitized photo-oxygenations. Other olefins can also be photo-oxygenated using n-π^* triplets as sensitizers. It is very probable that the singlet O_2 initially produced from these species would have a substantial $^1\Sigma_g^+$ contribution.

T. Matsuura (University of Kyoto): I wish to draw attention to the relationship between oxidation with singlet oxygen and biological oxidation. It has been reported that quercetin(Ia) is enzymatically converted to a depside(IIa) and carbon monoxide by the action of a dioxygenase. We found recently that the photosensitized oxygenation of 3-hydroxyflavone(Ib), followed by methylation of the products, gives a corresponding depside(IIb) in a 44% yield. We also found that carbon monoxide(88%) and carbon dioxide(18%) are liberated during oxygenation. A similar result was obtained with 5,7,3′,4′-tetramethylquercetin(IIc). This reaction represents a model for the enzymatic reaction. We propose possible mechanisms for both enzymatic and chemical reactions involving a hydroperoxide intermediate as shown below. [For more details *see,* T. Matsuura, H. Matsushima, H. Sakamoto, *J. Am. Chem. Soc.* **89,** 6370 (1967).]

Ia R = OH
Ib R = H
Ic R = OMe

IIa R = OH, R′ = H
IIb R = H, R′ = Me
IIc R = OMe, R′ = Me

72
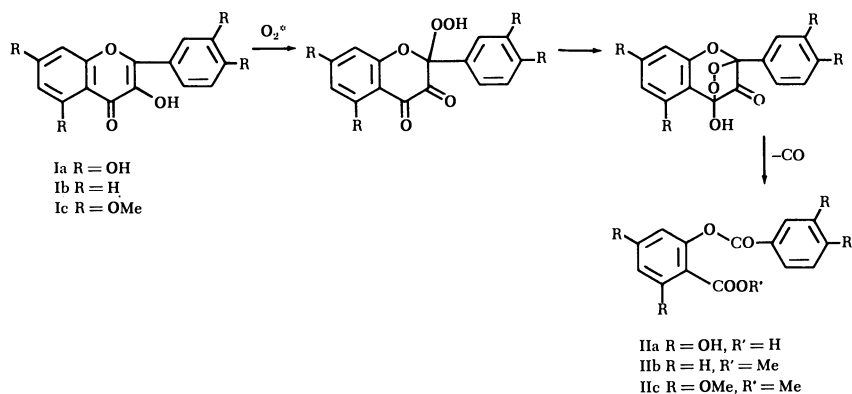
Biochemical Oxidations

SEYMOUR KAUFMAN

National Institutes of Health, Bethesda, Md. 20014

Oxygenases are enzymes which catalyze those biological oxidations which occur by addition of molecular oxygen to the organic molecule being oxidized. In reactions catalyzed by monooxygenases, the specific electron-donating cofactor utilized varies from one enzyme to another. Research on oxygenases has focused on cofactor requirements of the various oxygenases, the flow of electrons during the reaction, and the mechanism of the oxygenation step.

It is now well established that organic compounds can be oxidized by organisms in two different ways. The most common mode of biological oxidation is *via* dehydrogenation reactions. Almost all of the oxidative steps in carbohydrate, fat, and protein metabolism proceed by this pathway. Twelve years ago, it was shown by Mason and independently by Hayaishi that a second type of biological oxidative reaction can occur: addition of molecular oxygen onto the organic molecule being oxidized. The enzymes catalyzing this type of reaction have been called mixed function oxidases or oxygenases. Oxygenases have been further divided into two sub-categories: monooxygenases and dioxygenases, depending on whether one or two atoms of oxygen are incorporated into the organic molecule.

The reactions catalyzed by monooxygenases can be described by the following general equation where RH stands for the organic molecule being oxidized, and XH_2 is an electron donor:

$$RH + O_2 + XH_2 \rightarrow ROH + H_2O + X$$

The specific electron donor utilized in these reactions varies from one enzyme to another. Reduced pyridine nucleotides, tetrahydropteridines, and ascorbate have all been shown to function as electron-donating cofactors with different mono-oxygenases. These cofactor requirements are usually specific. Phenylalanine hydroxylase, for example, utilizes a

tetrahydropteridine and will not function with ascorbate or reduced pyridine nucleotides. The reason for this cofactor specificity is not known.

It is possible to discern three phases of research on oxygenases. In the first phase, the main effort was directed toward delineating the cofactor requirements of the various oxygenases. During this period new coenzymes, or new roles for old coenzymes, were uncovered. In the second phase, attempts were made to trace the flow of electrons from the electron donor to the enzyme itself. For microsomal and mitochondrial oxygenases, the flow of electrons may involve a complex series of intermediary electron carriers. In the third phase, attempts are being made to study the mechanism of the oxygenation step. In the following papers, all three areas of research in this field are touched.

73

The Mechanism of Action of Dopamine β–Hydroxylase

SEYMOUR KAUFMAN, WILLIAM F. BRIDGERS,[1] and JOSEPH BARON[2]

Laboratory of General and Comparative Biochemistry, National Institute of Mental Health, U. S. Department of Health, Education, and Welfare, Public Health Service, National Institutes of Health, Bethesda, Md. 20014

Dopamine β-hydroxylase catalyzes the side-chain hydroxylation of dopamine and other phenylethylamine derivatives. Ascorbic acid serves as a specific electron-donating cofactor. The enzyme from bovine adrenal glands contains Cu^{2+} and a smaller amount of Cu^+. When the enzyme oxidizes ascorbate to dehydroascorbate, most of the Cu^{2+} is reduced to Cu^+. Added substrate is hydroxylated, and Cu^+ is reoxidized to Cu^{2+}. This indicates that most of the protein-bound Cu^{2+} undergoes cyclic reduction and oxidation during hydroxylation. The results also rule out an oxygen-carrier function for ascorbate. The possibility that a β-substituted hydroperoxide of the substrate is formed as an intermediate in the reaction has been examined with the use of β,β'-tritium-labelled substrate. The results indicate that such an intermediate is unlikely.

Dopamine β-hydroxylase catalyzes the hydroxylation of dopamine (3,4-dihydroxyphenylethylamine) to norepinephrine according to Reaction 1 (*14*).

$$\text{Dopamine} + O_2 + \text{ascorbate} \rightarrow \text{norepinephrine} + H_2O + \text{dehydroascorbate} \tag{1}$$
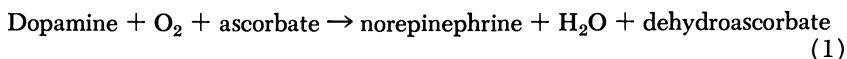
With catalytic amounts of enzyme, the hydroxylation reaction is specific for derivatives of ascorbate (*14*). The enzyme is relatively nonspecific for the substrate; the minimum structural requirements appear to be a benzene ring with a two-carbon side chain that terminates in an amino group (*2, 3, 6, 15*). The enzyme activity is stimulated markedly

---

[1] Present address: Department of Medicine, University of Miami School of Medicine, Miami, Fla. 33136.
[2] Present address: University of Chicago Medical School, Chicago, Ill.

by certain dicarboxylic acids such as fumarate and α-ketoglutarate (*14*). Recently, other hydroxylases have been reported to show a similar dual requirement for ascorbate and a dicarboxylic acid (*1, 7, 8, 13*).

Dopamine β-hydroxylase has been obtained in essentially pure form from bovine adrenal glands (*4*). It has a molecular weight of approximately 290,000. Although the protein is colorless, metal analysis showed that it is a copper protein containing between 0.65 and 1.0 μgram of copper per mg. of protein (4–7 moles of copper/mole protein). Part of the copper is present as Cu^+ and part as Cu^{2+}. Although the amount of Cu^+ varies from one enzyme preparation to another, the amount of Cu^{2+} is relatively constant and is equal to about two moles per mole of enzyme.

The copper is essential for enzyme activity. It can be removed by treating the enzyme with cyanide and ammonium sulfate, resulting in an apoenzyme without detectable hydroxylase activity. Copper is the only cation tested which can restore activity to the apoenzyme.

In the absence of substrate, the enzyme can rapidly oxidize an equivalent amount of ascorbate to dehydroascorbate. The other product of this reaction is a reduced form of the enzyme in which most of the Cu^{2+} has been reduced to Cu^+. The reduction of the enzyme by ascorbate can take place anaerobically. When the reduced enzyme is exposed to substrate and oxygen in the absence of ascorbate, part of the Cu^+ is reoxidized to Cu^{2+}, and an equivalent amount of substrate is converted to hydroxylated product. The valence changes in the protein-bound copper have been observed with both a colorometric method (*4*) and with ESR measurements (*5*).

Based on these results, the hydroxylation reaction has been formulated (*4, 5*) as shown in Reactions 2, 3, and 4, where RH stands for substrate and ROH for hydroxylated product.

$$E\text{-}(Cu^{2+})_2 + \text{ascorbate} \rightarrow E\text{-}(Cu^+)_2 + \text{dehydroascorbate} + 2H^+ \qquad (2)$$

$$E\text{-}(Cu^+)_2 + O_2 \rightleftarrows E\text{-}(Cu^+)_2\text{-}O_2 \qquad (3)$$

$$E\text{-}(Cu^+)_2\text{-}O_2 + RH + 2H^+ \rightarrow E\text{-}(Cu^{2+})_2 + ROH + H_2O \qquad (4)$$
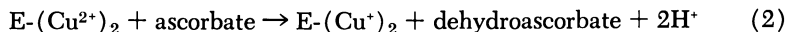
The scheme is undoubtedly oversimplified. It is possible, for example, that reduction of the enzyme by ascorbate involves the formation of semidehydroascorbate although dehydroascorbate is the only product that has so far been detected. It is also possible that Reaction 3, the combination of oxygen with the enzyme-bound copper, does not occur in the absence of substrate. It is of interest in this regard that the reduction of the enzyme by ascorbate occurs rapidly in the absence of substrate. This is in contrast to results obtained with salicylate hydroxylase, where rapid reduction of the enzyme-bound flavin by DPNH requires the presence of substrate (*9*).

Reactions 2, 3, and 4 tell us little about how oxygen is activated during the hydroxylation reaction, and at the moment one can only speculate about the details. The scheme and the results on which it is based do, however, rule out several general types of hydroxylation mechanism. The fact that the enzyme can be reduced anaerobically by ascorbate to a form which actively supports substrate hydroxylation in the absence of ascorbate rules out any mechanism for this enzyme-catalyzed reaction in which the ascorbate functions as an oxygen carrier. Such a role has been postulated for tetrahydropteridines (*16*), which can serve as specific electron-donating cofactors (just as ascorbate does with dopamine β-hydroxylase) in certain aromatic hydroxylation reactions (*10, 12*).

We have in the past considered another type of hydroxylation mechanism (Reactions 5 and 6) that involves the formation of a hydroperoxide of the substrate as an intermediate, followed by reduction of the peroxide to the hydroxylated product (*11*). A similar mechanism involving the formation of a transannular peroxide of the substrate has also been proposed recently for aromatic hydroxylations (*18*).

$$RH + O_2 \rightarrow ROOH \tag{5}$$

$$ROOH + \text{ascorbate} \rightarrow ROH + \text{dehydroascorbate} + H_2O \tag{6}$$
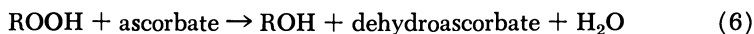
In the light of the results discussed earlier on the reduction of the enzyme by ascorbate, this old scheme would have to be modernized by replacing the ascorbate in Reaction 6 with the reduced enzyme, $E\text{-}(Cu^+)_2$. In this mechanism, it is assumed that the only role of the enzyme-bound copper is to allow transfer of electrons from ascorbate to the hydroperoxide of the substrate.

We have tried to detect the formation of a hydroperoxide of the substrate in the absence of the over-all reaction by using a substrate labelled with tritium in the β positions.

$$\begin{array}{ccc} & T & & T \\ & | & & | \\ R\text{—}C\text{—}CH_2\text{—}NH_2 + O_2 \rightarrow & R\text{—}C\text{—}CH_2\text{—}NH_2 \\ & | & & | \\ & T & & OOT \end{array} \tag{7}$$
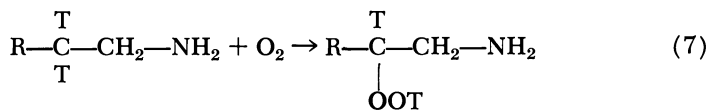
If Reaction 7 occurred, tritium should be released into the medium in the absence of ascorbate. Sufficient enzyme was used in these experiments to detect Reaction 7 even if the hydroperoxide formed did not exceed the amount of enzyme present.

Before experiments in the absence of ascorbate were performed, the extent of discrimination against the tritium-labelled substrate during the hydroxylation reaction was estimated. The hydroxylation of β-β′-tritium-labelled tyramine was studied as a function of time. The reaction was followed by measuring the amount of octopamine (1-[*p*-hydroxyphenyl]-

2-aminoethanol) formed and the amount of tritiated water released. The results (Table I) indicate that the isotope effect is about 1.8.

The results of experiments designed to detect Reaction 7 are shown in Table II. About 0.2% of the tritium initially present in the substrate was volatile under conditions of lyophilization. In the absence of ascorbate, no enzyme-dependent release of tritium was detectable. In the presence of ascorbate—*i.e.*, when the over-all hydroxylation raction took

Table I. Time-Course of the Conversion of Tyramine to Octopamine[a]

Incubation Time, min.	Octopamine Formed, μmoles	Tritium Release, CPM/0.05 ml.		Isotope Effect
		Found	*Expected*	
5	0.111	258	470	1.82
10	0.219	498	928	1.86
20	0.414	913	1760	1.92
40	0.685	1754	2900	1.65

[a] All tubes contained the following components (in μmoles unless stated otherwise): potassium phosphate, pH 6.5, 100; ascorbate, 6.0; fumarate, 50; tyramine-$\beta\beta'$-^{3}H, 2.0, specific activity 1.15×10^5 CPM/μmole; catalase, 300 units, dopamine β-hydroxylase (4). Final volume, 0.68 ml. at 25°C. Octopamine determined by a minor modification of a published procedure (17). A 0.05 ml. sample of water was obtained by lyophilization and dissolved in 10 ml. of Bray's scintillation mixture. Radioactivity determined in a Packard liquid scintillation spectrometer; total counts collected were sufficient to yield a 5% coefficient of variation. The expected tritium release was calculated from the octopamine formed, assuming that the amount of tritium was the same in both β positions of the tyramine. The results for the amount of tritium released have been corrected for the amount of exchangeable tritium initially present in the tyramine.

Table II. Reaction of Tyramine-β,β'-^{3}H with Dopamine β-Hydroxylase[a]

Experiment	Enzyme Added, mg.	Ascorbate	Tritium Released	
			CPM	*%*
1	0	—	3.20×10^3	0.18
2	0.884 (native)	—	3.25×10^3	0.18
3	1.37 (boiled)	—	3.20×10^3	0.18
4	1.37 (native)	—	3.11×10^3	0.17
5	0.069 (boiled)	+	3.11×10^3	0.17
6	0.069 (native)	+	7.85×10^5	43.0

[a] Complete reaction mixtures contained the following components (in μmoles): potassium phosphate, pH 6.5, 100; fumarate, 50; catalase, 300 units, tyramine, β-β'-^{3}H, 0.54, specific activity, 3.36×10^6 CPM/μmole. Ascorbate (6.0 μmoles) and dopamine β-hydroxylase (4) were added where indicated. Final volume, 0.68 ml.; incubation time, 20 min. at 25°C. Reactions were stopped by freezing. A 0.1-ml. sample of water was obtained by lyophilization and dissolved in 10 ml. of Bray's scintillation mixture. Radioactivity determined in a Packard liquid scintillation spectrometer; total counts collected were sufficient to yield 5% coefficient of variation.

place (Experiment 6), 43% of the radioactivity was released into the medium. Since a 5% difference in radioactivity between Experiments 1 and 2 and Experiments 3 and 4, could have been measured, these experiments were sensitive enough to detect a partial reaction (involving substrate and oxygen in the absence of ascorbate) occurring at 0.01% of the catalytic rate observed in Experiment 6.

If a β-substituted hydroperoxide of the substrate had been formed in amounts equal to the amount of enzyme present, the expected amount of tritium released in the presence of native enzyme (Experiment 4) should have exceeded that found in its absence (Experiment 3) by about 4000 CPM/0.1 ml.

These results show that it is unlikely that the hydroxylation reaction catalyzed by dopamine β-hydroxylase occurs as depicted in Reactions 5 and 6. A β-substituted hydroperoxide of the substrate could still be involved in the mechanism if the *formation* of the hydroperoxide required the participation of ascorbate.

Acknowledgment

Literature Cited

(1) Abbott, M. T., Schandl, E. K., Lee, R. F., Parker, T. S., Midgett, R. J., *Biochim. Biophys. Acta* **132,** 525 (1967).
(2) Bridgers, W. F., Kaufman, S., *J. Biol. Chem.* **237,** 526 (1962).
(3) Creveling, C. R., Daly, J. W., Witkop, B., Udenfriend, S., *Biochim. Biophys. Acta* **64,** 125 (1962).
(4) Friedman, S., Kaufman, S., *J. Biol. Chem.* **240,** 4763 (1965).
(5) *Ibid.*, **241,** 2256 (1966).
(6) Goldstein, M., Contrera, J. F., *J. Biol. Chem.* **237,** 1898 (1962).
(7) Hausmann, E., *Biochim. Biophys. Acta* **133,** 591 (1967).
(8) Hutton, J. J., Tappel, A. L., Udenfriend, S., *Biochem. Biophys. Res. Commun.* **24,** 179 (1966).
(9) Katagiri, M., Takemori, S., Suzuki, K., Yasuda, H., *J. Biol. Chem.* **241,** 5675 (1966).
(10) Kaufman, S., *J. Biol. Chem.* **234,** 2677 (1959).
(11) Kaufman, S., "Oxygenases," O. Hayaishi, Ed., p. 129, Academic Press, New York, 1962.
(12) Kaufman, S., *Proc. Natl. Acad. Sci.* **50,** 1085 (1963).
(13) Kivirikko, K. I., Prockop, D. J., *Proc. Natl. Acad. Sci.* **57,** 782 (1967).
(14) Levin, E. Y., Levenberg, B., Kaufman, S., *J. Biol. Chem.* **235,** 2080 (1960).
(15) Levin, E. Y., Kaufman, S., *J. Biol. Chem.* **236,** 2043 (1961).
(16) Mager, H. I. X., Berends, W., *Biochim. Biophys. Acta* **118,** 440 (1966).
(17) Pisano, J. J., Creveling, C. R., Udenfriend, S., *Biochim. Biophys. Acta* **43,** 566 (1960).
(18) Soloway, A. H., *J. Theoret. Biol.* **13,** 100 (1966).

Reaction Mechanism of FAD-Containing Monooxygenases

SHOZO YAMAMOTO, YOSHITAKA MAKI, TERUKO NAKAZAWA, YASUMICHI KAJITA, HIROSHI TAKEDA, MITSUHIRO NOZAKI, and OSAMU HAYAISHI

Department of Medical Chemistry, Kyoto University Faculty of Medicine, Kyoto, Japan

Imidazoleacetate and L-lysine monooxygenases from pseudomonads were obtained in crystalline form. Both enzymes were established to contain FAD probably as a sole cofactor. Available evidence indicates that the reaction catalyzed by these enzymes involves the reduction of FAD, the monooxygenation of substrate, and the reoxidation of reduced FAD. The mechanism of activating molecular oxygen by these FAD-containing monooxygenases is discussed.

Monooxygenase (mixed function oxidase) catalyzes the incorporation of one atom of molecular oxygen into substrate and the reduction of the other atom to water. For the reduction of the oxygen atom, some monooxygenases require an exogenous reductant such as reduced pyridine nucleotide and ascorbate, whereas others consume endogenous hydrogen atoms of substrate. Thus, the monooxygenase reaction involves both the oxidation (dehydrogenation) of a hydrogen donor and the oxygenation of substrate.

To clarify the reaction mechanism of monooxygenase, we have recently purified two monooxygenases from pseudomonads. Imidazoleacetate monooxygenase (5) and L-lysine monooxygenase (10) were obtained in crystalline form, and both were shown to be flavoproteins. The former requires an exogenous hydrogen donor, but the latter utilizes the hydrogen atoms of L-lysine.

This paper describes some of the results of our investigations of the two FAD (flavin adenine dinucleotide)-containing monooxygenases. We also discuss the mechanism of activation of molecular oxygen by these enzymes.

Imidazoleacetate Monooxygenase

Imidazoleacetate monooxygenase was purified about 250-fold from a cell-free extract of a pseudomonad and was obtained in crystalline form (Figure 1). The specific activity of the crystalline enzyme was 25.0 μmoles/min./mg. protein, and on the basis of a molecular weight of 90,000 its molecular activity was estimated to be 2000 at 24°C.
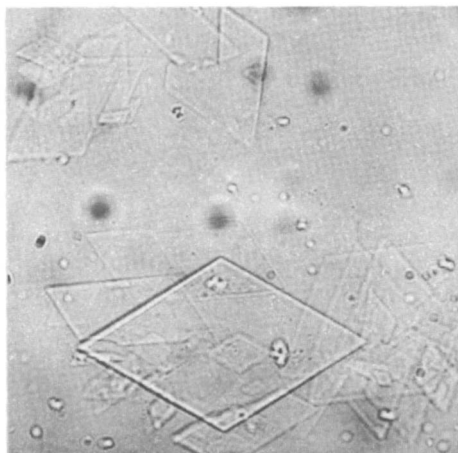
Figure 1. Crystalline imidazoleacetate monooxygenase

The enzyme catalyzes the incorporation of one atom of oxygen into imidazoleacetate, and the accumulation of imidazoloneacetate was observed. The reaction product was unstable and decomposed spontaneously. NADH (nicotinamide adenine dinucletotide hydrate) was consumed as a hydrogen donor. The enzyme assay was carried out either by the spectrophotometric measurement of NADH oxidation or

$$\text{HC}=\text{C}-\text{CH}_2\text{COOH} \; + \; \text{O}^*_2 + \text{NADH} + \text{H}^+ \longrightarrow \text{HO}^*-\text{C}=\text{C}-\text{CH}_2\text{COOH} \; + \; \text{NAD}^+ + \text{H}_2\text{O}^*$$
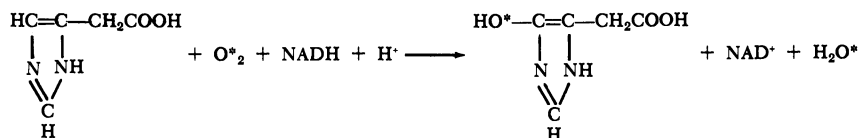
by the polarographic determination of oxygen consumption. K_m values for imidazoleacetate, NADH, and oxygen were estimated to be 0.3, 0.01, and 0.02 mM, respectively.

The crystalline enzyme was yellow, and its absorption spectrum is presented in Figure 2. The prosthetic group was identified as FAD, one mole of which was estimated per mole of the enzyme protein. The
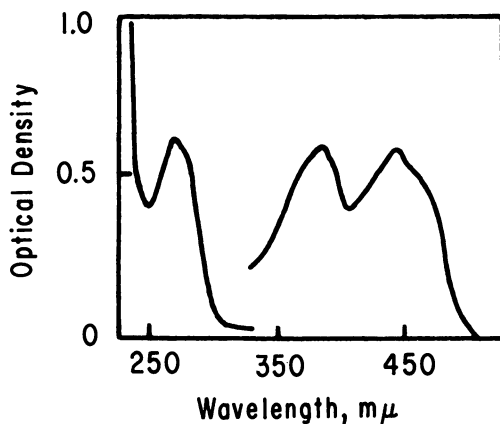
Figure 2. Absorption spectrum of imidazoleacetate monooxygenase. Protein, 0.45% for visible region and 0.045% for ultraviolet region

enzyme catalyzed the reduction of several dyes with NADH under anaerobic conditions; 2,6-dichlorophenolindophenol, FAD, FMN (riboflavine 5'-phosphate), and ferricyanide. In the absence of imidazoleacetate the enzyme could oxidize NADH at only 0.5% of the rate in its presence. K_m values of the NADH oxidase activity for NADH and oxygen were estimated to be 0.3 and 0.02 mM, respectively.

Analyses of the enzyme failed to detect significant amounts of iron and copper (Table I), and most metal chelating agents tested did not show significant inhibition of the enzyme activity (*11*).

Table I.   Estimations of Iron and Copper of Imidazoleacetate and L-Lysine Monooxygenases, μmole

Enzyme	Iron[a]	Copper[a]
Imidazoleacetate monooxygenase (0.120)	0.001	0.000
L-Lysine monooxygenase (0.103)	0.000	0.003

[a] Dry ashing of enzyme protein was carried out. Iron was estimated by *o*-phenanthroline method and copper by sodium diethyldithiocarbamate or dithizone method.

Reduction of the enzyme-bound FAD was observed on adding sodium dithionite at pH 10.5 (Figure 3). FAD reduction was also observed on adding NADH both in the presence of imidazoleacetate and in its absence (Figure 3). An absorption spectrum characteristic of the semiquinoid form of FAD appeared when the enzyme was half reduced with sodium dithionite but not with NADH.

When an equimolar amount of NADH was anaerobically added to the enzyme in the presence of imidazoleacetate, the reduction of FAD

was complete and immediate. Air was then introduced to reoxidize FAD, and the amount of imidazoleacetate was measured. On adding NADH (45 mμmoles), FAD (44 mμmoles) was reduced, and on the reoxidation of FAD, imidazoleacetate (42 mμmoles) was consumed.
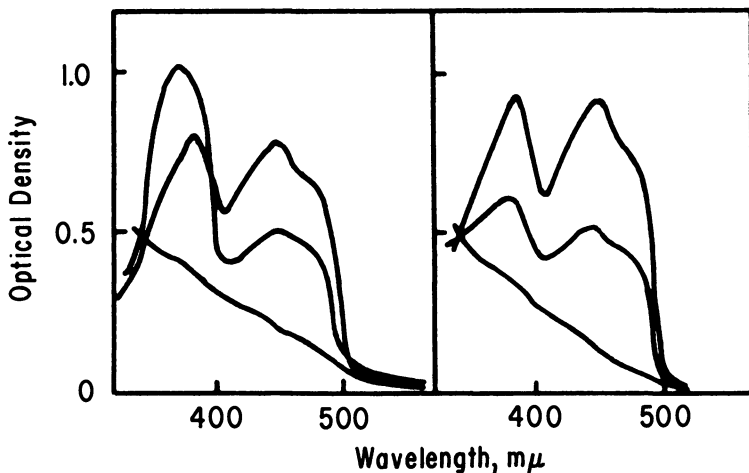
Figure 3. Reduction of imidazoleacetate monooxygenase with sodium dithionite at pH 10.5 (left) and with NADH (right)

L-*Lysine Monooxygenase*

L-Lysine monooxygenase from a pseudomonad was purified approximately 100-fold, and the enzyme was crystallized (*10*) (Figure 4). Its specific activity was 10.5 μmoles/min./mg. protein. The molecular weight was estimated to be 191,000 and the molecular activity was calculated to be 2082 at 34°C.

The enzyme catalyzes the incorporation of one atom of oxygen into L-lysine, and δ-aminonorvaleramide is formed concomitantly with the evolution of carbon dioxide. Enzyme activity was estimated by the polarographic determination of oxygen consumption. The concentration curve of L-lysine was sigmoidal, and 0.18 m*M* L-lysine was required for the half maximal velocity of the enzyme.

$$
\begin{array}{l}
\mathrm{CH_2NH_2} \\
| \\
\mathrm{(CH_2)_3} + \mathrm{O^*_2} \\
| \\
\mathrm{CH{-}NH_2} \\
| \\
\mathrm{COOH}
\end{array}
\quad\longrightarrow\quad
\begin{array}{l}
\mathrm{CH_2NH_2} \\
| \\
\mathrm{(CH_2)_3} + \mathrm{CO_2} + \mathrm{H_2O^*} \\
| \\
\mathrm{C{-}NH_2} \\
\| \\
\mathrm{O^*}
\end{array}
$$
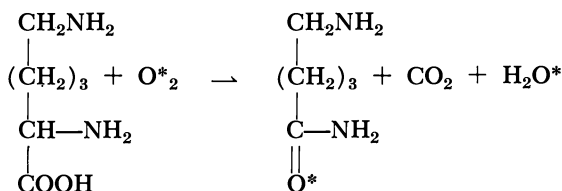
The enzyme was also shown to contain FAD. The absorption spectrum is shown in Figure 5. Two moles of FAD were estimated per mole of enzyme protein. The enzyme catalyzed the reduction of 2,6-dichlorophenolindophenol in the presence of phenazine methosulfate.

Analyses of the enzyme showed no iron, copper, or other metal present in significant quantities (Table I). Most metal chelating agents tested were not inhibitory to the enzyme (*11*).
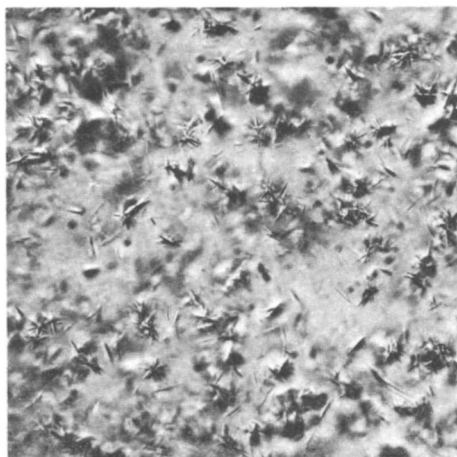
Figure 4. Crystalline L-*lysine monooxygenase*
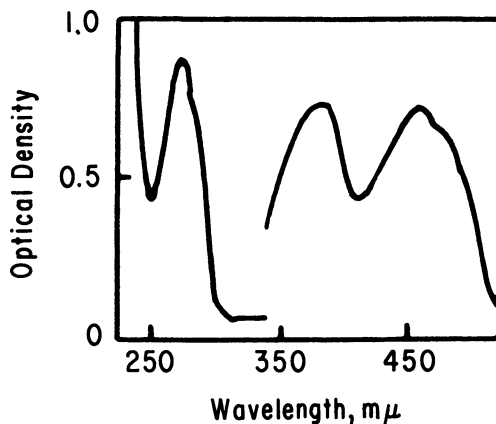
Figure 5. Absorption spectrum of L-*lysine monooxygenase. Protein, 0.62% for visible region and 0.048% for ultraviolet region*

The enzyme-bound FAD could be reduced by adding sodium di-thionite. Figure 6 presents the spectral change of FAD at pH 7.0, and an absorption of semiquinoid of FAD appeared during the reduction. When the enzyme was incubated with L-lysine under the anaerobic conditions, FAD was reduced at a rate which depended on the concentration of L-lysine. With 0.1 mM L-lysine the reduction occurred very slowly as presented in Figure 6.
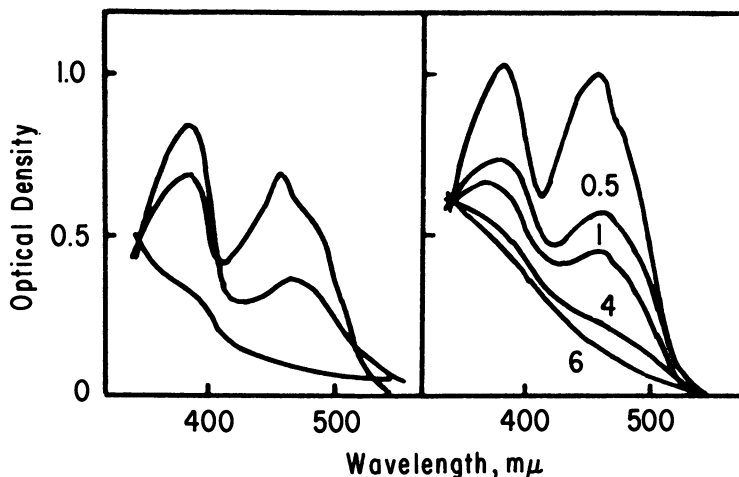
Figure 6.   Reduction of L-lysine monooxygenase with sodium di-thionite at pH 7.0 (left) and with L-lysine at 0.1 mM. Numbers in-dicate the incubation time in hours (right)

A stoichiometric amount (0.1 mM) each of enzyme-bound FAD and [41]C-u-L-lysine (u = uniformly labelled) was incubated anaerobically until FAD was fully reduced. After deproteinization the reaction mixture was subjected to high voltage paper electrophoresis and paper chroma-tography. Most of the radioactivity appeared at the area corresponding to piperidine 2-carboxylic acid (α-keto-ε-aminocaproic acid) (Figure 7), and a significant amount of carbon dioxide was not detected. When the reaction mixture was aerated to reoxidize FAD and then deproteinized, the radioactivity was also found at the position of piperidine 2-carboxylic acid.

Discussion

By incorporating one atom of molecular oxygen into substrate, monooxygenases catalyze a variety of reactions—namely, hydroxylation, dealkylation, epoxide and N-oxide formation, desaturation, aromatization of steroid, and acid amide formation. The participation of a flavin cofactor has been reported for each type of monooxygenase reaction.

An electron transport system is associated with several monooxygenase reactions. The steroid 11β-hydroxylating system of adrenal mitochondria consists of a flavoprotein, non-heme iron protein and homoprotein (*3*). Fatty acyl ACP desaturase from Euglena requires a flavoprotein and non-heme iron protein (*6*). In these monooxygenation systems FAD as a flavoprotein is a component of an electron transport system. However, imidazoleacetate and L-lysine monooxygenases, together with salicylate and *p*-hydroxybenzoate hydroxylases, appear to contain FAD as a sole cofactor since iron and copper were not detected in significant quantities in these enzymes (*11, 12*).

When FAD of imidazoleacetate monooxygenase was fully reduced with NADH in the presence of imidazoleacetate and reoxidized by aeration, an equimolar amount of imidazoleacetate was consumed probably to form imidazoloneacetate. An analogous result has been obtained with salicylate hydroxylase (*9, 13*). These findings indicate that the reduced form of enzyme-bound FAD serves as a hydrogen donor in the hydroxylation of substrate and reduces one atom of oxygen to water. When a similar experiment was carried out with L-lysine monooxygenase and ^{14}C-L-lysine, the radioactivity was

R: $H_2N—(CH_2)_3—$

Lysine — δ-Aminonorvaleramide — α-Keto-ε-aminocaproate — Piperidine 2-carboxylate
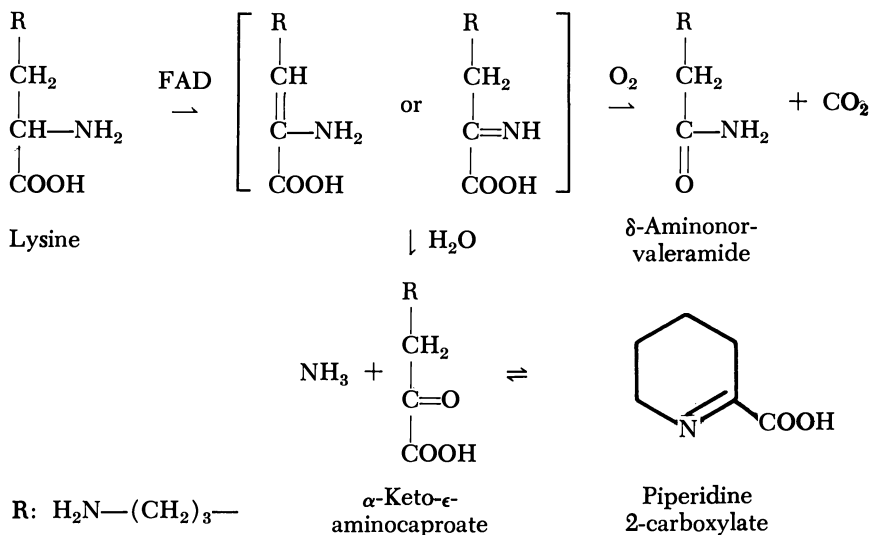
found at the area corresponding to piperidine 2-carboxylic acid but little at the position of δ-aminonorvaleramide. Under the experimental conditions, FAD was reduced very slowly, and a rather long incubation time was required for its full reduction. If an intermediate formed by the dehydrogenation of L-lysine is unstable and readily hydrolyzed, after the long incubation time the intermediate may be hydrolyzed to piperidine 2-carboxylic acid, which is not susceptible to monooxygenation.
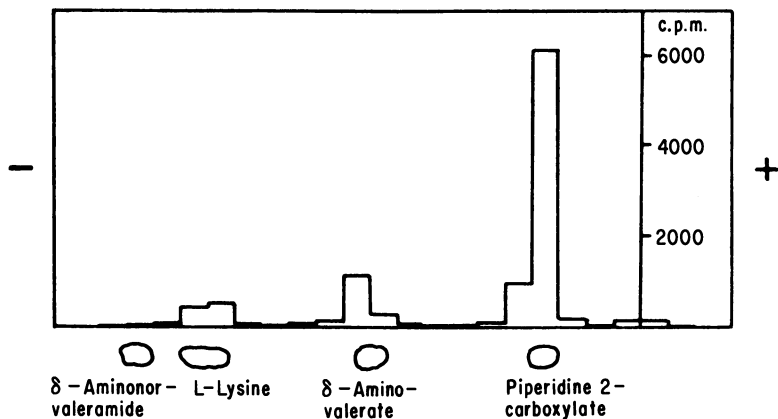
Figure 7. Formation of piperidine 2-carboxylic acid. The enzyme-bound FAD (0.1 mM) and ^{14}C-u-L-lysine (0.1 mM, 1,000,000 c.p.m.) were incubated anaerobically for 7 hours. After deproteinization by adding perchloric acid, an aliquot of the reaction mixture was subjected to high voltage paper electrophoresis (2000 volts) at pH 3.4 for 1 hour

Although the identification of the ^{14}C-labeled product as piperidine 2-carboxylic acid has not been established and the mechanism of its formation has not been clearly elucidated, the formation of the α-keto acid may suggest the intermediate formation of dehydrogenated L-lysine concomitant with the reduction of FAD.

The function of metal ion in activating molecular oxygen has long been investigated and discussed. Several dioxygenases have been established to contain iron which has been postulated to mediate the activation of molecular oxygen (7, 8). This is also the case with the copper contained in phenolase (2) and dopamine β-hydroxylase (1). As described above, however, iron and copper appear to be absent in some monooxygenases, and FAD seems to be a sole cofactor of these enzymes. Therefore, in the absence of metal ion, consideration of the mechanism of activating molecular oxygen suggests an additional function of reduced flavin in addition to its action as an electron carrier. The spontaneous oxidation of reduced flavin leading to a very reactive hydroperoxide has been reported by Mager and Berends (4). This hydroperoxide is supposed to arise by a reaction between a semiquinoid form of flavin and molecular oxygen. Whether or not such a hydroperoxide participates in the enzymatic activation of molecular oxygen will require evidence obtained from experiments with FAD-containing monooxygenases.

The semiquinoid form of FAD was observed spectrophotometrically when the enzymes were reduced with sodium dithionite. However, such a species could not be detected on reduction with substrate, and it has

not been established whether a semiquinone of FAD is involved in the catalyses of these enzymes.

Acknowledgment

Literature Cited

(1) Friedman, S., Kaufman, S., *J. Biol. Chem.* **240**, 4763 (1965).
(2) Kertesz, D., Zito, R., "Oxygenases," O. Hayaishi, Ed., p. 307, Academic Press, New York, 1962.
(3) Kimura, T., Suzuki, K., *J. Biol. Chem.* **242**, 485 (1967).
(4) Mager, H. I. X., Berends, W., *Biochim. Biophys. Acta* **118**, 440 (1966).
(5) Maki, Y., Yamamoto, S., Nozaki, M., Hayaishi, O., *Biochem. Biophys. Res. Commun.* **25**, 609 (1966).
(6) Nagai, J., Bloch, K., *J. Biol. Chem.* **241**, 1925 (1966).
(7) Nozaki, M., Kojima, Y., Nakazawa, T., Fujisawa, H., Ono, K., Kotani, S., Hayaishi, O., Yamano, T., "Biological and Chemical Aspects of Oxygenases," K. Bloch, O. Hayaishi, Eds., p. 347, Maruzen Co., Tokyo, 1966.
(8) Senoh, S., Kita, H., Kamimoto, M., "Biological and Chemical Aspects of Oxygenases," p. 378, Maruzen Co., Tokyo, 1966.
(9) Suzuki, K., Yasuda, H., Sei, K., Takemori, S., Katagiri, M., *Seikagaku* **38**, 521 (1966).
(10) Takeda, H., Hayaishi, O., *J. Biol. Chem.* **241**, 2733 (1966).
(11) Yamamoto, S., Takeda, H., Maki, Y., Hayaishi, O., "Biological and Chemical Aspects of Oxygenases," p. 303, Maruzen Co., Tokyo, 1966.
(12) Yano, K., Morimoto, M., Higashi, N., Arima, K., "Biological and Chemical Aspects of Oxygenases," p. 329, Maruzen Co., Tokyo, 1966.
(13) Yasuda, H., Suzuki, K., Takemori, S., Katagiri, M., *Biochem. Biophys. Res. Commun.* **28**, 135 (1967).

75

Oxidation of Iron(II) Chloride in Nonaqueous Solvents

GEORGE S. HAMMOND and CHIN-HUA S. WU

Gates and Crellin Laboratories of Chemistry, California Institute of Technology, Pasadena, Calif. 91109

Autoxidation of iron(II) chloride in nonaqueous solvents is much faster than in water. The rate is first order in oxygen, and under controlled conditions, second order in iron(II). Various additives have powerful catalytic or inhibitory effects. The inhibition by iron(III) disappears in the presence of excess lithium chloride, so inhibition is attributed to competition between iron(II) and iron(III) for chloride ions. Induced autoxidation of benzoin to benzil has the same rate-limiting step as the autoxidation of iron(II) without cosubstrate. The data can be accommodated by a mechanism in which the rate-limiting step is production of iron(IV) by dissociation of a binuclear complex having the composition $Cl_2FeOOFeCl_2$. In the presence of excess lithium chloride, intermediates containing more chloride bound to iron become involved.

A number of workers (8, 13, 14, 15, 20, 21, 22, 23, 33, 34, 35) have reported studies of the rates of air oxidation of iron(II) to iron(III) in aqueous solution and have discussed the mechanistic implications of the kinetic studies. Only Pound (28) has reported the results of a preliminary study of the reaction in nonaqueous solvents. We have investigated the reaction in organic solvents because the faster rates are more convenient to follow and because a wider range of organic cosubstrates can be included. The ultimate aim of this study is to increase our understanding of the various catalytic and inhibitory roles played by metallic compounds in autoxidations.

Experimental

Materials. Iron(II) chloride dihydrate was purified by a slight variation of the procedure described by Moeller (25). Reagent grade

$FeCl_2 \cdot 2H_2O$ (100 grams), water (40 ml.), 5 grams iron powder, and 5 ml. $6N$ HCl were heated under nitrogen at 120°C. for one hour. The hot suspension was filtered, and the filtrate was cooled, first at room temperature and then at ice temperature, and the green crystals of $FeCl_2 \cdot 4H_2O$ were removed by filtration. All of the last three operations were carried out in a nitrogen box. The crystals were dried to constant weight over phosphorus pentoxide in a vacuum desiccator. The ivory-colored dihydrate was obtained and stored in vacuum-sealed ampoules containing 2–3 grams. When ampoules were opened for use, the contents were transferred to screw-cap vials and stored in a vacuum desiccator. Various samples were analyzed for iron(II) by dichromate titration (*17*). Samples stored as described showed a maximum loss in titer of 1% over five-month periods. Analysis: calculated for $FeCl_2 \cdot 2H_2O$, Fe(II), 34.31. Found, 34.10-34.87. Methanol was first treated with aluminum amalgam (*32*) and then distilled. Tests for carbonyl compounds with alkaline mercuric cyanide (*12*) showed the presence of less than 0.002% of such materials. Ethanol was purified in the same way as methanol. The former was found to contain less than 0.005% carbonyl compounds. Ethylene glycol was purified by distillation from sodium (*36*). Pyridine, purified by distillation over pellets of potassium hydroxide, was supplied by James Waters. Dimethyl sulfoxide, purified by distillation and stored over molecular sieves, was provided by Robert C. Neuman, Jr. Reagent grade piperidine was dried over sodium and distilled; the fraction boiling at 105°C. was collected for use. Acetylacetone was purified by treatment with sodium hydroxide and distillation (*6, 7*). The fraction collected for use boiled at 133°–134°C. and initially had $n_D^{25} = 1.4525$; the value changed to $n_D^{25} = 1.4512$ after a few days. Dipivaloylmethane (*18*), purified by preparative vapor chromatography, was provided by Donald Paskovich. Other materials were reagent grade chemicals used as drawn from the stockroom.

Kinetic Procedures. The volumetric oxygen monitoring apparatus has been described by Boozer (*2*). The pressure of oxygen can be kept within ±2 mm. Hg. The gas buret reads with a precision ±0.01 ml. The O_2 uptake is independent of stirring speed, and the possibility of photocatalysis has been ruled out by dark experiments. The reaction vessel consists of a thermojacketed flask whose sidearm is equipped with a snug ground-glass chamber seat for iron(II) sample. Iron chloride is weighed in a small Pt boat, placed in the seat, then the chamber is closed. Under these circumstances, the sample is protected from solvent vapor during degassing. The reaction mixture is degassed, saturated with 1 atm. oxygen or air. Owing to the volatility of methanol, it is important to establish the near equilibrium between the oxygen gas and the liquid before the zero time is marked. A period of 15 to 20 minutes should be allowed. Then the iron sample is added. Within one to two minutes, a homogeneous reaction mixture results, and at this time the zero point of a run is marked.

Analytical Methods. IRON(II) AND IRON(III). Methanolic solutions of varying concentrations of iron(II) and iron(III) were made. Spectrophotometric analyses were performed and calibrated according to the reported procedure (*10, 37*). They both obey Beer's Law. In a kinetic

run an aliquot was removed and quenched by dilution with methanol. Total iron concentration was first obtained by reducing the iron(III) by hydroxylamine hydrochloride. The iron(II)o-phenanthroline complex was then developed at pH 2.9, and the optical density at 5100 A. was measured. The same procedure without reduction gave iron(II) [correction was made for absorbance owing to iron(III)o-phenanthroline]. By thiocyanate colorimetry at 4780 A. and pH 1.5, the iron(III) concentration was determined. The sum of the iron(II) and iron(III) concentrations was in good agreement with the assay for total iron.

BENZOIN AND BENZIL. Beer's Law was obeyed by a methanolic solution of benzoin and benzil at wavelengths 2500 to 2900 A. The relationship $\epsilon = \epsilon_N \cdot M_N + \epsilon_L \cdot M_L$ was established for a series of solutions containing these two compounds in different proportions. The values of ϵ, ϵ_N, ϵ_L are respectively the extinction coefficients of the mixture, benzoin, and benzil; M_N and M_L are the mole fractions of benzoin and benzil. In the kinetic work the optical density measured was corrected for the contributions by iron(II and III) species which were determined independently. The optical density was measured at more than one wavelength (usually 2700, 2800, 2600 A.), and the results were reproducible and agreed within $\pm 2\%$ error. A Cary model 11 spectrophotometer was used for this analysis.

Detection and Determination of Aldehyde. The amount of formaldehyde in methanolic reaction mixture was estimated quantitatively according to the procedure by Kolthoff (16). A series of solutions containing varying amounts (5×10^{-5} to $5 \times 10^{-4} M$) of formaldehyde as well as the unknown sample, with pH adjusted to 3 by phosphate-citric acid buffer, was treated with $1.5 \times 10^{-3} M$ Schiff's reagent (31). Thirty minutes later, the optical density at 5500 A. was determined by a Coleman Junior spectrometer. The unknown concentration of formaldehyde was estimated by interpolating the known values. This procedure was reproducible for autoxidation of ferrous chloride in methanol. However, in the presence of a reactive cosubstrate, such as benzoin, the color became unstable, and the analysis was only semiquantitative. It was possible to determine acetaldehyde quantitatively in ethanolic reaction mixtures by vapor chromatography using a decylphthalate column at 66°–68°C.

Detection and Determination of Hydrogen Peroxide. Titanyl sulfate solution (30) was used for qualitative detection of hydrogen peroxide. Control measurements showed that the sensitivity limit was $1 \times 10^{-4} M$. Iodometry with starch indicator was also used to detect hydrogen peroxide. Kolthoff's (17) procedure was followed strictly with respect to the exclusion of air oxidation and correction for blank.

Results

Rates were followed by monitoring oxygen uptake at constant pressure. In the earlier stages of this work, solid iron(II) samples were contaminated by iron(III) owing to a slight preoxidation at the surface during degassing and thermal equilibration. Careful duplication of ex-

periments gave reproducible results and allowed semiquantitative observation of the effects of various additives. In the later experimental stages, by using a specially designed reaction vessel, preoxidation was eliminated. Data from these runs gave reasonably accurate values of the true initial oxidation rates. In the tables relative reactivities are cited when data are compared that are only accurate to the order of magnitude.

Solvent Effects. A major aim of our study was to learn about the effects of ligands (solvents and chloride ions) on the reactivity of iron(II) with molecular oxygen. Table I shows that the rate of oxidation of iron(II) is three to 1000 times as fast in these organic solvents as in water. This increase in rate, as well as the large difference between methanol and ethanol, can be inferred or seen from previous reports.

Ligand effects in water have been attributed to their effects on binding iron(III) (*8, 13, 14, 15, 33, 34, 35*). However, we shall show that the acceleration of iron(II) oxidation by chloride ion in methanol solution is caused mostly by its effect on iron(II) rather than on iron(III). As a corollary we suggest that solvent effects are also largely associated with ligand effects on the reactivity of iron(II).

Table I.   Oxidation of Iron(II) Chloride in Various
Solvents at 39.8 $\pm$ 0.2°C.

Solvent	$[Fe(II)]_o$, M	Relative[a] R_o	$\frac{\Delta Fe(II)}{\Delta O_2}$
Water	0.176	<0.02	4
Ethylene glycol	0.136	0.06	–
Methyl alcohol	0.145	1.0	3
Dimethyl sulfoxide	0.123	2.6	2
Ethyl alcohol	0.176	20.0	~4

[a] Ratios of initial rates.

Some oxidations of methanol and dimethyl sulfoxide were apparently induced by the oxidation of iron(II). The theoretical value for $\Delta Fe(II)/\Delta O_2$ is 4.0 if only iron is oxidized. Table I shows that up to twice as much oxygen was consumed in the indicated solvents. Since the sulfoxide was more easily attacked than methanol, their oxidations probably are not associated with a free radical mechanism, although the oxidations of alcohols gave aldehydes.

Our further studies began in ethanol as solvent, but these results, summarized first below, are only semiquantitative. Our best data were obtained in methanol where slower rates of oxidation were more conveniently studied.

Oxidation in Ethanol. The data best fitted a second-order rate law in iron(II) and first-order rate law in oxygen. This was consistent with

Pound's (28) report. The ratio of $\Delta Fe(II)/\Delta O_2$ was 3.9 to 4.0. Acetaldehyde was detected in the product by vapor chromatography although only one-sixth the amount expected on the basis of excess oxygen consumption was found. No acetic acid and hydrogen peroxide could be detected.

A preliminary survey was made of the effects of additives such as acetylacetone (HAA), dipivaloylmethane (HDPM), and piperidine ($C_5H_{11}N$). Table II shows that the neutral β-diketones have no effect on the rates, but marked acceleration accompanies the addition of both a diketone and base. Base alone also accelerates the rate; however, the quantitative significance of the effect is not obvious because the mixture became heterogeneous during the reaction.

Table II. Effects of Chelating Ligands on Oxidation of Iron(II) Chloride in Ethanol

$[FeCl_2]_o$, M	T, °C.	[Additives], M		Relative[a] R_o	$\dfrac{\Delta Fe(II)^b}{\Delta O_2}$
0.18[c]	39.6	None		1.00	4.0
0.18	39.6	HAA	0.20	1.04	3.2
0.18	39.6	HAA	0.39	0.96	3.1
0.18	39.6	HAA	0.97	0.96	2.6
0.20	39.6	HDPM	0.20	1.04	4.0
0.20	39.6	HDPM	0.20	1.04	3.7
0.13	29.6	HAA + $C_5H_{11}N$	0.23 0.27	1.87	2.3
0.12	29.6	HDPM + $C_5H_{11}N$	0.30 0.28	1.52	2.3
0.15	29.6	HDPM + $C_5H_{11}N$	0.30 0.28	4.48	2.3
0.11[d]	29.6	$C_5H_{11}N$	0.25	2.17	3.6

[a] Relative initial rate.
[b] $\Delta Fe(II)/\Delta O_2$ represents the stoichiometry at the time oxidation of iron(II) to iron(III) was essentially complete.
[c] Experimental accuracy ±10%.
[d] Heterogeneous throughout the reaction.

Except for HDPM, all the additives decrease the stoichiometric ratio. Oxidation in the presence of $C_5H_{11}N$ and HDPM leads to precipitation of bis(dipivaloylmethanato)iron(III) ethoxide (38), and a small amount of acetaldehyde (0.2–0.5γ) was also detected. Tests for peroxides were negative. Consequently, we believe that the chelating agents themselves (HAA, AA⁻, and DPM⁻) are oxidized by some transient involved in the reaction.

Oxidation in Acetylacetone. Since iron(II) chloride is not very soluble in the neutral diketone, heterogeneous mixtures were used. As the reaction proceeded the mixtures became homogeneous and developed

the deep red color characteristic of $Fe(AA)_3$. Initial oxidation rates were slower at 39.6°C. than were reactions in any except the most dilute solutions in ethanol. The stoichiometric ratio was 1.51–1.76; the rate is proportional to the partial pressure of oxygen. The low rates of reaction and low solubility indicate that solvolytic dissociation of iron(II) chloride (Reactions 1 and 2) is limited even in a solvent that can provide a powerful chelating anion.

$$FeCl_2 + HAA \rightleftarrows ClFe(AA) + H^+ + Cl^- \tag{1}$$

$$ClFe(AA) + HAA \rightleftarrows Fe(AA)_2 + H^+ + Cl^- \tag{2}$$
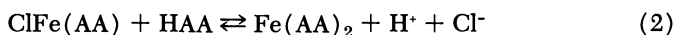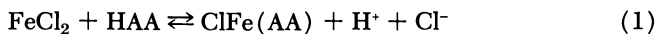
Consequently, we would also expect solvolysis to be limited in monohydric alcohols that are weaker acids and can provide only monodentate ligands.

The fact that values of $\Delta Fe(II)/\Delta O_2$ are persistently less than 2.1, averaging 1.7, indicates the stoichiometric factor of 2.0 is not a limit as might have been inferred from the measurements in ethanol containing HAA. Acetylacetone apparently behaves as a cosubstrate in much the same way as benzoin (*vide infra*) or hydrazobenzene (38) but with lower reactivity.

Oxidation of iron(II) chloride was immeasurably slow in HDPM at 40°C. and proceeded at a slow but detectable rate at 70°C. In one experiment carried to completion at the higher temperature, the measured value of $\Delta Fe(II)/\Delta O_2$ was 2.91. The system has not been studied further.

Oxidation in Methanol. STOICHIOMETRY. For nearly all the kinetic runs $\Delta Fe(II)$ was analyzed (10, 37) only at the end of the reaction. Therefore, the stoichiometric factor $\Delta Fe(II)/\Delta O_2$ (SF) actually is an average value over the reaction period. It was always found to be in the range of 3.0 ± 0.2 despite the addition of accelerator (LiCl, etc.) or inhibitor ($FeCl_3$, etc.) and regardless of the degree of completion of the reaction (20 to 80%). This implies that the SF does not vary much under the conditions of this investigation. To assure that the rate based on ΔO_2 is significant, attempts hade been made to determine $\Delta Fe(II)$ and ΔO_2 simultaneously. Two runs were made; one began with methanolic iron(II) chloride (0.145M), and the other began with a mixture of methanolic iron(II) chloride (0.145M) and iron(III) chloride (0.07M). Both were carried to 45% conversion. There was small decrease in the SF during the first 10% of reaction, but later the factor remained constant (3.0 ± 0.2). Since initial addition of a substantial amount of iron(III) chloride does not change the stoichiometry appreciably, the initial, apparent decrease in SF is attributed to inherent inaccuracy of volumetric data at the beginning of the run. Induced oxidation by iron(III) species must be relatively unimportant in this study; otherwise the SF would have changed throughout the course of a run.

In the analysis of our data to test rate laws and to calculate pseudo-rate constants, the value of $(\Delta O_2)_\infty$ is needed. We used the experimental value of the SF since it does not vary significantly from run to run.

KINETIC ORDER. The rate is first order with respect to oxygen, as was demonstrated by runs in which air replaced oxygen as the atmosphere in contact with the reaction mixture. The reaction order, n, with respect to iron(II) was first estimated by comparison of initial rates and by application of the fractional-lifetime method (11). A value of $n = 1.98$ was calculated from the initial rates of a number of runs made under comparable initial conditions; values of n estimated in several runs using $t_{1/3}$ and $t_{1/2}$ in the fractional-lifetime method ranged from 1.7 to 2.2. None of the estimates is really precise. If the data for runs followed to high conversion are plotted according to the integral form of the second-order law, the rates fall off at high conversion. The result might indicate that the dependence on iron(II) is more than second order or that the reaction is autoinhibitory. For reasons that will become clear, we prefer the latter explanation.

EFFECTS OF MISCELLANEOUS ADDITIVES. The rates are not significantly changed by adding 0.1 to 0.2M perchloric and p-toluenesulfonic acid although there is marked acceleration in the presence of 2M acetic acid. The rates are not affected by adding a small amount of water. A small, but significant, acceleration (1.5 times) in the presence of 0.3M phosphoric acid is reminiscent of the influence of phosphate in aqueous solution and is probably a ligand effect similar to that of chloride (*vide infra*). We interpret the absence of major effects of acids as indicating that in neutral media solvolysis according to Equation 3 is negligible.

$$FeCl_2 + CH_3OH \rightleftharpoons FeCl(OCH_3) + Cl^- + H^+ \tag{3}$$
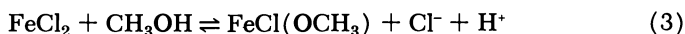
Tertiary amines greatly accelerate the reactions. The effect is complex since the amines will bind iron as ligands and also decrease proton activity in the medium. That the latter effect must be of major significance is demonstrated by comparing the effects of pyridine and 2,6-lutidine. The latter exerts a more powerful catalysis effect despite the fact that steric hindrance weakens its ligand effect. Consequently, we infer that solvolysis to produce species such as $FeCl(OCH_3)$ and $Fe(OCH_3)_2$ is extensive in the presence of bases and that the alkoxides must be more reactive than $FeCl_2$ as substrates. The rate in the presence of 0.4M piperidine was immeasurably fast. The powerful acceleration is attributed to the high basicity of piperidine ($pK_b = 2.80$ in 50% ethanol) compared with pyridine ($pK_b = 9.62$) and 2,6-lutidine ($pK_b = 8.23$).

EFFECTS OF IRON(III) AND LITHIUM CHLORIDE. Among mechanisms considered during our work were several in which intermediate oxidants are equilibrated with iron(III). We considered that the decrease in rates

during the latter part of the reactions might be caused by accumulation of trivalent iron. Consequently, runs were carried out in which ferric chloride or samples drawn from oxidation mixtures were added initially. Both forms of iron(III) inhibit oxidation, so the oxidation of iron(II) under the conditions of most of our experiments is autoinhibitory. However, the effect seems to be associated with the behavior of iron(III) as a Lewis acid, not to reversibility of some oxidation step. Other Lewis acids, mercuric chloride and zinc chloride, are also powerful inhibitors. On the other hand, lithium chloride and calcium chloride are catalysts. We infer that the reactivity of iron(II) is sensitive to the amount of chloride ion bound to the metal ion and that the autoinhibitory effect is caused by binding of chloride by the reaction product. Data are summarized in Table III, and plots of typical runs are shown in Figure 1.

Table III.   Effects of Chlorides on Oxidation of $FeCl_2$ in Methanol at 29.5°C. and 1 Atm. O_2

$[FeCl_2]_o$, M	$[Additives]$, M	$R_o{}^a \times 10^4$
0.143	none	3.5
0.145	0.420 LiCl	11.2
0.148	0.216 $CaCl_2$	11.2
0.144	0.217 $HgCl_2$	0.19
0.147	0.264 $ZnCl_2$	0.32
0.146	0.147 $FeCl_3$	0.57
0.144	0.840 LiCl	27.5
0.144	0.840 LiCl	25.5
	0.035 $FeCl_3$	
0.145	0.940 LiCl	28.3
	0.070 $FeCl_3$	
0.144	0.840 LiCl	27.1
	0.034 $FeCl_2(OCH_3)^b$	

^{a} R_o is the initial rate of absorption of oxygen in mole/min./liter of the reaction mixture.
^{b} $FeCl_2(OCH_3)$ provided by oxidation of $FeCl_2$ in CH_3OH.

Figure 2 shows the disappearance of autoinhibition in the presence of lithium chloride. Figure 3 shows the fit to second-order kinetics with excess chloride and also shows data for a comparable run without added lithium chloride. Evidently the reaction is second order with respect to iron(II) but slows down as iron(III) is produced unless a ligand is added to bind the latter. The effect of varying the amount of the excess lithium chloride is shown in Figure 4, and the data are summarized in Table IV. The rate is not a linear function of the concentration of lithium chloride; at higher concentrations the rate appears to increase with a greater than first-order dependence on chloride. However, the

concentrations of electrolyte are so high that no rigorous interpretation of the results can be offered.

Brealey and Uri (4) have shown spectrophotometrically that ferric chloride is only slightly dissociated in ethanol solution and that it is readily converted to $FeCl_4^-$ by adding excess lithium chloride. We find that quantitative conversion of $FeCl_3$ to $FeCl_4^-$ is effected in solutions containing 0.148M iron(II) chloride and 0.013M iron(III) chloride.
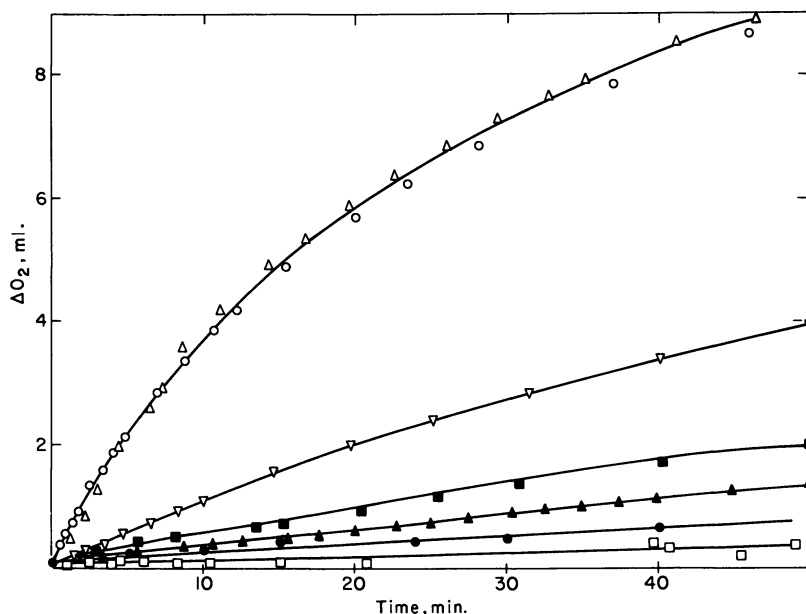
Figure 1.   Effect of metallic chlorides on the oxidation rate of ferrous chloride in methanol at 29.5°C. and 1 atm. O_2

$\triangle$, $[FeCl_2]_0 = 0.145M$, $[LiCl] = 0.420M$
$\bigcirc$, $[FeCl_2]_0 = 0.148M$, $[CaCl_2]_0 = 0.216M$
$\triangledown$, $[FeCl_2]_0 = 0.145M$
$\blacksquare$, $[FeCl_2]_0 = 0.134M$, $[FeCl_2(OCH_3)]_0 = 0.155M$
$\blacktriangle$, $[FeCl_2]_0 = 0.146M$, $[FeCl_3]_0 = 0.147M$
$\bullet$, $[FeCl_2]_0 = 0.147M$, $[ZnCl_2] = 0.264M$
$\square$, $[FeCl_2]_0 = 0.144M$, $[HgCl_2] = 0.217M$

Figure 5 shows that the absorption spectrum of the tetrachloroferrate ion, with a characteristic maximum at 3150 A., is completely developed in such a solution. The dotted line is the spectrum of an oxidation mixture. The spectrum resembles that of a solution of $FeCl_4^-$, but the characteristic maximum at 3600 A. appears to be shifted to 3580 A., and the extinction coefficient at the latter wavelength is lower than that at 3150 A. The result suggests that the principal iron(III) species in the oxidation mixtures is $Cl_3Fe(OCH_3)^-$. Figure 6 shows the effect of metallic chlorides on the spectrum of methanolic solutions of ferric chloride.
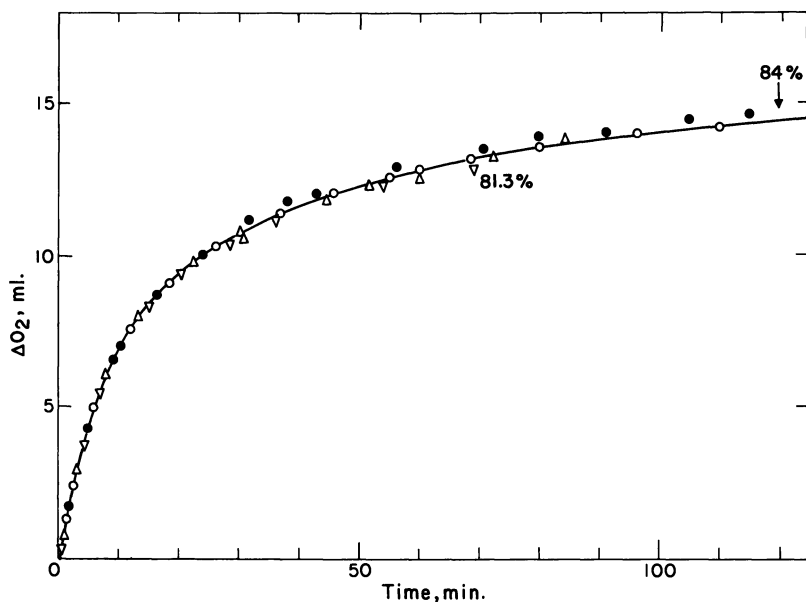
Figure 2.   Elimination of inhibitory effect of ferric chloride on oxidation of ferrous chloride by adding lithium chloride

O, $[FeCl_2]_0 = 0.144M$, $[LiCl] = 0.84M$, $[FeIII]_0 = 0$
△, $[FeCl_2]_0 = 0.144M$, $[LiCl] = 0.84M$, $[FeCl_2OCH_3]_0 = 0.034M$
●, $[FeCl_2]_0 = 0.145M$, $[LiCl] = 0.84M$, $[FeCl_3]_0 = 0.035M$
▽, $[FeCl_2]_0 = 0.144M$, $[LiCl] = 0.94M$, $[FeCl_3]_0 = 0.070M$

INDUCED OXIDATION OF BENZOIN. If benzoin is included in an oxidation mixture, it is oxidized cleanly to benzil.

$$2 \ C_6H_5CHOHCOC_6H_5 + O_2 \xrightarrow[\text{methanol}]{\text{FeCl}_2} C_6H_5COCOC_6H_5$$
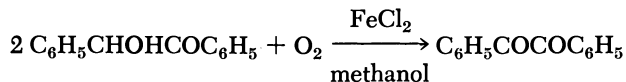
Figure 7 shows the representative runs, and Table V summarizes data for a number of runs. The reaction is zero order with respect to benzoin, and the specific rates of oxygen uptake are within experimental error the same as the initial rates in solutions containing the same amounts of iron(II) chloride without benzoin. Comparison among runs gives a good indication of the dependence of the initial rate on the concentration of iron(II) since all of the runs were carried out by our best procedure. Although the initial slopes may still be somewhat in error, the accuracy is good enough to indicate that the rates decrease with concentration more rapidly than is predicted by the second-order law. We are fairly well convinced by the kinetics obtained in the presence of excess chloride that the reaction is second order with respect to iron(II), so we need to account for the decrease in rate by some other explanation. A likely
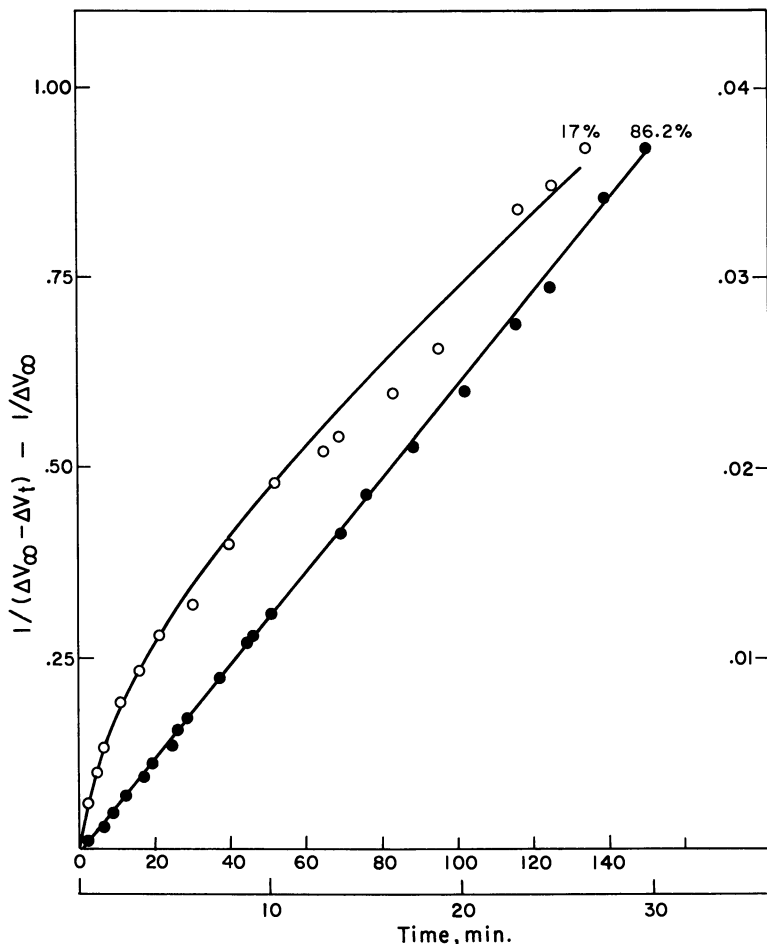
Figure 3.   Second-order plot of oxidation rate of ferrous chloride in methanol at 30°C. and 1 atm. O₂

●, *Left ordinate and lower abscissa* $[FeCl_2]_0 = 0.052M$, $[LiCl]_0 = 1.74M$
○, *Right ordinate and upper abscissa* $[FeCl_2]_0 = 0.051M$

candidate is ionic dissociation of $FeCl_2$ in the more dilute solutions, and the assumption that $FeCl^+$ is less reactive as a substrate than $FeCl_2$.

$$FeCl_2 \overset{K}{\rightleftharpoons} FeCl^+ + Cl^-.$$

If all of the rate is attributed to $FeCl_2$, the data at various concentrations can be fitted reasonably well with a value of $K = 5 \times 10^{-2}$. The study of the conductance of $FeCl_2$ in methanol by de Maine and McAlone (9) indicates that the compound behaves as a weak electrolyte. Although the data are not suitable for rigorous analysis, a value of the dissociation

constant of the order of 10^{-2} is compatible with the data which indicate the iron(II) chloride is partially dissociated in solutions in the concentration range 0.01–0.10M. This conclusion can also be reached by comparing the behavior of a strong electrolyte, such as LiCl, a medium strong electrolyte $CaCl_2$, and a weak electrolyte $ZnCl_2$.

Similar kinetic results are obtained in the presence of other cosubstrates (38), but the experiments with benzoin are especially significant because benzoin is not oxidized by iron(III). Consequently, the failure of substantial amounts of iron(III) to appear along with benzil in the reaction mixtures implies that iron(III) cannot be formed before a rate-determining step.

Discussion

Status of the Composition of the Iron(II) Chloride Species in Methanol. Since ferrous chloride behaves as a weak electrolyte in methanol and in our investigation solutions of relatively high concentra-
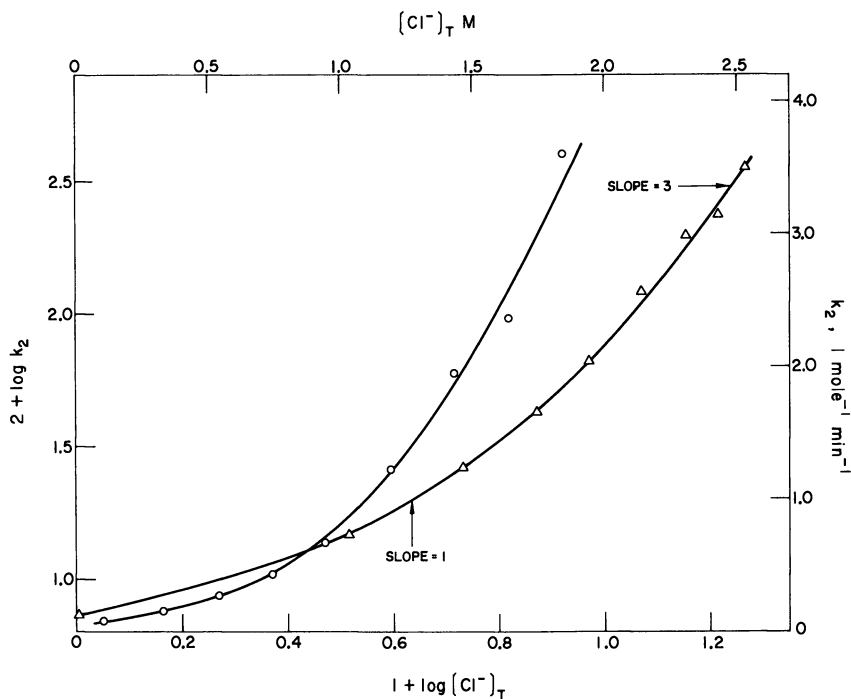
Figure 4. Effect of lithium chloride on the oxidation rate of ferrous chloride in methanol at 30°C. and 1 atm. O_2

$[FeCl_2]_0 = 0.05M$
△, *Left ordinate and lower abscissa* log k_2 vs. log $[Cl^-]_T$
○, *Right ordinate and upper abscissa* k_2 vs. $[Cl^-]_T$

Table IV. Effect of Lithium Chloride on Initial Rate of Oxidation of Ferrous Chloride in Methanol at 30°C. and 1 Atm. O_2

$[FeCl_2]_o$, M	$[LiCl]$,[a] M	$[Cl^-]_T$,[b] M	R_o[c] $\times 10^4$	k_2,[d] liter/mole/ min.	$\dfrac{\Delta[Fe(II)]}{[Fe(II)]_o}$[e]	$\dfrac{\Delta Fe(II)}{\Delta O_2}$[f]
0.0505	0.000	0.101	0.45	0.072[g]	0.170	3.52
0.0503	0.223	0.329	1.59	0.150[g]	0.388	2.84
0.0505	0.440	0.540	2.43	0.263	0.424	3.12
0.0498	0.645	0.744	4.39	0.431	0.620	2.99
0.0506	0.840	0.941	5.48	0.667	0.663	3.28
0.0506	1.09	1.19	8.97	1.220	0.700	3.11
0.0514	1.33	1.43	11.90	1.945	0.852	3.16
0.0501	1.54	1.64	17.40	2.360	0.882	3.21
0.0518	1.74	1.84	25.50	3.620	0.862	3.20

[a] LiCl · 0.345 H_2O was used.
[b] $[Cl^-]_T$ is $2[FeCl_2]$ + $[LiCl]$.
[c] R_o is the initial rate of oxygen uptake in mole/min./liter of reaction mixture.
[d] Second-order rate constant from $1/(\Delta O_2)_\infty - (\Delta O_2)_t$ vs. time.
[e] % Conversion when reaction terminated.
[f] Stoichiometric factor.
[g] Second-order plot is nonlinear owing to autoinhibition; k_2 is the intial slope of the plot.

tion of iron(II) chloride were used, more than one iron(II) species must have been present in solution. The distribution of these species can be formulated in terms of classical equilibrium constants, which may, unfortunately, depend upon the concentrations of the various solutes.

Equation 4 represents stepwise equilibrium between iron(II) chloride and chloride ion, without specifying the amount of methanol bound to each metal ion. Equation 5 shows that the concentration of any chloroiron(II) species can be represented as a function of the total iron(II) concentration, where A_i, the proportional constant, is a polynomial function of free chloride and equilibrium constants.

$$Cl_iFe(II) \overset{K_i}{\rightleftharpoons} Cl_{i-1}Fe(II) + Cl^- \quad i = 1,2,\ldots 6 \tag{4}$$
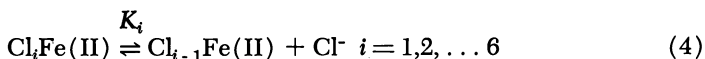
$$[Cl_iFe(II)] = A_i[Fe(II)]_T; A_i = \frac{[Cl^-]^i}{i \displaystyle\prod_{l=1} K_l}\left\{1 + \sum_{n=1}^{6} \frac{[Cl^-]^n}{n \displaystyle\prod_{l=1} K_l}\right\}^{-1} \tag{5}$$

It is evident that the relative amounts of the iron(II) species will vary when $[Cl^-]$ varies. When a kinetic run is carried out under ideal conditions such that the variation of $[Cl^-]$ is negligibly small during the reaction, the experimentally obtained kinetic dependence on total iron(II), $[Fe(II)]_T$, truly represents the kinetic contribution from all existing iron(II) species.

In the runs with excess chloride the data fit the second-order rate law as illustrated in Figure 3. As the data in Table IV show, the rate
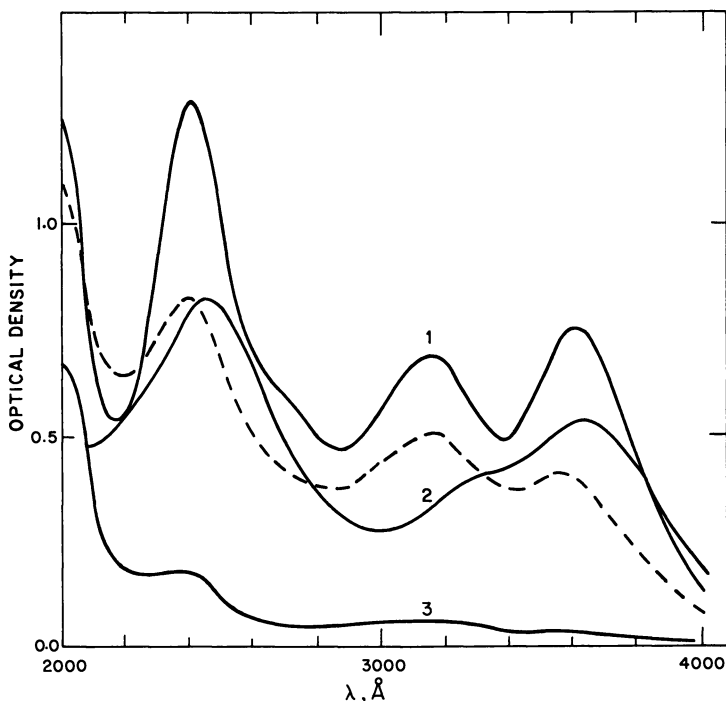
Figure 5.   Ultraviolet spectra of iron chlorides in methanol in 0.1-mm cells

(1): $FeCl_2$ 0.148M + $FeCl_3$ 0.0131M
(2): $FeCl_3$ 0.0131M
(3): $FeCl_2$ 0.148M
broken line, $FeCl_2$ 0.143M + Cl_2FeOCH_3 0.015M

constants increase as the concentration of chloride increases. Under these conditions, the generalized rate equation is as follows:

$$\frac{-d[Fe(II)]_T}{dt} = \sum_{ij=0}^{6} k_{ij}[Cl_iFe(II)][Cl_jFe(II)][O_2] \qquad (6)$$

$$= \left(\sum_{ij=0}^{6} k_{ij}A_iA_j \right) [Fe(II)]_T^2[O_2]$$

$$= k_2[Fe(II)]_T^2[O_2]$$

The second-order rate constant k_2 is, in reality, a pseudo-second-order constant of complexity. The shape of the plot of k_2 (Figure 4) *vs.* chloride is exponential as expected.

Equation 6 explains the irregularity of the rate law and the apparent inconsistency in rate constants when $FeCl_2$ is the only source of chloride.
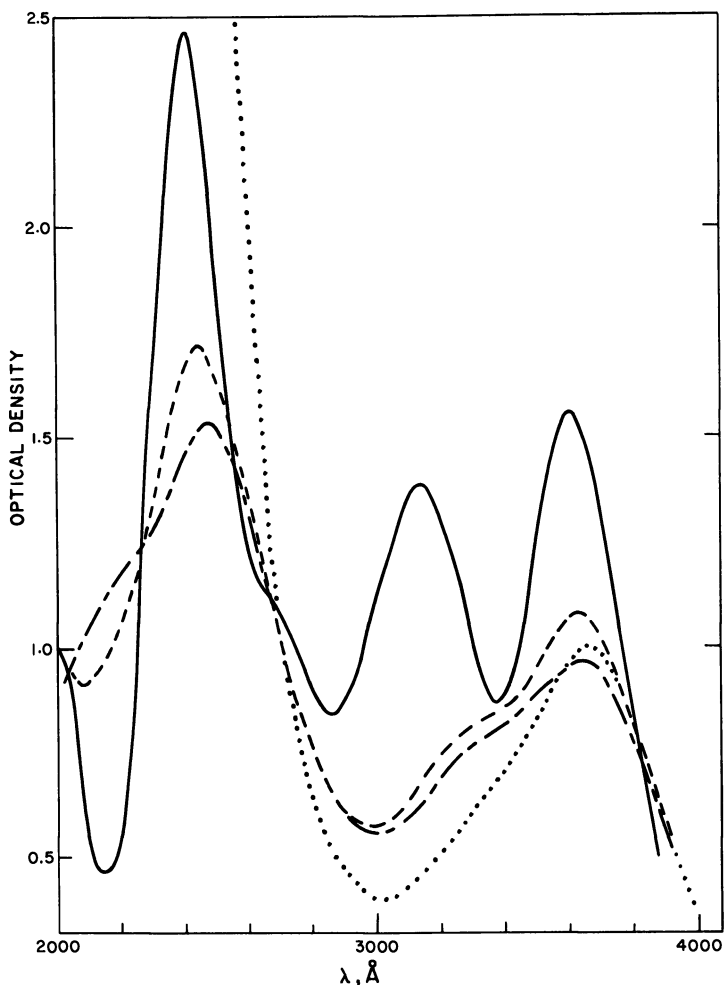
Figure 6.   Ultraviolet spectra of iron(III) chloride in methanol
with added metallic chlorides in 0.1-mm cells; FeCl$_3$, 0.0262M
in all cases

——————, CaCl$_2$ 0.204M, or LiCl 0.430M
– – – –, no additive
— – — –, ZnCl$_2$ 0.260M
· · · ·, HgCl$_2$ 0.247M

Since the equilibrium constants, K_i, and specific rate constants (k_{ii}, k_{jj}, and k_{ij}) are not available, we will discuss the mechanism simply on the assumption that the rate is second order in iron(II) and make only qualitative comments on the effects of bound chloride on reactivity.

    Mechanism. The first mechanism suggested for oxidation of iron(II) in aqueous solution (33) involved reversible electron transfer from

iron(II) to oxygen followed by rate-determining reaction of superoxide ion with ferrous ions.

$$Fe^{2+} + O_2 \rightleftharpoons Fe^{3+} + O_2^- \qquad (7)$$
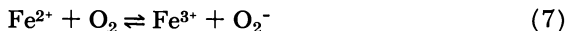
This mechanism, which has since been rejected (*34*) by Weiss who originally proposed it, is clearly not acceptable for the reaction in methanol since it predicts that inhibition by iron(III) should be observed under all conditions that do not reduce the kinetic order with respect to iron(II) to first order.

Weiss (*34*) and George (*14*) have suggested the following pair of closely related mechanisms.

Weiss: $$Fe^{2+} + O_2 \rightleftharpoons Fe^{2+}O_2 \qquad (8)$$

$$Fe^{2+}O_2 + Fe^{2+} \rightleftharpoons Fe^{2+}O_2Fe^{2+} \qquad (9)$$

$$Fe^{2+}O_2Fe^{2+} + H^+ \rightarrow 2Fe^{3+} + HO_2^- \qquad (10)$$

$$Fe^{2+}O_2 + X^- \rightarrow FeX^{2+} + O_2^- \qquad (11)$$
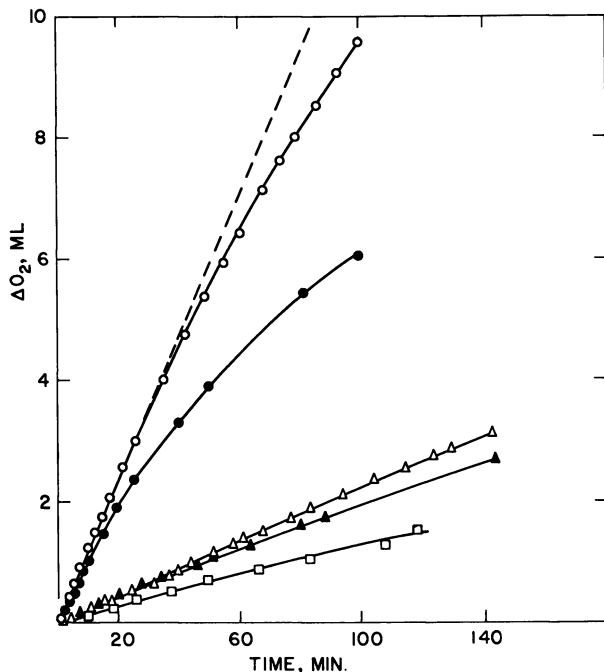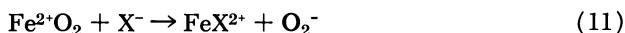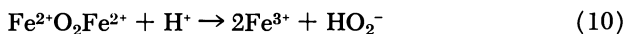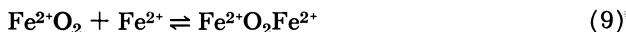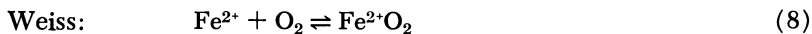
Figure 7.   Induced oxidation of benzoin by iron(II) chloride in methanol at 29.5°C.

$\bigcirc$, $[FeCl_2]_0 = 0.143M$, $[benzoin]_0 = 0.028M$
$\bullet$, $[FeCl_2]_0 = 0.145M$
$\triangle$, $[FeCl_2]_0 = 0.073M$, $[benzoin]_0 = 0.056M$
$\blacktriangle$, $[FeCl_2]_0 = 0.070M$, $[benzoin]_0 = 0.028M$
$\square$, $[FeCl_2]_0 = 0.070M$

George: $Fe^{2+}O_2 + H_2O + Fe^{2+} \rightarrow FeO_2H^{2+} + FeOH^{2+}$ (12)
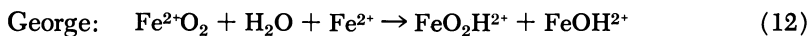
Reaction 11 was invoked by Weiss to account for the catalytic effects of ions such as fluoride or pyrophosphate. The particular form of the solvolytic reaction was chosen by George to accommodate his observations that the oxidation of ferrous perchlorate in water is second order with respect to iron(II) and only slightly dependent on the acidity of the system. The general mechanistic formulations were accepted by Davidson and co-workers (8, 13, 15), who observed both first- and second-order dependence on iron(II) under various conditions although it was pointed out (8) that iron(IV), rather than $HO_2 \cdot$, might be an intermediate in the reaction involving one ferrous ion. All mechanisms have presumed that hydrogen peroxide is an intermediate in the reaction and that it is rapidly reduced by the well-known reaction with iron(II). Catalytic effects of anions have inevitably been associated with stabilization of transition states in which iron(III) is being produced.

Experimentally it has usually been found that anion-catalyzed reactions are first order with respect to iron(II) (8, 13, 15, 33, 34, 35). The reaction in very concentrated hydrochloric acid solutions (27) should be included in this class. Uncatalyzed reactions have usually been reported to be second order in iron(II) (14, 19, 24), although King and Davidson (15) observed mixed-order kinetics at high temperatures. In no case has the influence of iron(III) been carefully investigated, although Pound (29) reported that addition of iron(III) had no influence on the oxidation rate of iron(II) sulfate.

This investigation has shown that in methanol solution the oxidation of iron(II) to iron(III) is clearly second order with respect to iron(II)

Table V.   Induced Oxidation of Benzoin in Methanol by Iron(II) Chloride at 29.5°C. and 1 Atm. Oxygen

$[FeCl_2]_o$, M	$[Benzoin]_o$, M	$R_o{}^a \times 10^4$	Reaction Time, min.	$\dfrac{[Fe(III)]^b}{[Fe(II)]_o}$	$\dfrac{[Benzil]^c}{[Benzoin]_o}$	$\dfrac{R_o \times 10^4}{[FeCl_2]_o{}^2}$	
0.220	none	13.4	54.0	0.352	—	277[d]	709[e]
0.219	0.057	11.4	53.3	0.163	1.00	238	607
0.155	none	5.17	90.0	0.346	—	215	666
0.155	0.057	5.33	57.4	0.044	0.65	222	685
0.070	0.028	0.63	144.0	0.050	0.50	128	638
0.073	0.055	0.66	144.0	0.033	0.28	125	627
0.143	0.028	3.4	100.0	0.135	1.00	165	548
0.204	0.058	1.8[f]	—	—	—	42	114

[a] The initial rate of oxygen uptake in mole/min./liter of reaction mixture.
[b] Iron(II) and iron(III) were determined (10, 37) at the end of the reaction period.
[c] Benzoin and benzil determined by ultraviolet spectrophotometry.
[d] Calculated from formal concentration.
[e] Calculated assuming the first dissociation constant for $FeCl_2$ to be 0.05.
[f] 1 atm. of air.

in the presence of excess chloride and probably is second order in all cases. The fact that inhibition by iron(III) disappears at high chloride concentration indicates that iron(III) is an important factor only to the extent that it regulates the activity of chloride ion in the reaction mixture. Our results are consistent with any mechanism in which two iron(II) species, an oxygen molecule, and some number of chloride ions in excess of the average number bound to iron(II) in the solution, are accumulated to form a transition state for the rate-determining step of the reaction. This would fit with assignment of the rate-determining step as a solvolysis similar to Reaction 12 suggested by George. However, the facts are in equally good agreement with a mechanism in which a binuclear oxygen complex undergoes any other unimolecular reaction as the rate-determining step. Reaction 13, which produces iron(IV), is an attractive candidate.

$$Cl_2FeOOFeCl_2 \rightarrow 2Cl_2FeO \qquad (13)$$

A choice between Reactions 12 and 13 can be made by considering the induced oxidation of benzoin. Oxidation of iron(II) to iron(III) and the induced oxidation apparently have the same rate-limiting step. Direct assay for iron(III) in runs with benzoin showed that very little is produced during the early stages though significant amounts start to appear as the runs progress and the concentration of benzoin falls to low levels. Consequently, we infer that the rate-determining step does not produce iron(III). Therefore, Reaction 12, or an analog involving methanolysis instead of hydrolysis, cannot be involved in the mechanism. We suggest that iron(IV) is produced by Reaction 13 and subsequently destroyed by Reactions 14 and 15 which are competitive.

$$Cl_2FeO + FeCl_2 \rightarrow 2FeIII \qquad (14)$$

$$Cl_2FeO + C_6H_5CHOHCOC_6H_5 \rightarrow FeCl_2 + C_6H_5COCOC_6H_5 + H_2O \qquad (15)$$
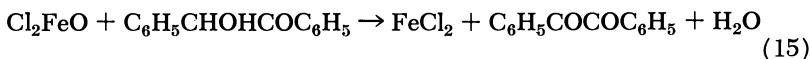
The rate increase caused by excess lithium chloride suggests that there are other mechanisms in which additional chloride ions are accumulated before the rate-determining step. The following equations would accommodate this hypothesis:

$$Cl_3\overline{Fe}OOFeCl_2 \rightarrow Cl_3\overline{Fe}O + Cl_2FeO \qquad (16)$$

$$Cl_3\overline{Fe}OO\overline{Fe}Cl_3 \rightarrow 2Cl_3\overline{Fe}O \qquad (17)$$
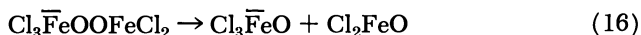
Iron(IV) was suggested many years ago by Bray (3), Taube (5), and their respective co-workers as an intermediate formed from iron(II) and iron(III) with hydrogen peroxide.

The ligand effects on rates are all very reasonable. Weiss (33, 34, 35) and Davidson (8, 13, 15) have previously reasoned that attachment of ligands, such as chloride or phosphate, which tend to stabilize iron(III)

should also stabilize transition states leading to that species. The same should hold true for reactions in which iron(IV) is produced. In this work we have observed catalysis by chloride, methoxide, and the anions of β-diketones. The former two are strong field ligands which have no low-lying vacant π-orbitals capable of stabilizing iron(II) by back bonding (26). The diketone ligands are unsaturated, and their absorption spectra show relatively low-lying π-π^* transitions ($\lambda_{max} \cong$ 3000 A.). Consequently, they might have been expected to decrease reactivity because of backbonding. However, the net effect is clearly that of providing driving force for the reactions which produce higher oxidation steps.

The ligand effects could, in principle, be dissected and allocated to the various equilibria involved as well as to the rate-determining reaction.

$$FeCl_2 + Cl^- \rightleftharpoons FeCl_3^- \qquad (18)$$

$$FeCl_2 + O_2 \rightleftharpoons Cl_2FeO_2 \qquad (19)$$

$$FeCl_3^- + O_2 \rightleftharpoons Cl_3\overline{Fe}O_2 \qquad (20)$$

$$Cl_2FeO_2 + FeCl_2 \rightleftharpoons Cl_2FeOOFeCl_2 \qquad (21)$$

$$Cl_3\overline{Fe}O_2 + FeCl_2 \rightleftharpoons Cl_3\overline{Fe}OOFeCl_2 \qquad (22)$$

$$Cl_3\overline{Fe}O_2 + FeCl_3^- \rightleftharpoons Cl_3\overline{Fe}OO\overline{Fe}Cl_3 \qquad (23)$$

Some cosubstrates (38)—i.e., ascorbic acid—appear to intercept an intermediate containing only one atom of iron. We believe that such substrates react with Cl_2FeO_2; hence, study of ligand effects on this second group of induced oxidation reactions should provide information concerning effects on the earlier steps in the reaction. We cannot make any firm decision as to whether or not O_2 should be regarded essentially as a π-ligand or as a σ-ligand. Both types of binding may be involved although it seems probable that the σ-configuration must be involved in Reaction 13, our postulated rate-determining step.

The relationship between the reaction in nonaqueous solvents and that in water is obscure. Since the kinetics are different, it is likely that the mechanism is also different. In methanol the chloride-catalyzed reaction is second order with respect to iron(II) whereas ligand-catalyzed reactions show only first-order dependence on ferrous ion in aqueous solution. In water, rate-limiting solvolysis of species such as XFe^+O_2, to produce $HO_2\cdot$, may occur simply because formation of the binuclear compound, required for the rate-limiting step in methanol, is inhibited by strong solvation of iron(II) in aqueous solution.

Finally, the induced oxidation of alcoholic solvents can be formulated readily within the framework of the suggested mechanism. The

$$\text{Cl}_2\text{Fe} \overset{\displaystyle \text{OH}}{\underset{\displaystyle \text{O}-\text{CH}_2-\text{H} : \text{B}}{\Big\backslash}} \longrightarrow \text{Cl}_2\text{FeOH}^- + \text{CH}_2{=}\text{O} + \text{BH}^+$$
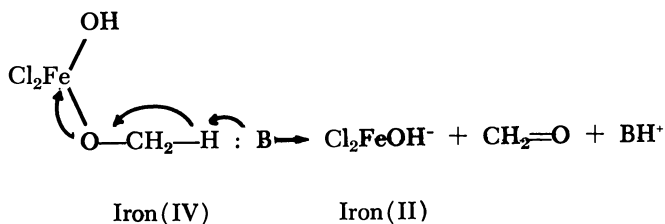
Iron(IV)　　　　　　Iron(II)

iron(IV) species seems ideally constituted to undergo oxidative elimination with regeneration of iron(II). In other words, the alcohols simply function as two-electron reductants of low reactivity. The above scheme is one of several tenable hypotheses for the detailed mechanism.

Acknowledgment

Literature Cited

(1) Bolland, J. L., *Proc. Roy. Soc. (London)* **A186**, 218 (1946).
(2) Boozer, C. E., Hammond, G. S., Hamilton, C. E., Sen, J. N., *J. Am. Chem. Soc.* **77**, 3237 (1955).
(3) Bray, W. C., Gorin, M. H., *J. Am. Chem. Soc.* **54**, 2124 (1932).
(4) Brealey, G. J., Uri, N., *J. Chem. Phys.* **20**, 257 (1952).
(5) Cahill, A. E., Taube, H., *J. Am. Chem. Soc.* **74**, 2312 (1952).
(6) Charles, R. C., Barnartt, S., *J. Phys. Chem.* **62**, 315 (1958).
(7) Charles, R. C., Barnartt, S., *J. Am. Chem. Soc.* **73**, 4416 (1951).
(8) Cher, M., Davidson, N., *J. Am. Chem. Soc.* **77**, 793 (1955).
(9) de Maine, P. A. D., McAlonie, G. E., *J. Inorg. Nucl. Chem.* **18**, 286 (1961).
(10) Fortune, W. B., Mellon, M. G., *Ind. Eng. Chem., Anal. Ed.* **10**, 60 (1938).
(11) Frost, A. A., Pearson, R. C., "Kinetics and Mechanism," p. 41, 2nd ed., Wiley, New York, 1961.
(12) Hartley, H., Raikes, H. R., *J. Chem. Soc.* **127**, 524 (1925).
(13) Huffman, R. E., Davidson, N., *J. Am. Chem. Soc.* **78**, 4836 (1956).
(14) George, P., *J. Chem. Soc.* **1954**, 4349.
(15) King, J., Davidson, N., *J. Am. Chem. Soc.* **80**, 1542 (1958).
(16) Kolthoff, I. M., Medalia, A. I., *J. Am. Chem. Soc.* **71**, 3783 (1949).
(17) Kolthoff, I. M., Sandell, E. B., "Textbooks of Quantitative Analysis," pp. 608-632, Macmillan Co., New York, 1948.
(18) Kopecky, K. R., Nonhebel, D., Morris, G., Hammond, G. S., *J. Org. Chem.* **27**, 1036 (1962).
(19) Lamb, A. B., Elder, L. W., *J. Am. Chem. Soc.* **53**, 137 (1931).
(20) Macejevskis, B., Vlasova, A., Liepina, L., *Latvijas PSR Zinatnu Akad. vestis* **12**, 85 (1960).
(21) *Ibid.* **2**, 123 (1961).
(22) Macejevskis, B., Liepina, L., *Latvijas PSR Zinatnu Akad. vestis* **9**, 109 (1960).
(23) *Ibid.* **10**, 91 (1960).

(24) McBain, J. W., *J. Phys. Chem.* **5**, 623 (1901).
(25) Moeller, T., *Inorg. Syntheses* **5**, 179 (1957).
(26) Orgel, L. E., "An Introduction to Transition-Metal Chemistry," p. 152, Wiley, New York, 1960.
(27) Posner, A. M., *Trans. Faraday Soc.* **49**, 382 (1953).
(28) Pound, J. R., *J. Phys. Chem.* **43**, 971 (1939).
(29) *Ibid.* **42**, 955 (1938).
(30) Satterfield, C. N., Bonnell, A. H., *Anal. Chem.* **27**, 1174 (1955).
(31) Tobie, W. C., *Ind. Eng. Chem., Anal. Ed.* **14**, 405 (1942).
(32) Vogel, A. I., "Practical Organic Chemistry," p. 198, Longman Green and Co., London, 1956.
(33) Weiss, J., *J. chim. Phys.* **48**, 6 (1951).
(34) Weiss, J., *Experientia* **9**, 61 (1953).
(35) Weiss, J., *Proc. Roy. Soc. (London)* **A222**, 124 (1954).
(36) Weissberger, G., "Techniques of Organic Chemistry," Vol. V, p. 362, Interscience, New York, 1955.
(37) Wood, J. T., Mellon, M. G., *Ind. Eng. Chem., Anal. Ed.* **13**, 551 (1941).
(38) Wu, C.-H. S., unpublished observations.

Discussion

Adolfo Aquilo: Have you investigated the autoxidation of ferrous fluoride and ferrous pyrophosphate?

Chin-Hua S. Wu: Fluoride and pyrophosphate are known to be good complexing agents for iron(III) species. They are good candidates for studying ligand effects. Owing to their limited solubility in methanol we have not used them in our work.

N. Uri: According to my understanding, the acceleration by chloride is not primarily caused by the suppression of a back reaction by formation of $FeCl_4^-$, and there is an important ligand effect on the reactivity of iron(II). A species like $FeCl_4^{2-}$ can be present in the solution. Have the authors considered this?

Dr. Wu: Yes, we have indeed. The matter is treated in the first part of the discussion section of the paper, "Status of the composition of the iron(II) chloride species in methanol." Participation by such a species is compatible with our data, but can not be proved rigorously for a number of reasons.

Dr. Uri: Does water affect the rate?

Dr. Wu: Water is expected to slow down the rate. However, a small quantity of water (0.1 to $1M$ in methanol) has no measurable effect.

Dr. Uri: Do you intend to detect experimentally the existence of the transient $[Cl_2FeO]$?

Dr. Wu: We will be happy to detect the transient if we can. However, we are far from certain as to the most appropriate tools to use. The species may be paramagnetic but might be hard to find by spin resonance spectroscopy because of the presence of other paramagnetic species in solution. At present we have no basis for guessing its lifetime or concentration level.

Cheves Walling: I wonder if you considered the "Fenton" scheme for your reaction mechanism. This scheme, in its simplest version would predict that benzoin would not affect the rate of oxygen uptake but would reduce the $Fe:O_2$ stoichiometry from 4 to 2.

$$2Fe(II) + O_2 \rightarrow 2Fe(III) + H_2O_2$$

$$H_2O_2 + Fe(II) \rightarrow Fe(III) + \cdot OH$$

$$\cdot OH + Fe(II) \rightarrow Fe(III)$$

$$\cdot OH + \phi CHOHCO\phi \rightarrow \phi \overset{.}{C}OHCO\phi$$

$$Fe(III) + \phi COHCO\phi \rightarrow \phi COCO\phi + Fe(II)$$
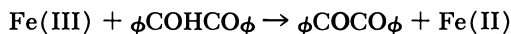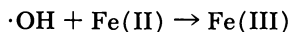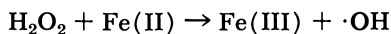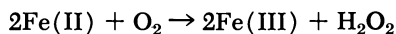
A quick look suggests that some, not all, of your data may agree with this.

Dr. Wu: The Fenton-type mechanism has been seriously considered, but it was abandoned because iron(III) production becomes very small in the presence of the higher concentrations of benzoin. The above scheme will require stoichiometric relationship,

$$Fe(III) : benzil \geqslant 2:1.$$

The fact that $\dfrac{dFe(III)}{d\,benzil}$ is proportional to $\dfrac{[Fe(II)]}{[benzoin]}$ is consistent with our proposed mechanism. We have not found a modification of the Fenton mechanism that accommodates the data.

76

Spectral Characteristics and Autoxidation of Hematin *a*-Globin and Polyhistidine

F. C. YONG and TSOO E. KING

Oregon State University, Corvallis, Ore. 97331

The complex formed from hematin a and native globin (from crystalline hemoglobin) possesses an approximate ratio of 4 to 1 and shows low spin characteristics in both oxidized and reduced forms. The reduced complex, when oxidized by either oxygen or ferricyanide, is converted to a yellow compound whose spectra differ from those of the initial compound. The conversion is reversed by dithionite but not by prolonged deaeration. We concluded that the hematin a–globin complex is autoxidizable but possesses no oxygenative property and is not reduced by ferrocytochrome c. The hematin a–polyhistidine complex also shows low spin characteristics. Its reduced form is even more autoxidizable than hematin a–globin. The implications of these observations are discussed, with heme protein interactions and the structural specificities required for oxygenation and autoxidation.

The oxygenative activity of hemoglobin and myoglobin is dramatically different from the autoxidative reaction of cytochrome oxidase. [The term "oxygenation" as used in this paper is defined as the reaction between oxygen and hemoprotein to form a stable, long-lived oxygen-hemoprotein complex without change of the valence of iron, such as oxyhemoglobin, which can be isolated and purified. Consequently, for example, the binding of oxygen and cytochrome a_3 as postulated for the oxidation of cytochrome oxidase (*21*) or the reaction of oxygen and cytochrome oxidase to form the "oxygenated complex," which is not stable (*23, 25*), is not considered as oxygenation.] Such a unique disparity has been a subject of discussion in a number of symposia and reviews (*1, 6, 8, 10, 16, 19, 27*). The easy accessibility of a large quantity of purified hemoglobin and myoglobin has enabled workers to undertake extensive

investigation of their structures and physicochemical properties. In addition, these proteins have been resolved into heme and protein components which have been in turn successfully recombined or reconstituted (*3, 15*). From these studies has accumulated a wealth of information about the correlation between the structure and function.

Recombination studies have given useful insight to the interactions between the heme and protein. Globin from hemoglobin, for example, is able to recombine not only with protoheme to form hemoglobin but also with other hemes to form so-called synthetic hemoglobins in a well-defined stoichiometry (*2*). These results have been correlated with the linear free energy change and the stability constants (*7*) and also in terms of the interaction between the metal-ligand σ-bonding and the π-electron systems (*11*). Consequently, valuable explanations have been advanced for the mechanisms of oxygenation.

From x-ray analysis, it is certain that histidine residue coordinates with iron in both myoglobin and hemoglobin. Likewise, histidine has been proposed as a ligand for several heme enzymes.

However, still left to be answered is the basic question: why are hemoglobin and myoglobin active in oxygenation while cytochrome oxidase results in autoxidation. Obviously, this query cannot be solved until the knowledge of cytochrome oxidase approximates that of hemoglobin. Unfortunately, not only is the protein structure of cytochrome oxidase completely unknown, but its resolution into active components has always eluded success. Moreover, the elucidation of the structure is not in sight, but the heme moiety of cytochrome oxidase, known as hematin *a*, has been isolated into presumably unmodified form. Thus, every conceivable means must be used, for example, to probe its interactions with known proteins and in turn to examine the behavior of the artificial complexes so formed. Among these complexes, the hybrid molecule formed from hematin *a* and the globin (of hemoglobin) possesses special interest.

With these considerations in mind, we have studied the spectral characteristics, oxygenation, and autoxidation of the hematin *a*-globin and the hematin *a*-polyhistidine complexes. This report communicates some results along these lines.

Experimental

Hematin *a* was prepared from purified cytochrome oxidase as described (*29*). The hematin solution was made by dissolving the dried samples in phosphate buffer containing 1% Emasol 1130. Its concentration was determined by the pyridine hemochromogen method in a mixture of 20% pyridine and 0.05N NaOH; an extinction coefficient of 27.4 mM^{-1} cm.$^{-1}$ at 589 mμ was used (*29*).

Globin was prepared from crystalline bovine oxyhemoglobin by the method originally developed for *Palemyssarda* by Rossi Fanelli, Antonini, and Caputo (28) with our adaptation (20). The globin content was determined spectrophotometrically at 280 mμ with $A^{1\%} = 8.5$. A sample of polyhistidine was obtained from the Biophysics Department, Weizmann Institute of Science. All other chemicals were purchased from commercial sources.

To demonstrate reversible oxygenation and autoxidation, a scheme as shown in Figure 1 was designed. The solution was placed in a Thunberg cuvette. Whenever deaeration was employed, the cuvette was evacuated and subsequently flushed with helium; the cycle was repeated three times and ended in a helium atmosphere. Ferricyanide or dithionite, always in a very slight excess, was added under helium atmosphere without contamination of air.

Spectrophotometric measurements were conducted at room temperature (22° to 25°C.) in a Cary recording spectrophotometer, model 11, or a Zeiss manual spectrophotometer, PMQ III. Activities of cytochrome oxidase and tetrahydroquinone oxidase were measured with a GME Oxygraph at room temperature according to the method reported previously (5).

Results

Interactions of Hematin *a* and Globin. The "nativeness" of the globin preparations was ascertained by the reconstitution technique with proto-
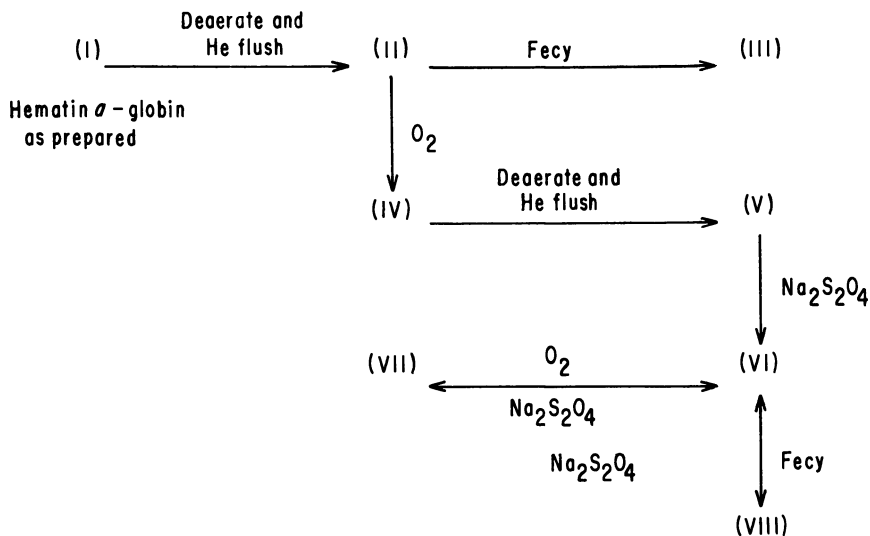
Figure 1.   Design of reaction scheme to demonstrate reversible oxygenation of hematin a–globin complex

System contained 927 μgrams of globin and 42 mμmoles of hematin a in 2.5 ml. of 0.02M phosphate buffer, pH 7.0 and 0.1% Emasol 1130. He, helium; Fecy, ferricyanide; Na$_2$S$_2$O$_4$, sodium dithionite; O$_2$, oxygen.
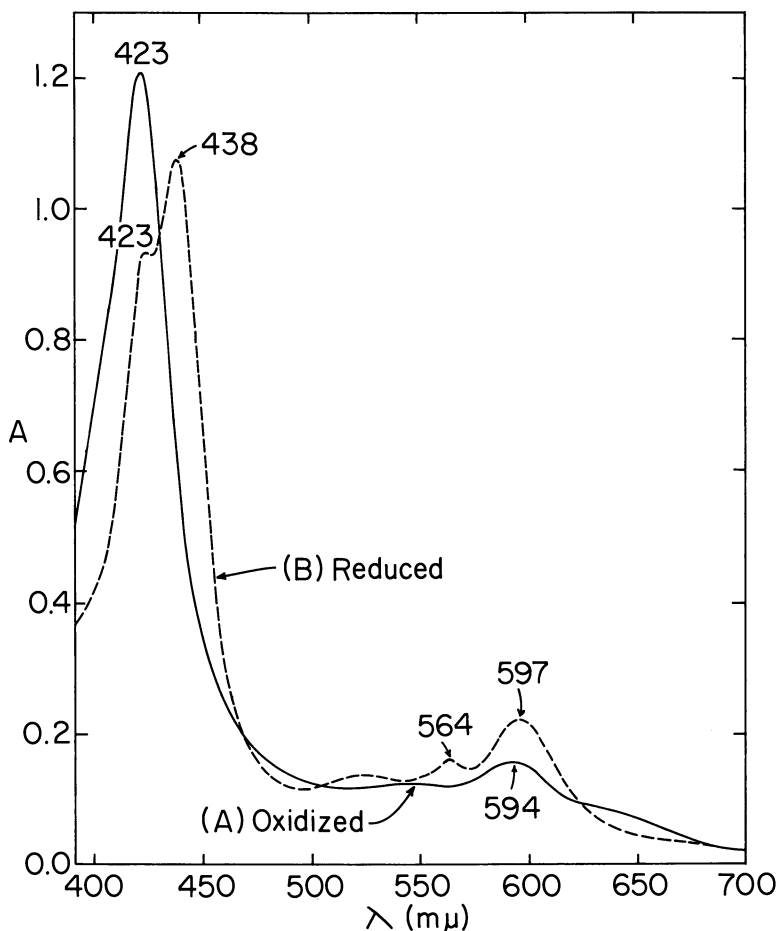
Figure 2. Absorption spectra of hematin a–globin complex in neutral medium

A, oxidized; B, dithionite reduced. System contained 14.8μM hematin a and 6.6μM globin in 0.02M phosphate buffer, pH 7.0.

hematin to give hemoglobin (actually the primary product is methemoglobin) by the criteria of spectral behavior and spectrophotometric titration (*28*). The protohematin-to-globin ratio was 4, in agreement with values established in the literature (*1, 27*).

Hematin *a* interacted with globin in neutral medium to form a green complex which exhibited absorption maxima at 593 to 595 and 422 mμ, as shown in Figure 2. Adding ferricyanide did not change the spectrum, indicating that the heme-iron in the complex was already in the ferric state. Reduction by dithionite shifted the absorption maxima of the complex to 596 and 437 mμ with less prominent peaks at 564, 524, and

424 mμ. The complex was essentially "low spin" as indicated by the ratio, $\epsilon_{596\ m\mu}/\epsilon_{635\ m\mu}$, for the ferric complex (24) and also by the difference between the positions of the Soret absorption maxima of the ferrous and ferric forms of the complex (12, 32).

When the reaction between hematin a and globin was titrated spectrophotometrically, a ratio between 4 and 5 moles (average 4.7) of heme per mole of globin (66,000 grams) was obtained. The rate of recombination of protoheme and globin to form hemoglobin is very high (13). The reaction of globin with deutero-, meso-, or hematohematin is also very fast (2, 14), but the reaction between hematin a and globin was slow; about 45 minutes were required to complete the reaction. The slow rate of reaction for hematin a is probably caused by the structure of the heme molecule. A large side chain in position 2 of the porphyrin ring may make it difficult for hematin a to orient itself into the crevice of the globin molecule if the binding is indeed the same as that in hemoglobin, whereas other hematins tested do not have the bulky group.

Through the conventional enzyme assay in the ascorbate-cytochrome c system, it was found that the hematin a–globin complex was devoid of either the cytochrome oxidase or the tetrahydroquinone oxidase activity. Adding phospholipids did not alter the activity.

Since the spectra of the hematin a–globin complex were established in its Fe(III) and Fe(II) states, its oxygenative and oxidative activities could then be studied spectrally. Thus an experiment, as schematically shown in Figure 1, was designed. Prior to the actual experiment some preliminary controls were investigated to test the suitability of the operation. First, it was found that ferricyanide did not change the spectra of hematin a solution. This observation indicates that free hematin a as prepared was completely in the ferric state. Second, a sample of purified cytochrome oxidase was deaerated, then reduced with a slight excess of dithionite in an inert atmosphere, subsequently made to react with oxygen, and finally reduced again with dithionite; a spectrum was taken in each stage. With respect to the absorption spectra, the deaerated cytochrome oxidase showed the same spectrum as the stock enzyme as well as the reoxidized oxidase after dithionite reduction; all were in the oxidized state. The dithionite-reduced oxidase in both stages was the same as the reduced oxidase usually prepared. Indeed, this type of cycle could be repeated several times. Quantitatively the absorbance as well as the ratio of γ- to α-peaks did not change more than 10%. Therefore, the technique employed was considered satisfactory.

Following the scheme as shown in Figure 1, the absorption spectrum of hematin a–globin complex in each state was carefully determined. It was found that state I was identical with states II, III, IV, and V and remained in the ferric form. State VI showed a spectrum typical of

dithionite-reduced complex. The spectrum (*cf.* Figure 3) of state VII, which was obtained by admitting oxygen to state VI, was different from that of state I but practically identical to that of state VIII (*cf.* Figure 4). The conversions among states VI, VII, and VIII could be repeated several times without changes of absorbance, and the spectrum of state I did not appear. However, the processes from states I through VII decreased the absorption intensity by about 25% of the original. Furthermore, if ferricyanide was used instead of oxygen, the resulting spectrum (state VIII) was also different from that of state I but resembled, though it was not identical with, that of state VII. Several experiments, as described or with minor modifications, gave similar results.

These observations, especially the practical identity of state VII with the ferricyanide-oxidized form (state VIII), strongly suggest that the hematin *a*–globin complex does not possess any oxygenative property or at least does not show up in the spectral behavior as myoglobin or hemoglobin does. All of these results, however, only show that the reduced form of the complex is autoxidizable but that the oxidized form cannot be reduced by reduced cytochrome *c* or by tetrahydroquinone. Why the oxidized form in state VII differs from that in state I is discussed below.

Interactions of Hematin *a* and Polyhistidine. In acidic media, hematin *a* reacted with polyhistidine to form a complex, exhibiting absorption maxima at 594 and 423 mμ. The ratio, $\epsilon_{594\,m\mu}/\epsilon_{635\,m\mu}$, indicated
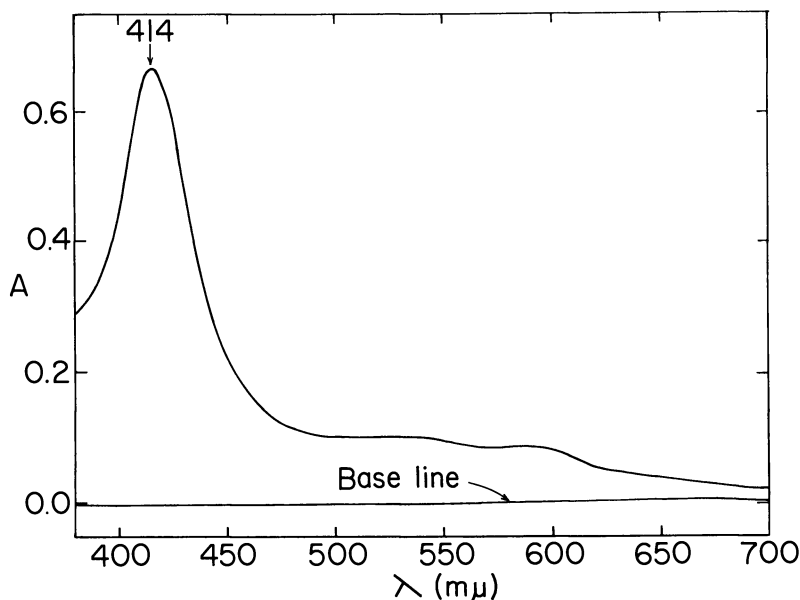
Figure 3.   Absorption spectrum of hematin a*–globin complex at state VII. See* Figure 1 *for description of states*

that the complex was "low spin." Upon reduction with dithionite, the solution became turbid. However, maxima at 592, 562, and 423 mμ with a shoulder at about 442 mμ were still discernible (Figure 5). The reduced form of the complex was found to be extremely autoxidizable, as evidenced by the almost instantaneous return of the absorption maxima to the oxidized form when exposed in air. In contrast, free heme a under the same conditions was relatively stable and did not undergo autoxidation as readily. If the solution containing the ferric hematin a–polyhistidine complex was adjusted to a pH > 6, a green precipitate was formed. The precipitate could be dissolved in dimethyl sulfoxide, giving an apparent pH of $ca.$ 8. The solution did not exhibit a distinct α-band ($cf.$ Figure 6); by contrast, free hematin a in dimethyl sulfoxide showed maxima at 631 and 405 mμ (20). Upon dithionite reduction in dimethyl sulfoxide, heme a–polyhistidine showed absorption maxima at 588, 523, and 421 mμ, whereas free heme a exhibited maxima at 583 and 432 mμ with a shoulder at 430 mμ (20).

Discussion

The complete structures of myoglobin and hemoglobin deduced from x-ray studies ($17, 26$) serve as useful models for investigating heme-protein interactions in these as well as in "synthetic" hemoglobin or myoglobin. In myoglobin, for example, hydrophobic interactions are many. There are 60 atom-to-atom contacts of less than 4 A. and 150 of less than 4.3 A. (31). The stability of the hemoprotein, therefore, depends to a great extent upon the hydrophobic interactions. When hematin a combines with globin, the hydrophobic side chains of the heme group are probably buried inside the protein crevice to render the complex water soluble. Although hydrophobic interactions might stabilize the complex, the presence of the bulky group at position 2 of the porphyrin ring could cause a considerable constraint inside the crevice and therefore could affect the stability of the metal-ligand coordinations. Any reactions that tend to release such a constrained situation in order to accommodate the bulky group would be favored. Thus, the attempt to reduce the complex by dithionite and subsequently its reoxidation must have brought about the release of the constrained situation and in turn altered the coordination sphere of the heme-iron. Such a change is suggested if one compares the spectrum of the complex before going through the redox cycle ($cf.$ Figure 2) with that after reoxidation (Figures 3 and 4). The significant decrease in absorption intensity after going through the redox cycle is also an indication of an altered structure. The possibility of modification of the heme moiety in the complex can be ruled out by the observation that spectrum VI (reduced form) reappeared when both
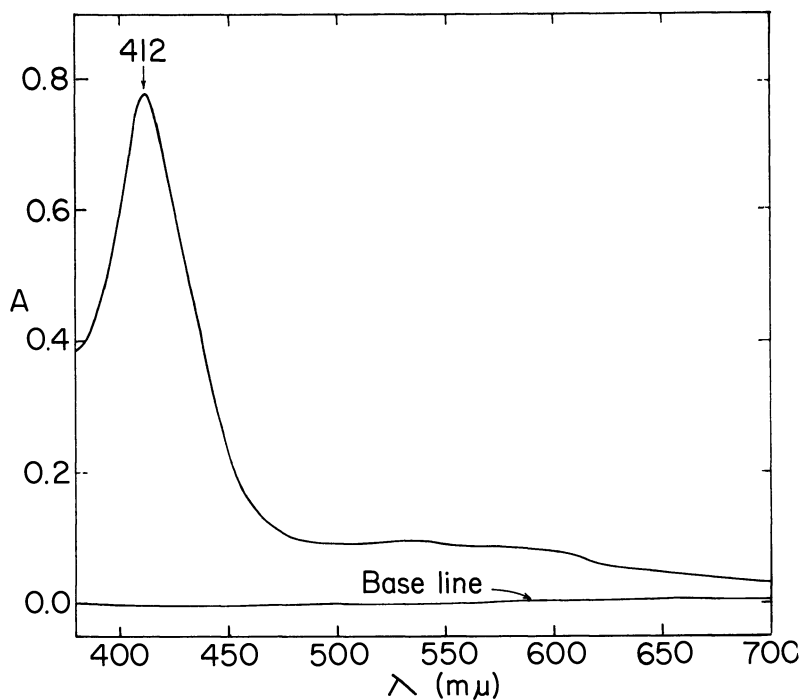
Figure 4.   Absorption spectrum of hematin a–globin complex at state VIII. See Figure 1 for description of states

states VII and VIII were reduced. Indeed, the process of oxidation-reduction could be repeated several times. There was no change in absorbance in either the 460-mμ or the 420-mμ regions—*i.e.*, no slightest indication of the formation of any mitochrome (9).

However, the lack of oxygenative property of the complex is more than simply the consequence of the structural alterations as described above. The availability of π-electrons to the heme-iron for $d\pi$-$p\pi$ bonding with the ligand is also an important factor (11). Antonini *et al.* (1, 2) have observed that the presence of electrophilic groups which draw electrons towards the periphery of the heme molecule tends to decrease the oxygen affinity of the corresponding heme-globin complex. In the case of hematin *a,* it contains two electrophilic groups: vinyl and formyl, which are situated diagonally across the heme plane (22). It is not unreasonable, then, that the reduced hematin *a*–globin complex should exhibit no oxygenative property. Lemberg (22) and Kiese and Kurz (18) had also reported that the complex did not bind oxygen reversibly; however, their studies were conducted in alkaline media, about pH 9.

The unprotected ferrous heme is subjected to immediate oxidation by air (30). Theoretical computations of the ligand field interactions in
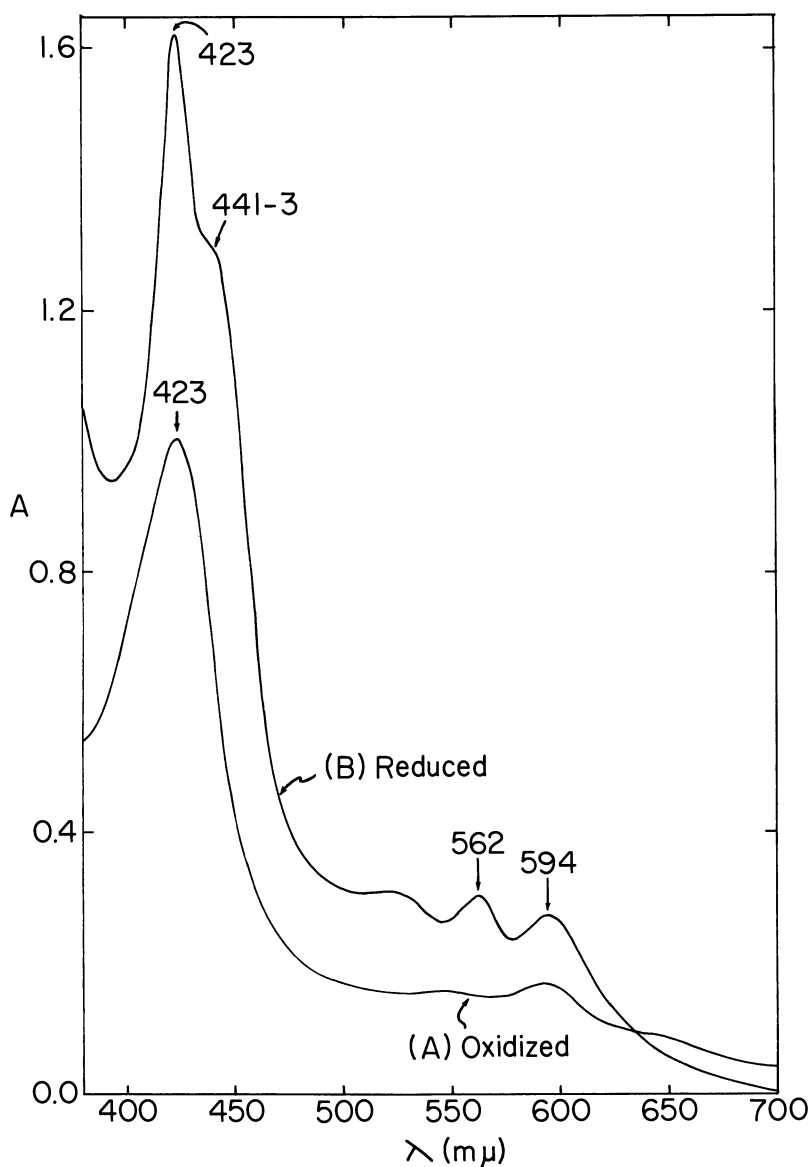
Figure 5.   Absorption spectra of hematin a–polyhistidine complex in acid medium

A, oxidized; **B,** dithionite reduced. Setting for reduced spectrum adjusted by 0.2 absorbance unit downward at 700 mμ because turbidity developed upon addition of dithionite. System contained 50 mμmoles of hematin **a** and 3.3 mg. of polyhistidine in 3 ml. of 0.01M phosphate buffer, pH 5.7.

a hypothetical heme model where oxygen interacts coaxially with the heme-iron suggest that such a geometry would be unstable and would lead to oxidation of the heme-iron (*33*). Thus, the autoxidizability of both the heme *a*–globin and heme *a*–polyhistidine complexes may be caused either by one or both of these situations.
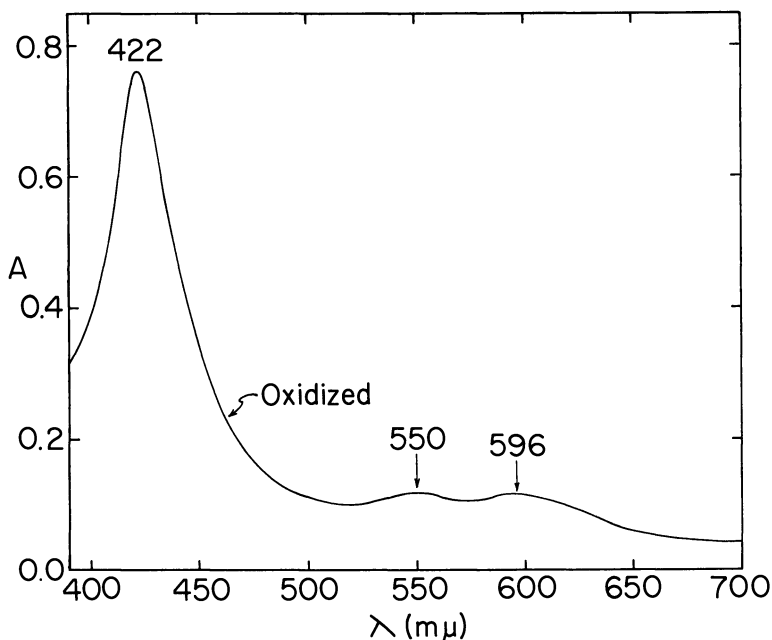
Figure 6. Absorption spectrum of hematin a*–polyhistidine complex in dimethyl sulfoxide*

System containing 16.7μM hematin a and 140μM polyhistidine in 0.01M phosphate buffer was adjusted to pH 11.6. Precipitate formed was separated and dissolved in dimethyl sulfoxide. Solution gave an apparent pH 8.

It may be pertinent to point out that the characteristics of hemoproteins toward oxygen are determined by the combined effect of the heme and protein moieties. Most hemoproteins may be generally classified into the following three groups: (1) able to form oxygenated complex easily but not as readily oxidized by oxygen (*e.g.*, myoglobin and hemoglobin), (2) no known oxygenative nor autoxidative function (*e.g.*, cytochrome *c*), and (3) no oxygenation but capable of autoxidation (*e.g.*, cytochrome oxidase). The fact that a number of protoheme-linked hemoproteins exhibit different behavior towards oxygen, as shown in the above classification, would suggest that the functional role of the protein or enzyme is determined primarily by the protein moiety of the complex. Unpublished results from optical rotatory dispersion studies on a number of

cytochromes done in this laboratory have uniformly shown that the conformations of these cytochromes depend on their oxidation states. Likewise, the conformation (*see* Ref. 4) of oxyhemoglobin differs from that of deaerated hemoglobin. (Although oxymyoglobin shows approximately the same magnitude of rotation for the 233-mμ trough as myoglobin, the detailed conformations of these two species may still be different.)

These ORD results and the difference between Figure 2 on one hand and Figures 3 and 4 on the other for hematin *a*–globin complex are in accord with the role of the protein in determining the specificity and function of a hemoprotein.

Literature Cited

(1) Antonini, E., *Physiol. Rev.* **45**, 123 (1965).
(2) Antonini, E., Brunovi, M., Caputo, A., Chiancone, E., Rossi Fanelli, A., Wyman J., *Biochim. Biophys. Acta* **79**, 284 (1964).
(3) Antonini, E., Gibson, Q. H., *Biochem. J.* **76**, 534 (1960).
(4) Brunori, M., Engle, J., Schuster,, T. M., *J. Biol. Chem.* **242**, 773 (1967).
(5) Camerino, P. W., King, T. E., *J. Biol. Chem.* **241**, 970 (1966).
(6) Chance, B., Estabrook, R., Yonetani, T., eds., "Hemes and Hemoproteins," Academic Press, New York, 1967.
(7) Da Silva, J. J. R. F., Calado, J. G., *J. Inorg. Nucl. Chem.* **28**, 125 (1966).
(8) Dickens, F., Neil, E. eds., "Oxygen in the Animal Organism," Pergamon Press, Oxford, 1963.
(9) Elliott, W. B., Hulsmann, W. C., Slater, E. C., *Biochim. Biophys. Acta* **33**, 509 (1959).
(10) Falk, J. E., Lemberg, R., Morton, R. K., eds., "Hematin Enzymes," Pergamon Press, New York, 1961.
(11) Falk, J. E., Phillips, J. N., Magnusson, E. A., *Nature* **212**, 1531 (1966).
(12) George, P., Beetlestone, J., Griffith, J. S., "Hematin Enzymes," J. E. Falk, R. Lemberg, and R. K. Morton, eds., p. 105, Pergamon Press, London, 1961.
(13) Gibson, Q. H., Antonini, E., *Biochem. J.* **77**, 328 (1960).
(14) Gibson, Q. H., Antonini, E., *J. Biol. Chem.* **238**, 1384 (1963).
(15) Hill, R., Holden, H. F., *Biochem. J.* **20**, 1326 (1926).
(16) *J. Gen. Physiol.* **49** (1), part 2 (1965).
(17) Kendrew, J. C., Watson, H. C., Strandberg, B. E., Dickerson, R. E., Phillips, D. C., Shore, V. C., *Nature* **190**, 666 (1961).
(18) Kiese, M., Kurz, H., *Biochem. Z.* **330**, 117 (1958).
(19) King, T. E., Mason, H. S., Morrison, M., eds., "Oxidases and Related Redox Systems," Vol. I, II, Wiley, New York, 1965.
(20) King, T. E., Yong, F. C., Takemori, S., *J. Biol. Chem.* **242**, 819 (1967).
(21) Lee, C. P., King, T. E., *Biochim. Biophys. Acta* **59**, 716 (1962).
(22) Lemberg, R., *Advan. Enzymol.* **23**, 265 (1961).
(23) Lemberg, R., Mansley, G. E., *Biochim. Biophys. Acta* **118**, 19 (1966).
(24) Lemberg, R., Morell, D. B., Newton, N., O'Hagan, J. E., *Proc. Roy. Soc. (London)* **B155**, 339 (1961).
(25) Orii, Y., Okunuki, K., *J. Biochem. (Tokyo)* **53**, 489 (1963); **57**, 45 (1965).
(26) Perutz, M. F., Bolten, W., Diamond, R., Muirhead, H., Watson, H. C., *Nature* **203**, 687 (1964).
(27) Rossi Fanelli, A., Antonini, E., Caputo, A., *Advan. Prot. Chem.* **19**, 74 (1964).

(28) Rossi Fanelli, A., Antonini, E., Caputo, A., *Biochim. Biophys. Acta* **30,** 608 (1958).
(29) Takemori, S., King, T. E., *J. Biol. Chem.* **240,** 504 (1965).
(30) Wang, J. H., "Oxygenases," Hayaishi, O., ed., Chap. 11, Academic Press, New York, 1962.
(31) Watson, H., "Hemes and Hemoproteins," B. Chance, R. Estabrook, T. Yonetani, eds., p. 109, Academic Press, New York, 1967.
(32) Williams, R. J. P., "Hematin Enzymes," J. E. Falk, R. Lemberg, R. K. Morton, eds., p. 41, Pergamon Press, London, 1961.
(33) Zerner, M., Gouterman, M., Kobayashi, H., *Theoret. Chim. Acta (Berlin)* **6,** 363 (1966).

The Role of Cytochrome P-450 in Mixed–Function Oxidations

D. Y. COOPER, S. NARASIMHULU, and O. ROSENTHAL

Harrison Department of Surgical Research

R. W. ESTABROOK

Department of Biophysics and Physical Biochemistry, University of Pennsylvania, Philadelphia, Pa. 19104

The photochemical action spectrum method demonstrates that cytochrome P-450 functions as the O_2-activating enzyme of TPNH-dependent mixed-function oxidase systems concerned with metabolism of steroids and various xenobiotics (drugs, poisons) in vertebrate tissues. The steroid 11β-hydroxylase of adrenocortical mitochondria can be resolved into (a) a particle containing cytochrome P-450 and the substrate-specific enzyme component, and (b) a soluble TPNH-cytochrome P-450 reducing system consisting of a flavoprotein (Fp) and a non-heme iron protein (NHI). Activity and biophysical properties of the system can be fully restored when the molar ratios of NHI : Fp : cytochrome P-450 are approximately 50 : 1 : 1. Steroid hydroxylations by the fungus Rhizopus nigricans *display light-reversible CO inhibition. The fungus, however, contains a CO-combining pigment with an absorption maximum at 414 mμ rather than 450 mμ.*

In the past few years considerable information has accumulated regarding hydroxylating enzymes which form a subgroup of the class termed mixed-function oxidases by Mason (*15*) or monooxygenases by Hayaishi (*13*). The reactions catalyzed by these enzymes are characterized by their dependence on TPNH and molecular oxygen of which one atom is incorporated into a lipid-soluble specific substrate. For the most part these oxidases are localized in the endoplasmic reticulum (the microsome

fraction) of the cytoplasm, although in endocrine tissues they are found also in the mitochondria.

The fact that cytochrome P-450 functions as terminal oxidase for these reactions is supported by both indirect and direct evidence: (a) the drug-induced increase in the hydroxylase activity of liver microsomes is accompanied by a similar increase in microsomal cytochrome P-450 (25, 26), an indication that this pigment participates in the mixed-function oxidation of drugs; (b) maximal reversal of the characteristic CO inhibition of mixed function oxidations is accomplished by illuminating the enzyme assay system with monochromatic light of 450 mµ wavelength, the absorption maximum of the CO compound of reduced cytochrome P-450 (P-450 · CO).

If the degree of reversal of the CO inhibition by different monochromatic light bands of equal quantum intensity is plotted as function of wavelength, a photochemical action spectrum is obtained which agrees with the spectrophotometric difference spectrum of P-450 · CO. Hydroxylase reactions for which the participation of cytochrome P-450 has been established by the action spectrum are listed in Table I. There is evidence that the hydroxylations of cholesterol by liver microsomes at position 6β (rats) (32) and 7α (rabbits) (30) may also belong to this group of reactions.

It is important to note that the CO inhibition of the hydroxylation reaction is competitive, the degree of inhibition being a function of the CO/O_2 ratio rather than of the CO concentration. Since CO combines only with reduced cytochrome P-450, O_2 must also react with this form of the pigment to be utilized in the oxygenation reaction.

Thus, the reduced form of cytochrome P-450 functions as the oxygen-activating biocatalyst of a wide variety of mixed-function oxidations by vertebrate tissues effecting biosynthesis and catabolism of steroid hormones, bile acid formation, and the metabolism of drugs and other xenobiotics (16). Since reduced pyridine nucleotides do not react directly with hemoproteins, the hydroxylase systems must include components that mediate the electron transport from TPNH to cytochrome P-450. There also must be distinctive differences in composition causing the substrate specificity of the oxygenations.

Attempts to resolve the enzyme systems, which are tightly bound to mitochondrial or endoplasmic membranes, usually yield enzymatically inactive preparations. Only for the steroid 11β-hydroxylase system of adrenocortical mitochondria has resolution into the following three components been accomplished (18, 21, 22, 31): (1) a particulate fraction containing cytochrome P-450; (2) a flavine-adeninedinucleotide flavoprotein (MW 60,000); and (3) a non-heme iron protein (MW 20,000). The latter two constitute the TPNH-cytochrome P-450 reducing system. Full 11β-hy-

Table I.   Demonstration of Function

No.	Substrate	Group Removed or Added	Products
1	17-OH-Progesterone	(+) 21-OH	Cortexolone
2	Cortexone	(+) 11β-OH	Corticosterone
3	Corticosterone	(+) 18-O	Aldosterone
4	Codeine	(−) CH$_3$	Morphine + HCHO
5	4-Methylaminoanti-pyrine	(−) CH$_3$	4-Aminoantipyrine + HCHO
6	Acetanilide	(+) OH	p-Hydroxyacetanilide
7	Testosterone	(+) OH[b]	Total products
8		(+) 6β-OH	6β-OH testosterone
9		(+) 7α-OH	7α-OH testosterone
10		(+) 16α-OH	16α-OH testosterone
11	Cholesterol	(−) C$_6$H$_{12}$O$_2$	Pregnenolone + isocaproic acid

[a] mcs = microsomes; mtch = mitochondrial particles.

droxylase activity is restored when these components are recombined in appropriate amounts.

The present paper presents a summary of the properties of the reconstituted bovine adrenocortical 11β-hydroxylase and compares this system with the previously studied non-resolved microsomal hydroxylases of the liver and adrenal. Terminology and abbreviations used are as follows:

Cortexone = deoxycorticosterone (DOC) = pregn-4-en-21-ol-3,20-dione

Corticosterone = (Cpd. B) pregn-4-en-11β,21-diol-3,20-dione
Cortexolone = (Subst. S) pregn-4-en-17α,21-diol-3,20-dione
17-Hydroxyprogesterone = pregn-4-en-17α-ol-3,20-dione
Pregnenolone = pregn-5-en-3β-ol-20-one
TPN and TPNH = triphosphopyridine nucleotide and its reduced form, respectively.

Resolution of the Steroid 11β-Hydroxylase System

Pooled cortex tissue of about 20 steer adrenals is homogenized in 0.25M sucrose solution, and the mitochondrial fraction is isolated by fractional centrifugation (5). The final mitochondrial sediment is suspended in distilled water and sonicated for 15 minutes (20 kc., 60-watt output) in an ice-cooled vessel. The fractionation of the sonicate is shown in Figure 1.

The specific flavoprotein (Fp) and the non-heme iron protein (NHI) were isolated from the supernatant fraction S-2 according to Omura et al. (22, 24). Additional amounts of NHI can be extracted from the precipi-

of P-450 by the Action Spectrum Method

Organ	Intracellular Location[a]	Species	Ref.
adrenal	mcs	steer	4, 8
adrenal	mtch	steer	6
adrenal	mtch	bullfrog Rana catesbiana	11
liver	mcs	rat	4
liver	mcs	rat	4
liver	mcs	rat	4
liver	mcs	rat	3
liver	mcs	rat	3
liver	mcs	rat	3
liver	mcs	rat	3
adrenal	mtch	steer	1, 9

[b] Total of individual hydroxylations.

tate P-1. For large scale preparations of NHI, extracts of acetone-dried (*31*) or freeze-dried mitochondria (*18*) are the most convenient starting material. The purification procedure is that described by Omura *et al.* (*23, 24*). No additional source for preparing Fp has as yet been found.

The hemoprotein content of the final precipitate, P-3, can be virtually completely accounted for by cytochrome P-450 and smaller quantities of its inactive derivative P-420. The particles also contain the substrate-specific component of the 11β-hydroxylase system and presumably of

Mitochondrial Sonicate

centrifuged 30 min.
at 105,000 x g.

Supernatant (S-1)   ppt (P-1) alternate
centrifuged 3 hours   source of NHI protein
at 105,000 x g

Supernatant (S-2)   ppt (P-2)
source of NHI and Fp   sonicate 30 seconds in 0.15 M KCl
                            10 m M K. Pi, pH 7.4 centrifuge 30
                            minutes 105,000 x g

Supernatant   ppt. (P-3)
discarded   source of P-450
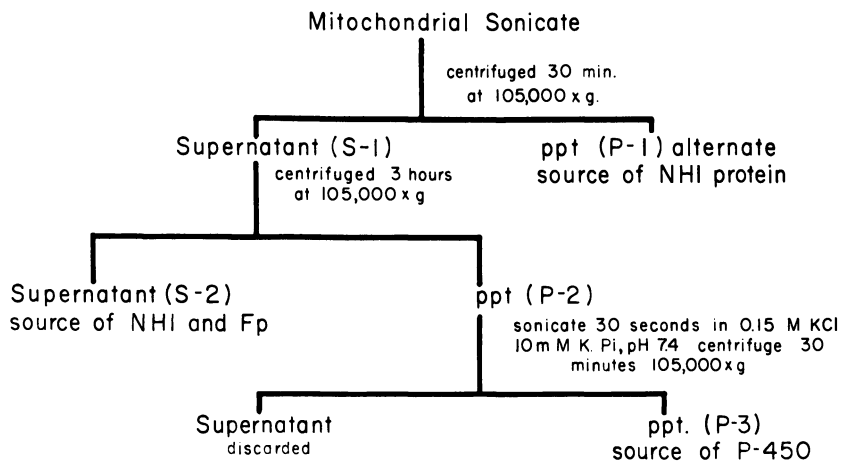
Figure 1.   Flow scheme for resolution of the 11β-hydroxylase system

other hydroxylase systems which are localized in adrenocortical mito-chondria. There is evidence that small amounts of NHI and Fp are still adhering to the particles.

The P-3 particles are dispersed in 10 mM potassium phosphate buffer, pH 7.4, by sonication for 30 seconds, and the tubes are kept in ice until used within one to two days.

The suspensions of P-3 particles and the solutions of NHI and Fp are standardized on the basis of protein content (biuret method) as well as of the millimolar extinction coefficients for P-450 · CO (20), NHI and Fp (24).

Reconstitution of the 11β-Hydroxylase System

Although the supernatant fraction S-1 [similar to the "solubilized" preparation described by Sharma et al. (29)] of the mitochondrial sonicate displayed 11β-hydroxylase activity, reaction rates were not pro-portional to the amount of mitochondrial protein added, but they de-creased precipitously with increasing dilution of the preparation (15). This observation, indicating a dissociating enzyme system, prompted the separation of the sample into the particulate fraction and the two soluble components of the reducing system.

While enzyme activity was partially restored easily by recombining the particles with the soluble components, the particles could be saturated with the soluble reducing system only when we realized that unexpectedly high concentrations of the non-heme iron protein were required. After the approximate saturation levels for NHI and Fp had been estimated, a set of assays was performed (Table II).

In the absence of NHI and Fp, hydroxylase activity of the P-3 par-ticles was barely detectable and was only slightly increased by adding Fp, whereas supplementation with NHI caused a significant increase in activity. The P-3 particles are thus relatively more deficient in NHI than in Fp. Maximal activity in this test series was obtained with 0.72 μM Fp in combination with 36.8 μM NHI (Flask 8). Under these conditions the ratio of NHI : Fp : P-450 was 55 : 1.1 : 1.0. What necessitates the large excess of NHI for restoring full activity of the system is not under-stood at present and requires further study.

Some Properties of the Reconstituted 11β-Hydroxylase System

Specific Activity. At the saturating levels of Fp, NHI, TPNH, and cortexone, the time course of the reaction was linear for at least 20 minutes, and the rates were proportional to the amount of P-3 protein present within the range studied (0.2 to 0.8 mg. per ml.). The maximum

Table II.   Reconstitution of the 11β-Hydroxylase System[a]

| Flask No. | Additions (μM) | | | | Corticosterone Formation | |
| | NHI | | F_p | | Absolute, $nmole \times min.^{-1}$ mg. P-3 protein | Relative, % of maximum |
	18.4	36.8	0.72	1.44		
1	−	−	−	−	0.1	0.7
2	−	−	+	−	0.2	1.5
3	−	−	−	+	0.2	1.5
4	+	−	−	−	1.6	11.8
5	−	+	−	−	1.6	11.8
6	+	−	+	−	11.2	82.5
7	+	−	−	+	10.8	79.0
8	−	+	+	−	13.6	100.0
9	−	+	−	+	13.4	99.0

[a] Reaction carried out in 15-ml. conical Warburg flasks attached to manometers and shaken in water bath at 25°C. Gas phase, 4% O_2 in N_2; fluid volume, 2.5 ml.; pH, 7.4. Reaction was started by adding a TPNH-generating system from sidearm of flask. Final concentrations of constituents of reaction mixture were: P-3 particle protein, 0.4 gram/liter (= 0.675 μM cytochrome P-450); cortexone 0.24, mM; NaCl, 57.5 mM; KCl, 44.4 mM; MgCl₂, 0.43 mM; glycylglycine, 11.5 mM; tris · HCl, 9.1 mM; KPO₄, 0.6 mM; crystalline bovine serum albumin, 7.7 grams/liter; glucose-6-phosphate, 4.25 mM; TPN, 1.01 mM; glucose-6-phosphate dehydrogenase, 200 Kornberg units/liter. Reaction terminated by rapidly transferring 2 ml. of reaction mixture to 15 ml. ice-cold dichloromethane. Corticosterone formed was determined with the fluorometric method of Mattingly (*17*).

activity of 13.5 nmole of corticosterone formed per minute per mg. of P-3 protein (Table II) is 35% lower than the average of 20 per mg. of mitochondrial protein reported by Cammer *et al.* (*2*) for suspensions of intact adrenocortical mitochondria of steers, even though the cytochrome P-450 concentration is nearly identical in both types of preparation. Since the particles contained considerable amounts of cytochrome P-420, the inactive derivative of P-450, it is possible that some loss of enzyme activity occurred during separation of the particles from the mitochondria. Nevertheless, when compared on a protein basis, the specific activity of the 11β-hydroxylase preparations was appreciably higher than that of the microsomal hydroxylases of adrenal cortex and liver (*4, 8*), which ranged from 1.5 to 7.0 nmoles of hydroxylation product formed per minute per milligram of protein.

CO Inhibition. Before saturation levels for the reducing system were determined, CO inhibition of reconstituted 11β-hydroxylase preparations varied so greatly that neither partition constants (K) nor light reversibility of the inhibition could be established. The probable reasons for the abnormal behavior of preparations, in which the capacity of the reducing system is rate limiting, have been discussed (*28*).

When the mitochondrial particle preparations were reinforced with increasing amounts of NHI and Fp, the competitive character of the CO

inhibition became evident. As Figure 2 shows, the percent inhibition of hydroxylation by gas mixtures containing either 4% CO and 4% O_2, or 20% CO and 20% O_2, is virtually identical. Conversely, the inhibition increases at a fixed CO concentration of about 10% when the CO/O_2 ratio is raised from 0.5 to 2.0.
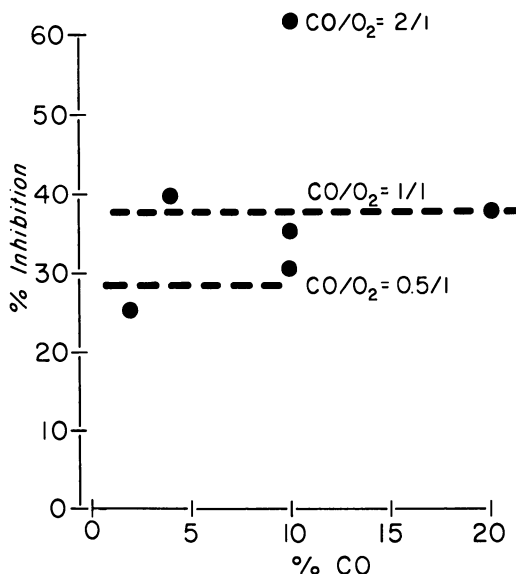
Figure 2.   Dependence of CO inhibition of 11β-hydroxylation on the CO/O_2 ratio. Percentage inhibition of 11β-hydroxylation is plotted as a function of CO concentration in CO–O_2–N_2 mixtures. Ratio of CO/O_2 is indicated above the horizontal lines. Inhibitions are calculated with reference to the rate in a CO-free control sample equilibrated with the same oxygen concentration as the sample exposed to CO. Incubation system is described in Table II

Warburg's partition constant $K = (n/(1 - n))x(CO/O_2)$, where n is the ratio of reaction rate with CO to rate without CO, lies between 0.6 and 2.5 in mixed-function oxidase systems (4). In the experiments included in Figure 2, K was around 1.4, while in other experiments K values between 0.6 and 1.0 were observed. Partition constants around unity differentiate the oxygenation reactions catalyzed by cytochrome P-450 from cell respiration catalyzed by cytochrome oxidase, where the K values are higher by one order of magnitude.

Photochemical Action Spectrum. The relative photochemical action spectrum of reconstituted 11β-hydroxylase preparations is shown in Figure 3. The photochemical action of the individual monochromatic
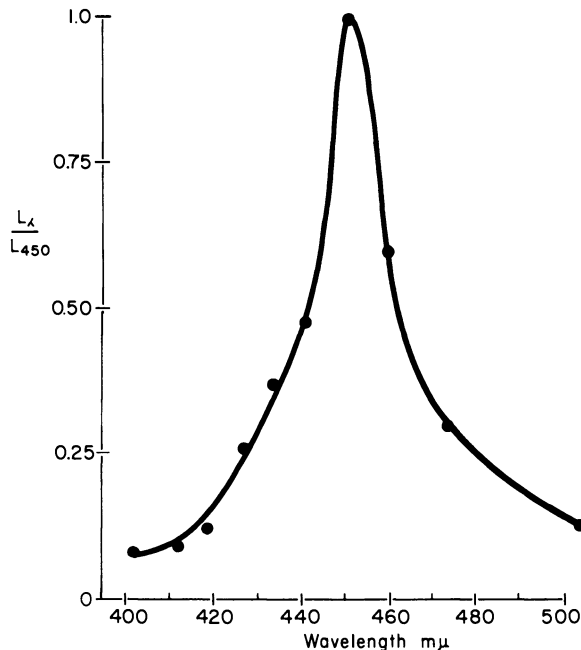
Figure 3. *Photochemical action spectrum of reconstituted 11β-hydroxylase system. Curve is a composite of five experiments, three in the range 450–401 mμ and two in the range 450–500 mμ. Experimental procedure and composition of reaction mixture are described in Table II; concentrations of Fp and NHI given in Flask 6 of Table II. Rate of corticosterone formation in the absence of CO averaged 9 nmole/mg. P-3 protein/min. Flasks were gassed with 4% O₂– 96% N₂ or 4% O₂–4.2% CO–91.8% N₂(CO/O₂ ratio = 1.05). The ordinate scale is relative light sensitivity L_x/L_450. L is calculated as described in Table III. The wavelength of monochromatic light of approximately equal intensity illuminating the reaction vessels is plotted on the abscissa*

light bands has been expressed in terms of the light sensitivity factor, L, introduced by O. Warburg (33) and defined as the reciprocal of the quantum energy required for doubling the distribution constant K. In Figure 3 the ratios of L for each light band to L for the 450 mμ band have been plotted as a function of wavelength. [Warburg (33) notes that $L = (\phi \cdot \beta)/z_d$ where ϕ is the quantum yield, β the absorption coefficient, and z_d the dark decomposition constant of the CO compound. Since the velocity constant z_d decreases with temperature, L increases with decreasing temperature. If z_d and ϕ can be measured or ϕ can be assumed to be 1, β can be determined.]

The 450-mμ band effected maximal reversal of the CO inhibition of the reconstituted 11β-hydroxylase system, and the effectiveness of the irradiation decreased rapidly above and below this wavelength. The action spectrum is in harmony with the spectrophotometric difference spectrum of cytochrome P-450 · CO in this preparation (Figure 4). The 420-mμ peak in the latter spectrum, which is caused by cytochrome P-420 · CO, is not reflected in the action spectrum. This proves that P-420 is not functioning in 11β-hydroxylation.
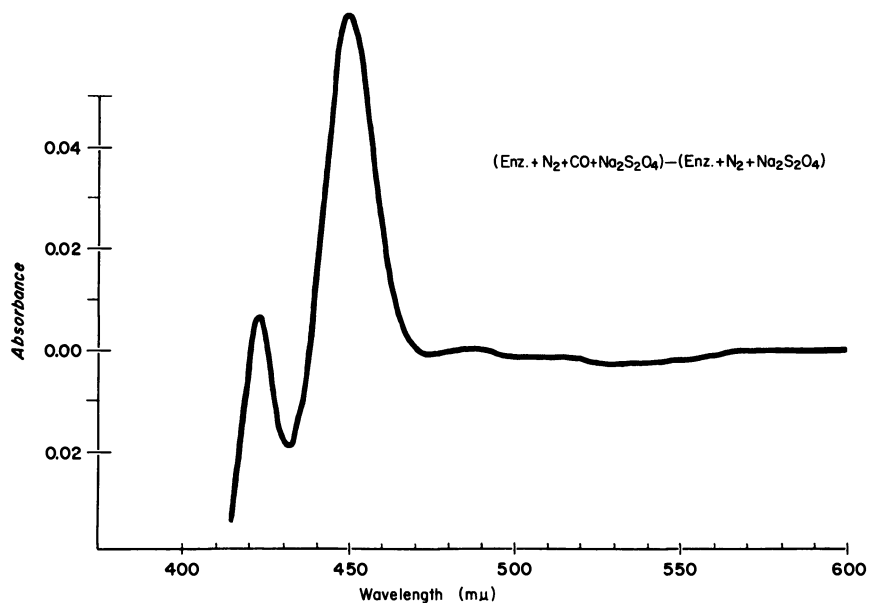
Figure 4. Difference spectrum of P-450 · CO measured with the Cary model 14 split-beam recording spectrophotometer. A suspension of P-3 particles containing 0.95 mg. of protein per ml. of 10 mM phosphate buffer (pH 7.4) was equally divided between two anaerobic optical cuvettes having $Na_2S_2O_4$ in the sidearms. Both cuvettes were gassed for 5 min. with N_2, and a base line of equal optical density was established. Experimental cuvette was then gassed with CO for 2 min., dithionite was added to both cuvettes from the sidearms, and the change in optical density was recorded

The photochemical action spectra of the various hydroxylase systems listed in Table I show only minor differences. In some of them (*e.g.*, the 21-hydroxylase of adrenocortical microsomes), the chief decline of the short wave limb of the spectrum occurs below 433 mμ, resulting in a broader peak. The maximum of the action spectra, however, is always around 450 mμ. As shown in Table III, L values computed for the 450 mμ band ranged from 4.9 to 27 $\times$ 10^6 in the different hydroxylase systems, although the order of magnitude is the same. Warburg's L values

Table III. Light Sensitivity of Co-Inhibited Mixed-Function Oxidases

450 mμ; 25°C.

No.[a]	Substrate	K[b]	$10^{-6} \times L$[c]	Ref.
1	17-OH Progesterone	0.97	27.0	8
2	Cortexone	0.86	8.9	6
3	Corticosterone	1.73	12.4	11
4	Codeine	0.96	9.3	4
5	4-Methylaminoantipyrine	1.14	10.3	4
6	Acetanilide	0.82	15.3	4
7	Testosterone (total)	1.34	4.9	3
8	Testosterone 6β	1.6	5.6	3
9	Testosterone 7α	2.74	11.8	3
10	Testosterone 16α	0.96	8.2	3

[a] Reactions numbered as in Table I.

[b] $K = \dfrac{n}{1-n} \cdot \dfrac{CO}{O_2}$, where $n =$ (rate with CO)/(rate without CO). All gas mixtures contained 4% O_2. CO/O_2 ratio was 1.05 in Expts. 2, 4, and 6, and 2.16 in all others. Balance was made up with nitrogen.

[c] $L = \dfrac{1}{i} \cdot \dfrac{K_h - K_d}{K_d} = \dfrac{1}{i} \cdot \dfrac{\Delta K}{K_d}$; K_h and K_d are partition constants with and without illumination respectively; $i =$ mole quanta $\times$ sq. cm. $\times$ min.$^{-1}$.

(10°C., 436 mμ) for the CO complex of the respiration enzymes of yeast and acetic acid bacteria are about one order of magnitude higher. This might be a consequence of the lower temperature. Whether the differences between the various mixed function oxidations catalyzed by cytochrome P-450 are real, or whether they are caused by differences in the accuracy of the analytical procedures used, remains undecided. [The first light sensitivities reported (8) were too low because of the wide band width of the 450-mμ interference filter used to measure light intensity. The L values reported (4, 11, 28) are one order of magnitude too low since the radiant flux was expressed in gram cal./10 sq. cm. rather than per sq. cm.]

Substrate Binding Reaction

Narasimhulu *et al.* (19) and Cooper *et al.* (7) observed that the addition of 17-hydroxyprogesterone to adrenocortical microsome preparations in the absence of TPNH produced a change in the difference spectrum characterized by the formation of an absorption minimum at 420 mμ and the simultaneous appearance of an absorption maximum at 390 mμ. Supplementation of the system with TPNH resulted in a gradual disappearance of the spectral change. Readdition of steroid substrate started a new cycle of appearance and disappearance of the spectral change.

While these cyclic spectral changes in conjunction with the hydroxylation of the substrate can be most clearly demonstrated in the steroid 21-hydroxylase system of adrenocortical microsomes, substrate-produced spectral changes have been described in several mixed-function oxidase systems, such as the induced drug hydroxylations of rat liver microsomes (27) and the 11β-hydroxylation of cortexone by intact mitochondria (2, 12) or by the supernatant S₁ of mitochondrial sonicates (5).

There is agreement that the spectral changes presumably reflect changes in the optical density of cytochrome P-450. Indeed these changes furnish the first information on the spectral properties of the functioning form of cytochrome P-450, of which only the 450-mμ absorption band of the inactive CO compound of its reduced form was known. Although the mechanism of interaction between substrate and cytochrome has not been established, the following have been proposed: (1) conformational changes of the hemoprotein; (2) changes in the oxidation state; and (3) a combination of 1 and 2. These interpretations have been discussed (7, 19).

Figure 5 shows the effect of adding cortexone on the formation of the 420-mμ trough in the difference spectrum of a suspension of P-3 particles. In contrast to the preparations discussed above, the hydroxylase system of the P-3 suspension has been freed of most of the TPNH cytochrome P-450 reducing system. Yet the spectral change occurs as readily as in the complete system previously studied. This indicates that the substrate-binding component of the 11β-hydroxylase system is bound to the particles as tightly as the oxygen-activating cytochrome P-450.

The apparent substrate dissociation constant K_s for cortexone of $4 \times 10^{-6}M$ is quite similar to that of 17-hydroxyprogesterone in steroid 21-hydroxylase preparations from bovine adrenocortical microsomes (7). This distinguishes the adrenal steroid hydroxylases from the drug hydroxylases of rat liver where K_s values of about $10^{-4}M$ were observed (27).

Cytochrome P-450 and Substrate Specificity of Mixed Function Oxidases

The experimental results given above clearly indicate that cytochrome P-450 is the oxygen-activating catalyst of a wide variety of mixed-function oxidations in tissues of vertebrate animals. Spectrophotometric measurements and determinations of the photochemical action spectra did not reveal any significant differences between the pigments from different sources. Yet the substrate specificity of these mixed-function oxidase systems is pronounced, as shown by studies on the induction of microsomal hydroxylase activity toward different xenobiotics (27) and on the affinity of different C-21 methyl corticosteroids toward
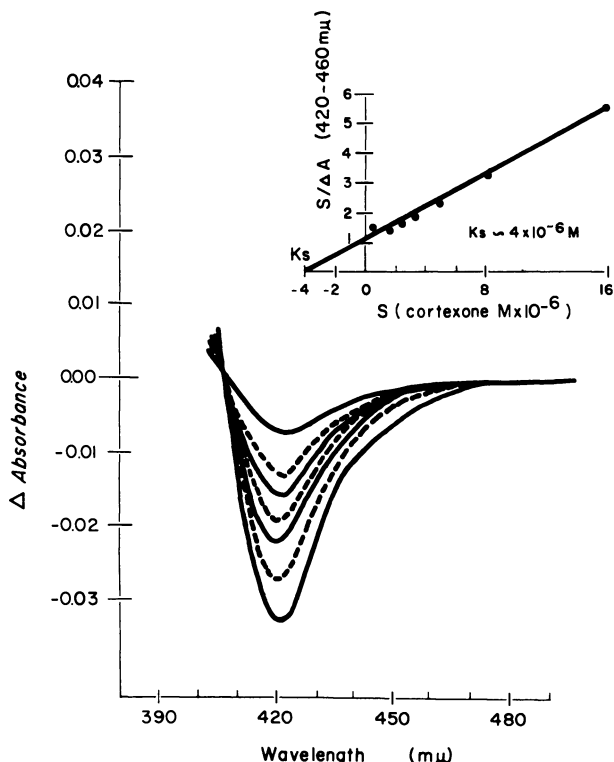
Figure 5. Spectrophotometric titration with cortexone of a P-3 particle suspension. Difference spectra were determined with the Yang-Chance split-beam recording spectrophotometer developed for studying turbid solutions. A suspension of P-3 particles, containing 1.93 mg. protein with 1.74 nmole cytochrome P-450 per ml. of 50 mM K-phosphate buffer (pH 7.4) was equally divided between experimental and reference cuvette, and a base line of equal optical density was established. Microliter volumes of a methanolic cortexone solution were then added to the experimental cuvette, and the change in optical density between 500 and 410 mµ was recorded after each addition. Because of the high turbidity of the preparation, the spectral region below 410 mµ could not be resolved. Upper corner shows relation between change in light absorbance and cortexone concentration as a reciprocal Lineweaver-Burk plot according to the equation:

$$\frac{S}{\Delta A} = \frac{Ks}{\Delta A_m} + \frac{1}{\Delta A_m} S$$

where S is the cortexone concentration, ΔA the density differences between 460 and 420 mµ for individual S values, and ΔA_m the maximal value of ΔA for saturating substrate concentrations

the steroid 21-hydroxylase system of adrenocortical microsomes (7). Hence, there remains the question whether the term cytochrome P-450 actually embraces a group of hematin enzymes with identical hemes bound to substrate specific proteins or whether cytochrome P-450 is associated with specific substrate-binding proteins which put the substrate in the proper position for interaction with the oxygenated heme. The decision between these alternatives must be left to future research.

Evidence for the direct utilization of molecular oxygen in the OH function introduced into the steroid molecule has been obtained largely with fungoid systems acting upon various steroid substrates in the presence of ^{18}O (14). Studies in our laboratory (10) concerning the 11α-hydroxylation of progesterone by the fungus *Rhizopus nigricans* indicate that this reaction is inhibited by CO and that the inhibition is reversed by illuminating the reaction system with white light. However, this fungus contains only a CO-combining pigment with an absorption maximum at 414 mμ. Similar findings have been reported (34) regarding steroid hydroxylations by *Bacillus cereus*. It appears that microbiological mixed-function oxidase systems do not require cytochrome P-450.

Acknowledgment

Literature Cited

(1) Boyd, G. S., Simpson, E. R., "Function of the Adrenal Cortex," K. McKerns, Ed., Appleton-Century-Crofts, New York, in press.
(2) Cammer, W., Cooper, D. Y., Estabrook, R. W., "Function of the Adrenal Cortex," in press.
(3) Conney, A. H., Ikeda, M., Levin, W., Cooper, D. Y., Rosenthal, O., Estabrook, R. W., *Federation Proc.* **26**, 462 (1967).
(4) Cooper, D. Y., Levin, S., Narasimhulu, S., Rosenthal, O., Estabrook, R. W., *Science* **147**, 400 (1965).
(5) Cooper, D. Y., Narasimhulu, S., Slade, A., Raich, W., Foroff, O., Rosenthal, O., *Life Sci.* **4**, 2109 (1965).
(6) Cooper, D. Y., Novack, B., Foroff, O., Slade, A., Sanders, E., Narasimhulu, S., Rosenthal, O., *Federation Proc.* **26**, 341 (1967).
(7) Cooper, D. Y., Narasimhulu, S., Estabrook, R. W., Rosenthal, O., "Function of the Adrenal Cortex," in press.
(8) Estabrook, R. W., Cooper, D. Y., Rosenthal, O., *Biochem. Z.* **338**, 741 (1963).

(9) Ferguson, J. J., Yun, J., Cooper, D. Y., Rosenthal, O., in preparation.

(10) Foroff, O., Cooper, D. Y., unpublished results.

(11) Greengard, P., Psychoyos, S., Tallan, H., Cooper, D. Y., Rosenthal, O., Estabrook, R. W., *Arch. Biochem. Biophys.* **121**, 298 (1967).

(12) Harding, B. W., Oldham, S. B., Wilson, L. D., "Function of the Adrenal Cortex," in press.

(13) Hayaishi, O. (July, 1964), *Proc. Plenary Session Intern. Congr. Biochem., 6th, New York*, p. 31.

(14) Hayano, M., Saito, A., Stone, D., Dorfman, R. I., *Arch. Biochem. Biophys.* **21**, 380 (1956).

(15) Mason, H. S., *Advan. Enzymol.* **19**, 79 (1957).

(16) Mason, H. S., North, J. C., Vanneste, M., *Federation Proc.* **24**, 1172 (1965).

(17) Mattingly, D., *J. Clin. Pathol.* **15**, 374 (1962).

(18) Nakamura, Y., Otsuka, H., Tamaoki, B., *Biochim. Biophys. Acta* **122**, 34 (1966).

(19) Narasimhulu, S., Cooper, D. Y., Rosenthal, O., *Life Sci.* **4**, 2101 (1965).

(20) Omura, T., Sato, R., *J. Biol. Chem.* **239**, 2379 (1964).

(21) Omura, T., Sanders, E., Cooper, D. Y., Rosenthal, O., Estabrook, R. W., *Proc. Kettering Symp., Yellow Springs*, 1965, p. 401.

(22) Omura, T., Sato, R., Cooper, D. Y., Rosenthal, O., *Federation Proc.* **24**, 1181 (1965).

(23) Omura, T., Sanders, E., Estabrook, R. W., Cooper, D. Y., Rosenthal, O., *Arch. Biochem. Biophys.* **117**, 660 (1966).

(24) Omura, T., Sanders, E., Cooper, D. Y., Estabrook, R. W., "Methods in Enzymology," S. P. Colowick, N. O. Kaplan, Eds., Vol. 10, p. 362, Academic Press, New York, 1967.

(25) Orrhenius, S., Dallner, G., Ernster, L., *Biochem. Biophys. Res. Comm.* **14**, 329 (1964).

(26) Remmer, H., Mercker, H. J., *Ann. N.Y. Acad. Sci.* **123**, 79 (1965).

(27) Remmer, H., Schenkman, J. B., Estabrook, R. W., Sasame, H., Gilette, J., Cooper, D. Y., Narasimhulu, S., Rosenthal, O., *Mol. Pharmacol.* **2**, 187 (1966).

(28) Rosenthal, O., Cooper, D. Y., "Methods in Enzymology," Vol. 10, p. 616, Academic Press, New York, 1967.

(29) Sharma, D. C., Forchielli, E., Dorfman, R. I., *J. Biol. Chem.* **237**, 1495 (1962).

(30) Staple, E., Shah, P., Cooper, D. Y., Rosenthal, O., unpublished results.

(31) Suzuki, K., Kimura, T., *Biochem. Biophys. Res. Comm.* **19**, 340 (1965).

(32) Voigt, W., Hsia, S. L., *Federation Proc.* **26**, 341 (1967).

(33) Warburg, O., "Heavy Metal Prosthetic Groups and Enzyme Action," Clarendon Press, Oxford, 1949.

(34) Wilson, J. E., Ober, R. E., Vestling, C. S., *Arch. Biochem. Biophys.* **114**, 166 (1966).

Discussion

F. C. Yong: We have some evidence which suggests that the conformation of the enzyme P-450 depends on the oxidation state of the

heme-iron. In collaboration with Dr. Mason's group, we have studied the optical rotatory dispersion properties of the enzyme in 50% glycerol phosphate buffer. The oxidized form showed a simple Cotton effect whose crossover point corresponded quite closely to the Soret absorption maximum of the enzyme. Upon reduction, the Cotton effect was practically abolished, giving a levorotatory dispersion corresponding to the protein backbone rotation.

The Role of Heme in the Tryptophan Pyrolase Reaction

YUZURU ISHIMURA, MITSUHIRO NOZAKI, and OSAMU HAYAISHI

Department of Medical Chemistry, Kyoto University Faculty of Medicine, Kyoto, Japan

MAMORU TAMURA and ISAO YAMAZAKI

Biophysics Division, Research Institute of Applied Electricity, Hokkaido University, Sapporo, Japan

Ferrous tryptophan pyrolase, when mixed with oxygen in the presence of tryptophan, showed a new spectrum which was caused by neither the ferrous nor ferric state of the heme in the enzyme. The spectral characteristics of the new species (λ_{max}: 415, 545, and 580 mμ), together with its absolute dependency upon oxygen, indicated that the new spectrum was caused by oxygenated heme in the enzyme. In the absence of tryptophan, this spectrum was not observed. There was evidence that a combination of tryptophan with the enzyme resulted in an increased reactivity of its heme towards ligands such as cyanide and CO. The significance of these findings in terms of the catalytic reaction mechanism is discussed.

Tryptophan pyrolase (tryptophan 2,3-dioxygenase) catalyzes the conversion of L-tryptophan to formylkynurenine and has been isolated from mammalian liver and *Pseudomonas* (*5, 12*). Hayaishi *et al.* (*6*) showed by using the heavy isotope of oxygen that this enzyme is an oxygenase. Tanaka and Knox (*16*) identified this enzyme as an iron-porphyrin protein using partially purified preparations from *Pseudomonas* as well as from rat liver. Subsequently, Feigelson and Greengard found that an inactive apo-enzyme could be obtained from rat liver, and the catalytic activity was restored upon adding exogeneous hematin (*3, 4*). However, the detailed mechanism of the catalytic process, especially the role of the heme, remained uncertain and has been the subject of controversy (*7, 11, 13, 14, 17*).

This paper describes a summary of our recent studies on the mechanism of the tryptophan pyrrolase reaction. Particular emphasis is placed on the role of heme as oxygen binding site.

Results and Discussion

Tryptophan pyrrolase was purified about 200-fold from cells of *Pseudomonas fluorescens* grown on L-tryptophan as described previously (9). The purified enzyme exhibited absorption spectra characteristic of a high spin hemoprotein both in its ferric state (λ_{max}: 405, 500, and 635 mμ) and ferrous state (λ_{max}: 432, 553, and 588 mμ) as shown in Figure 1. We confirmed the finding of Maeno and Feigelson (14) that adding tryptophan either to the ferric or to the ferrous enzyme results in slight shifts of the Soret bands. This indicates that tryptophan combines with enzyme irrespective of the valence state of the heme.

The purified enzyme had practically no catalase or peroxidase activity, as measured by the spectrophotometric method of Chance (1) and by the pyrogallol test (2), respectively.
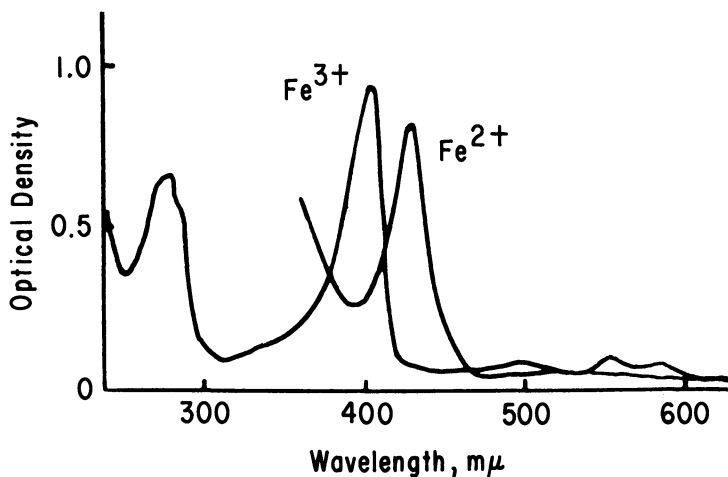
Figure 1. Absorption spectra of tryptophan pyrrolase. 0.96 mg. of tryptophan pyrrolase (specific activity 5.7) and 200 μmoles of potassium phosphate buffer, pH 7.0, in 1.6 ml.

Valence State of Heme in Active Tryptophan Pyrrolase. The purified enzyme was found to be active in its ferrous form, whereas it was almost inactive in its ferric form. The ferric enzyme could be activated by adding an appropriate amount of ascorbate (Figure 2) or hydrogen peroxide in the presence of tryptophan as originally reported (16). These
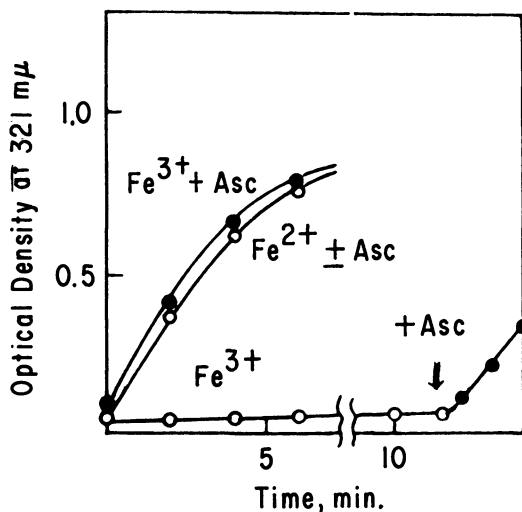
Figure 2. Effect of ascorbate (Asc) on the activity of tryptophan pyrrolase. Fe^{3+}, ferric enzyme; Fe^{2+}, ferrous enzyme

activators are known to reduce the ferric enzyme to the ferrous enzyme in the presence of tryptophan (*16*).

We reported previously that the enzyme was reduced and activated by light under anaerobic conditions (*7, 8*). This finding was confirmed by Maeno and Feigelson (*14*). Using this phenomenon, we examined further the above-mentioned relationship between the redox state of the heme and the activity. As represented in Figure 3, reduction of the heme resulted in a proportional increase in the activity. Thus, the ferrous form is an active species of tryptophan pyrrolase.

State of Heme during the Reaction. As we previously reported, when the valence state of heme in the enzyme was examined, a new spectrum in the Soret region appeared during the steady state of the reaction. This spectrum could not be ascribed to either ferric heme, ferrous heme, or a mixture of these and indicated the presence of a transient intermediate (*7, 8*). This finding was further extended in the following experiments (*10*), carried out at 5°C. to slow down the reaction rate. We used a special cuvette which allowed a continuous supply of oxygen through bubbling without interference in the optical measurements. When oxygen was bubbled into a mixture of ferrous enzyme and tryptophan, a new spectral species with absorption maxima at 415, 545, and 580 mμ appeared immediately (Figure 4). The absorption maxima of the new species were found to be similar to those of known oxygenated hemoproteins such as hemoglobin, myoglobin, and peroxidase. When

the bubbling of oxygen was discontinued, the spectrum reverted almost instantaneously to that of the ferrous state. This process could be repeated until all the tryptophan in the system had been consumed. With ferric enzyme in the presence of tryptophan, no such spectral changes were observed. Taken together, the above results indicate strongly that the new species is an oxygenated form of tryptophan pyrrolase.
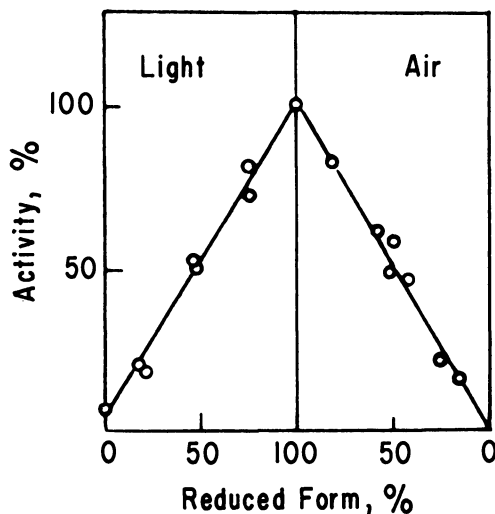
Figure 3.   Relationship of the redox state of the heme in tryptophan pyrrolase to the activity of the enzyme

When oxygen was introduced to the ferrous enzyme in the absence of tryptophan, the spectrum converted very slowly to that of ferric enzyme, showing an isosbestic point at 416 mμ, in contrast to the immediate spectral change owing to oxygenation observed in the presence of tryptophan. Thus, the formation of the intermediate depends on the simultaneous presence of ferrous heme and the substrate, tryptophan.

Activation of Enzyme Heme by Tryptophan. The above-mentioned requirement of tryptophan for the oxygenation of enzyme suggested that the reactivity of the heme toward oxygen is altered by combination with tryptophan. This hypothesis was examined further by using heme-binding substances such as cyanide and CO instead of oxygen. As shown in Figure 5, the affinity of the ferric enzyme toward cyanide was remarkably augmented by the presence of tryptophan. The concentrations required for half-maximal conversion of the ferric enzyme to the cyanide complex were $1.5 \times 10^{-6}M$ and $2.8 \times 10^{-4}M$ in the presence and absence of tryptophan, respectively. The corresponding values for the complex
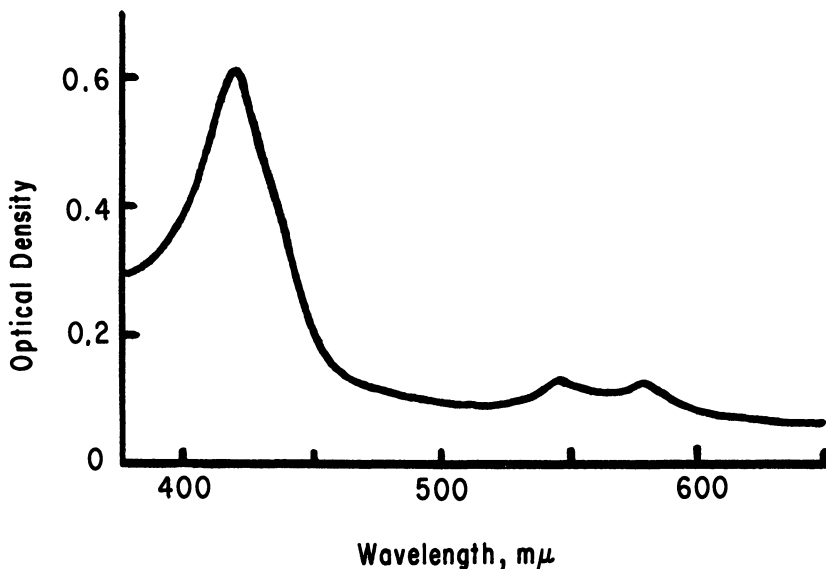
Figure 4. Oxygenated form of tryptophan pyrrolase. Spectrum was recorded during the continuous bubbling of oxygen to the reaction mixture at 5°C. Reaction mixture contained ferrous tryptophan pyrrolase (specific activity 3.7), 11.4 mg.; L-tryptophan, 50 μmoles; potassium phosphate buffer, pH 7.0, 500 μmoles, in a final volume of 5.0 ml.
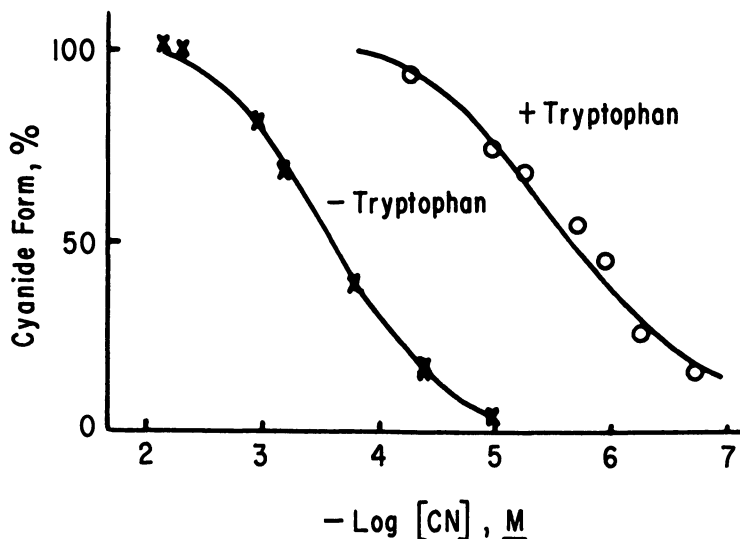
Figure 5. Conversion of the ferric enzyme to cyanide complex in the presence and absence of tryptophan. Reaction mixture contained tryptophan pyrrolase, 0.47 mg. (specific activity 2.5); potassium phosphate buffer, pH 7.0, 1.1. mmoles; L-tryptophan, 0.28 mmoles in a final volume of 28 ml. Cyanide was added in the presence (O) and absence (×) of tryptophan as indicated

of the ferrous enzyme and CO were $5 \times 10^{-6}M$ and $2.8 \times 10^{-4}M$ in the presence and absence of tryptophan, respectively.

Reaction Mechanism. The following reaction mechanism is compatible with the above data. Tryptophan first combines with ferrous enzyme and activates the heme in the enzyme. The activated enzyme then reacts with oxygen to form an intermediary ternary complex. Both substrates, tryptophan and oxygen, are activated in the complex and interact, yielding formylkynurenine as product.

Recently, Maeno and Feigelson (14) proposed a reaction mechanism which postulates the participation of ferric enzyme in the catalytic process. Their postulate is based mainly on the observation that no ferrous enzyme was formed during the steady state of catalysis. However, this does not necessarily mean that the enzyme is in the ferric state. The present data have revealed that the enzyme is mainly in an oxygenated state during the reaction.

The oxygenated iron compound reported here requires much more detailed characterization. Nevertheless, our findings are quite consistent with the view that dioxygenase reactions in general involve a ternary complex of enzyme, oxygen, and organic substrate (7, 15). The role of tryptophan in the complex is now under investigation.

Literature Cited

(1) Chance, B., "Methods of Biochemical Analysis," D. Glick, Ed., Vol. 1, p. 408, Interscience, New York, 1954.
(2) Chance, B., Maehly, A. C., "Methods in Enzymology," S. P. Colowick, N. O. Kaplan, Eds., Vol. 2, p. 764, Academic Press, New York, 1955.
(3) Feigelson, P., Greengard, O., *Biochim. Biophys. Acta* **50**, 200 (1961).
(4) Greengard, O., Feigelson, P., *J. Biol. Chem.* **237**, 1903 (1962).
(5) Hayaishi, O., Stanier, R. Y., *J. Bacteriol.* **62**, 691 (1951).
(6) Hayaishi, O., Rothberg, S., Mehler, A. H., Saito, Y., *J. Biol. Chem.* **229**, 889 (1957).
(7) Hayaishi, O., *Proc. Intern. Congr. Biochem., 6th, 1964,* p. 31.
(8) Ishimura, Y., Hayaishi, O., *J. Japan Biochem. Soc.* **36**, 502 (1964).
(9) Ishimura, Y., Okazaki, T., Nakazawa, T., Ono, K., Nozaki, M., Hayaishi, O., "Biological and Chemical Aspects of Oxygenases," K. Bloch, O. Hayaishi, Eds., p. 416, Maruzen Co., Tokyo, 1966.

(10) Ishimura, Y., Nozaki, M., Hayaishi, O., Tamura, M., Yamazaki, I., *J. Biol. Chem.* **242,** 2574 (1967).

(11) Knox, W. E., Tokuyama, K., "Oxidases and Related Redox Systems," T. E. King *et al.*, Eds., Vol. 1, p. 514, Wiley, New York, 1965.

(12) Kotake, Y., Masayama, T., *Z. Physiol. Chem.* **243,** 237 (1936).

(13) Maeno, H., Feigelson, P., *Biochem. Biophys. Res. Commun.* **21,** 297 (1965).

(14) Maeno, H., Feigelson, P., *J. Biol. Chem.* **242,** 596 (1967).

(15) Nakazawa, T., Kojima, Y., Fujisawa, H., Nozaki, M., Hayaishi, O., Yamano, T., *J. Biol. Chem.* **240,** PC3224 (1965).

(16) Tanaka, T., Knox, W. E., *J. Biol. Chem.* **234,** 1162 (1959).

(17) Tokuyama, K., Knox, W. E., *Biochim. Biophys. Acta* **81,** 201 (1964).

Role of Iron in Dioxygenase Reactions

MITSUHIRO NOZAKI, TERUKO NAKAZAWA, HITOSHI FUJISAWA, SHIGEKO KOTANI, YUTAKA KOJIMA, and OSAMU HAYAISHI

Department of Medical Chemistry, Kyoto University Faculty of Medicine, Kyoto, Japan

Physicochemical and kinetic analyses of dioxygenases, including metapyrocatechase, pyrocatechase, and protocatechuate 3,4-dioxygenase, suggest that the number of iron atoms in the enzymes coincide with the number of subunits and with the number of substrate molecules that bind to the enzyme. These enzymes may consist of several subunits, each of which contains one atom of iron, and all of the iron in the total molecule participates in these enzyme reactions as a part of the substrate binding sites. The suggested reaction mechanism for these dioxygenases is that the enzyme combines with organic substrate first and then reacts with oxygen to form an oxygenated end product.

A major reaction of the dioxygenases is the cleavage of various aromatic rings with the insertion of two atoms of molecular oxygen. Several dioxygenases, including metapyrocatechase (catechol 2,3-dioxygenase) and protocatechuate 3,4-dioxygenase, have recently been obtained in a crystalline form in our own and other laboratories (*1, 2, 6, 10*). When dihydroxyphenyl compounds are cleaved by the action of individual dioxygenases, two general modes of ring fission have so far been demonstrated: intradiol-type and extradiol-type (*9, 12*). Iron has been found to be a sole cofactor of these dioxygenases, and its role in their reactions has been extensively studied (*9, 11, 12, 14*). Electron spin resonance (ESR) and chemical analyses of these two types of enzymes revealed that the intradiol-type enzymes such as pyrocatechase (catechol 1,2-dioxygenase) and protocatechuate 3,4-dioxygenase contain the ferric form of iron, and the extradiol-type enzymes such as metapyrocatechase contain the ferrous form of iron (*11, 12*). We have previously suggested that iron in these dioxygenases is intimately involved in their catalytic

functions as an interacting site of substrates, regardless of the valence of the iron (*11, 12*).

Here we present further evidence to support the above proposal and a possible reaction mechanism of dioxygenases by which the enzyme first combines with an organic substrate to form a binary complex and then reacts with oxygen to yield an oxygenated end product.

Results and Discussion

Iron Content and Interaction with Substrate. METAPYROCATECHASE. Crystalline metapyrocatechase was obtained from a strain of *Pseudomonas arvilla* by the method previously described (*10*). The enzyme catalyzes the conversion of catechol by extradiol cleavage to α-hydroxymuconic ε-semialdehyde with the insertion of two atoms of molecular oxygen (Reaction 1).

$$\text{(structure with } OH, OH) + O_2 \longrightarrow \text{(structure with } OH, COOH, CHO) \tag{1}$$
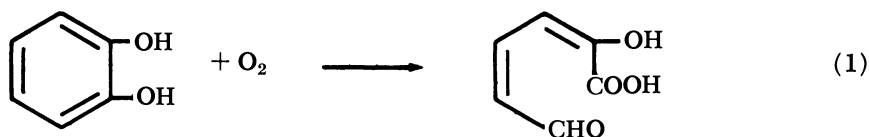
The enzyme contained three atoms of iron per molecule of the enzyme (molecular weight = approximately 140,000). All the iron in the native enzyme was shown to be in the divalent state, by ESR and colorimetric determinations. The enzyme was easily inactivated by an equimolar amount of H_2O_2 preincubated with the enzyme. Evidence indicates that inactivation is caused by simple oxidation of the ferrous ion to its ferric form (*13*). As Figure 1 shows, however, inactivation of the enzyme was completely counteracted by the presence of substrate, catechol. The reaction mixture contained 50 m*M* potassium phosphate buffer, pH 7.5, about 10 μgrams of dialyzed enzyme, 5 μ*M* H_2O_2, and catechol (concentrations as indicated), in a final volume of 1.0 ml. All incubations were carried out at 24°C. for 10 minutes under anaerobic conditions. Activities were measured by the standard assay method (*10*) with an aliquot of the mixture.

The concentration of catechol required for half-maximal counteraction is estimated to be 8×10^{-6} *M*, which is of the same order as the *Km* value, 5×10^{-6} *M*, suggesting that the organic substrate interacts with the iron in the enzyme.

PYROCATECHASE. Pyrocatechase which catalyzes an oxygenative intradiol cleavage of catechol to form *cis,cis*-muconic acid (Reaction 2), was purified from cells of *Pseudomonas arvilla C-1* according to the method previously described (*7*). The native enzyme was found to con-

$$\text{(catechol)} + O_2 \longrightarrow \text{(muconic acid)} \qquad (2)$$

tain two atoms of iron per molecule of the enzyme, whose molecular weight was estimated as 95,000 (7). The enzyme shows a distinct red color with a broad absorption peak at around 440 mμ and a sharp ESR signal at $g = 4.2$. The red color and the ESR signal were interpreted to arise from ferric form of iron bound to the enzyme (7, 11). Upon adding substrate (catechol) to the native enzyme under anaerobic conditions, the visible absorption spectrum of the enzyme showed an increase in absorbance at around 710 mμ (Figure 2A), with simultaneous disappearance of the ESR signal. When oxygen was admitted and the substrate was exhausted, the optical and ESR spectra were reversed to the original ones. These changes could be observed repeatedly by the alternate addition of catechol and oxygen and are probably caused by a modification of the ligand structure of the iron caused by its interaction with organic substrate (11). In contrast, no significant differences in the optical and ESR spectra of the enzyme were observed in the absence and presence of the other substrate, oxygen.
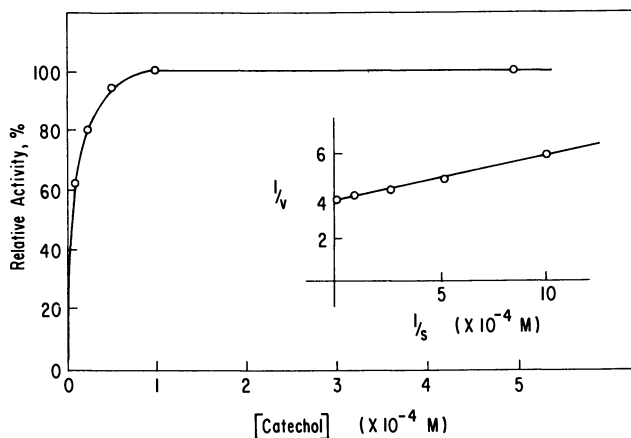
Figure 1.   Protection by catechol against H₂O₂ inactivation of metapyrocatechase

PROTOCATECHUATE 3,4-DIOXYGENASE. Crystalline preparations of the enzyme were obtained as described previously (2). The enzyme catalyzes the intradiol cleavage of protocatechuic acid with the insertion of two atoms of molecular oxygen to form β-carboxy *cis,cis*-muconic acid (Reaction 3).

$$+ O_2 \longrightarrow \qquad\qquad (3)$$
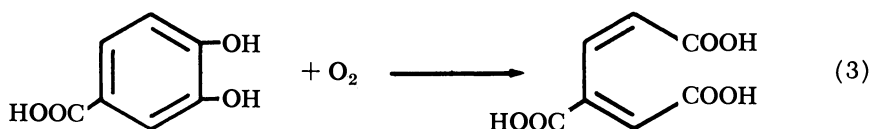
The enzyme was found to contain about eight atoms of iron per molecule of enzyme (molecular weight 700,000), and the iron seemed to be in the trivalent state (3). The enzyme showed an absorption spectrum and ESR signal similar to those of pyrocatechase. The increase in the visible absorption and the disappearance of the ESR signal were also caused by adding substrate (protocatechuic acid). A similar spectral change was also observed when protocatechualdehyde, a competitive inhibitor, was added to the enzyme. Figure 2B shows the absorption spectra of native enzyme and its complex with substrate.
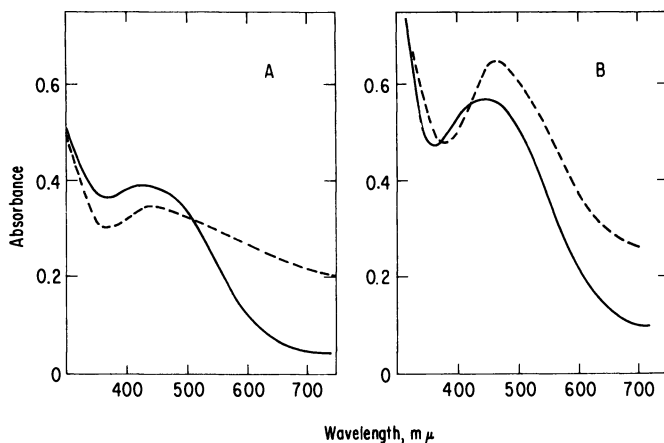
Figure 2. Visible absorption spectra

A. *Pyrocatechase*
B. *Protocatechuate 3,4-dioxygenase*
        — *Native enzyme*
        - - - *After adding 1μ mole of each substrate*
Protein concentrations in final volume of 3.0 ml., pH 8.0
        Pyrocatechase 24 mg.
        Protocatechuate 3,4-dioxygenase, 53 mg.

These results, together with other evidence described elsewhere (3, 8), suggest that during catalysis iron in the dioxygenases, irrespective of its valence, is intimately involved in the substrate binding sites.

Number of Substrate Molecules Bound to Enzyme. The number of substrate molecules bound to metapyrocatechase was determined by equilibrium dialysis.

One-half ml. each of approximately $4.5 \times 10^{-5}M$ metapyrocatechase (MPC) was dialyzed for 15 hours at 24°C. against 15 ml. of 50 mM potassium phosphate buffer, pH 7.5, containing 0.2M NaCl and catechol (concentrations as indicated) under strict anaerobic conditions. After dialysis, concentrations of catechol in inner and outer solutions were determined enzymatically with metapyrocatechase. Equilibrium dialysis of approximately $8.5 \times 10^{-5}M$ bovine serum albumin (BSA) was also carried out in a manner entirely analogous to metapyrocatechase.

As shown in Figure 3, 2 to 3 moles of substrate combined with the enzyme during equilibrium dialysis against different concentrations of catechol under anaerobic conditions. Assuming 2 moles of substrate bound to the enzyme at equilibrium, the dissociation constant of the enzyme-substrate complex was similar to or rather smaller than the Km value obtained by rate measurement. Bovine serum albumin did not combine with catechol under the same conditions. These results suggest that the complex is not caused by nonspecific binding but is involved in the catalytic reaction.
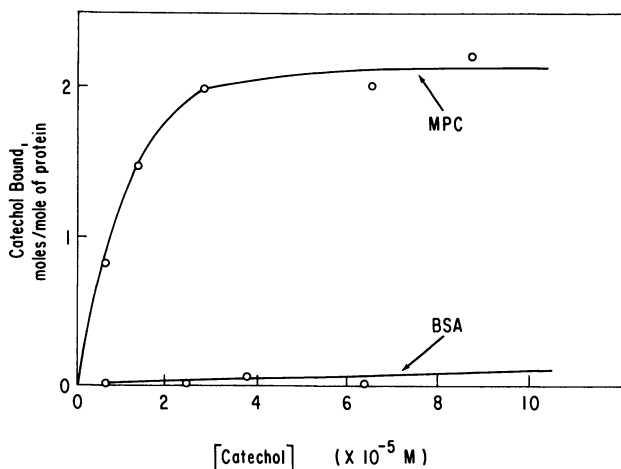
Figure 3.   Equilibrium dialysis of metapyrocatechase

When pyrocatechase was titrated with the substrate catechol under anaerobic conditions, about 1.6 moles of catechol per mole of enzyme were required to bring about maximum increase in absorbance at 710 mμ, suggesting that 2 moles of catechol can combine with the enzyme (Figure 4 A). Similarly, when protocatechuate 3,4-dioxygenase was titrated with protocatechualdehyde, a competitive inhibitor, under aerobic conditions, approximately 8 moles of the compound per mole of enzyme were required to cause a maximal increase in absorption, suggesting that 8 moles of substrate can combine with the enzyme (Figure 4 B).
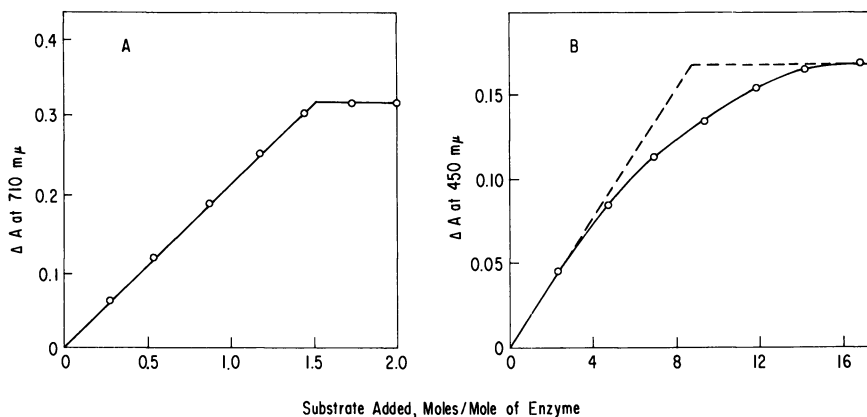
Figure 4. Titration

A. $2 \times 10^{-4}M$ pyrocatechase in 0.05M tris-HCl buffer, pH 8.0, titrated with catechol under anaerobic conditions
B. $1.42 \times 10^{-5}M$ protocatechuate 3,4-dioxygenase in 0.05M tris-HCl buffer, pH 8.5, titrated with protocatechualdehyde under aerobic conditions

Subunit Structure of Enzyme. Determination of the N-terminal amino acid in metapyrocatechase revealed that it contains about 2 moles of serine per mole of the enzyme, indicating that the enzyme consists of at least two peptide chains. Ultracentrifugal and diffusion analyses of the enzyme suggested that it was dissociated in 0.03N NaOH into two to three subunits. Likewise, protocatechuate 3,4-dioxygenase (19.4s) was dissociated into small subunits (5.0s) in 0.05N NaOH, and electron microscope observation of the enzyme suggested that it consists of eight subunits.

Iron content, number of substrate binding sites, and number of subunits of these dioxygenases are summarized in Table I.

Table I. Properties of Dioxygenases

	Metapyrocatechase	Pyrocatechase	Protocatechuate 3,4-Dioxygenase
Type of reaction	Extradiol	Intradiol	Intradiol
Molecular weight	140,000	95,000	700,000
Valence of iron	Ferrous	Ferric	Ferric
Iron content, atoms/mole of enzyme	3	2	8
No. of subunits	2 to 3	—	~8 [a]
Substrate bound to enzyme, moles of substrate/mole of enzyme	2 to 3	~2	~8

[a] Electron microscope observation.

These results indicate that the number of iron atoms in these dioxygenases may coincide with the number of subunits and the number of substrate binding sites. Although attempts to obtain an active subunit have so far been unsuccessful, it is plausible to assume that each subunit of enzyme contains one atom of iron and that all of the iron in the total molecule participates in these enzyme reactions as a part of the substrate binding sites. This explanation is consistent with our previous proposal that iron interacts with both organic substrate and oxygen during catalyses (4, 11), but is inconsistent with the interpretation by Senoh's group concerning the action of 3,4-dihydroxyphenylacetate 2,3-oxygenase. They reported that the enzyme contains 4 atoms of iron per mole of enzyme and that some of the iron atoms participate in the aggregation of the subunits, although at least one of them is involved in enzyme activity (14).

Reaction Mechanism of Dioxygenase. According to Weiss (15), oxygen preferentially combines with ferrous ion to form $Fe^{2+}O_2$, which is in equilibrium with $Fe^{3+}O_2^-$. On the other hand, ferric ion easily forms a complex with catechol. On the basis of these theoretical considerations, we postulated in a previous paper (11) a sequential reaction mechanism for dioxygenases as follows. Pyrocatechase, a ferric ion containing enzyme, combines with catechol, resulting in the reduction of the iron, and then reacts with oxygen to form a ternary complex, which subsequently yields an oxygenated end product. On the other hand, metapyrocatechase, a ferrous ion–containing enzyme, reacts with oxygen first and then with substrate to form a product.

To test the validity of the above hypothesis, we have attempted to demonstrate the existence of an oxygenated form of metapyrocatechase. Oxyhemoglobin is an oxygenated form of hemoglobin and should contain one mole of oxygen per mole of heme in the protein. Accordingly, the total oxygen content in an oxyhemoglobin solution which is equilibrated with air at a fixed temperature should be the sum of dissolved oxygen and oxygenated oxygen to the heme. When metapyrocatechase and catechol were added to an oxyhemoglobin solution in a closed system, all the oxyhemoglobin was converted to the deoxygenated hemoglobin, judging from the spectra. This indicates that the oxygenating oxygen was utilized for the metapyrocatechase reaction to form a product, α-hydroxymuconic ϵ-semialdehyde. Therefore, from the amount of the product formed, it is possible to determine the total oxygen content of an oxyhemoglobin solution. As expected, the total oxygen content in an oxyhemoglobin solution, determined as mentioned above, is proportional to the amount of the protein added (Figure 5).

To an oxyhemoglobin solution (2.5 ml.) which was equilibrated with air, 10 μmoles of catechol and about 100 μgrams of metapyrocatechase were added in a closed system. The reactions were carried out in a
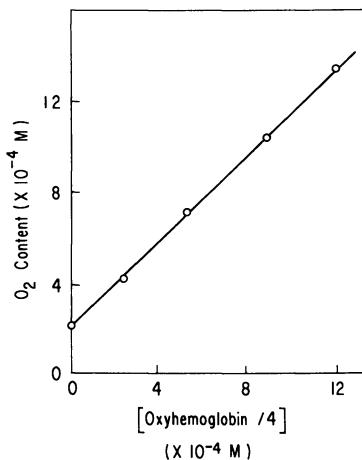
*Figure 5. Total oxygen content
of oxyhemoglobin solution*

syringe at 20°C. When the reaction was complete (about 2 minutes), an aliquot of the mixture was transferred to 1M trichloroacetic acid solution, avoiding contact with air. After removing protein and neutralizing the supernatant, the amount of product α-hydroxymuconic ϵ-semialdehyde was determined spectrophotometrically at 375 mμ.

If the oxygenated form of metapyrocatechase is similar to that of hemoglobin, it would be possible to demonstrate this by the same technique.

To a metapyrocatechase solution in 0.05M potassium phosphate buffer, pH 7.5 (approximately 2.5 ml.), which was equilibrated with air 5 μmoles of catechol were added in a closed system. The reactions were carried out in a cuvette with a 0.5-cm. light path at 24°C. The cuvette was filled with reaction mixture and covered with a glass plate to avoid contact with air. The product formed was directly determined spectrophotometrically at 430 mμ.

Figure 6, in which the dashed line indicates a theoretical curve assuming that one mole of oxygen combines with a mole of the enzyme, shows that the total oxygen content in a metapyrocatechase solution does not depend on the enzyme added but is the same as that of dissolved oxygen in a buffer solution. Furthermore, no oxygenated form of the enzyme has been detected in the presence of a substrate analog or a competitive inhibitor such as o-aminophenol, o-phenylenediamine, or m-phenanthroline. These results indicate that free metapyrocatechase cannot be oxygenated, or else that its oxygenated form is not as stable as oxyhemoglobin.

On the other hand, as discussed above, organic substrate can combine with these enzymes regardless of the presence of oxygen. These
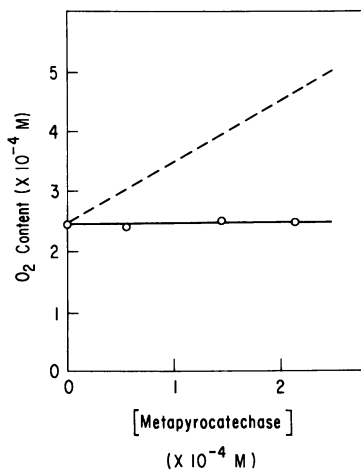
Figure 6.   Total oxygen content
of metapyrocatechase solution

observations are consistent with the explanation that the organic substrate combines with the enzyme first, irrespective of the valence of the iron, and then reacts with oxygen to form an oxygenated end product. This explanation is compatible with that of tryptophan pyrrolase, a heme-containing dioxygenase, in which the enzyme combines with tryptophan first, resulting in an increase in reactivity of heme. Subsequently, the binary complex reacts with oxygen to form a ternary complex; tryptophan-enzyme-oxygen, which has been spectrophotometrically characterized as an oxygenated intermediate (5).

An oxygenated intermediate of the nonheme iron-containing dioxygenases has never been detected as a discernible entity, so that the interaction between enzyme and oxygen remains to be elucidated. However, the iron appears to be involved in a binding site for organic substrate. It is plausible to assume that oxygen, too, combines with the iron, forming a ternary complex of iron, oxygen, and organic substrate during the enzyme reaction. To clarify this interaction, kinetic analyses of the enzyme reaction are being undertaken in our laboratory.

Acknowledgment

Literature Cited

(1) Adachi, K., Iwayama, Y., Tanioka, H., Takeda, Y., *Biochim. Biophys. Acta* **118,** 88 (1966).

(2) Fujisawa, H., Hayaishi, O., *J. Biol. Chem.*, in press.

(3) Fujisawa, H. *et al.*, unpublished data.

(4) Hayaishi, O., *Proc. Plenary Sessions, Intern. Congr. Biochem.*, 6th, *New York,* **1964,** 31.

(5) Ishimura, Y., Nozaki, M., Hayaishi, O., Tamura, M., Yamazaki, I., *J. Biol. Chem.* **242,** 2574 (1967).

(6) Kita, H., Kamimoto, M., Senoh, S., Adachi, K., Takeda, Y., *Biochem. Biophys. Res. Commun.* **18,** 66 (1965).

(7) Kojima, Y., Fujisawa, H., Nakazawa, A., Nakazawa, T., Kanetsuna, F., Taniuchi, H., Nozaki, M., Hayaishi, O., *J. Biol. Chem.* **242,** 3270 (1967).

(8) Nakazawa, T. *et al.*, unpublished data.

(9) Nozaki, M., Fujisawa, H., Kotani, S., *Proc. Intern. Congr. Biochem.*, 7th, *Tokyo,* 1967, p. 565.

(10) Nozaki, M., Kagamiyama, H., Hayaishi, O., *Biochem. Z.* **338,** 582 (1963).

(11) Nakazawa, T., Kojima, Y., Fujisawa, H., Nozaki, M., Hayaishi, O., Yamano, T., *J. Biol. Chem.* **240,** PC3224 (1965).

(12) Nozaki, M., Kojima, Y., Nakazawa, T., Fujisawa, H., Ono, K., Kotani, S., Hayaishi, O., Yamano, T., "Biological and Chemical Aspects of Oxygenases," K. Bloch and O. Hayaishi, eds., p. 347, Maruzen Co., Japan, 1966.

(13) Nozaki, M., Ono, K., Nakazawa, T., Kotani, S., Hayaishi, O., *J. Biol. Chem.*, in press.

(14) Senoh, S., Kita, H., Kamimoto, M., "Biological and Chemical Aspects of Oxygenases," K. Bloch and O. Hayaishi, eds., p. 378, Maruzen Co., Japan, 1966.

(15) Weiss, J. J., *Experientia* **9,** 61 (1953).

80

A New Ring Cleavage Enzyme : 2,3-Dihydroxybenzoate Oxygenase

DOUGLAS W. RIBBONS[1] and ROBERT J. WATKINSON

Milstead Laboratory of Chemical Enzymology, "Shell" Research, Ltd., Broad Oak Road, Sittingbourne, Kent, England

2,3-Dihydroxybenzoate is oxidized by extracts of Pseudomonas fluorescens *with the consumption of one mole of oxygen per mole of substrate. An equivalent amount of carbon dioxide is evolved, and α-hydroxymuconic semialdehyde is formed. Intermediates between 2,3-dihydroxybenzoate and α-hydroxymuconic semialdehyde have not been detected, nor has the site of ring cleavage been established. The enzyme is inactivated rapidly by air and other oxidants, but the activity may be restored by anaerobic incubation of the enzyme with reducing agents or Fe^{2+} ions. The enzyme is inhibited by iron chelating agents such as α,α'-dipyridyl.*

2,3-Dihydroxybenzoate occurs as a metabolite of plants and microorganisms (8, 16). Certain fungi decarboxylate it to catechol after which it is oxygenated and converted by known pathways to 3-oxoadipate (11, 14). *Pseudomonas fluorescens,* however, utilizes 2,3-dihydroxybenzoate as its sole carbon source and cleaves the benzenoid ring of this substrate (9). The enzyme(s) catalyzing the oxygenation of 2,3-dihydroxybenzoate to α-hydroxymuconic semialdehyde is named 2,3-dihydroxybenzoate oxygenase; a preliminary report has described the stoichiometry of the reaction(s) (9).

Extracts of *Pseudomonas fluorescens* 23D-1, grown in the presence of 2,3-dihydroxybenzoate, catalyze the rapid oxidation of 2,3-dihydroxybenzoate to a yellow acidic intermediate with the spectral characteristics of α-hydroxymuconic semialdehyde (2, 5), which is also the product of the oxidation of catechol by catechol 2,3-oxygenase. Carbon dioxide is also evolved during dihydroxybenzoate oxidation in amounts equivalent to those of the substrate added to the enzyme (Table I).

[1] Permanent address: Department of Biochemistry, School of Medicine, P. O. Box 875, Biscayne Annex, University of Miami, Miami, Fla. 33152.

Table I.   **Stoichiometry of Gaseous Exchange during 2,3-Dihydroxybenzoate Oxidation**

2,3-Dihydroxybenzoate Supplied, μmoles	Oxygen Consumed, μmoles	Carbon Dioxide Evolved, μmoles
5	4.9	4.7
10	9.9	9.8
10	10.2	9.7

The product, α-hydroxymuconic semialdehyde, was isolated and characterized from a large scale incubation. Its elemental analysis, infrared, ultraviolet and visible absorption spectra, and its rapid decomposition to pyruvate by extracts of *Pseudomonas aeruginosa* T1 (*10*) are all consistent with this structure.

Intermediates between 2,3-dihydroxybenzoate and α-hydroxymuconic semialdehyde have not been detected. It is evident, however, that catechol is not an intermediate in the formation of 2,3-dihydroxybenzoate since extracts catalyze neither its formation anaerobically from 2,3-dihydroxybenzoate nor its oxidation. In fact, catechol is an inhibitor of 2,3-dihydroxybenzoate oxygenase. The exclusion of catechol as intermediate in this metabolic transformation leaves two possibilities: (a) decarboxylation and oxygenation of the benzene nucleus are simultaneous, yielding α-hydroxymuconic semialdehyde directly, or (b) oxygenation precedes decarboxylation, and a second oxo-acid is intermediate.

Our results so far do not differentiate between these possibilities. When purified extracts are oxidizing 2,3-dihydroxybenzoate, the rates of oxygen consumption, carbon dioxide evolution, and α-hydroxymuconic semialdehyde formation cannot be distinguished (Figure 1). With either possibility, the site of ring cleavage remains to be determined. As seen in Figure 2, cleavage of the nucleus between carbon atoms 3 and 4 would yield an oxo-acid, which could decarboxylate at carbon atom 7 to yield α-hydroxymuconic semialdehyde. Cleavage of 2,3-dihydroxybenzoate between carbon atoms 1 and 2 would yield a dioxodicarboxylic acid that could decarboxylate at either end of the carbon chain to give α-hydroxymuconic semialdehyde with its carbon atoms differently derived.

Stability of 2,3-Dihydroxybenzoate Oxygenase

The enzyme is usually unstable in air in both crude extracts and purified fractions. Loss of activity is attributed to oxidation and is fairly common to oxygenases of this type (*13*). The oxidation may be induced by oxygen itself since preparations are more stable if stored under nitrogen or *in vacuo* or by the oxidized form of some of the usual sulfhydryl-
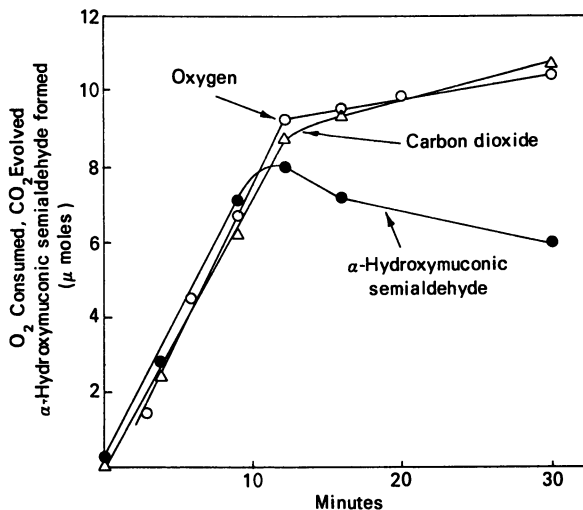
Figure 1. 2,3-Dihydroxybenzoate oxidation by partially purified extracts of Pseudomonas fluorescens

Each Warburg flask contained: 20% KOH in the center well (0.2 ml.) during measurements of oxygen consumption, or 2N H_2SO_4 in the second sidearm (0.2 ml.) for determining carbon dioxide evolved; 25mM 2,3-dihydroxybenzoate in sidearm (0.2 ml.); 0.067 M-KH_2PO_4, pH 7.1 (0.6 ml.); and enzyme solution (1 ml. of a P-300 eluate fraction). Oxygen consumption was followed in duplicate flasks, and acid was tipped into the others at the times indicated. Portions of the arrested reaction mixtures were taken to determine α-hydroxymuconic semialdehyde formation spectrophotometrically

protecting reagents such as mercaptoethanol. This is based on evidence that the rate of inactivation by mercaptoethanol is greatly accelerated by adding factor B [which catalyzes the autoxidation of mercaptoethanol (7) (Figure 3)]. Hydrogen peroxide has been suggested as the inactivator under similar circumstances (6), but the product of factor B catalyzed oxidation of mercaptoethanol is not hydrogen peroxide but water (7). Activity of the enzyme may be restored by various reducing reagents, usually by preincubation under anaerobic conditions. The more successful of these has been anaerobic incubation with sodium borohydride, cysteine, Fe^{2+}, and ascorbate. Ascorbate will also give quick reactivation by aerobic incubation which led to the inclusion of ascorbate in the assay system. The response of different batches of enzyme to reactivation by various reducing agents is quite variable.

Purification of 2,3-Dihydroxybenzoate Oxygenase

Table II shows the steps used in purifying 2,3-dihydroxybenzoate oxygenase.

The cells were harvested by centrifugation, washed with 0.01*M* tris buffer pH 7.0 and stored as cell pastes at −14°C. until required. Crude extracts were prepared by suspending cells in 0.01*M* tris buffer pH 7.0 (0.5 gram wt. wt./ml.) and disrupting with an MSE 100 watt ultrasonic disintegrator for 2 minutes and centrifuging at 5000 *g* for 15 minutes. High speed supernatants of extracts were prepared by centrifuging crude extracts at 100,000 *g* for 2 hours.

2,3-Dihydroxybenzoate was assayed at 30°C. in a fully automated Unicam SP800 spectrophotometer at 430 mμ. The reaction cuvettes contained: 0.067*M* phosphate buffer, pH 7.1 (2.5 ml.); 25 m*M* 2,3-dihydroxybenzoate (20 μliters); enzyme solution (as required but usually between 5 and 50 μliters). Under these conditions the molar extinction coefficient of α-hydroxymuconic semialdehyde at 430 mμ is 3.2×10^3. The assays were conducted at 430 mμ because this is a more convenient wavelength when simultaneous measurements of oxygen consumption and product formation are made, although it is much less sensitive an assay than that used by Kojima *et al.* (5).

Properties of 2,3-Dihydroxybenzoate Oxygenase

The purest preparations obtained catalyze the formation of 7.3 μmoles of α-hydroxymuconic semialdehyde/min./mg. protein after reactivation with NaBH$_4$, anaerobically.
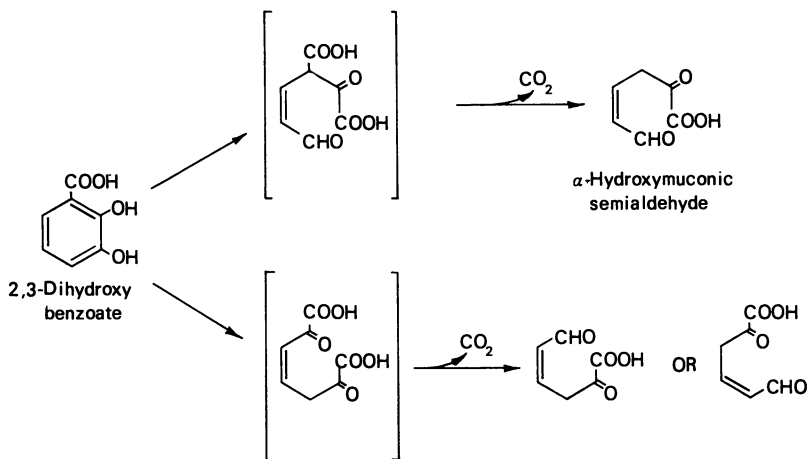
Figure 2. Possible routes of α-hydroxymuconic semialdehyde formation from 2,3-dihydroxybenzoic acid
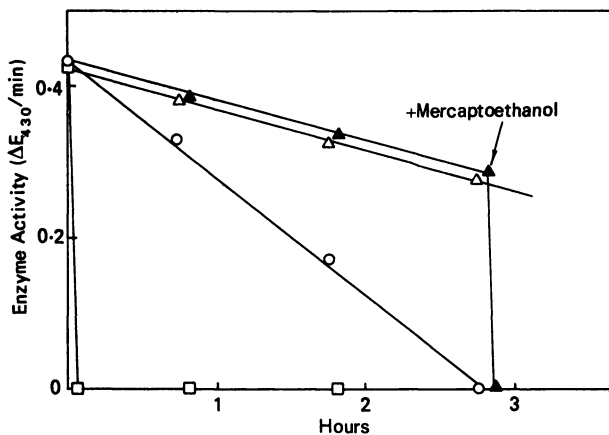
Figure 3. Effect of oxidized and reduced forms of mercaptoethanol on 2,3-dihydroxybenzoate oxygenase activity

△, *enzyme alone*
▲, *enzyme + factor B (10^{-6}M), mercaptoethanol (3.9 × 10^{-3}M) added as indicated*
○, *enzyme + mercaptoethanol (3.9 × 10^{-3}M)*
□, *enzyme + factor B (10^{-6}M) + mercaptoethanol (3.9 × 10^{-3}M)*
The enzyme (P-300) eluate was incubated in 0.01M tris/HCl buffer pH 7.0, in air or in vacuo with 1-mM solutions of either cysteine, HCl, or $FeSO_4$ and assayed spectrophotometrically at the times indicated

Table II.   Purification of 2,3-Dihydroxybenzoate Oxygenase

	Total Protein, mg.	Total Activity, μmoles/min.	% Yield	Specific Activity, μmoles/min./mg. of Protein
High Speed Supernatant	1000	470	100	0.5
(NH_4)$_2SO_4$ ppt. (33–45%)	—	—	—	—
Biogel P300	220	137	30	0.62
Hydroxylapatite	41	100[a]	21	2.40
DEAE Cellulose	12	88[a]	19	7.35

[a] After reactivation with NaBH$_4$.

The K_m value for 2,3-dihydroxybenzoate is 7.5 × 10^{-6}M. The enzyme was non-competitively inhibited by ⍺,⍺'-dipyridyl (K_i = 6 × 10^{-6}M) and was competitively inhibited by catechol (K_i = 10^{-5}M). 4-Methylcatechol and 4-ethylcatechol both inhibit the reaction at 2 × 10^{-4}M. Neither phenol nor salicylate inhibit at 2 × 10^{-4}M. o-Phenanthroline (10^{-5}M) and KCN (10^{-3}M) inhibit the reaction. Inhibition by o-phenan-

throline, α,α'-dipyridyl and KCN is more complete when the inhibitors are preincubated with the enzyme rather than added to the assay system.

Reactivation of 2,3-Dihydroxybenzoate Oxygenase

Some preparations of 2,3-dihydroxybenzoate oxygenase may be reactivated by anaerobic incubation with $NaBH_4$, Fe^{2+}, ascorbate, cysteine,
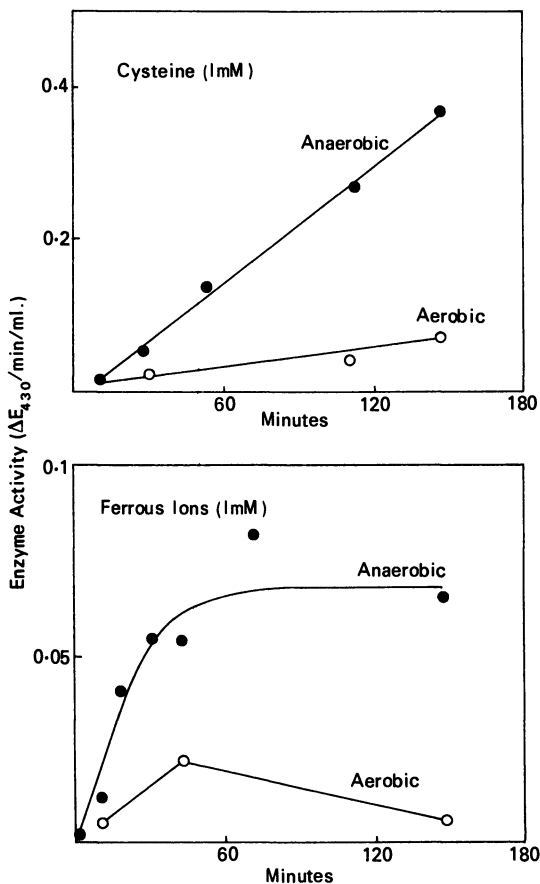
Figure 4.   Time course of reactivation of 2,3-dihydroxybenzoate oxygenase by cysteine and Fe^{2+}

The enzyme (P-300 eluate) was incubated in air or in vacuo with 1-mM solutions of either cysteine, HCl, or $FeSO_4$ and assayed spectrophotometrically at the times indicated. All enzyme incubations were performed in 0.01M tris/HCl buffer pH 7.0, and portions were taken for the standard assay

or glutathione. Figure 4, shows the reactivation with Fe^{2+} and cysteine as a function of time. In some cases the effect of $NaBH_4$ and Fe^{2+} was additive. Of these reagents, only ascorbate induced reactivation when added to the assay system (Figure 5).
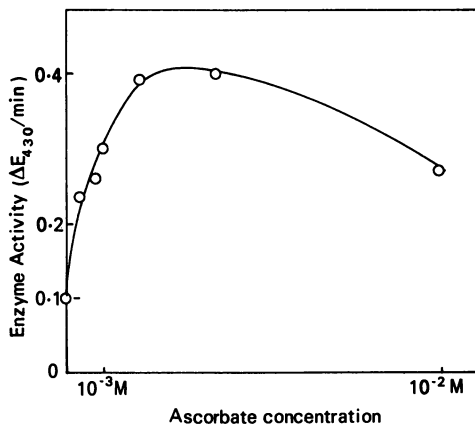
Figure 5. *Effect of ascorbate concentration on 2,3-dihydroxybenzoate oxygenase activity. Ascorbate was added to the standard assay mixture*

Our results indicate that 2,3-dihydroxybenzoate oxygenase is similar to other dioxygenases that yield oxo-acids—*e.g.,* catechol 2,3-oxygenase (*3*) and 3,4-dihydroxyphenylacetic acid 2,3-oxygenase (*1*). All are unstable in air and inactivated by oxidizing agents; they are reactivated by reducing agents under anaerobic conditions and are inhibited by Fe^{2+} chelating agents.

Decarboxylating oxygenases have been described previously. Salicylate and anthranilate hydroxylases (*12, 17*), lysine oxygenase (*3*), lactate oxygenase (*4*), and arginine oxygenase (*15*) all oxygenate the carbon atom from which the carboxyl is lost. External electron donors are required for the two hydroxylases, but the substrates of the last three enzymes presumably reduce the second oxygen atom to water. In addition, 2,3-dihydroxybenzoate oxygenase catalyzes a second carbon-carbon scission of the substrate to yield an aliphatic product. A common mechanism for these decarboxylating oxygenases might exist; in the latter case both atoms of oxygen are incorporated into the product with consequent ring opening.

Acknowledgments

Literature Cited

(1) Adachi, K., Takeda, Y., Senoh, S., Kita, H., *Biochim. Biophys. Acta* **93**, 483 (1964).
(2) Dagley, S., Evans, W. C., Ribbons, D. W., *Nature* **188**, 560 (1960).
(3) Hayaishi, O., *Bact. Rev.* **30**, 720 (1966).
(4) Hayaishi, O., Sutton, W. B., *J. Am. Chem. Soc.* **70**, 4809 (1957).
(5) Kojima, Y., Itada, N., Hayaishi, O., *J. Biol. Chem.* **236**, 2223 (1961).
(6) Nozaki, M., Kojima, Y., Nakazawa, Y., Fujisawa, H., Ono, K., Kotani, S., Hayaishi, O., Yamamo, T., "Biological and Chemical Aspects of Oxygenases," p. 347, K. Bloch, O. Hayaishi, eds., Maruzen Co. Ltd., Tokyo, 1966.
(7) Peel, J. L., *Biochem. J.* **88**, 296 (1963).
(8) Pittard, A. J., Gibson, F., Doy, C. H., *Biochim. Biophys. Acta* **57**, 290 (1962).
(9) Ribbons, D. W., *Biochem. J.* **99**, 30P (1966).
(10) Ribbons, D. W., *J. Gen. Microbiol.* **44**, 221 (1966).
(11) Shepherd, C. J., Villanueva, J. R., *J. Gen. Microbiol.* **20**, vii (1964).
(12) Taniuchi, H., Hatanaka, M., Kuno, S., Hayaishi, O., Nakajima, M., Kurihara, N., *J. Biol. Chem.* **239**, 2204 (1964).
(13) Taniuchi, H., Kojima, Y., Kanetsuna, F., Ochiai, H., Hayaishi, O., *Biochem. Biophys. Res. Comm.* **8**, 97 (1962).
(14) Terui, G., Enatsu, T., Tokaku, H., *J. Ferment. Technol.* **31**, 65 (1963).
(15) Thoai, N. V., Olomucki, A., *Biochim. Biophys. Acta* **59**, 533 (1962).
(16) Towers, G. H. N., "Biochemistry of Phenolic Compounds," p. 249, J. B. Harborne, ed., Academic Press, London, 1964.
(17) Yamamoto, S., Katagiri, M., Maeno, H., Hayaishi, O., *J. Biol. Chem.* **240**, 3408 (1965).

RECEIVED October 9, 1967.

81

Hydroxylation of Aromatic Compounds Induced by the Activation of Oxygen

M. B. DEARDEN, C. R. E. JEFCOATE, and J. R. LINDSAY SMITH

University of York, York, England

Two chemical systems that induce the hydroxylation of aromatic compounds to phenols are described. The first system involves the autoxidation of metal salts in the presence of aqueous suspensions of aromatic compounds; during this process the aromatic compounds are oxidized to phenols. The phenolic isomer ratios depend strongly on the initial concentration of the metal salts. Possible reaction mechanisms are discussed involving metal-oxygen species as the hydroxylating entities. The second system comprises ferric ion, N-benzyl-1-4-dihydronicotinamide and oxygen together with the aromatic substrate. Evidence is described that indicates that the hydroxylating species arises from the reaction of oxygen with a complex of the ferric ion and the reduced nicotinamide.

Oxidation-reduction processes are well known both in chemical and in living systems (*22, 23, 34*). Despite this apparent similarity, the biological processes can rarely be reproduced chemically. This difficulty to simulate synthetically the biological redox systems arises from the fact that the chemical systems are generally less specific and require more vigorous conditions than their biological counterparts.

The aromatic hydroxylases or mixed-function oxidases are no exception to the above generalization. For maximum activity they require a transition metal ion and an electron donor such as one of the pyridine or flavin nucleotide coenzymes; further, they probably utilize molecular oxygen as the source of the hydroxylic oxygen; an example is the liver microsomal hydroxylating system (*27*). As yet there is no comprehensive explanation to cover the mode of action of these enzymes, for on the one hand there are the specific hydroxylases which catalyze such conversions as L-phenylalanine to L-tyrosine (*26*) or tryptophan to 5-hydroxytrypto-

phan (35), and on the other hand there are the nonspecific hydroxylases where the aromatic substrate is converted into two or more isomeric phenols (48). Moreover, a consideration of the aromatic substrates involved in the two types of hydroxylation reveals that specific hydroxylation generally embodies naturally occurring benzenoid compounds, whereas the nonspecific counterpart occurs with benzene derivatives foreign to the animal body.

Chemical models for mixed-function oxidases can be divided into two groups, the classification depending on the origin of the oxygen of the entering hydroxyl group: (1) those that require hydrogen peroxide as the source of oxygen; (2) those that involve molecular oxygen. This work is concerned with model systems that belong to the latter group.

Since Udenfriend and his colleagues discovered that a mixture of ferrous ions, ascorbic acid, ethylenediaminetetraacetic acid (EDTA), and oxygen is capable of hydroxylating aromatic compounds (39), work on several other model systems involving molecular oxygen has been published (7, 13, 14, 29, 31, 37). We have directed our attention toward two types of hydroxylating systems involving either the autoxidation of metal ions or the autoxidation of organic compounds.

Experimental

Materials. Most of the chemicals were obtained commercially and were AnalaR or reagent grade when available. The aromatic substrates were purified by distillation, and their purities were checked by gas chromatography. N-benzyl-1,4-dihydronicotinamide (NBNH) was prepared by the method of Mauzerall and Westheimer (24).

Gas-Liquid Chromatography. Oxidation products were analyzed using either a Pye Argon, Perkin-Elmer F11 or Pye F104 gas chromatograph. The stationary phases and operating conditions have been reported previously (21). An improved method for separating cresol isomers (28) was introduced in this research in place of the previous method which used tris(2,4-xylenyl)phosphate as the liquid phase.

Oxidations. FERROUS SULFATE SYSTEM. An aqueous solution of ferrous sulfate with EDTA (500 ml.) was added to the aromatic reactant (2 ml.) in water (500 ml.). A steady rate of addition was maintained during 20 minutes by a capillary tube while oxygen was bubbling through the solution at 30 ml./min. The initial concentrations of ferrous sulfate are given in Tables I to IV; a 1:1 molar ratio of ferrous ion : EDTA was used. In experiments where the concentration of ferrous sulfate was kept constant, but the amounts varied, the procedure adopted was the same as that described above except that the volume of ferrous sulfate solution added was varied (Table V).

Anisole was also oxidized by mixing the reactants before introducing oxygen. The total yield of hydroxylated products and the isomer distributions of methoxyphenols together with those obtained by the dropwise

Table I.   Hydroxylation of Toluene by Metal Ion–Oxygen Systems

	Concentration, $\times 10^3 M$	Yield, Relative to a Standard	Orientation		
			o	m	p
Fe^{2+}	1.4	1.0	39	24	37
	7.2	4.7	46	26	28
	14.4	7.7	50	26	24
	29.0	12.3	50	31	19
	58.0		42	45	13
Ti^{3+}	1.0	0.49	60	17	23
	3.0	1.54	58	18	24
	5.0		54	21	25
	10.0	4.54	51	27	22
	15.0	13.3	49	31	20
Cu^{+}	1.3		22	31	47
	2.5		27	31	42
	3.8		26	38	36
	5.0		28	50	22
	10.0		33	46	21
	20.0		35	42	23
	40.0		37	36	27
Sn^{2+}	0.9		45	41	14
	4.9		34	54	12

Table II.   Hydroxylation of Anisole by Metal Ion–Oxygen Systems

	Concentration, $\times 10^3 M$	Orientation		
		o	m	p
Fe^{2+}	3.6	54	11	35
	18.0	57	12	31
	22.0	55	14	31
	54.0	51	27	22
Ti^{3+}	0.5	58	4	38
	1.0	61	8	31
	3.0	62	19	19
	5.0	57	28	15
	10.0	51	36	13
Cu^{+}	1.3	53	27	20
	2.5	40	28	32
	5.0	29	43	28
	10.0	32	47	21
	20.0	43	24	33
Sn^{2+}	1.1	51	31	18
	2.2	35	55	10
	6.0	36	59	5

Table III. Hydroxylation of Fluorobenzene by Metal Ion–Oxygen Systems

	Concentration, $\times 10^3 M$	Orientation		
		o	m	p
Fe^{2+}	1.4	4	53	43
	3.6	7	59	34
	7.2	11	65	24
	11.0	13	69	18
	14.5	17	69	14
	29.0	22	74	4
Ti^{3+}	1.0	5	41	54
	3.0	8	54	38
	5.0	12	61	27
	10.0	17	70	13
Cu^+	2.5	29	69	2
	5.0	28	70	2
	10.0	27	70	3
	20.0	23	68	9
	40.0	22	67	11

Table IV. Hydroxylation of Nitrobenzene by Ferrous Ion–Oxygen System

Ferrous Ion, $\times 10^3 M$	Orientation		
	o	m	p
0.7	5	36	59
3.0	1	50	49
7.2	2	57	41
11.5	6	70	24

procedure above in otherwise identical conditions are recorded in Table VI.

Effect of Catalase. Catalase was added to the aqueous suspension (pH 7) of the aromatic compound, and a solution of ferrous sulfate (29.0×10^{-3} mole/liter) with EDTA was added. The procedure was the same as described above.

Substrate	Catalase, grams	Yield relative to standard	Orientation of phenols		
			o	m	p
Fluorobenzene	0.05	2.1	28.2	68.7	3.1
	—	5.6	25.2	70.6	4.2
Toluene	0.05	2.8	42.3	39.3	18.4
	—	5.8	46.7	37.0	16.3

Oxidation of Cresols. An equimolar solution of cresols (1×10^{-3} gram) in water was oxidized by adding ferrous sulfate (1 gram) with EDTA in the presence of oxygen. The reaction was repeated using 5×10^{-3} gram of each cresol.

	Relative Proportions of Cresols Recovered		
Each Cresol, gram	o	m	p
1×10^{-3}	1.00	0.99	1.06
5×10^{-3}	1.00	1.02	1.01

TITANOUS CHLORIDE SYSTEM. For the oxidation of toluene and fluoro-benzene, oxygen was bubbled (30 ml./min.) through titanous chloride (1–15 ml.) in $0.05N$ sulfuric acid (1 liter) containing the aromatic re-actant (2 ml.). Under these conditions, the oxidation of anisole was negligible, and instead sulfuric acid was replaced by distilled water. The concentrations of titanous ion used are given in Tables I–III.

CUPROUS CHLORIDE SYSTEM. Cuprous chloride (0.05–0.8 gram) was dissolved in $4N$ hydrochloric acid (10 ml.) and added steadily (15 sec.) to a vigorously stirred suspension of the aromatic reactant (1 ml.) in aqueous phosphate buffer (200 ml., pH 7) through which oxygen was bubbled (30 ml./min.). Bubbling and stirring were continued for 10 minutes after addition was complete. The concentrations of cuprous chloride used are given in Tables I–III.

STANNOUS PYROPHOSPHATE SYSTEM. Stannous chloride (0.05–0.27 gram) was added to a solution of tetrasodium pyrophosphate (2.7 grams) in water (200 ml.) containing the aromatic reactant (1 ml.). Oxygen was bubbled (30 ml./min.) through the solution for 20 minutes. The concentrations of stannous ions used are given in Tables I and II.

Table V. Hydroxylation of Anisole with the Ferrous Ion–Oxygen System Ferrous Sulfate Concentration, $5.0 \times 10^{-3}M$

Ferrous Sulfate Used, grams	*Yield of Methoxyphenols Relative to a Standard*	*Orientation of Methoxyphenols*		
		o	m	p
0.2	0.7	57	12	31
1.0	3.0	64	14	22
2.0	6.7	57	12	31
3.0	8.4	60	12	28

Table VI. Hydroxylation of Anisole Using the Ferrous Ion–Oxygen System

Ferrous Sulfate, grams	*Yield, Relative to a Standard*	*Orientation of Methoxyphenols*		
		o	m	p
1 (present initially)	9.8	53	39	8
1 (added dropwise)	9.7	54	12	34
3 (present initially)	23.8	39	50	11
3 (added dropwise)	24.5	51	27	22

Table VII. Hydroxylation of Anisole and Toluene by NBNH–Ferric Ion–Oxygen System

$FeCl_3$:NBNH, Molar Ratio	Methoxyphenols				Cresols			
	Yield[a]	Orientation			Yield[a]	Orientation		
		o	m	p		o	m	p
0.08	—	—	—	—	0.6	44	24	32
0.19	2.5	58	9	33	—			
0.38	3.3	50	10	40	1.0			
0.77	4.1	48	8	44	1.5			
0.96	4.1	47	7	46	1.0			
1.16	3.7	48	5	47	1.0			
1.54	2.5	50	8	42	1.5			
1.92	1.8	55	7	38	—			
2.31	—	—	—	—	1.1			
3.84	1.3	62	7	31	1.2			

[a] Yield relative to a standard.

Table VIII. Hydroxylation of Toluene with NBNH–Ferric Ion–Oxygen System

Ferric Salt, 3.7×10^{-4} mole	pH	Yield of Cresols Relative to a Standard	Orientation of Cresols		
			o	m	p
$FeCl_3$	2.6	0.9	46	22	32
	3.2	0.6	46	20	34
	4.2	0.9	46	21	33
	5.2	1.0	43	25	32
	5.8	0.6	45	18	37
	6.4	0.2	40	21	39
$K_3Fe(CN)_6$	4.2	0.7	55	15	30
$Fe_2(SO_4)_3$	4.2	1.6	40	24	36
$FeCl_3$ + EDTA (3.7×10^{-4} mole)	4.2	0.1	44	23	33

COBALTOUS CHLORIDE SYSTEM. Cobaltous chloride (4.25 grams) was added to an aqueous solution of potassium cyanide (6.9 grams), containing anisole (2 ml.) and cooled to 0°C. Oxygen was passed through the solution for 45 minutes. The experiment was repeated except that the anisole was added after 15 minutes. Under both conditions little hydroxylation occurred; the main product was phenol.

NBNH–OXYGEN SYSTEM IN WATER. The aromatic compound was suspended in an aqueous phosphate–citrate buffer (1 liter; pH 2.6–6.4) with NBNH (9.3×10^{-4} mole) and ferric chloride (0.72–36.0×10^{-4} mole). Oxygen was bubbled through the mixture (30ml./min.) for one hour (Table VII).

Ferric chloride was replaced with other metal salts (cupric or ferrous sulfate, or ceric sulfate in acid) and with FMN (9.3×10^{-4} mole). Only other ferric salts induced hydroxylation (Table VIII).

NBNH in Nonaqueous Solvents. Standard solutions of NBNH (0.0688 gram) in ethyl alcohol (50 ml.) and of ferric chloride (0.1146 gram) in ethyl alcohol (50 ml.) were prepared. These solutions were used to prepare 2.0-ml. samples for spectrometric analysis. The initial absorption at 590 mμ and rate of decay of this absorption were recorded (Tables IX and X, Figure 1). Ethanolic solutions of NBNH with salts of metals other than ferric produced no visible color change.

ESR Studies on NBNH Oxidation. Solutions of NBNH (10.0 grams) in water or ethyl alcohol (3 liters) were flowed against ferric chloride (12.5 grams) in either water or ethanol (3 liters) through the ESR spectrophotometer. The flow apparatus was the same as that used by Dixon and Norman (10). Ferric chloride showed a broad signal which disappeared when the flow of the NBNH solution was increased to at least equal to that of the ferric chloride. No other signal was observed.

Extraction of Phenolic Products. Reaction mixtures were acidified and extracted with ether (4 × 100 ml.). The combined ether extracts were evaporated to a small volume (1–2 ml.) and analyzed by gas-liquid chromatography. By using synthetic mixtures, this procedure was shown not to lead to preferential loss of any component.

Table IX. Dependence of Initial Absorbance of the Blue-Green Complex with the Proportion of Ferric Chloride to NBNH

Molar Ratio of Ferric Chloride:NBNH	Initial Optical Density, D
0.33	0.35
0.49	0.39
0.66	0.44
0.82	0.54
0.99	0.69
1.15	0.68
1.32	0.81
1.51	0.76
1.76	0.75
2.12	0.74
2.64	0.80

Table X. Change in Absorbance of the Blue-Green Complex with Time

Time, min.	Optical Density, D	1/D
0.5	0.670	1.49
1.0	0.560	1.79
1.5	0.480	2.08
2.0	0.421	2.38
2.5	0.370	2.70
3.0	0.335	2.98
3.5	0.303	3.30
4.0	0.278	3.60
4.5	0.256	3.90
5.0	0.235	4.25
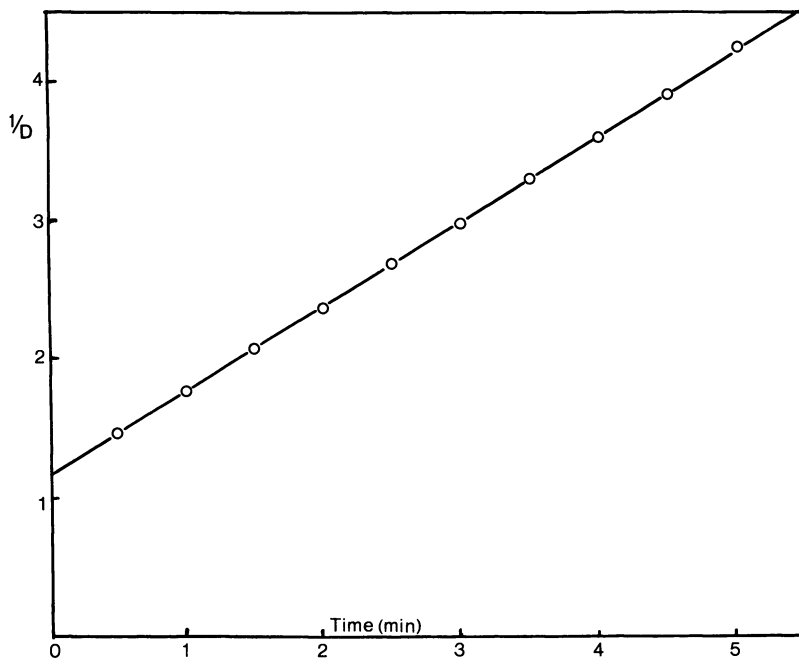
Figure 1.   Second-order rate plot for the decay of the blue-green ferric-NBNH complex

Results

Hydroxylation by the Metal Ion–Oxygen Systems. A monosubstituted benzene was suspended in aqueous solution of a metal salt through which oxygen was bubbled. Two aromatic compounds (toluene and anisole) were treated this way with each of four metal salts (ferrous sulfate in the presence of EDTA, titanous chloride, cuprous chloride and stannous pyrophosphate); a third compound (fluorobenzene) was oxidized with the ferrous, titanous, and cuprous systems, and a fourth aromatic compound (nitrobenzene) was treated with ferrous ion with EDTA. The initial concentration of the metal ion was varied.

In each case at least four products were obtained—namely, the three isomeric phenols derived by the replacement of hydrogen by hydroxyl and phenol itself. The conditions were such that the extent of hydroxylation was always less than 2%, thereby reducing the possibility of further hydroxylation (*see also below*). The orientations of phenolic isomers are recorded in Tables I–IV.

No trace could be detected of bibenzyl or bitolyls from experiments with toluene, or of bianisyls from those with anisole. Treatment of benzene with the ferrous ion and titanous ion systems gave no biphenyl.

The addition of catalase (4% by weight, based on the metal ion) to the ferrous ion system reduced the yields of hydroxylated products from toluene and fluorobenzene by approximately 50%, although the ratios of *o*-, *m*-, and *p*-phenolic products were essentially unchanged. Catalase activity was confirmed by its marked effect on a reaction by a model system involving hydrogen peroxide (*17*).

Anisole treated with an aqueous solution of cobaltous chloride and potassium cyanide in the presence of oxygen gave negligible amounts of methoxyphenols.

Further oxidation was excluded as a source of the change in isomer ratios (Tables I–IV) by the following experiments.

There was no significant change in the isomer distribution of the methoxyphenols when anisole was hydroxylated in the presence of larger amounts of ferrous sulfate, at the same concentration, although the total yield of phenolic products increased proportionately with the amount of ferrous sulfate used (Table V).

When toluene was hydroxylated with the titanous ion–oxygen system in a constant volume of water, the yield of phenolic products depended on the amount of metal salt. The yield increased proportionately with the concentration of the metal ion. Under these conditions the phenolic isomer ratios changed continuously, the proportion of the meta isomer increasing with the metal ion concentration (Table I).

When anisole was hydroxylated by slowly adding ferrous sulfate solution to a suspension of anisole in water through which oxygen was bubbled, the total yield of methoxyphenols was the same as when the ferrous sulfate solution was initially mixed with anisole, although the isomer distribution of methoxyphenols was markedly altered (Table VI).

Solutions of the three isomeric cresols, of similar concentrations to those obtained from reactions on toluene, were oxidized, using the ferrous ion–oxygen system. Isolation of the unreacted cresols showed that the relative reactivity of the three compounds was close to one, and no isomer was selectively oxidized.

Anisole was hydroxylated by the ferrous ion–oxygen system in the presence of increasing amounts of added ferric ions. This resulted in a decrease rather than an increase in the proportion of *m*-methoxyphenol (Table XI).

Hydroxylation Induced during the Autoxidation of *N*-benzyl-1,4-dihydronicotinamide. Oxygen was bubbled through the aromatic compound suspended in an aqueous solution of *N*-benzyl-1,4-dihydronicotinamide and ferric chloride. Four compounds were oxidized by this model system: benzene to phenol and no biphenyl; toluene to benzyl alcohol, cresols, phenol, and no bibenzyl; anisole to phenol and methoxyphenols; fluorobenzene to phenol and fluorophenols. Even under optimum

Table XI. Hydroxylation of Anisole by Ferrous Ion–Oxygen
System in the Presence of Ferric Ion

	Ferric Ion × 10³M	Methoxyphenol Distribution		
		o	m	p
Ferrous Ion Added				
Slowly (5.9×10^{-3}M)	0	51	20	29
	7.4	62	7	31
	14.8	76	12	12
Ferrous Ion Present				
Initially (7.2×10^{-3}M)	0	53	39	8
	3.7	56	36	8
	7.4	66	24	10
	18.5	76	14	10

conditions the yield of fluorophenols was extremely low; the major product was phenol (Table VII).

The molar ratio of NBNH to ferric chloride was varied, and the yield and isomer ratios of phenolic products from toluene and anisole were recorded (Table VII).

The pH dependence of the system was investigated using toluene as substrate in a phosphate-citrate buffer. In the pH range 2.6–5.2 the yield and cresol isomer ratios remain unchanged; above this value the yield decreases (Table IV).

Ferric chloride was omitted from the system and then replaced successively by either cupric sulfate, ceric sulfate, ferrous sulfate, or flavin mononucleotide (FMN). In each experiment the yield of methoxyphenols from anisole was negligible. Other ferric salts, however, were found to induce hydroxylation (Table VIII). The addition of EDTA to the ferric chloride–NBNH system markedly reduced the yield of cresols from toluene.

Solutions of NBNH in nonaqueous solvents (methyl cyanide, ethyl alcohol, and dimethyl sulfoxide) developed a blue-green color in the presence of ferric chloride; the salts of the other metals listed above induced no visible color change, suggesting that NBNH forms a complex specifically with ferric ions. The intensity of the absorption of the complex in ethyl alcohol (E_{max} = 590 mμ), which decays rapidly, was examined spectrophotometrically in solutions containing varying amounts of ferric chloride and NBNH. In each case a decay dependent on the second power of the absorbing species was observed (Table X, Figure 1). The initial absorption of the complex for solutions containing constant amounts of NBNH showed a maximum value when the molar ratio of ferric chloride to NBNH was 1 : 1 (Table IX).

Aqueous or ethanolic solutions of NBNH were mixed with the corresponding solutions of ferric chloride and flowed through an ESR spectro-

photometer. The only signal observed was a broad line from the ferric chloride; no organic radicals were detected.

Discussion

Metal Ion–Oxygen Systems. Hydroxylation of aromatic compounds occurs during the autoxidation not only of ferrous ion but also of other metal ions. The ions we have investigated are all capable of undergoing one-electron oxidation. [This is well known for ferrous, titanous, and cuprous ions and has recently been demonstrated also for stannous ion (*43*).] The main problem in elucidating the course of the hydroxylations is determining the nature of the hydroxylating species.

In part of a previous publication (*31*), we reported some preliminary conclusions on the hydroxylation of aromatic compounds by the metal ion–oxygen systems. This work has been extended, and it is clear that the most interesting feature is the strong dependence of the distribution of phenolic products on the initial concentration of the metal ions. In general, the proportion of the meta derivative formed from each of the four monosubstituted aromatics increases and the para isomer decreases with increase in the metal ion concentration.

The anomalous behavior of fluorobenzene which gives a high proportion of *m*-fluorophenol, even in very dilute solutions of metal ions, has been discussed (*31*). The intermediates which would otherwise lead to *o*- and *p*-fluorophenols are diverted to give *o*- and *p*-hydroquinones, respectively.

A possible explanation for these variations might be that, as the metal ion concentration is increased, a proportion of the phenolic products is removed by further reaction, the three isomers reacting at different rates. However, strong evidence against this interpretation has been presented, except perhaps at the highest metal ion concentrations studied; in particular with the cuprous ion system where the proportion of the meta derivative at the highest cuprous concentrations is less than would have been predicted from the results in more dilute cuprous solution (Tables I and II). Thus, it seems likely that hydroxylation by each metal ion–oxygen system is induced by more than one hydroxylating species, their concentrations being determined by the concentration of reduced metal ion.

Of possible hydroxylating species, the two most obvious for consideration are the hydroxyl and perhydroxyl radicals. Nofre *et al.* (*29*) suggest that the former is the active species in the metal ion–oxygen systems, while Staudinger and his colleagues (*37*) propose that these systems involve a combination of both species. The hydroxyl radical is involved in hydroxylations by Fenton's reagent and the closely related

system of titanous ion and hydrogen peroxide (*20*). However, it is characteristic of these two systems that benzene is oxidized partly to biphenyl and toluene partly to bibenzyl (*20*), whereas a dominating feature of the metal ion–oxygen systems is the complete absence of these and related dimeric products. Moreover, the addition of catalase by no means inhibits hydroxylation completely. Finally, the isomer ratios of phenolic products obtained from the metal ion–oxygen systems are very different from those obtained from Fenton's reagent (*32*). Thus, it seems unlikely that oxygen is first reduced to hydrogen peroxide, which is in turn reduced to the hydroxyl radical.

The perhydroxyl radical is known to result from the one-electron oxidation of hydrogen peroxide—*e.g.*, by ceric ion (*36*). We might anticipate its formation by the one-electron reduction of oxygen during autoxidation of metal ions, followed by the uptake of a proton. However, attempts to induce the hydroxylation of aromatic compounds by the perhydroxyl radical have been unsuccessful (*20*).

It seems unlikely that hydroxylation of aromatic compounds by the metal ion–oxygen systems is induced by either the hydroxyl or perhydroxyl radicals. This is confirmed by extrapolating the values for the isomer distributions of phenolic products obtained at different metal ion concentrations to zero concentration of metal ion. The values obtained [some of which have been reported (*31*)] depend on the nature of the metal ion (Table XII). This evidence argues against a simple hydroxylating species being common to the metal ion–oxygen systems and suggests that a metal ion is intimately involved in the reactive species.

More information concerning possible hydroxylating entities can be obtained by investigating the autoxidation of the metal ions. The nature of the reaction involved in the autoxidation depends strongly on the redox potentials, $E°$, for the various oxidation-reduction couples. It is probably significant that the values for the metal ions used here are as follows:

$$E°$$

$$Fe^{2+}(EDTA) = Fe^{3+}(EDTA) + e^- \qquad -0.12 \ (pH \ 7) \qquad (48)$$

$$Cu^+ = Cu^{2+} + e^- \qquad -0.15 \qquad (20)$$

$$Ti^{3+} = Ti^{4+} + e^- \qquad -0.15 \qquad (20)$$

$$Sn^{2+} = Sn^{4+} + 2e^- \qquad -0.15 \qquad (20)$$
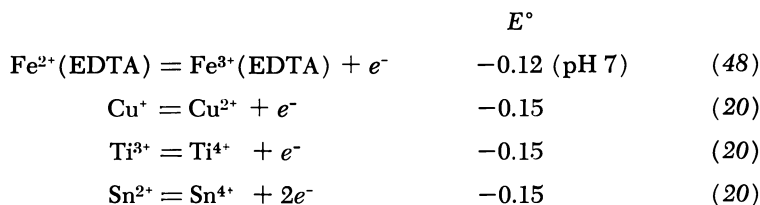
and each system is effective in inducing hydroxylation, whereas in the absence of EDTA, ferrous sulfate is ineffective.

$$Fe^{2+} = Fe^{3+} + e^- \qquad -0.77 \qquad (20)$$

Table XII. Isomer Distribution of Monosubstituted Phenols Extrapolated to Zero Metal Ion Concentration

	Cresols			Methoxyphenols			Fluorophenols			Nitrophenols		
Metal Ion	o	m	p	o	m	p	o	m	p	o	m	p
Fe^{2+}	38	24	38	56	8	36	2	45	53	4	36	60
Ti^{3+}	61	16	23	54	0	46	2	33	65			
Cu^+	22	29	49	75	8	17	30	68	2			
Sn^{2+}	46	38	16	53	20	27						

A mechanistic similarity is suggested. Now the value of $E°$ for the couple $HO_2 \cdot - O_2$ is between 0.1 and 0.55 (*19, 38*), so that the reaction of the metal ions with oxygen studied here is unlikely to proceed *via* $HO_2 \cdot$ for thermodynamic reasons. However, the autoxidation of the metal and reduction of oxygen may well occur *via* the formation of a complex, such as FeO_2^{2+}.

Further, the kinetics of the autoxidation of ferrous ion has been interpreted as proceeding through the formation of an iron-oxygen complex,

$$Fe^{2+} + O_2 \rightarrow FeO_2^{2+}$$
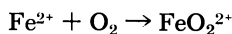
which undergoes one of the two reactions, either (*11*):

$$FeO_2^{2+} + H_2OFe^{2+} \rightarrow FeO_2H^{2+} + FeOH^{2+}$$

or (*38, 42*):

$$FeO_2^{2+} + Fe^{2+} \rightarrow (FeO_2Fe)^{4-}$$
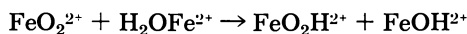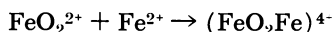
Whether the rate of autoxidation is first or second order in ferrous ion depends on the medium. In perchlorate (*11*) or sulfate (*6*) the rate is $K[Fe^{2+}]^2[O_2]$, and in phosphate (*8*) the rate is $K[Fe^{2+}][O_2]$ $[H_2PO_4^-]^2$. The autoxidation of cuprous ion can also show either a first- or second-order dependence on cuprous ion concentration (*15, 30*). Binuclear complexes, as proposed in the second scheme above, are well known in the reactions of Co(II) (*12*) and Cr(II) (*18*) in the presence of appropriate ligands. It is possible that the binuclear iron complex breaks down to another species, FeO^{2+}, analogous to a step reported during the autoxidation of Cr(II)–ammonia solutions (*18*). Thus, it is possible that any one of the species FeO_2^{2+}, $FeOOH^{2+}$, $(FeO_2Fe)^{4+}$, and FeO^{2+}, is capable of hydroxylating aromatic compounds in the ferrous ion–oxygen system.

The general meta orientation of phenolic products obtained at high metal ion concentrations, irrespective of the type of substituent, is difficult to reconcile with any established mode of aromatic substitution. It seems logical that in dilute metal ion solution such a species as FeO_2^{2+} which would be formed in the initial step of the autoxidation of ferrous ion could be the hydroxylating species. Such complexes for cuprous and

ferrous ion are well established among the biological (*46*) and synthetic (*40*) oxygen carriers and have been suggested as active oxidants in numerous biological (*22, 23, 34*) and chemical systems (*33, 49*). At higher concentrations the aromatic substrate will compete with other metal ions for these species, and hydroxylation may arise from a combination of FeO_2^{2+} with one or more of FeO_2H^{2+}, $(FeO_2Fe)^{4+}$, and FeO^{2+}. Previously (*31*) we suggested tentatively that the meta substituted phenol arise from an initial complex between the ortho and para positions of the aromatic ring and the hydroxylating species, followed by intramolecular transference of oxygen to the meta position. The main advantage of this scheme was that it offered a simple explanation for the variation of phenolic isomer ratios with the metal ion concentration. Alternative explanations are discussed below.

A comparison of the phenolic isomer ratios from the metal ion–oxygen systems with those from Fenton's reagent shows that the metal–oxygen complexes are less selective than the hydroxy radical; this is particularly apparent at high metal ion concentrations. The attacking species, however, is unlikely to be a free radical for the product isomer distribution from homolytic aromatic phenylation or methylation indicates that even the reactive phenyl and methyl radicals show moderate selectivity (*45*). Another possible reactive entity is an oxenoid species capable of direct oxygen atom transfer into the aromatic substrate; this type of process was proposed by Hamilton for the mechanism of aromatic hydroxylation by Udenfriend's system (*13*). The oxygen atom transferred can be either a singlet or triplet species. A random distribution of phenolic products will arise if the predominant reaction leading to phenols is oxygen insertion into the aromatic C—H bonds; such a reaction will be favored by a singlet rather than triplet species. In agreement with these conclusions the methylation of anisole with carbene (a singlet species) results in a random distribution of methyl anisoles (*25*). A triplet oxygen species would add predominantly to the aromatic nucleus to give cyclohexadienylepoxides, which could rearrange to phenols; the isomer distribution would now resemble that from an electrophilic substitution. Dewar and Narayanaswami (*9*) and Abramovitch and his colleagues (*1*) have observed this type of aromatic substitution from carbon and nitrogen species containing six electrons. Some recent ESR studies suggest that the attacking entities here are probably triplet and not singlet species (*41*). It is possible that at low metal ion concentration the predominant attacking species is a reduced metal ion–oxygen complex—*e.g.*, FeO_2^{2+}— while at higher concentrations, it is mainly a complex capable of singlet oxygen insertion—*e.g.*, $(FeO_2Fe)^{4+}$.

One further mechanism which does not require a highly unselective hydroxylating entity is worth considering (Scheme 1). The first step

involves an initial addition of a metal–oxygen species, such as FeO_2^{2+}, to the aromatic nucleus; the resulting adduct then decomposes to a phenol or cyclizes to a cyclic peroxide.
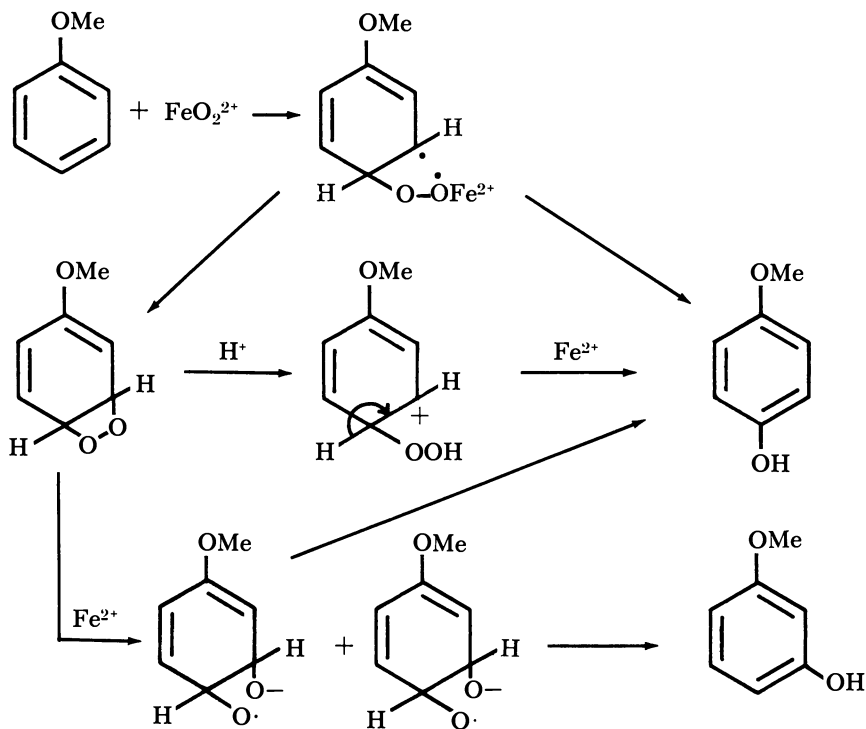
Scheme 1

Such cyclic peroxides have been proposed as intermediates in photochemical and chemiluminescent reactions of aromatic compounds with oxygen (*4*, *5*, *44*) and in the biological hydroxylation of aromatic compounds (*22*, *23*, *34*). In dilute ferrous ion solution the cyclic peroxides could decompose ionically to give a predominantly electrophilic distribution of substituted phenols, while at higher concentrations the ferrous ion would cleave the peroxide bond homolytically; this, followed by loss of water, would give a more random pattern of substituted phenols.

A common metabolite from the nonspecific hydroxylation of aromatic compounds foreign to animals is the 3,4-dihydrodiol (*48*). This compound could arise by either solvolysis of the 3,4-dihydroepoxides or reduction of the 3,4-dihydroperoxides proposed in the mechanisms above.

At present it is not possible to make a final decision as to the mechanism of hydroxylation by the metal ion–oxygen systems. Work is, however, in progress which, it is hoped, will resolve this interesting problem.

The NBNH–Oxygen System.   Since biological hydroxylases are known to involve both a metal ion and a reducing agent, a number of workers have investigated the activity of related model systems involving molecular oxygen. A selection of different reducing agents has been used —namely, ascorbic acid (Udenfriend's system) (*39*), 2,4,5-triamino-6-hydroxypyrimidine (*13*), tetrahydropteridines (*7*), reduced flavin (*16*), and nicotinamide coenzymes (*37*). We have found that benzenoid compounds are hydroxylated by a system comprising ferric ion, *N*-benzyl-1,4-dihydronicotinamide, and oxygen.

Unlike Udenfriend's system, which is active with several different metal ions (*29*), hydroxylation of aromatic compounds using NBNH and oxygen occurs only in the presence of ferric ions. Ceric or cupric sulfate are unable to activate the system, and more surprisingly, ferrous sulfate is ineffective. Ferrous ions under the reaction conditions (pH 4.2) are relatively stable and are oxidized only slowly to ferric ions by molecular oxygen; thus, it would seem that only negligible amounts of ferric ions are formed during the reaction period, and hence no hydroxylation occurs.

In agreement with these conclusions only ferric ion shows evidence of forming a complex with NBNH in nonaqueous solvents. NBNH with ferric salts in ethyl alcohol, produces a blue-green colored solution, which decays rapidly to yellow both in the presence and absence of oxygen. The initial intensity of the absorption from the species depends strongly on the molar ratio of ferric ion to NBNH and is maximal at a value close to 1 : 1. This suggests that the colored species is either a 1 : 1 complex of NBNH with ferric ion or that each NBNH is oxidized rapidly by one ferric ion to a colored oxidation product, which in turn is destroyed more slowly. In this latter explanation the initial steady-state concentration of the colored species would be maximal at *ca.* 1 : 1.

ESR studies showed that no measurable amounts of a radical oxidation product from NBNH are present when the blue-green species is generated in alcohol. A broad line spectrum, typical of a paramagnetic metal ion (*2*) is present when ferric ion is in molar excess; this disappears as the amount of NBNH is increased, suggesting a complete incorporation of the ferric ion into a complex (*3*). This evidence suggests that the blue-green species is a complex perhaps of the type I.

I
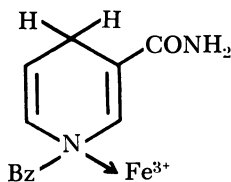
The active hydroxylating species in this system is unlikely to be either the hydroxyl or perhydroxyl radical for the same reasons as discussed above for the metal ion–oxygen systems—namely, the lack of dimeric aromatic products and the difference in phenolic isomer ratios from those obtained using Fenton's reagent.

We believe that the active hydroxylating species is derived from the blue-green ferric-NBNH complex. The evidence for this conclusion can be summarized as follows:

(1) Ferric ion is the only metal ion studied which induces hydroxylation in the presence of NBNH and oxygen and the only one that shows evidence of forming a complex with NBNH. The other metal ions and FMN neither complex with NBNH nor produce any hydroxylating activity.

(2) EDTA, rather than increasing the yield of hydroxylation, as has been observed in several other model hydroxylases (7, 29), reduces it drastically. The role of EDTA is twofold; first, it chelates preferentially with the ferric ions decreasing the amount of ferric–NBNH complex; second, it reduces the oxidizing ability of ferric. The monodentate ligands —sulfate, chloride, and cyanide—do not act in the same way.

(3) The yield of methoxyphenols from anisole varies with the initial molar proportion of NBNH to ferric ion reaching a maximum at a 1 : 1 ratio. The 590-mμ absorption of the ferric–NBNH complex in ethyl alcohol shows a similar variation with the proportion of ferric ion to NBNH. A possible reaction scheme is outlined in Scheme 2.
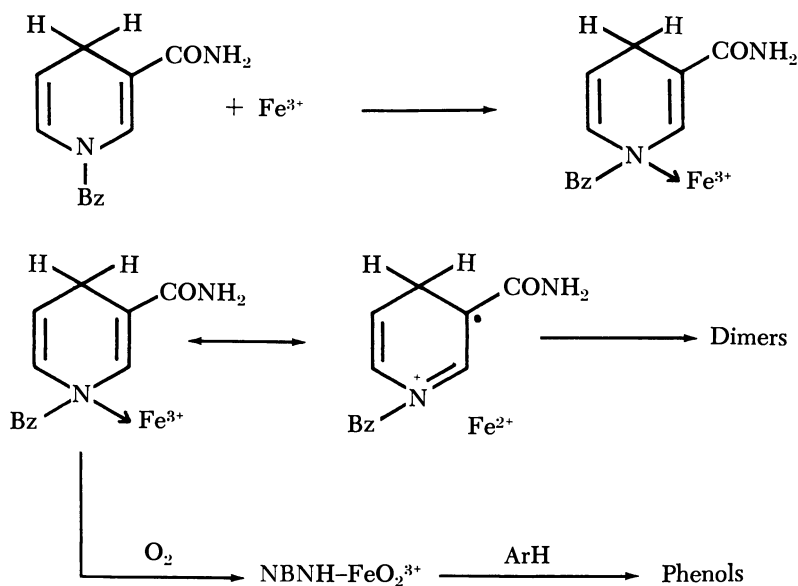
Scheme 2

The major portion of the NBNH in air or nitrogen leads to dimeric products. In air, however, a small part of the complex is diverted to give an active species that hydroxylates the aromatic substrate.

It is interesting to compare the phenolic isomer distributions from hydroxylation using the ferric–NBNH system with those from the ferrous–oxygen system (Tables I, II, and VIII). The strong similarity suggests that they involve similar hydroxylating entities. However, the role of NBNH cannot be merely to reduce the ferric ions to ferrous to produce a simple ferrous–oxygen system since ferrous ions with NBNH is an ineffective hydroxylating system.

We believe that the ferric–NBNH complex interacts with oxygen to give the active hydroxylating species $NBNH–Fe^{3+}O_2$. This active complex can act as a FeO_2^{2+} species (the proposed hydroxylating species in the ferrous oxygen system), by donating an electron from the NBNH to the ferric ion. Thus, the specific role of ferric ion is to complex the reduced nicotinamide and act as an electron bridge between the NBNH and the oxygen.

Acknowledgment

Literature Cited

(1) Abramovitch, R. A., Roy, J., Ulma, V., *Can. J. Chem.* 43, 3407 (1965).
(2) Al'tshuler, S. A., Kozirev, B. M., "Electron Paramagnetic Resonance," p. 168, Academic Press, London, 1964.
(3) *Ibid.*, 233.
(4) Arbuzov, Y. A., *Uspekhi Khim.* 34, 1332 (1965).
(5) Arbuzov, Y. A., *Russ. Chem. Rev.* 1965, 588.
(6) Belopal'ski, A. P., Urusov, V. V., *Zh. Prikl. Khim.* 21, 903 (1948).
(7) Bobst, A., Viscontini, M., *Helv. Chim. Acta.* 49, 884 (1966).
(8) Cher, M., Davidson, M., *J. Am. Chem. Soc.* 77, 793 (1955).
(9) Dewar, M. J. S., Narayanaswami, K., *J. Am. Chem. Soc.* 86, 2422 (1964).
(10) Dixon, W. T., Norman, R. O. C., *J. Chem. Soc.* 1963, 3119.
(11) George, P., *J. Chem. Soc.* 1954, 4349.
(12) Haim, A., Wilmarth, W. K., *J. Am. Chem. Soc.* 83, 509 (1961).
(13) Hamilton, G. A., *J. Am. Chem. Soc.* 86, 3391 (1964).
(14) Hamilton, G. A., Giacin, J. R., *J. Am. Chem. Soc.* 88, 1584 (1966).
(15) Henry, P. M., *J. Inorg. Chem.* 5, 688 (1966).
(16) Higgins, R., *D. Phil. Thesis*, Oxford (1965).
(17) Jefcoate, C. R. E., *D. Phil. Thesis*, Oxford, 1966.
(18) Joyner, T. B., Wilmarth, W. K., *J. Am. Chem. Soc.* 83, 516 (1961).
(19) Latimer, W. M., "Oxidation Potentials," Prentice-Hall Inc., New York, 1952.
(20) Lindsay Smith, J. R., Norman, R. O. C., *J. Chem. Soc.* 1963, 2897.
(21) Lindsay Smith, J. R., Norman, R. O. C., Radda, G. K., *J. Gas Chromatog.* 2, 146 (1964).

(22) Mason, H. S., *Advan. Enzymol.* **19,** 79 (1957).
(23) Mason, H. S., *Ann. Rev. Biochem.* **34,** 595 (1965).
(24) Mauzerall, D., Westheimer, F. H., *J. Am. Chem. Soc.* **77,** 2261 (1955).
(25) Meerwein, H., Disselnkötter, H., Rappen, F., von Rintelen, H., van de Vloed, H., *Ann.* **604,** 151 (1957).
(26) Mitoma, C., *Arch. Biochem. Biophys.* **60,** 476 (1956).
(27) Mitoma, C., Posner, H. S., Reitz, H. C., Udenfriend, S., *Arch. Biochem. Biophys.* **61,** 431 (1956).
(28) Mortimer, J. V., Gent, P. L., *Anal. Chem.* **36,** 755 (1964).
(29) Nofre, C., Cier, A., Lefier, A., *Bull. Soc. Chim. France* **1961,** 530.
(30) Nord, H., *Acta Chem. Scand.* **9,** 430 (1955).
(31) Norman, R. O. C., Lindsay Smith, J. R., "Oxidases and Related Redox Systems," p. 131, T. King, H. S. Mason, M. Morrison, eds., Wiley, New York, 1965.
(32) Norman, R. O. C., Radda, G. K., *Proc. Chem. Soc.* **1962,** 138.
(33) Ochiai, E., *Tetrahedron* **20,** 1819 (1964).
(34) "Oxygenases," O. Hayaishi, ed., Academic Press, New York, 1964.
(35) Renson, J., Weissbach, H., Udenfriend, S., *J. Biol. Chem.* **237,** 2261 (1962).
(36) Saito, E., Bielski, B. H. J., *J. Am. Chem. Soc.* **83,** 4467 (1961).
(37) Staudinger, Hj., von Kerékjártó, B., Ullrich, V., Zubrzycki, Z., "Oxidases and Related Redox Systems," p. 815, T. King, H. S. Mason, M. Morrison, eds., Wiley, New York, 1965.
(38) Taube, H., *J. Gen. Physiol.* **49,** 29 (1965).
(39) Udenfriend, S., Clark, C. T., Axelrod, J., Brodie, B. B., *J. Biol. Chem.* **208,** 731 (1954).
(40) Vogt, L. H., Faigenbaum, H. M., Wiberley, S. E., *Chem. Rev.* **63,** 269 (1963).
(41) Wasserman, E., Murray, R. W., *J. Am. Chem. Soc.* **86,** 4203 (1964).
(42) Weiss, J., *Nature* **181,** 825 (1958).
(43) Wetton, E. A. M., Higginson, W. L. E., *J. Chem. Soc.* **1965,** 5890.
(44) White, E. H., Harding, M. J. C., *Photochem. Photobiol.* **4,** 1129 (1965).
(45) Williams, G. H., "Homolytic Aromatic Substitution," Pergamon Press, London, 1960.
(46) Williams, R. J. P., "Enzymes," P. Boyer, H. Lardy, K. Myrback, eds., Vol. I, p. 41, Academic Press, New York, 1961.
(47) Williams, R. J. P., Tomkinson, J. C., *J. Chem. Soc.* **1958,** 2010.
(48) Williams, R. T., "Detoxication Mechanisms," Chapman & Hall, London, 1959.
(49) Wüthrich, K., Fallab, S., *Helv. Chim. Acta* **47,** 1440 (1964).

Intramolecular Migrations during Hydroxylation of Aromatic Compounds

The NIH Shift

JOHN DALY, GORDON GUROFF, DONALD JERINA, SIDNEY UDENFRIEND, and BERNHARD WITKOP

National Institutes of Health, Bethesda, Md.

When selectively deuterated or tritiated aromatic substrates undergo enzymatic hydroxylation, a fundamental 1,2 shift of deuterium or tritium, from the point of substitution by oxygen, to the adjacent position in the aromatic ring is observed. Migrations of chloro, bromo, and methyl substituents also occur. The extent and direction of migration observed with tritiated and deuterated aromatic compounds agrees with predictions based on the major canonical forms of cationoid intermediates. Phenolic compounds and aniline show almost negligible migration of tritium while in other compounds such as anisole and the alkylbenzenes the initial positive charge is not delocalized, and significant migrations of deuterium or tritium occur. Migrations are observed during hydroxylation with the electrophilic reagent, peroxytrifluoroacetic acid, but not with other nonenzymatic hydroxylating systems.

D uring studies at NIH, it was discovered that enzymatic hydroxylation of (deuterated or tritiated) substrates leads to a novel and mechanistically important shift of the deuterium or tritium from the point of substitution by oxygen to an adjacent position in the aromatic ring (*12*). [It has been found recently that arene oxides are likely intermediates in the metabolism of aromatic compounds. They rearrange to phenols with concomitant "NIH Shift," and they are enzymatically converted to dihydrodiols and premercapturic acids. In addition, naphthalene oxide has now been demonstrated as an intermediate in the conversion of naphthalene to α-naphthol, *trans*-1,2-dihydro-1,2-dihydroxynaphthalene, and

S-(1,2-dihydro-2-hydroxynaphthyl)glutathione. This is the first direct demonstration of an arene oxide as an intermediate in enzymatic hydroxylation.]. This observation has been extended to include the migration of chlorine, bromine and alkyl groups.

With the enzyme, phenylalanine hydroxylase, a variety of substrates have been found to undergo hydroxylation-induced migrations. 4-Deutero- (15), 4-tritio- (14), 4-chloro-, 4-bromo- (13), or 4-methylphenylalanine (7) are hydroxylated to the corresponding 3-substituted tyrosines, while only small amounts of unsubstituted tyrosine are formed (Figure 1). By contrast, hydroxylation of 4-fluorophenylalanine leads to formation of tyrosine with complete loss of the substituent as fluoride ion (20).
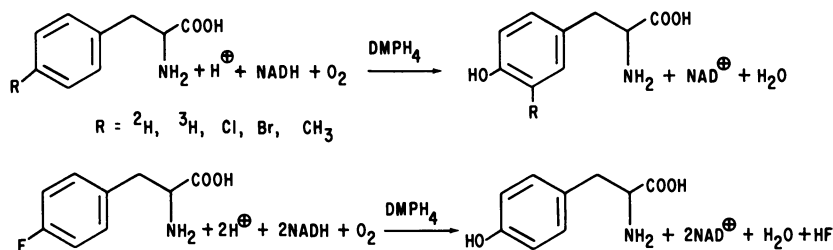
Figure 1. Hydroxylation of 4-substituted phenylalanines with phenylalanine hydroxylase from either rat liver or Pseudomonas *(DMPH$_4$ = dimethyltetrahydropteridine)*

Another amino acid hydroxylase, tryptophan-5-hydroxylase, catalyzes the conversion of 5-tritiotryptophan to 4-tritio-5-hydroxytryptophan (Figure 2) (24). With this substrate, exchange experiments have shown that only the 4-tritio isomer is formed rather than a mixture of the 4- and 6-tritio compounds.

A third amino acid hydroxylase, tyrosine hydroxylase, causes the "NIH Shift" with phenylalanine (21) but not with its normal substrate, tyrosine (Figure 3). Thus, the hydroxylation of 4-tritiophenylalanine with either tyrosine hydroxylase or phenylalanine hydroxylase leads to migration and retention of tritium in the product, tyrosine. However, with 3,5-ditritiotyrosine as substrate for tyrosine hydroxylase, complete loss of one tritium occurs in the conversion to 3,4-dihydroxy-5-tritiophenylalanine.

The hydroxylation of 4-tritio- and 4-deuteroacetanilide with the aryl hydroxyases of liver microsomes was studied in detail (28). Migration of 45% of the tritium or 30% of the deuterium (previously reported as 15%) to the 3-position occurred during formation of 4-hydroxyacetanilide (Figure 4). No primary isotope effect was observed in this hydroxylation (28) or in the hydroxylation of 4-deutero- or tritiophenylalanine with
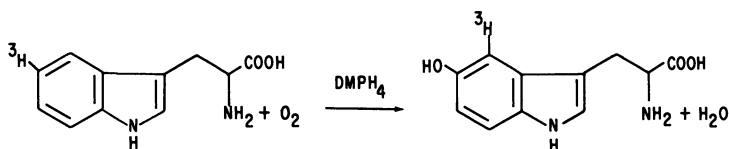
Figure 2. *Hydroxylation of 5-tritiotryptophan with tryptophan-5-hydroxylase from mast cells (DMPH$_4$ = dimethyltetrahydropteridine)*
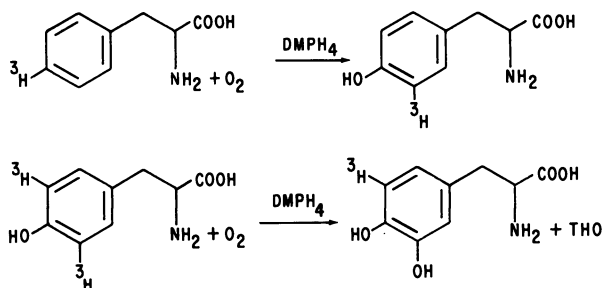
Figure 3. *Hydroxylation of 4-tritiophenylalanine or 3,5-ditritiotyrosine with tyrosine hydroxylase from adrenal glands (DMPH$_4$ = dimethyltetrahydropteridine)*
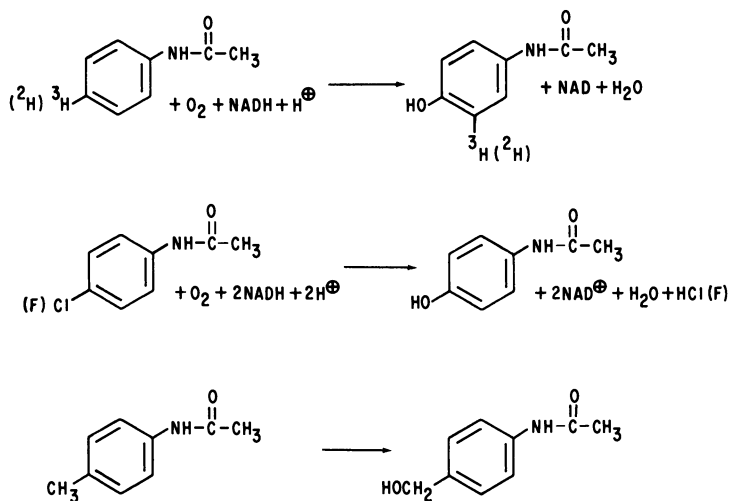
Figure 4. *Hydroxylation of 4-substituted acetanilides with microsomal aryl hydroxylases*

phenylalanine hydroxylase (11). No migration or loss of label occurred before hydroxylation. Retention was similar with rabbit or rat liver microsomes but depended on the pH of the incubation and varied from 63% at pH 7.0 to 36% at pH 9.2. When 4-tritioacetanilide was given to rats and 4-hydroxyacetanilide was isolated from urine, a retention of 36% was found (8). Attempts to demonstrate migration of halogen or alkyl substituents, in analogy to migrations observed with phenylalanine hydroxylase, were unsuccessful. Both the 4-fluoro- and 4-chloroacetanilide were converted to 4-hydroxyacetanilide with loss of halogen (9). [Migration of halogen using microsomes from rats induced with phenobarbital has now been reported (29).] Alkylacetanilides were selectively hydroxylated in the benzylic position rather than in the aromatic ring (9).

To determine whether the enzyme participated in these reactions by abstraction of the hydrogen at the position adjacent to oxygen substitution, the hydroxylations of 3,5-ditritiophenylalanine, 4-tritiotryptophan, and 3,5-ditritioacetanilide were studied with the appropriate enzymes (Figure 5) (12).

The results clearly showed no significant loss of tritium with any of these substrates and indicated no other function for the enzyme but selective introduction of the oxygenating species. The retentions obtained with the preceding examples and with a variety of other specifically deuterated or tritiated substrates during hydroxylation are given in Table I. The net retentions are related to the electron-donating ability of the
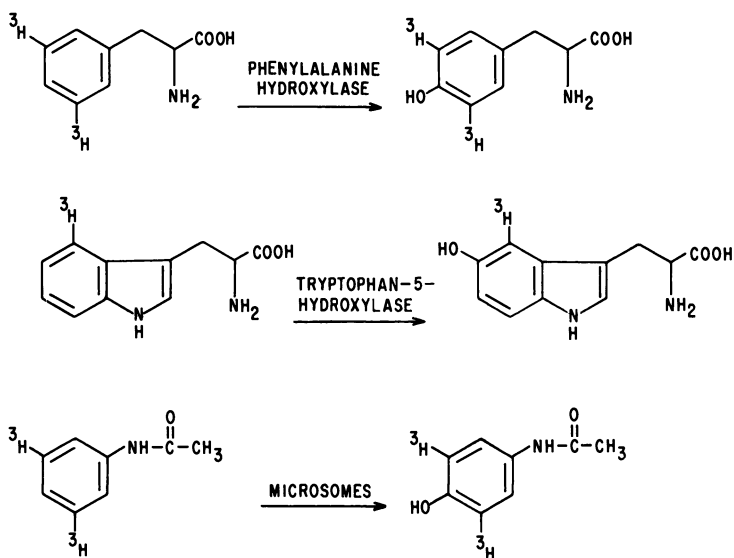
Figure 5.   Hydroxylation of substrates containing tritium label
in the position adjacent to oxygen substitution

Table I.   Migration and Retention of Deuterium or Tritium During Enzymatic Hydroxylation of Specifically Labeled Substrates

Substrate	Product	% Migration and Retention of:	
		Tritium	Deuterium
4-Tritiophenylalanine[a]	3-Tritiotyrosine	94	—
4-Deuterophenylalanine[a]	3-Deuterotyrosine	—	>70
4-Tritioamphetamine[b]	3-Tritio-4-hydroxy-amphetamine	91	—
5-Tritiotryptophan[c]	4-Tritio-5-hydroxy-tryptophan	>85	—
4-Deuterochlorobenzene[b]	3-Deutero-4-hydroxy-chlorobenzene	—	54
4-Tritioacetanilide[b]	3-Tritio-4-hydroxy-acetanilide	45	—
4-Deuteroacetanilide[b]	3-Deutero-4-hydroxy-acetanilide	—	30
4-Tritioaniline[b]	3-Tritio-4-hydroxy-aniline	12	—
4-Deuteroanisole[b]	3-Deutero-4-hydroxy-anisole	—	60
5-Tritiosalicylic acid[b]	Tritiogentisic acid	4	—
3,5-Ditritiotyrosine[d]	3-Tritio-4,5-dihydroxy-phenylalanine	0	—
3,5-Ditritio-N-acetyl-tyramine[b]	3-Tritio-N-acetyldop-amine	0	—

[a] Enzyme: phenylalanine hydroxylase.
[b] Microsomal aryl hydroxylase.
[c] Tryptophan-5-hydroxylase.
[d] Tyrosine hydroxylase.

aromatic substituents and are compatible with the stabilization or delocalization of charge in cationoid intermediates. Compounds which have strong electron donating (ionizable) substituents, such as phenols and aniline exhibit very low degrees of migration and retention. Compounds such as acetanilide, which donate electrons by ionization to a lesser extent, exhibit higher values for migration and retention (*17*). Compounds, such as tryptophan, phenylalanine, and amphetamine, in which no delocalization of charge can take place in a cationoid intermediate, exhibit very high retentions. The charge on the cationoid intermediate formed during 5-hydroxylation of tryptophan is best stabilized in the 4-position. This explains the almost exclusive formation of 4-tritio-5-hydroxytryptophan rather than a mixture of the 4- and 6-tritio isomers.

Pathways and intermediates in the hydroxylation of various substrates are shown in Figure 6. If the charge is partially delocalized by an unshared pair of electrons from the substituent R, as in 4-tritioacetanil-

ide, the label is partially lost *via* path A. This path will be favored at higher pH, and the degree of tritium retention during hydroxylation of 4-tritioacetanilide decreases with increasing pH. As expected, the loss of deuterium by this path was higher than that of tritium. The degree of retention in the final product will depend not only on the relative importance of paths A and B, but also on the ratio of paths C and D (k_H/k_T) in the rearomatization of the cyclohexadienone intermediate. Double-labeling experiments with 3,5-dideutero-4-tritioacetanilide indicate that the latter reaction involves a large isotope effect in analogy to the rather large ($k_H/k_T \sim 6$–7) isotope effects found for the enolization of simple ketones. This was expected from the data on phenylalanine hydroxylation, where direct loss *via* path A is very small (less than 6%), so that the observed 94% retention is the result of a large isotope effect in the enolization of the intermediate cyclohexadienone.

It is known that the metabolism of chlorobenzene *in vivo* leads to a variety of products including 4-chlorophenol, 4-chlorocatechol, 4-chlorophenylmercapturic acid, and 4-chloro-1,2-*trans*-dihydrodihydroxybenzene (*26*). When the metabolism of 4-deuterochlorobenzene was studied in this laboratory, 3-chlorophenol and an *O*-methylated chlorocatechol were isolated in addition to the products reported above (*19*). The products isolated, the proposed intermediates, and their deuterium contents are summarized in Figure 7. An intermediate, X, is postulated for this scheme
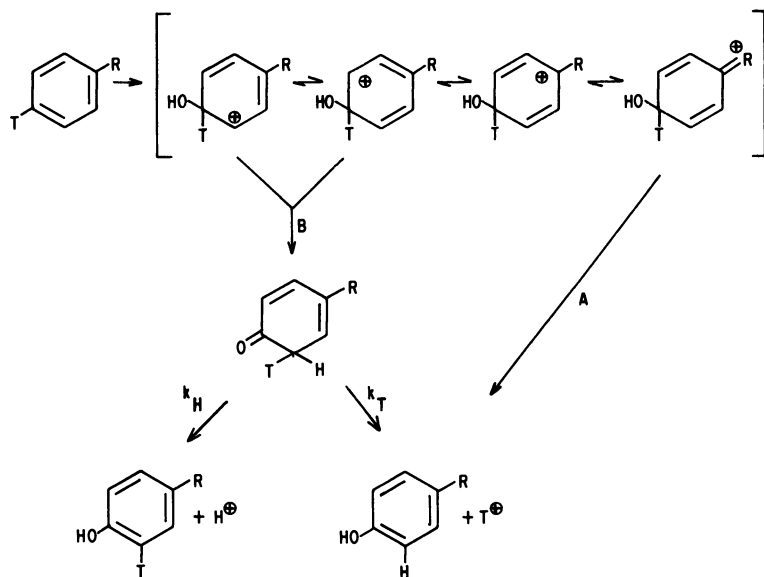
Figure 6. Postulated intermediates formed during enzymatic hydroxylation and their relation to the NIH Shift
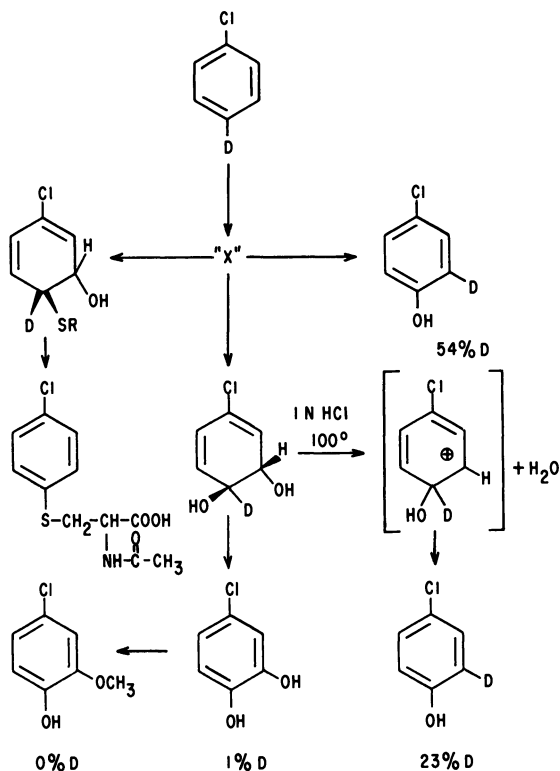
Figure 7. Metabolism in vivo of 4-deuterochloro-benzene and the acid-catalyzed dehydration of 4-chloro-1,2-dihydrodihydroxybenzene-1-^2H

of enzymatic oxidation. This X could be a cationoid structure or an epoxide, either of which could react with nucleophiles, such as "activated glutathione" (2), or with water to form dihydrobenzene derivatives. X could also undergo rearomatization reactions as shown earlier (Figure 6). The 4-chlorophenol retained 54% of the deuterium while the 4-chlorocatechol and the O-methyl-4-chlorocatechol contained only insignificant amounts of deuterium. This indicates that the catechol derivatives arise by dehydrogenation of the diol rather than by hydroxylation of the 4-chlorophenol; if the catechols had arisen from 4-chlorophenol, they would have contained at least one-half of its deuterium content (27%). The possibility that they arise from 3-chlorophenol is under investigation. The 3-chlorophenol, contained 84% of the deuterium, but its metabolic origin is not certain. The mercapturic acid contained very little (∼ 2%) deuterium, and its formation is being studied further. As expected, the isolated 4-chloro-1,2-*trans*-dihydrodihydroxybenzene contained one deu-

terium atom. On treatment with 1N HCl at 100°C. this material de-
hydrates to form 4-chlorophenol with a concomitant migration and
retention of 23% of the deuterium. This nonenzymatic migration and
retention of deuterium demonstrates that cationoid intermediates of the
type generated in this dehydration are compatible with the migrations
observed during enzymatic hydroxylations. Similar studies are planned
with 4-substituted-1-deutero-1,2-benzene epoxides.

The migration of alkyl substituents during the hydroxylation of
4-hydroxyphenylpyruvic acid (25) and 4-fluorophenylpyruvic acid (27)
(Figure 8) provides another example of the NIH Shift and was formerly
thought to be a unique phenomenon. It is in a sense atypical since a
decarboxylation accompanies the hydroxylation and side chain migration.

Nonenzymatic examples of intramolecular migrations are known,
such as the migration of tritium during oxidative polymerization of
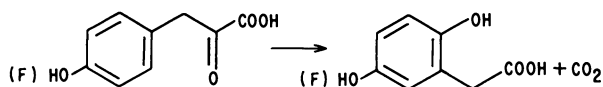
*Figure 8. Migration of the side chain during hy-
droxylation of phenylpyruvates with (hydroxy) phenyl-
pyruvic acid oxidase*

4-tritio-2,6-xylenol (Figure 9) for which a cationoid intermediate has also
been proposed (6). Oxidation of 4-alkylphenols with Caro's reagent or
lead tetraacetate (30, 31) leads to migration of the alkyl substituent and
formation of 2-alkylhydroquinones (Figure 10). Caro's acid is a source
of OH$^+$ as is peroxytrifluoroacetic acid. With the latter reagent, methyl
migrations occur during oxidation of 1,2,3,4-tetramethylbenzene (Figure
10) (5).

The enzymatic migration of chloro and bromo groups, but not of
fluoro substituents, by a cationoid mechanism is supported by observations
on aluminum chloride-catalyzed isomerizations of halo arenes (22),
where all halogens except fluorine migrate by a mechanism involving
cationoid intermediates. For the enzymes, however, fluorine appears to
be removed reductively, so that it is lost as fluoride ion rather than as
positive fluorine.

The reagent, peroxytrifluoroacetic acid, also causes migrations of
tritium and deuterium during 4-hydroxylation of 4-tritio(deutero)
acetanilide and 4-deuterochlorobenzene (Figure 11). The retentions
with the acetanilides are lower (8 and 10% vs. 30 and 45%) than those
obtained on enzymatic hydroxylation while the retention obtained with
the chlorobenzene is higher (70% vs. 54%) than the value obtained on
enzymatic hydroxylation. Other hydroxylating systems as those of
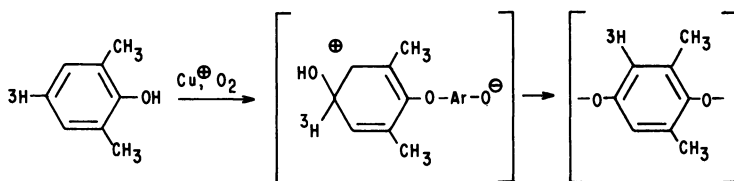
Figure 9. *Migration of tritium during oxidative polymerization of 4-tritio-2,6-xylenol*
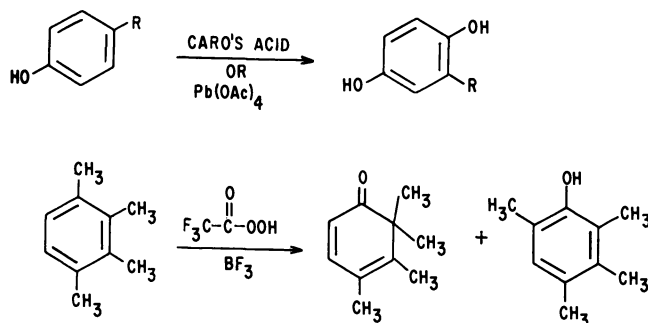
Figure 10. *Migration of alkyl substituents during non-enzymatic hydroxylations*
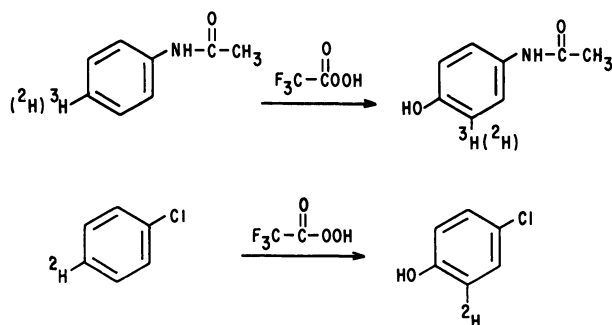
Figure 11. *Migration of tritium and deuterium during hydroxylation of acetanilides and chlorobenzene with peroxytrifluoroacetic acid*

Fenton (*4*), Udenfriend (*3*), Hamilton (*16*), or Viscontini (*1*) which have been considered as possible models for enzymatic hydroxylation do not lead to significant migration and retention of tritium during the formation of 4-hydroxyacetanilide (Table II). Thus, only model hydroxylating systems proceeding *via* cationic intermediates produce the migration of substituents characteristic of enzymatic hydroxylation. It appears

Table II.   Retention of Tritium in 4-Hydroxyacetanilide Formed from 4-Tritioacetanilide with a Variety of Nonenzymatic Hydroxylating Systems (18) [a]

Hydroxylating System	Retention of Tritium, %
F_3CCO_3H	9.6 [b]
H_2O_2, Fe^{2+}, EDTA	1.9
H_2O_2, catalytic amounts of Fe^{3+} and catechol	1.0
O_2, Fe^{2+}, ascorbic acid, EDTA	1.2
O_2, Fe^{2+}, $DMPH_4$, EDTA	1.9

[a] The 2- and 3-hydroxyacetanilides produced retained at least 80% of the original activity of 4-tritioacetanilide ($DMPH_4$ = dimethyltetrahydropteridine).
[b] Retention of deuterium with this reaction was 7.5%.

most likely that the migrations observed on enzymatic hydroxylation are a function of both the structure of the substrate and the nature of the oxygenating species.

The discovery of the NIH Shift has provided new insights into the mechanisms of aromatic hydroxylation and a new criterion for studying model hydroxylating systems. It is also important in studies on drug metabolism and has led to the development of new enzyme assays for at least two important hydroxylases, phenylalanine hydroxylase (10) and tryptophan hydroxylase (23).

Literature Cited

(1) Bobst, A., Viscontini, M., *Helv. Chim. Acta* **49**, 884 (1966).
(2) Booth, J., Boyland, E., Sims, P., *Biochem. J.* **79**, 516 (1961).
(3) Brodie, B., Axelrod, J., Shore, P., Udenfriend, S., *J. Biol. Chem.* **208**, 741 (1954).
(4) Breslow, R., Lukens, L. N., *J. Biol. Chem.* **235**, 292 (1960).
(5) Buehler, C., Hart, H., *J. Am. Chem. Soc.* **85**, 3177 (1963).
(6) Butte, W. A., Jr., Price, C. C., *J. Am. Chem. Soc.* **84**, 3567 (1962).
(7) Daly, J., Guroff, G., *Arch. Biochem. Biophys.* **125**, 136 (1968).
(8) Daly, J., Guroff, G., Udenfriend, S., Witkop, B., *Arch. Biochem. Biophys.* **122**, 218 (1967).
(9) Daly, J. W., Guroff, G., Udenfriend, S., Witkop, B., *Biochem. Pharmacol.* **17**, 31 (1968).
(10) Guroff, G., Abramowitz, A., *Anal. Biochem.* **19**, 548 (1967).
(11) Guroff, G., Daly, J., *Arch. Biochem. Biophys.* **122**, 212 (1967).
(12) Guroff, G., Daly, J. W., Jerina, D., Renson, J., Witkop, B., Udenfriend, S., *Science* **157**, 1524 (1967).
(13) Guroff, G., Kondo, K., Daly, J., *Biochem. Biophys. Res. Commun.* **25**, 622 (1966).
(14) Guroff, G., Levitt, M., Daly, J., Udenfriend, S., *Biochem. Biophys. Res. Commun.* **25**, 253 (1966).
(15) Guroff, G., Reifsnyder, C. A., Daly, J., *Biochem. Biophys. Res. Commun.* **24**, 720 (1966).
(16) Hamilton, G., Hanifin, J., Friedman, J., *J. Am. Chem. Soc.* **88**, 5266 (1966).
(17) Jerina, D., Guroff, G., Daly, J., *Arch. Biochem. Biophys.* **124**, 612 (1968).

(18) Jerina, D., Daly, J., Landis, W., Witkop, B., Udenfriend, S., *J. Am. Chem. Soc.* **89**, 3347 (1967).
(19) Jerina, D., Daly, J., Witkop, B., *J. Am. Chem. Soc.* **89**, 5488 (1967).
(20) Kaufman, S., *Biochim. Biophys. Acta* **51**, 619 (1961).
(21) Levitt, M., unpublished data.
(22) Olah, G. A., Tolgyesi, W. S., Dear, R. E. A., *J. Org. Chem.* **27**, 3441 (1962).
(23) Renson, J., unpublished data.
(24) Renson, J., Daly, J., Weissbach, H., Witkop, B., Udenfriend, S., *Biochem. Biophys. Res. Commun.* **25**, 504 (1966).
(25) Schepartz, B., Gurin, S., *J. Biol. Chem.* **180**, 663 (1949).
(26) Smith, J. N., Spencer, B., Williams, R. T., *Biochem. J.* **47**, 284 (1950).
(27) Taniguchi, K., Kappe, T., Armstrong, M. D., *J. Biol. Chem.* **239**, 3389 (1964).
(28) Udenfriend, S., Zaltzman-Nirenberg, P., Daly, J., Guroff, G., Chidsey, C., Witkop, B., *Arch. Biochem. Biophys.* **120**, 413 (1967).
(29) Ullrich, V., Wolf, J., Amadori, E., Staudinger, H., *Z. Physiol. Chem.* **349**, 85 (1968).
(30) Witkop, B., Goodwin, S., *Experientia* **8**, 377 (1952).
(31) Witkop, B., Goodwin, S., *J. Am. Chem. Soc.* **79**, 179 (1957).

83

Analysis of the O₂ Reduction Process by the Peroxidase System

I. YAMAZAKI, H. YAMAZAKI, M. TAMURA, T. OHNISHI,
S. NAKAMURA, and T. IYANAGI

Biophysics Division, Research Institute of Applied Electricity,
Hokkaido University, Sapporo, Japan

The reaction of O_2 in the peroxidase system is initiated in two different ways. First, O_2 accepts an electron from the semioxidized organic molecule produced in the presence of peroxidase and H_2O_2, forming perhydroxyl radical which is an active intermediate in the chain reaction and which causes the oxidation of other organic molecules. In this reaction O_2 is reduced to H_2O_2 via the perhydroxyl radical. Second, O_2 combines with ferroperoxidase, which is reduced by the semioxidized organic molecule, and forms oxygenated enzyme (Compound III). O_2 in Compound III is activated and reacts with many hydrogen donors, especially rapidly with indoleacetate and p-phenylenediamine. The mechanism of oxygen activation by peroxidase provides some insight into the catalytic activation of O_2 in general.

Although the redox potential of the O_2–H_2O system is much more positive than that of organic molecules which appear in the ordinary metabolic paths in biology, these molecules are usually non-autoxidizable under physiological conditions. The sluggish activity of O_2 toward these molecules seems to arise from the fairly low redox potential of the first one-equivalent reduction of O_2,

$$O_2 + e^- \rightleftharpoons O_2^- \tag{1}$$

and from the high redox potential of one-equivalent oxidation of organic molecules,

$$H_2A \rightleftharpoons HA\cdot + e^- + H^+ \tag{2}$$

General considerations of the one-equivalent redox potential in the two-equivalent redox system were made by Michaelis (*18*) for organic

molecules and by George (8) for O_2. According to Michaelis, normal potentials of the first (E_1) and second (E_2) oxidations are

$$E_1 = E_m - \frac{RT}{2F} \ln K_s \qquad (3)$$

$$E_2 = E_m + \frac{RT}{2F} \ln K_s \qquad (4)$$

where E_m is the normal potential of the over-all two-equivalent oxidation process, and K_s is the semiquinone formation constant,

$$K_s = \frac{(HA\cdot)^2}{(H_2A)(A)} \qquad (5)$$

Michaelis *et al.* (16, 17) have estimated E_1 and E_2 for several molecules by analyzing the potentiometric titration curve. This method can be applied only to redox systems which give a large equilibrium concentration of semiquinone, usually for systems for which $K_s > 0.01$. Direct estimation of semiquinone concentration by ESR (electron spin resonance) is about 10^{10} times more sensitive for the K_s estimation than analysis of titration curves. Some values are shown in Table I. The K_s for NADH (reduced form of nicotineamide adenine dinucleotide) is too small to be measured even by ESR, and only an approximate upper limit is given.

Table I. First One-Equivalent Oxidation Potential (E_1) and Autoxidation Velocity

	pH	E_m	$-\log K_s$	E_1	E_2	k, $sec.^{-1}\,M^{-1}$	$E_1 + 0.06\,\log k$
Hydroquinone	7.3	0.26	6	0.45	0.07	10^{-2}	0.33
Ascorbic acid	7.5	0.05	8.8	0.31	−0.21	10^{-1}	0.25
Vitamin K₃	6.5	0.02	9	0.30	−0.26	1	0.30
Methylene blue	6.0	0.045	4.1	0.17	−0.09	3	0.20
NADH	7.0	−0.2	(~20)	(0.39)		3×10^{-2}	

Table I shows that the autoxidation velocity of the organic molecules depends on E_1 rather than E_m. $E_1 + 0.06 \log k$ gives about 0.3 volt, which might be called an "autoxidation constant." The approximate uniformity of the value can be understood by assuming the following imaginary isolated redox reaction,

$$H_2A + O_2 \underset{k_{-1}}{\overset{k_1}{\rightleftharpoons}} HA\cdot + O_2^{-\cdot} + H^+ \qquad (6)$$
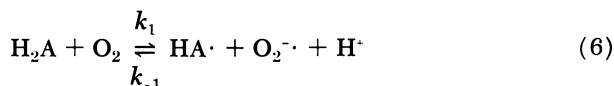
with an approximate constant value for k_{-1}, which seems to be almost diffusion limited. The apparent rate constant, k, may deviate slightly

from k_1 because of the possible participation of chain reactions, discussed later. If Reaction 6 is an elementary process, the equilibrium constant is equal to the ratio of forward and reverse rate constants, k_{-1}/k_1, and at room temperature (34),

$$E_1 + 0.06 \log k_1 = E_{H_2O_2,2} + 0.06 \log k_{-1} \tag{7}$$

where $E_{H_2O_2,2}$ is the second oxidation potential of H_2O_2 which corresponds to the potential of Reaction 1. The autoxidation constant may be only approximate, but it makes possible the evaluation of the autoxidizability of molecules where over-all redox potential (E_m) and semiquinone formation constant are known. NADH is very stable against autoxidation despite its low redox potential. Rough values for E_1 and K_s of NADH can be estimated (Table I). The value for K_s suggests that the equilibrium concentration of semiquinone is much smaller than ESR spectroscopy can detect under the most suitable conditions. The extreme stability of many biological metabolites against autoxidation may be explained in the same way. Most of these molecules do not give equilibrium semiquinones detectable by ESR.

How does the oxidase remove these potential barriers? The oxidase can activate either electron donor or electron acceptor or both simultaneously. The activation of the substrate by the oxidase might be considered as the movement of the potential of the first one-equivalent reduction of
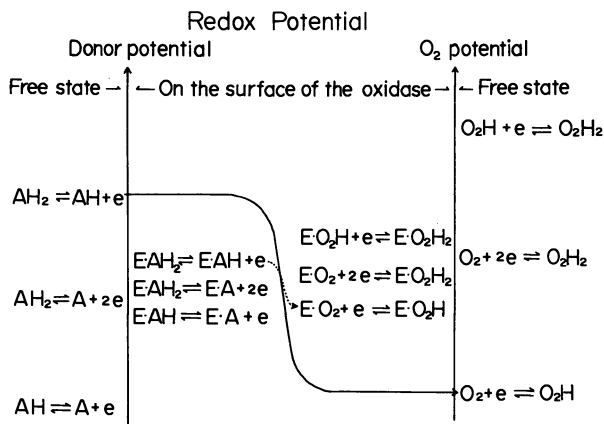
Figure 1. Tentative mechanism for activation of electron donors and O_2 by the oxidase

Strong affinities of the oxidase for AH_2 and O_2 increase the E_m of donors and decrease E_m for O_2. Electron transfer from donors to O_2 becomes much easier on the surface of oxidase (dotted line) than in the free state (solid line) because of the possible proximity of both molecules and the decrease in the potential barrier

O_2 ($E_{H_2O_2,2}$) to the positive side and of the first one-equivalent oxidation of electron donors to the negative side, as shown in Figure 1. The E_m of these molecules in the bound state on the oxidase will be the same as in the free state provided the affinities of the oxidase for the reduced and oxidized forms are equal. The one-order-of-magnitude difference between these affinities will make 0.03 volt difference in the normal potentials (E_m) between the free and bound state. It may be said that hydrogen donors and O_2 are activated by the oxidase when it stabilizes the intermediates and increases the semiquinone formation constant, K_s. An increase in K_s results in a rise of E_2 and a drop of E_1.

Peroxidase as an Oxygen-Activating Enzyme

Besides the ordinary H_2O_2-consuming oxidation, peroxidase also catalyzes O_2-consuming oxidation (the peroxidase-oxidase reaction). In recent years considerable attention has been directed to elucidating the peroxidase-oxidase mechanism. Controversy was centered about the participation of ferrous enzyme in O_2 activation. Is peroxidase reduced to the ferrous state during the reaction (*3, 13, 19, 21, 23*)? Does peroxidase compound III, which appears in the reaction, correspond to oxygenated ferroperoxidase (*3, 5, 15*)? If so, is O_2 in Compound III activated (*15*)? As discussed here, these problems seem to be almost solved, and it is very likely that the peroxidase-oxidase reaction is a good model for analyzing the mechanism of other oxidases.

O₂ Reduction by Semiquinones. The most typical feature of the peroxidase reaction is the oxidation of a number of organic molecules at the expense of H_2O_2 to produce free radicals of the donor molecules used. The following mechanism for the peroxidase reaction was established by George (*7*) and Chance (*4*).

$$\text{Peroxidase} + H_2O_2 \longrightarrow I \tag{8}$$

$$I + H_2A \longrightarrow II + HA\cdot + (H_2O) \tag{9}$$

$$II + H_2A \longrightarrow \text{Peroxidase} + HA\cdot + (H_2O) \tag{10}$$
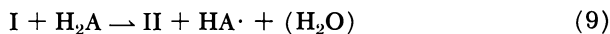
They confirmed that conversions from I to II and from II to free peroxidase correspond to single-equivalent reductions. Since II was observable as an intermediate in the steady state of the ordinary peroxidase reactions, it was suggested that organic molecules are oxidized to semi-oxidized free radicals. We have confirmed the mechanism by titrating the radicals with suitable electron acceptors (*26*) and finally by using ESR spectroscopy (*29*). Kinetic analysis of free radical formation during the peroxidase reaction made it possible to conclude that most of the free radicals formed in Reactions 9 and 10 dismutate with each other rather than react further with the enzyme in the oxidized state (*30*).

We have never succeeded in detecting by ESR the free radicals of important biological molcules such as IAA (indoleacetic acid) and NADH which are substrates for the peroxidase-oxidase reaction. When an electron acceptor such as ferric ion with o-phenanthroline is added to the peroxidase system, one can observe the stoichiometric reduction of iron (Figure 2) described in the following reactions (28).

$$2 \text{ IAA} + \text{H}_2\text{O}_2 + 2 \text{ Fe}^{3+} \xrightarrow{\text{peroxidase}} 2 \text{ IAAox} + 2 \text{ Fe}^{2+} (+2 \text{ H}_2\text{O}) \quad (11)$$

$$2 \text{ NADH} + \text{H}_2\text{O}_2 + 2 \text{ Fe}^{3+} + 2 \text{ H}^+ \xrightarrow{\text{peroxidase}} 2 \text{ NAD}^+ + 2 \text{ Fe}^{2+} + 2 \text{ H}_2\text{O} \quad (12)$$
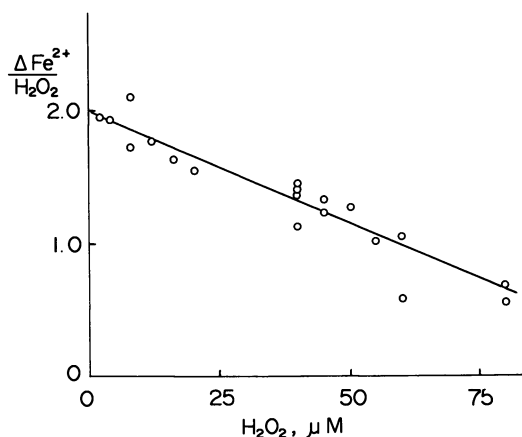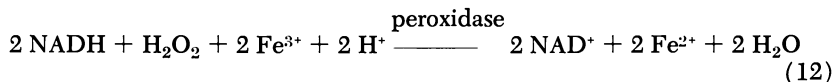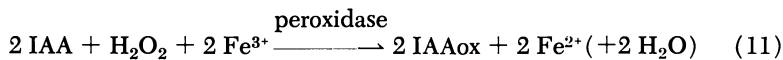
Figure 2.   Molar ratio of reduced iron to H_2O_2 added in the $NADH$–H_2O_2–peroxidase reaction. 2 μM HRP, 1 mM NADH, 40 μM FeCl$_3$, 1.2 mM o-phenanthroline, 0.05M phosphate, pH 6.0, 25°C.

The stoichiometric reduction of iron can be explained only by assuming that in the presence of peroxidase H_2O_2 produces two free radicals which are very reactive and effectively reduce the added electron acceptor. There are two types of free radicals which appear in the peroxidase reaction. We have classified them into redogenic and oxidogenic ones (26). Redogenic donors can give rise to two-equivalent oxidized forms, but oxidogenic donors cannot.

Redogenic

$$\text{H}_2\text{A} \rightleftharpoons \text{HA} \cdot \rightleftharpoons \text{A}$$

Oxidogenic

$$\text{HX} \rightleftharpoons \text{X} \cdot$$
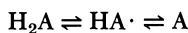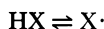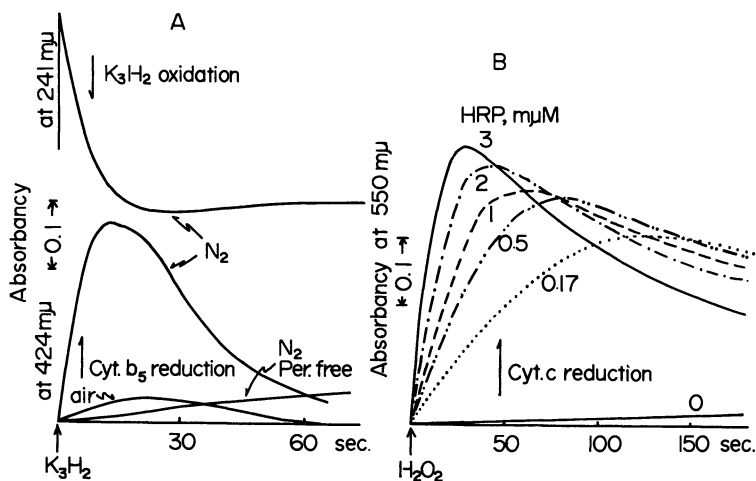
Figure 3.   Reduction of cytochromes by semiquinones formed in the peroxidase reaction. 0.05M phosphate, pH 6.5. Reoxidations of cytochromes are caused by the accumulation of quinones

(A) Cytochrome b_5 reduction by K_3 semiquinone. 10 mμM HRP, 3.7 μM cyt. b_5, 10 μM H_2O_2, 20 μM reduced vitamin K_3 (K_3H_2), 20°C. Reaction was started by adding K_3H_2. Cyt. b_5 reduction and K_3H_2 oxidation were measured separately but under the same conditions
(B) Cytochrome c reduction by p-benzosemiquinone. 33 μM cytochrome c, 50 μM H_2O_2, 100 μM hydroquinone at different HRP concentrations, 25°C. Reaction was started by adding H_2O_2

Semiquinones of redogenic molecules can reduce not only ferric ions but also dyes (27), cytochromes, and O_2 as shown in Figure 3 and Table II. Since the reduction product of O_2 is H_2O_2, a trace amount of H_2O_2 initiates a peroxidase-catalyzed aerobic oxidation, and further addition

Table II.   Reducing Activity of Semiquinones Derived from Donors by Peroxidase

		Electron Acceptors for Semiquinones				
Electron Donors	O_2	*Methylene Blue*	*Cyt. b_5*	*Cyt. c*	*Ferric Peroxidase*	*Fe^{3+}* [b]
NADH	+		+	+	++ [a]	+
IAA	+			+	++ [a]	+
Triose reductone	+	+		+	+	
DHF	++ [a]	+		+	+	
Vitamin K_3	+		+	+	+	
Ascorbic acid	−			+	−	
Hydroquinone	−	−		+	−	

[a] Reaction of the acceptors with these semiquinones are much faster than the others.
[b] Reactions carried out in the presence of o-phenanthroline.

of H_2O_2 is no longer necessary for the reaction to proceed. The direct demonstration of the reaction of O_2 with such semiquinone intermediates was made with ESR in the DHF–H_2O_2–pedoxidase–O_2 system (31). From the experiments it was concluded that O_2 reacts very rapidly with DHF (dihydroxyfumaric acid) semiquinone but slowly with triose-reductone semiquinone. No measurable reactions of O_2 with semiquinones of ascorbate or hydroquinone were observed. Reduced vitamin K_3 is known to be oxidized by the peroxidase system (12, 13). An active intermediate in the reaction seems to be K_3 semiquinone which is able to reduce O_2. The ESR signal of the semiquinone formed in the peroxidase reaction is shown in Figure 4. The reaction of O_2 with this semiquinone is not as fast as with that of DHF. A role of K_3 semiquinone as a mediator of electron transfer to O_2 was also suggested by Sato *et al.* (20) for the microsomal NADPH–cytochrome c reductase reaction. The semiquinones of hydrogen donors in the peroxidase-oxidase reaction thus

During continuous flow

(Reaction time ≑ 30 m sec)

10 gauss

After stopping the flow
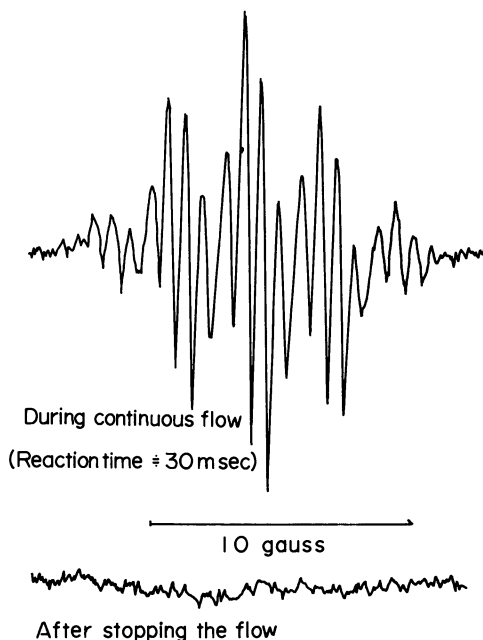
Figure 4.   ESR signal of vitamin K_3 semi-quinone which appears during peroxidase reaction under anaerobic conditions

1 mM reduced vitamin K_3, 1 mM H_2O_2, 5 μM HRP, 0.05M phosphate, pH 7.0, 9% ethyl alcohol at room temperature; 0.2 gauss modulation. Flow method used (29). Reduced K_3 plus H_2O_2 solution was mixed with HRP solution
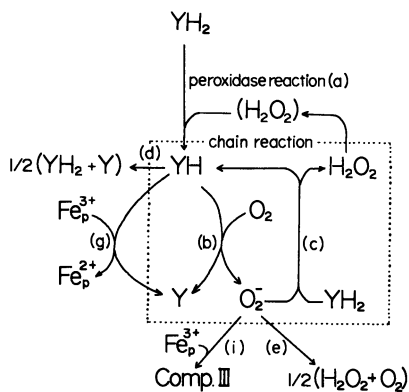
Figure 5.   Chain mechanism in the peroxidase-oxidase reaction.   The mechanism can explain the majority of O_2-consuming oxidations of various electron donors catalyzed by peroxidases

seem able to reduce O_2 to perhydroxyl radical, O_2^-. Since the first one-equivalent reduction potential of O_2 is fixed, there may be an approximate upper limit for the E_2 of donor molecules causing an appreciable reduction of O_2 by their semiquinones. This potential may be about -0.25 volt. The perhydroxyl radical thus formed acts as a strong oxidant rather than a reductant and can oxidize donor molecules to the semiquinones again. The chain reaction will be completed as shown in Figure 5. The efficiency of the chain reaction depends mainly on Reaction c which is activated by Mn^{2+}. The gain of the chain reaction (36) =

$$\frac{v_b}{(v_b + v_d + v_g)} \cdot \frac{(3v_c + v_e)}{(v_c + v_e + v_i)} \qquad (13)$$

O₂ Activation by the Ferrous Enzyme. REDUCTION OF PEROXIDASE. The great controversy over the peroxidase-oxidase reaction has centered about the participation of the ferrous enzyme. We pointed out the possibility of a partial contribution of the ferrous enzyme, especially when IAA or NADH was used as a hydrogen donor (32). Although it is still impossible to detect the semiquinones of these molecules by ESR, it may be concluded from the stoichiometric results of Reactions 11 and 12 that H_2O_2 produces two semiquinone molecules of IAA and NADH. When excess peroxidase rather than the added acceptors is present, peroxidase itself will be reduced by the semiquinones. Ferroperoxidase can be observed easily even in the absence of CO when NADH is used as donor (33). The semioxidized IAA molecule seems to have unusual reactivity

toward peroxidase protein, and it is not easy to observe the formation of ferroperoxidase in the absence of CO.

FORMATION AND REACTIVITY OF III. Peroxidase III was found by Keilin and Mann (11) in the presence of excess H_2O_2 and was observed by Swedin and Theorell (23) during the aerobic oxidation of DHF catalyzed by this enzyme. An oxy-ferroperoxidase structure was suggested for III (6, 15). This idea, however, has not been generally accepted since ferroperoxidase is thought to be oxidized directly to ferriperoxidase without the formation of an oxygenated compound (5, 9, 24). Recently, experimental evidence has accumulated which suggests that ferroperoxidase reacts with O_2 to form III (22, 25, 31, 33, 35). The possible contribution of an O_2^- structure in III may suggest the following three tentative mechanisms for the decomposition of III.
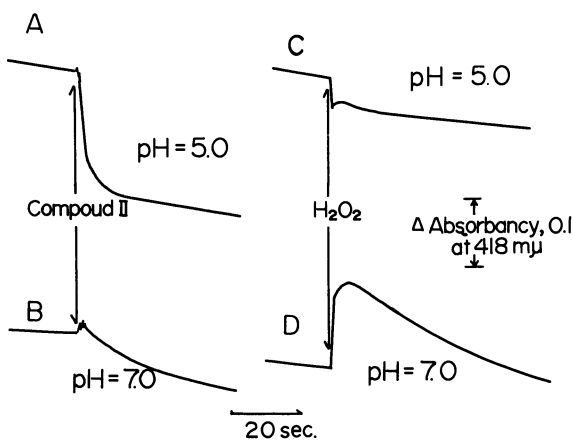
Figure 6.   Decomposition of III by adding II and a small amount of H_2O_2

A and B: 2 ml. of II solution were added to 2 ml. III solution. III was prepared by photodissociation of CO-ferroperoxidase in the presence of O_2. HRP concentrations were II μM in both solutions. II was prepared from ferriperoxidase by adding 11 μM H_2O_2 and 5.5 μM ascorbate. 0.1M acetate, pH 5.0 (A) and 0.1M phosphate pH 7.0 (B). In A, II and III disappeared immediately after mixing, and they both converted to ferriperoxidase. In B, a mixture of II and III was observed, and the decomposition of III was slightly accelerated
C, D: H_2O_2 (final concentration = 5 μM) was added to III solution (HRP = 11 μM, about 20% III had already converted to ferriperoxidase). 0.1M acetate, pH 5.0 (C) and 0.1M phosphate, pH 7.0 (D). In C a mixture of I and III, and in D a mixture of II and III were observed, respectively

Comp. I
(+5)

H₂O₂ | (a₁)   (a₂) | e⁻

Ferroperoxidase $\underset{(g)}{\overset{e^-}{\rightleftharpoons}}$ Peroxidase $\underset{(a_3)}{\overset{e^-}{\longleftarrow}}$ Comp. II
(+2)   (+3)   (+4)

O₂⁻ (j)   (i) | O₂⁻   (h) H₂O₂

Comp. III
(+6)

(c) | e⁻

(Comp. I)
(+5)
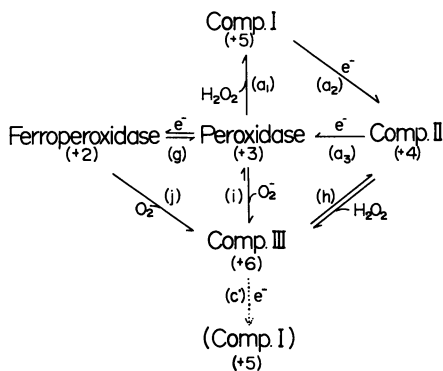
Figure 7. Tentative scheme for the relationship between peroxidase compounds which appear during the peroxidase-oxidase reactions

Numbers in parentheses show the "oxidation level" of the iron of peroxidase compounds. Peroxidase cycle is composed of Reactions a₁, a₂, and a₃. No direct evidence has been obtained which indicates that III is reduced to I itself by the introduction of a single electron

Reductive Decomposition. III reacts with many electron-donors (2, 37). Ferroperoxidase itself is a very good electron-donor in Reaction 14,

$$Fe_p{}^{3+}O_2{}^-(III) \quad \overset{+e^-}{\underset{(2H^+)}{\longrightarrow}} \quad Fe_p{}^{3+} + H_2O_2(I) \tag{14}$$
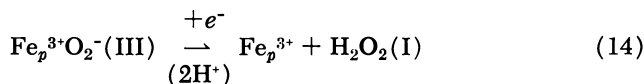
and thus III is not observed if O_2 is introduced into a ferroperoxidase solution little by little.

Oxidative Decomposition. Figures 6A and B show that III reacts with II more rapidly at pH 5.0 than at 7.0. H_2O_2 catalyzes the decomposition

$$Fe_p{}^{3+}O_2{}^-(III) \quad \overset{-e^-}{\longrightarrow} \quad Fe_p{}^{3+} + O_2 \tag{15}$$
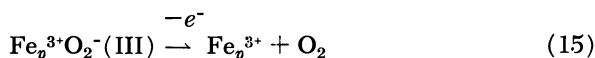
of III in the presence of ferriperoxidase, and it is suggested that I and II participate in the reaction. Figures 6C and D show that adding a small amount of H_2O_2 causes different effect on the absorbance at 418 mμ, and scans of wavelength show a mixture of I and III at pH 5.0 and a mixture of II and III at pH 7.0. Since I and II are stable for this enzyme preparation, it is suggested that the reaction of III with I is fast at pH 7.0 and slow at pH 5.0. Since I and II are strong oxidants, it is reasonable to assume that this type of decomposition is oxidative.
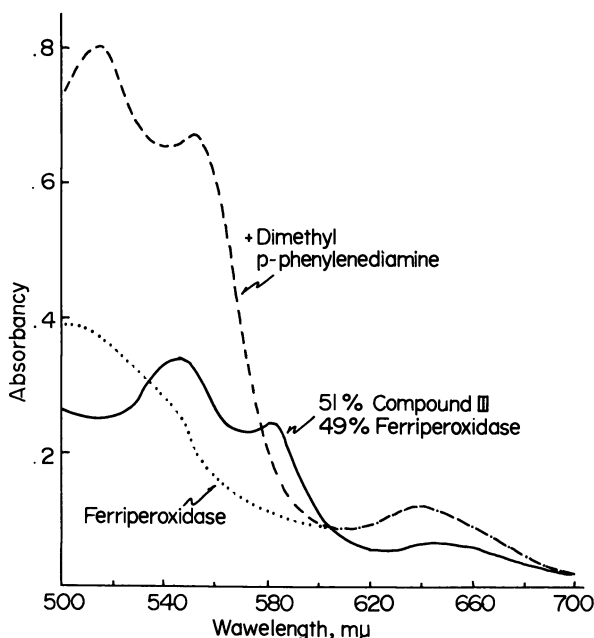
Figure 8A. Stoichiometry of the reaction of III with dimethyl-p-phenylenediamine. Experiments carried out strictly at 0°C. to avoid decomposition of III. Milli-molar extinction coefficient of dimethyl-p-phenylene-diamine radical was 8.7 at 515 mμ

Horseradish peroxidase. After HRP was treated with 0.1 mM DHF, pH 5.0, the enzyme was isolated by passing the solution through Sephadex G-25 column; 51% of III remained about 40 minutes after the treatment started (solid line). 1 mM dimethyl-p-phenylenediamine was added to this solution at pH 6.0 (broken line). Dotted line is spectrum of the solution in which all of III autodecomposed to ferriperoxidase

Autodecomposition. III decomposes to give ferriperoxidase without any observable intermediates (25, 35). Reactions 16 and 17 are suggested for the initial autodecomposition of III

$$\text{Fe}_p{}^{3+}\text{O}_2{}^-(\text{III}) \xrightarrow{\text{H}_2\text{O}} \text{Fe}_p{}^{3+}\text{OH}(\text{II}) + \text{HO}_2{}^- \tag{16}$$

$$\text{Fe}_p{}^{3+}\text{O}_2{}^-(\text{III}) \longrightarrow \text{Fe}_p{}^{3+} + \text{O}_2{}^-(\tfrac{1}{2}\,\text{O}_2 + \tfrac{1}{2}\,\text{H}_2\text{O}_2) \tag{17}$$
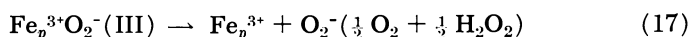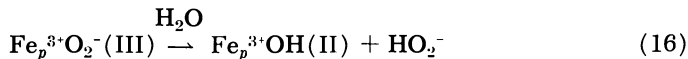
Both reactions produce H_2O_2. Hence, I and II must be intermediates in this reaction. Since these intermediates decompose III oxidatively, it is reasonable to assume that the rate-limiting step in the autodecomposition is either Reaction 16 or 17.

CONFIRMATION OF THE REDOX STATE OF III. Three possible paths for the formation of III were suggested (*35*) (Figure 7). Consequently, the structure of the compound may be $Fe_p{}^{2+}O_2$, $Fe_p{}^{3+}O_2{}^-$, $Fe_p{}^{4+}O_2{}^{2-}$, or a hybrid; All these structures are in the three-equivalent oxidized state when compared with the ferric enzyme, but direct evidence has never been reported to support this fact. Figure 8 shows the stoichiometric relationship of the reaction between III and dimethyl-*p*-phenylenediamine. This donor is known to be oxidized in a one-equivalent step and gives a stable color-free radical. When this donor is added in excess of III, the molar
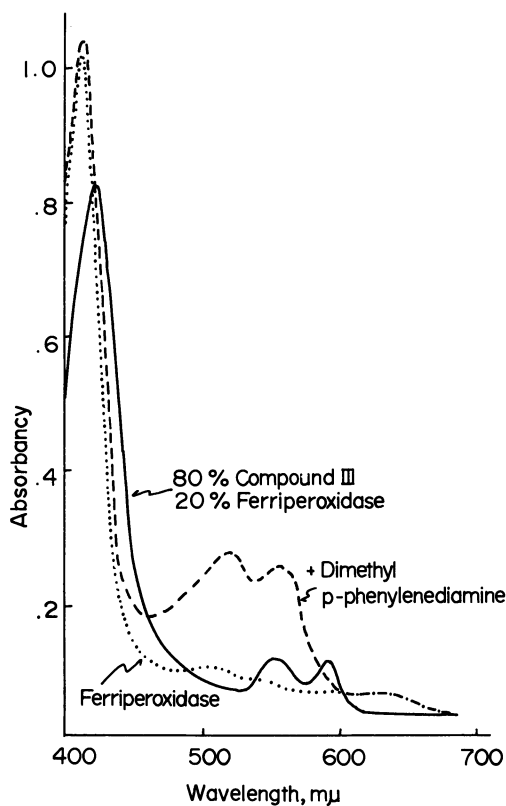
Figure 8B.   Lactoperoxidase

After LP was treated with 1 mM NADH and 0.1 mM Mn^{2+} at pH 7.0, the enzyme was isolated as in Figure 8A. 80% of III solution was obtained (solid line). 0.1 mM dimethyl-p-phenylenediamine was added to this solution (broken line). Increase in the donor concentration up to 1 mM gave the same spectra as the broken line. Dotted line is spectrum of ferriperoxidase at the same LP concentration

ratio of free radical formed to III decomposed is very close to 3, both for HRP (horseradish peroxidase) and LP (lactoperoxidase). The final state of peroxidase is ferric. Since dimethyl-*p*-phenylenediamine is a very fast substrate for I and II which are possible intermediates in the reductive decomposition of III, the participation of oxidative decomposition of III with such intermediates is negligible in this case where excess dimethyl-*p*-phenylenediamine is present, as shown in Figures 8A and B. It is suggested that three donor molecules are consumed to reduce one molecule of III. This seems to be the first demonstration which shows that III is at the three-equivalent oxidized level above that of the ferric enzyme.

   Various attempts have been made, without success, to derive CO-ferroperoxidase from HRP III. LP III is about 10 times more stable than HRP III, and its half-life is more than a half day at $0°C$. When LP III is kept for several hours in an O_2-free and CO-saturated solution, a CO-ferroperoxidase complex cannot be observed. Hence, the dissociation of III into ferrous enzyme and O_2 does not occur at a measurable rate, as indicated in Figure 7.
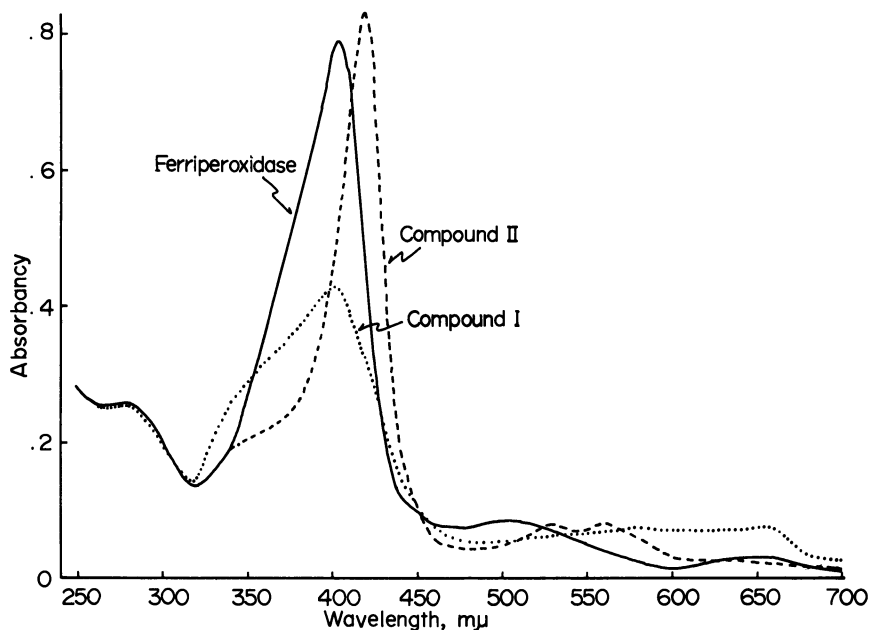
Figure 9A.   Absorption spectra of redox compounds of HRP
I (broken line), 14 μM H_2O_2 were added to the ferriperoxidase (solid line). Our preparation gave very stable I under these conditions. II (dotted line), a slight excess of ascorbate was added to I solution. 0.05M phosphate, pH 7.0 at 6°C.
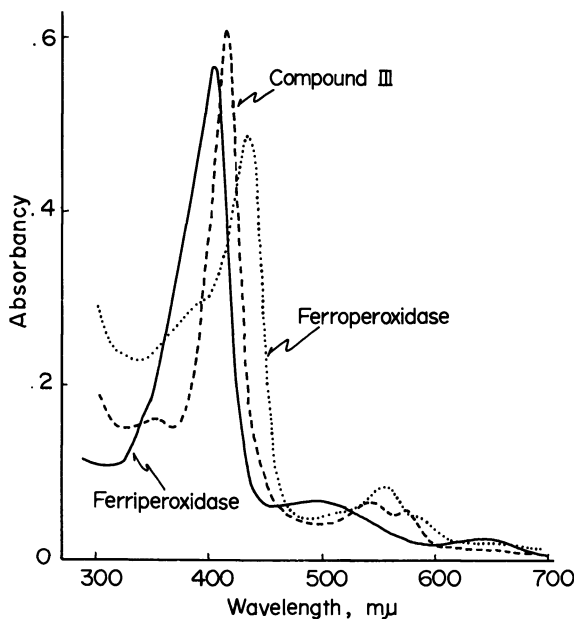
Figure 9B. Absorption spectra of redox compounds of HRP

III (broken line), 0.1 mM DHF and 12 μM H₂O₂ were added to ferriperoxidase, 0.05M acetate, pH 5.0. The same spectrum could be obtained when NADH was added. Ferroperoxidase (dotted line), reduced by Na₂S₂O₄. Ferroperoxidase can be observed in the presence of NADH but only in the mixture with ferriperoxidase (38)

Discussion

Five oxidation states of peroxidase which are catalytically active are clearly identified. All these peroxidase compounds can be obtained in fairly stable states under suitable experimental conditions, shown in Figure 9. III is found to be at the three-equivalent oxidation state above that of the ferric enzyme. It still remains to be shown whether III can be converted to I by a single-equivalent reduction. All the electron donors are known so far to react with I and II faster than with III, and it is difficult to observe intermediates on the way to the ferric enzymes. This difficulty is compounded by the unusually rapid reactions of III with I and II.

Undoubtedly, O₂ is activated as it combines with ferroperoxidase since it reacts with many nonspecific electron donors which are not autoxidizable. This activation is usually explained in terms of partial migration of electron from iron to O₂. It is reasonable to expect a high
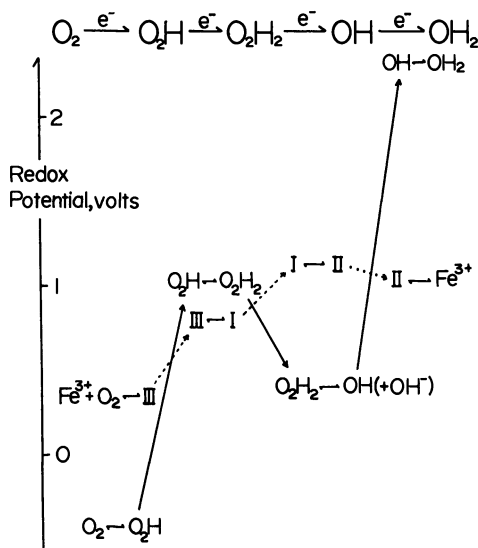
Figure 10. Approximate reduction potential of four single-equivalent steps from O₂ to H₂O in the free state and in the bound state to HRP. Here, 10⁻¹⁰ is used for the dissociation constant of ferroperoxidase and O₂. Rough calculation shows that this is the upper limit. The other values are cited from George's paper (7, 8)

oxidation potential for O_2^- in the bound state as well as in the free state. A rough calculation of the reduction potential of III is possible if one assumes a reversible redox system (Figure 10).

$$\text{III} + e \longleftrightarrow \text{I} \tag{18}$$
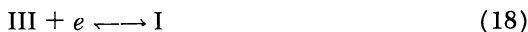
From this potential diagram it may be concluded that peroxidase activates H_2O_2 and O_2 by stabilizing II (HO radical) and III (HO₂ radical). The first one-equivalent reduction potential of H_2O_2 increases remarkably in the form of I. O_2 is also activated in III as a consequence of its semiquinone character.

Figure 11 shows the mechanism of O_2 activation caused by introducing a single electron into the system. The sources of such an electron may be a key point in certain O_2-activating enzymes. For the peroxidase system, they are free radicals of electron donors, as shown by a series of ESR experiments (29, 30). A strong single-equivalent oxidant produces a powerful reductant in the two-equivalent system. In the peroxidase-oxidase reaction the reductant is used for direct reduction of O_2 or formation of ferrous enzyme. The peroxidase-oxidase reaction has mixed

features, as shown in Figure 11, and the reaction mechanism varies slightly from donor to donor. The details were reported elsewhere (*32, 38*).

The mechanism of hydroxylation of aromatic compounds catalyzed by peroxidase in the presence of DHF and O_2 has been discussed by Mason *et al.* (*1, 14, 15*). Probably, the activated species of O_2 is perhydroxyl ion in this reaction (*1*), but the possible transfer of an oxygen atom from III to the organic molecule as suggested by Mason, may not be excluded (*15*). The similarity of this enzyme to tryptophan pyrrolase has been discussed. Now it is found that tryptophan pyrrolase shows

$$Fe_P^{3+} + O_2$$

$$\downarrow + e^- (YH \rightarrow Y + H^+ + e^-)$$

$$Fe_P^{2+}$$

$$(O_2) \quad (Fe_P^{3+})$$

$$Comp.\,III \longleftarrow O_2^-$$

$$\downarrow + e^- (YH_2 \rightarrow YH + H^+ + e^-)$$

$$Fe_P^{3+} + H_2O_2$$
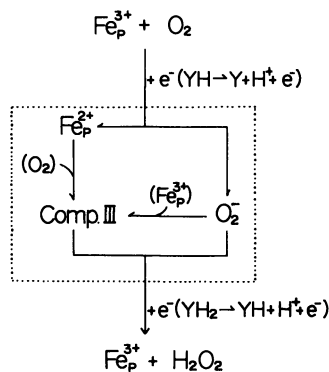
Figure 11. Mixed mechanism for O_2 reduction by peroxidase system

Mechanism on the right is the main path which is shown in Figure 5. Mechanism on the left shows the participation of ferrous enzyme which takes a part of mechanism in the IAA oxidation. Experimental evidence has not yet been obtained which indicates direct oxygen transfer from III to organic molecules

some characteristic properties similar to peroxidase when the enzyme combines with tryptophan. A clear reaction intermediate which shows a spectrum typical of peroxidase III is observed when the reduced enzyme is mixed with O_2 in the presence of tryptophan (*10*). It may be concluded that the intermediate is an oxygenated form of the enzyme resembling peroxidase III.

Literature Cited

(1) Buhler, D. R., Mason, H. S., *Arch. Biochem. Biophys.* **92**, 424 (1961).
(2) Chance, B., *Advan. Enzymology* **12**, 153 (1951).

(3) Chance, B., *J. Biol. Chem.* **107,** 577 (1952).
(4) Chance, B., *Arch. Biochem. Biophys.* **41,** 416 (1952).
(5) Chance, B., "Oxidase and Related Redox Systems," T. E. King, H. S. Mason, M. Morrison, Eds., p. 504, Wiley, New York, 1965.
(6) George, P., *Advan. Catalysis* **4,** 367 (1952).
(7) George, P., *Biochem. J.* **54,** 267 (1953).
(8) George, P., "Oxidases and Related Redox Systems," p. 3, Wiley, New York, 1965.
(9) Harbury, H. S., *J. Biol. Chem.* **225,** 1009 (1957).
(10) Ishimura, Y., Nozaki, M., Hayaishi, O., Tamura, M., Yamazaki, I., *J. Biol. Chem.* **242,** 2574 (1967).
(11) Keilin, D., Mann, T., *Proc. Roy. Soc. (London)* **122 B,** 119 (1937).
(12) Klapper, M. H., Hackett, D. P., *J. Biol. Chem.* **238,** 3736 (1963).
(13) *Ibid.,* p. 3743.
(14) Mason, H. S., Onoprienko, I., Buhler, D. R., *Biochim. Biophys. Acta* **24,** 225 (1957).
(15) Mason, H. S., *Proc. Intern. Symp. Enzyme Chem., Tokyo-Kyoto, 1957,* p. 220.
(16) Michaelis, L., *Chem. Rev.* **16,** 243 (1935).
(17) Michaelis, L., Schwarzenbach, G., *J. Biol. Chem.* **123,** 527 (1938).
(18) Michaelis, L., Schubert, M. P., *Chem. Rev.* **22,** 437 (1938).
(19) Morita, Y., Kameda, K., *Mem. Res. Inst. Food Sci., Kyoto Univ.* **23,** 1 (1961).
(20) Nishibayashi, H., Omura, T., Sato, R., *J. Biochem.* **60,** 172 (1966).
(21) Ray, P. M., *Arch. Biochem. Biophys.* **87,** 19 (1960).
(22) Richard, J., Nari, J., *Biochim. Biophys. Acta* **132,** 321 (1967).
(23) Swedin, B., Theorell, H., *Nature* **145,** 71 (1940).
(24) Theorell, H., *Advan. Enzymol.* **7,** 265 (1947).
(25) Wittenberg, J., Noble, R. W., Wittenberg, B. A., Antonini, E., Brunori, M., Wyman, J., *J. Biol. Chem.* **242,** 626 (1967).
(26) Yamazaki, I., *Proc. Intern. Symp. Enzyme Chem., Tokyo-Kyoto, 1957,* p. 224.
(27) Yamazaki, I., Fujinaga, K., Takehara, I., *Arch. Biochem. Biophys.* **72,** 42 (1957).
(28) Yamazaki, I., Souzu, H., *Arch. Biochem. Biophys.* **86,** 294 (1960).
(29) Yamazaki, I., Mason, H. S., Piette, L. H., *J. Biol. Chem.* **235,** 2444 (1960).
(30) Yamazaki, I., Piette, L. H., *Biochim. Biophys. Acta* **50,** 62 (1961).
(31) Yamazaki, I., Piette, L. H., *Biochim. Biophys. Acta* **77,** 47 (1963).
(32) Yamazaki, I., Yokota, K., Nakajima, R., "Oxidases and Related Redox Systems," p. 485, Wiley, New York, 1965.
(33) Yamazaki, I., Yokota, K., *Biochem. Biophys. Res. Comm.* **19,** 249 (1965).
(34) Yamazaki, I., Ohnishi, T., *Biochim. Biophys. Acta* **112,** 469 (1966).
(35) Yamazaki, I., Tamura, M., Yokota, K., "Hemes and Hemoproteins," B. Chance, R. Estabrook, T. Yonetani, Eds., p. 319, Academic Press, New York, 1966.
(36) Yamazaki, I., Yokota, K., *Biochim. Biophys. Acta* **132,** 310 (1967).
(37) Yokota, K., Yamazaki, I., *Biochem. Biophys. Res. Comm.* **18,** 48 (1965).
(38) Yokota, K., Yamazaki, I., *Biochim. Biophys. Acta* **105,** 301 (1965).

INDEX